

“Researchers confirmed an exoplanet, a planet that orbits another star, using NASA’s James Webb Space Telescope for the first time.

Formally classified as LHS 475 b, the planet is almost exactly the same size as our own, clocking in at 99% of Earth’s diameter.”

NASA

VOLUME:7 / ISSUE:2 / YEAR:2023
ISSN:2651-401X / e-ISSN:2651-4028

Owner

Assoc.Prof.Dr. Hamza Kandemir
Kutbilge Association of Academicians, Türkiye

Editor-in-chief

Assoc.Prof.Dr. Mustafa Karaboyacı
Suleyman Demirel University, Türkiye

Co-Editors

Asst. Prof.Dr. Abdullah Beram
Pamukkale University, Türkiye

Asst. Prof.Dr. Serkan Özdemir
Isparta University of Applied Sciences, Türkiye

Technical Editors:

Res. Asst. Tunahan Çınar
Düzce University, Türkiye

Language Editor

Instructor Berna Yakçinkaya
University of Delaware, USA

Layout Editor

Instructor Şerafettin Atmaca
Süleyman Demirel University, Türkiye

Dr. Ahmet Acarer
Isparta University of Applied Sciences, Türkiye

Press:

Kutbilge Association of Academicians
Distribution, Sales, Publisher;
Certificate No: 42086
32040, Isparta, Türkiye

Contact:

Kutbilge Association of Academicians, 32040,
Isparta, TÜRKİYE

Web Site:

<https://dergipark.org.tr/tr/pub/bilgesci>

E-mail:

bilgesci@gmail.com

Editors

Prof. Dr. Steve Woodward
University of Aberdeen, United Kingdom

Assoc. Prof. Dr. Grzegorz Kowaluk
Warsaw University of Life Sciences-SGGW, Poland

Assoc. Prof. Dr. Halil Suel
Isparta University of Applied Sciences, Türkiye

Assoc. Prof. Dr. Joanna Boguniewicz-Zablocka
Opole University of Technology, Poland

Assoc. Prof. Dr. Emrah Altun
Bartın University, Türkiye

Prof. Dr. Halil Gökce
Giresun University, Türkiye

Prof. Dr. Alaattin Kaçal
Kutahya Dumlupınar University, Türkiye

Assoc. Prof. Dr. Özdemir Şentürk
Burdur Mehmet Akif University, Türkiye

Dr. Müge Ünal Çilek
Fırat University, Türkiye

Dr. Mehmet Tekin
Akdeniz University, Türkiye

Assoc. Prof. Dr. Kubilay Taşdelen
Isparta University of Applied Sciences, Türkiye

Dr. Izabela D. Czabak-Górska
Opole University of Technology, Poland

Dr. Muhamet Ahmeti
University Of Business and Technology, Kosovo

Dr. Cengiz Çesko
University Of Business and Technology, Kosovo

Dr. Ali Sihahtar
Sakarya University, Türkiye

VOLUME:7 / ISSUE:2 / YEAR:2023
ISSN:2651-401X / e-ISSN:2651-4028

A peer reviewed international journal, published biannually by Kutbilge Association of Academicians.

The journal is indexed in **Index Copernicus**, **Crossref**, **AcademicKey**, **Araştırmaz**, **CiteFactor**, **Eurasian Scientific Journal Index (ESJI)**, **Infobase Index**, **ROAD**, **JIFACTOR**, **Rootindexing**, **Science Library Index**, **Cosmos Index**, **Directory of Research Journals Indexing (DRJI)**, **International Institute of Organized Research (I2OR)**, **Journal Factor**, **Google Scholar**, **Researchbib**, **Scientific Indexing Service (SIS)**, **ISI (International Scientific Indexing)**, **IPIndexing**, **ASOS Indeks**, **ScienceGate**, **Scilit**, **IJI Factor** and **ACAR Indeks**.



VOLUME:7 / ISSUE:2 / YEAR:2023
ISSN:2651-401X / e-ISSN:2651-4028

CONTENTS

Research Articles

- Effective Dye Adsorption with Cross-linked Hexagonal Boron Nitride Spheres
Sahra Dandıl, Abdullah Düzgün 95-104
- Automatic detection of water surfaces using K-means++ clustering algorithm with Landsat-9 and Sentinel-2 images on the Google Earth Engine Platform
Osman Salih Yılmaz 105-111
- A Retrospective Study on Wild Animals Admitted to Animal Rescue and Rehabilitation Centres in Türkiye
Emrah Bozkaya, Tamay Başağaç Gül..... 112-116
- Use of Spinning Roller in Cylindrical Densification; Spring back in Black Poplar, Larch and Cedar of Lebanon after Densification
Zafer Kaya, Sait Dündar Sofuoğlu 117-127
- Prediction of Turkish Constitutional Court Decisions with Explainable Artificial Intelligence
Tülay Turan, Ecir Uğur Küçüksille, Nazan Kemaloğlu Alagöz 128-141
- Modeling of *E. coli* Inactivation from Solutions using GInaFiT via Hybrid Electrode Connected Electro-Disinfection Process
Murat Solak, Rüya Tekin Karaköse 142-155
- Biometric Personal Classification with Deep Learning Using EMG Signals
Bekir Bilgin, Mehmet İsmail Gürsoy, Ahmet Alkan..... 156-161
- Perception of Yachts by Non-Owners
Murat Aydın 162-171
- Effects of Contamination Agent for Tissue Culture Applications of *Bacopa monnieri*
Onur Sinan Türkmen, Zeynep Karaceylan, Melike Küçük, Refika Ceyda Beram 172-176
- City and Brain Analogy: a Sample for Conservative Versus Adaptive Phenotypical Vision of a Genotypical Heritage
Ozgu Hafizoğlu, Kader Reyhan 177-186
- A Bibliometric Analysis of Wearable Health Technology Research
Pelin Yılık 187-197
- Reading The World with Statistical Literacy: Results of An Empirical Study
Deniz Ünal, Begüm Çiğşar, Dibanur Alam, Şerife Ezgi Atalar, Sait İsmail Gümüş, Ali Çakitli..... 198-203

Effective Dye Adsorption with Cross-linked Hexagonal Boron Nitride Spheres

Sahra Dandil^{1*}, Abdullah Düzgün¹

Abstract: In this study, cross-linked spheres (CS) were synthesized with chitosan and hexagonal boron nitride (h-BN) to investigate the efficiency of h-BN as an adsorbent and reveal an alternative adsorbent for adsorption processes. CS were used in Reactive Blue 3R (RB3R) and Red P4BN (RP4BN) dye adsorption from wastewater. Surface characteristics of the CS were investigated by Scanning Electron Microscopy (SEM) with Energy Dispersive X-ray (EDX) analysis. The behavior of the adsorption processes with varying effective parameters was investigated. The highest removals were obtained at pH 3 for the RB3R and RP4BN removal processes as 62.8 and 74.2%, respectively. The equilibrium time of the processes was determined as 150 min. The pseudo-first-order kinetic model best explained the adsorption rates of the processes. The Freundlich isotherm model was fitted to define the adsorption mechanisms for both dyes. The positive ΔH values obtained as 24.27 and 16.59 kJ mol⁻¹ for the RB3R and RP4BN adsorption processes, respectively, showed that the processes were endothermic. For the RB3R and RP4BN dye removal processes, ΔS values were calculated as 93.38 and 72.23 J mol⁻¹K⁻¹, respectively. Positive ΔS value indicates the processes that occur with an increase in disorder at the interface. The results described that the CS can be used in the adsorption of RB3R and RP4BN dyes from wastewater.

Keywords: Chitosan, Cross-linked Spheres, Dye Adsorption, Hexagonal Boron Nitride.

¹**Address:** Bilecik Şeyh Edebali University, Faculty of Engineering, Department of Chemical Engineering, 11100, Bilecik, Türkiye.

***Corresponding author:** sahra.ugur@bilecik.edu.tr

Citation: Dandil, S., Düzgün, A. (2023). Effective Dye Adsorption with Cross-linked Hexagonal Boron Nitride Spheres. *Bilge International Journal of Science and Technology Research*, 7(2): 95-104.

1. INTRODUCTION

Decreased water resources around the world have made the issues of more conscious use of existing resources and reuse of wastewater important. Pollutants that cause a danger to the environment and living things by mixing with wastewater can be exemplified as pesticides, herbicides, pharmaceuticals, heavy metals, industrial dyes and detergents (Peng et al., 2022; Ewis et al., 2022). Among these, dyes cause environmental problems even at very low concentrations. They are preferred for coloring in the textile, leather and paper industries (Duan et al., 2022). Synthetic dyes, which can be ionic (cationic and anionic) and non-ionic, cause serious problems by mixing with water during or after production (Tara et al., 2021; Chouaybi et al., 2022). In addition, their complex molecular structure gives them durability and resistance (Qasem et al., 2022).

Adsorption is one of the preferred effective methods in wastewater treatment. To remove pollutants from wastewater, adsorption describes a mass transfer that occurs

in the form of physical or chemical bonding of dissolved pollutants in the liquid phase (adsorbate) onto a solid phase (adsorbent) (Artioli, 2008; Liyanag and Walpita, 2020; Hu and Xu, 2020). The method is frequently preferred for industrial dye removal due to its low cost, controllability and high performance.

One of the most researched aspects of the adsorption method is the synthesis of new adsorbents. The adsorbents to be used in adsorption processes are expected to be high-capacity, porous, cheap and stable, and provide high efficiency. One of the materials frequently used in adsorbent synthesis is chitosan. Chitosan is a natural polysaccharide synthesized by the N-deacetylation of chitin (Chen et al., 2022). Chitosan has applications in adsorption because it can interact with pollutants with amino (-NH₂) and hydroxyl (-OH) groups in its molecules (Verma and Dutta, 2020). Synthesis of various adsorbents using chitosan and their use in different adsorption processes are included in the literature. Among the studies in recent years, Chen et al. synthesized chitosan-based aerogel and used it in thorium adsorption (Chen et al.,

2022). Yeo et al. synthesized bentonite-chitosan composites for use in the removal of antibiotics (Yeo et al., 2023). Wang et al. prepared magnetic chitosan using chitosan and iron oxide (Fe_3O_4) as an adsorbent and used it in dye adsorption (Wang et al., 2022). Xu et al. studied the adsorption of heavy metals with composite beads synthesized with paper waste and chitosan (Xu et al., 2022).

It is known that two-dimensional materials have excellent electrical, mechanical and thermal properties compared to their bulk forms (An et al., 2022). Hexagonal boron nitride (h-BN) is a two-dimensional material with a structure similar to graphene (Yun et al., 2022). h-BN has many uses with its excellent mechanical, electrical, thermal and chemical properties (Chen et al., 2022). In this study; in order to investigate the efficiency of h-BN in wastewater treatment and to reveal an alternative adsorbent that can be used in adsorption processes, cross-linked spheres (CS) containing h-BN and chitosan were synthesized and used in dye adsorption processes. This study is important in terms of examining the usability of h-BN, which draws attention to its superior properties, as an adsorbent in adsorption processes, in addition to its usage areas. Reactive Blue 3R (RB3R) and Red P4BN (RP4BN) dyes were chosen as dyes. RB3R (C.I. Reactive Blue 28) belongs to the vinyl sulfone dye group (Emco, 2023). RP4BN (C.I. Reactive Red 3.1) is also in a reactive dye group (Aditya, 2023). The effective parameters (pH, time, dye concentration, adsorbent dosage and temperature) of both dye removal processes were examined. Kinetic, equilibrium and thermodynamic data of the processes were performed to describe the RB3R and RP4BN dye adsorption by the spheres.

2. MATERIAL AND METHOD

2.1. Materials

Chitosan and hexagonal boron nitride (h-BN) were used to synthesize cross-linked spheres (CS) to use as an adsorbent. h-BN (micron size) was supplied from BORTEK. The acetic acid solution was purchased from Merck. Glutaraldehyde solution (50%) was used as a cross-linker and supplied from Fluka. RB3R and RP4BN dyes used as adsorbates were obtained from a textile dye production factory in Turkey. Various concentrations of hydrochloric acid (HCl) and sodium hydroxide (NaOH) solutions were used to adjust the pH of the dye solutions.

2.2. Synthesis and characterization of adsorbent

Synthesis of the adsorbent was carried out similarly to the study previously presented by Dandil et al (Dandil et al., 2019). 1.5 g chitosan was added to 75 mL of 5% by volume acetic acid solution and left to stir overnight. After mixing was complete, 0.5 g of h-BN was added to the mixture and stirred overnight. The mixture was added to a 1M NaOH solution with a syringe. It was observed that each drop of the mixture became spherical particles. The spheres were left to mix overnight. Then, the spheres were washed with distilled water. Several washes were continued until pH 7. The spheres were added to a 2.5% glutaraldehyde - ethyl alcohol solution by mass and kept in a shaker at 60 °C for 15 hours. The spheres washed with distilled water were held at -80 °C

for a night. Then the spheres were kept in a freeze-dryer for 24 hours.

The surface characteristics of the CS were determined with Scanning Electron Microscopy (SEM) analysis. Zeiss Supra 40VP was used to investigate the surface porosity and pore distribution of the sample. Also, Energy Dispersive X-ray (EDX) technique was performed for the chemical characterization of the CS.

2.3. Adsorption

The synthesized spheres were used for the adsorption of RB3R and RP4BN dyes from aqueous solutions. The effective parameters such as pH (3-9), time (0-150 min), dye concentration (25-150 ppm), adsorbent dosage (0.2-0.8 g/L) and temperature (25-45 °C) on the removal processes were investigated. The same parameter values were studied for both dyes.

Adsorption studies were carried out with 50 mL dye solutions. The aqueous dye solutions were prepared with deionized water. The experiments were performed in a shaker (Thermal H11960) at 200 rpm. Absorbance values of the samples taken at certain time intervals to determine the dye concentrations in aqueous solutions were obtained with the Ultraviolet-Visible region (UV-GB) spectrophotometer (Perkin Elmer, Elmer Analyst 800) at a wavelength of 585 and 535 nm, where the maximum absorbance values for RB3R and RP4BN dyes was observed, respectively.

The adsorption data of the processes were studied with the adsorption capacity and removal percentage equations given below (Long et al., 2022):

$$q_e = \frac{(C_0 - C_e) \times V}{m} \quad (1)$$

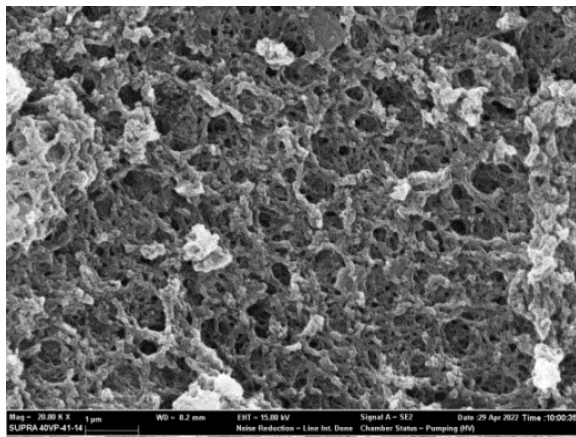
$$\% \text{Removal} = \frac{(C_0 - C_e) \times 100}{C_0} \quad (2)$$

where q_e ; the amount of dye adsorbed at equilibrium (mg g^{-1}), C_0 and C_e ; initial and equilibrium dye concentrations of dye solution (mg L^{-1}), respectively, V ; volume (L), M ; adsorbent mass (g) (Long et al., 2022).

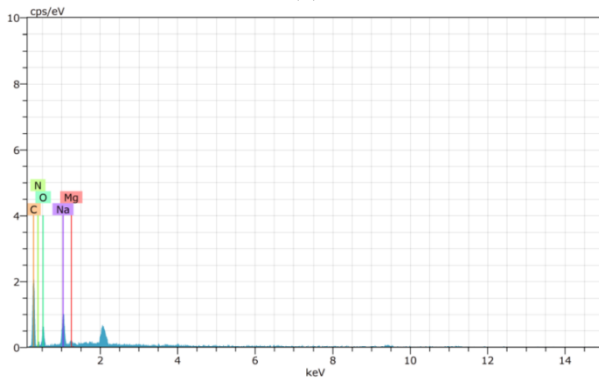
3. RESULTS AND DISCUSSION

3.1. Characterization of the spheres

The surface characteristics of the CS were observed by SEM images. SEM micrograph of the CS at 20000 magnifications is presented in Figure 1 (a). The porous and uniform texture of the spheres is shown in microscopic observation. The elemental composition of the adsorbent was examined by EDX analysis. As given in Figure 1 (b), carbon (C) and oxygen (O) elements were observed in the EDX image of the CS. According to the quantitative analysis of the CS given in Table 1, the mass fraction of C and O are determined as 51.21 and 25.78%, respectively.



(a)



(b)

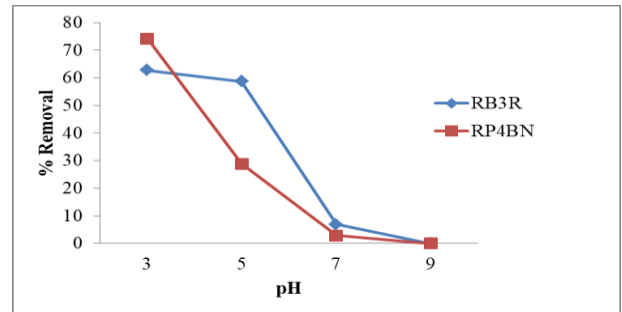
Figure 1. (a) SEM and (b) EDX images of the CS**Table 1.** Quantitative results of EDX analysis for the CS

Elements	Mass%	Atomic%
Carbon	51.21	59.30
Oxygen	25.78	22.41
Sodium	11.05	6.68
Nitrogen	11.31	11.23
Magnesium	0.66	0.38

3.2. Effect of pH of the dye solutions and contact time

The pH of the RB3R and RP4BN dye solutions has a great effect on the adsorption processes due to changing the surface charge of the CS. The surface charge of an adsorbent is significant since it affects the adherence of the ionized RB3R and RP4BN dye molecules on the CS surface. To investigate the effect of various pH values on the RB3R and RP4BN dye adsorption on the CS, experiments were done for pH values in the range of 3-9 of dye solutions. The concentration of the dye solutions was 50 ppm, the adsorbent dosage was 0.4 g/L and the temperature was 25 °C in the experiments. The processes were followed for 150 minutes. pH effect on the removal percentages of RB3R and RP4BN dyes by the CS is given in Figure 2. According to Figure 2, it was observed that RB3R and RP4BN removal percentages decreased with the increase of pH values from 3 to 7, and no removal occurred for both dyes at pH 9. The percentages of RB3R dye removal by the CS were determined as 62.8, 58.7 and 6.9% at pH of 3, 5 and 7, respectively. And also for the RP4BN dye adsorption process from aqueous solution 74.2, 28.8 and 2.8% removal efficiencies were observed at pH of

3, 5 and 7, respectively. Thus, the effect of pH on adsorption was confirmed. The highest removals were obtained at pH 3 for both processes. Due to the positive charge density in the aqueous solution medium at pH 3, the adsorption of anionic RB3R and RP4BN dyes on the CS was effective. As the pH increased, the adsorption efficiencies of the dyes decreased with the decrease of the positively charged sites (Mahmoodi and Mokhtari-Shourijeh, 2015).

**Figure 2.** Effect of pH on the removal percentages of RB3R and RP4BN dyes by the CS (Initial dye concentrations: 50 mg/L, adsorbent dosage: 0.4 g/L, temperature: 25 °C, time: 150 min)

The RB3R and RP4BN adsorption processes on the CS were followed with time in the range of pH 3-9 of the dye solutions and results were given in Figure 3. According to the graphs given in Figure 3 (a) and (b) for RB3R and RP4BN dye removal processes, respectively, regular increases were observed in the removal percentages for both dyes over time at all pH values. After 90 minutes for both processes, the increase in removal percentages started to decrease and the processes reached equilibrium in 150 minutes at pH 3, where the highest removal was determined. Also, a higher removal of RP4BN dye (74.2%) than RB3R dye (62.8%) was obtained at pH 3 in 150 minutes. In the early times of adsorption, the unoccupied sites of the CS allowed more efficient and rapid adsorption of the RB3R and RP4BN molecules. However, due to the active sites that start to occupy the dye molecules with time, the removal percentages decrease and reach an equilibrium where there is no dye removal (Wong et al., 2020).

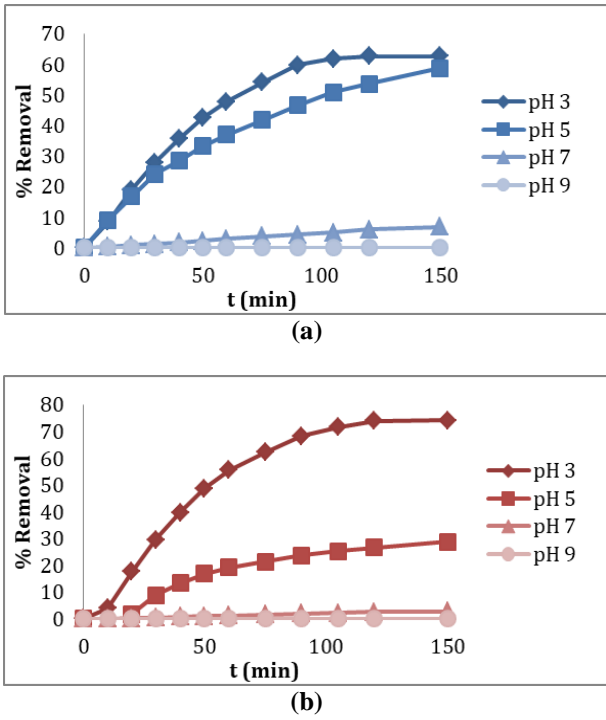


Figure 3. Effect of contact time on the removal percentages of (a) RB3R and (b) RP4BN dyes by the CS (Initial dye concentrations: 50 mg/L, adsorbent dosage: 0.4 g/L, temperature: 25 °C)

3.3. Adsorption kinetics

The experimental data obtained for the RB3R and RP4BN dye adsorption with the synthesized spheres were evaluated with the two most used kinetic models. The adsorption kinetics of the dye adsorption processes were studied with the pseudo-first-order and pseudo-second-order models.

The pseudo-first-order and pseudo-second-order kinetic model equations were presented in Equations (3) and (4), respectively (Loganathan et al., 2022):

$$\log(q_e - qt) = \log q_e - \frac{k_1}{2.303}t \tag{3}$$

$$\frac{t}{qt} = \frac{1}{k_2 q_e^2} + \frac{t}{q_e} \tag{4}$$

where t; time (min), qt; adsorbed dye at time t (mg g⁻¹), k₁ and k₂; first-order kinetic model rate constant (min⁻¹) and second-order kinetic model rate constant (g mg⁻¹ min⁻¹), respectively and C; constant (Loganathan et al., 2022).

The pseudo-first-order and pseudo-second-order kinetic model plots of the RB3R and RP4BN dye removal processes by the CS are seen in Figure 4 (a) and (b), respectively. The parameters of the kinetic models were also presented in Table 2. The correlation coefficients (R²) of the RB3R and RP4BN adsorption processes seen in Table 2 were interpreted to decide on the kinetic model that best describes the processes. The R² values of the pseudo-first-order kinetic model were higher than the R² values of the second-order kinetic model for both dyes. Thus, the pseudo-first-order

kinetic model was found as compatible with the removal of RB3R and RP4BN dyes by the CS. The highest R² values of the pseudo-first-order model indicate the RB3R and RP4BN dye removal processes by the CS occur physically (Zaini et al., 2022). In addition, the calculated q_e value for the RP4BN dye was found to be higher than that of the RB3R dye.

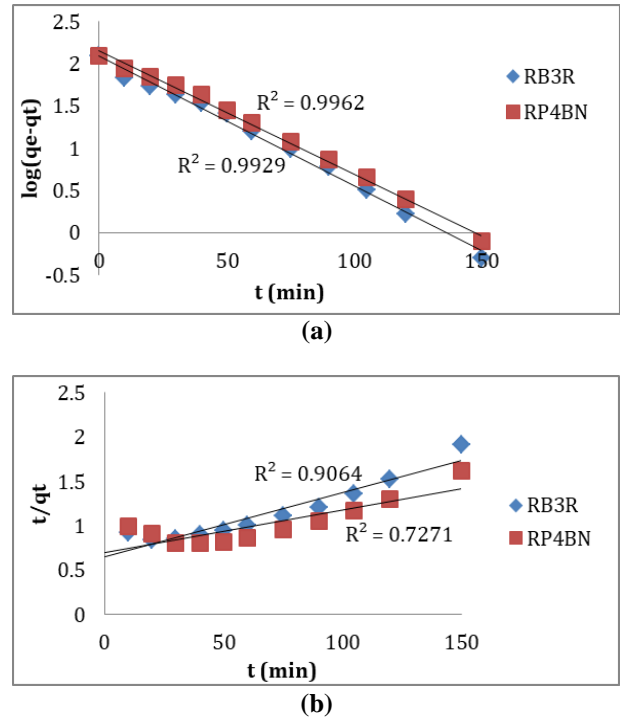


Figure 4. (a) Pseudo-first-order, and (b) pseudo-second-order kinetic model plots for the RB3R and RP4BN dye adsorption processes

Table 2. Kinetic parameters of the RB3R and RP4BN dye adsorption processes

	Pseudo-First-Order Kinetic Model			Pseudo-Second-Order Kinetic Model		
	k ₁ (x10 ²) (min ⁻¹)	q _{e,cal} (mg g ⁻¹)	R ²	k ₂ (x10 ⁵) (g mg ⁻¹ min ⁻¹)	q _{e,cal} (mg g ⁻¹)	R ²
RB3R	3.55	125.6	0.992	7.98	138.8	0.906
RP4B	3.36	142.3	0.996	3.30	208.3	0.727
N		3	2		3	1

3.4. Effect of initial concentration of the dye solutions and isotherm studies

To examine the dye concentration effect on removal efficiency, the adsorption processes of RB3R and RP4BN dyes on the CS were studied in the range of 25-150 ppm dye solution concentrations. The processes were followed at 0.4 g/L adsorbent dosage and 25 °C for 150 minutes. The effect of initial dye concentration on the removal percentages of the processes is given in Figure 5. In Figure 5 (a) and (b), it is observed that the removal efficiencies increase over time for each concentration according to the graphs showing the change in the percentage of removal of RB3R and RP4BN dyes, respectively. At the end of 150 minutes, 48.0, 62.8,

67.6 and 42.1% removals were obtained for RB3R dye at 25, 50, 100 and 150 ppm, respectively. Removal percentages of 63.3, 74.2, 71.2 and 63.0% were obtained for RP4BN at 25, 50, 100 and 150 ppm, respectively. It is seen that higher removals were obtained for RP4BN than RB3R at all concentration values. For both dyes, the removal percentages increased with increasing dye concentration but decreased after a high concentration. Up to a certain concentration, the number of unoccupied sites for adsorption is high, and the driving force for mass transfer also increases. After a high concentration, the removal efficiency decreases as the number of sites required to increase the concentration will be limited. The results agree with other adsorption studies presented previously (Pathania et al., 2017; Salimi et al., 2017; Farouq, 2022;).

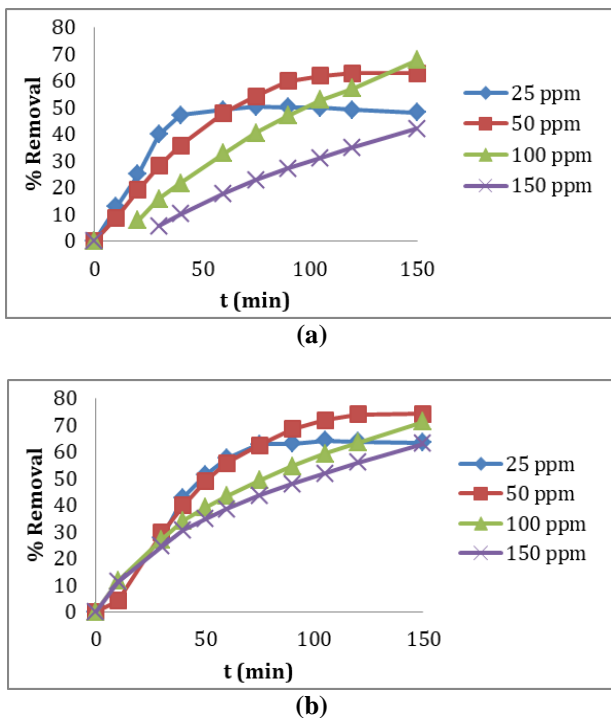


Figure 5. Effect of initial concentrations of (a) RB3R and (b) RP4BN dye solutions on the removal efficiencies of the RB3R and RP4BN dye adsorption processes (Adsorbent dosage: 0.4 g/L, time: 150 min, temperature: 25 °C)

Langmuir and Freundlich models were studied to explain the mechanisms of the RB3R and RP4BN dye adsorption processes on the spheres. Langmuir and Freundlich equations are given below respectively (Dandil et al., 2019):

$$\frac{C_e}{q_e} = \frac{C_e}{q_m} + \frac{1}{(q_m K_L)} \quad (5)$$

$$\ln q_e = \ln K_F + \frac{1}{n} \ln C_e \quad (6)$$

where K_L ; Langmuir isotherm constant ($L g^{-1}$), q_m ; maximum adsorption capacity ($mg L^{-1}$), K_F ; Freundlich isotherm constant, and n ; linearity constant for Freundlich isotherm (Dandil et al., 2019).

The plots of Langmuir and Freundlich isotherm are seen in Figure 6. In addition, the isotherm parameters of both

processes were calculated and presented in Table 3. As given in Table 3, the R^2 values of the isotherm models exhibit that the Freundlich isotherm model clarifies better isotherm studies of both processes than the Langmuir model. The Freundlich isotherm model for the RB3R and RP4BN dye removal processes describes that the RB3R and RP4BN dye is adsorbed on the surface of the CS with multilayer sorption (Salim et al., 2021). The n value indicates the heterogeneity of the CS surface and being below unity explains cooperative adsorption (Ojediran et al., 2021; Salim et al., 2021).

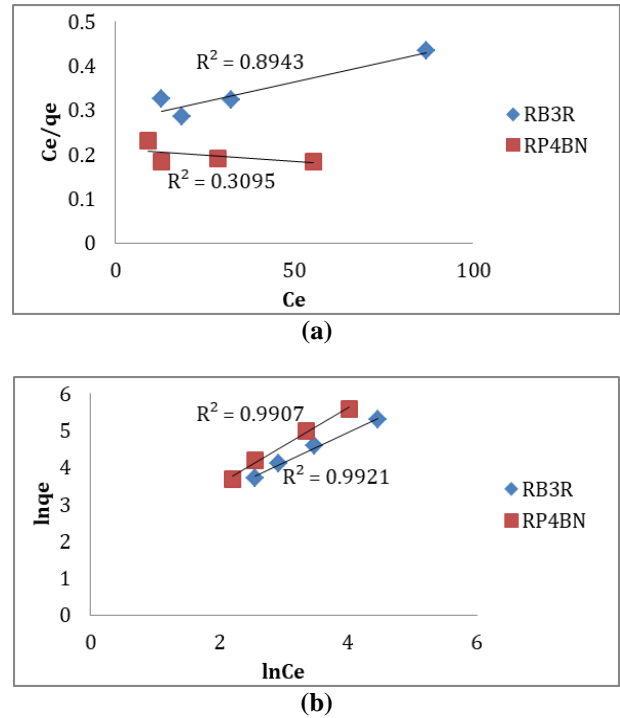


Figure 6. (a) Langmuir and (b) Freundlich isotherms for the RB3R and RP4BN dye adsorption processes

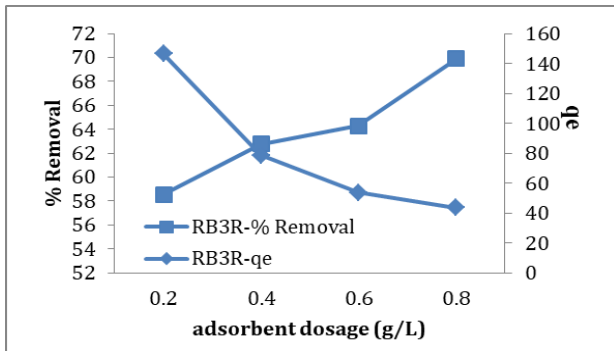
Table 3. Freundlich and Langmuir isotherm model parameters for the RB3R and RP4BN dye adsorption processes

	Langmuir Isotherm			Freundlich Isotherm		
	$K_L(x10^3)$ (L/mg)	$q_m(x10^3)$ ($mg g^{-1}$)	R^2	K_F ($mg g^{-1}$ (L/g) ^{1/n})	n	R^2
RB3R	6.55	0.55	0.8943	5.16	1.206	0.9921
RP4BN	-2.8	-1.67	0.3095	4.23	0.956	0.9907

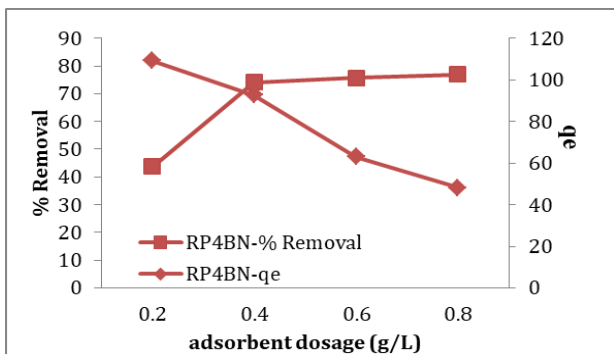
3.5. Effect of adsorbent dosage

To investigate the CS amount effect on the RB3R and RP4BN dye removal processes, studies were performed at various adsorbent dosages (0.2-0.8 g/L). Data were obtained for 150 minutes at 25 °C at a concentration of 50 ppm dye solutions. The behavior of RB3R and RP4BN dye removal processes at different adsorbent dosages are given in Figure 7 (a) and (b), respectively. For both processes, the removal percentages increased with the increasing adsorbent dosage, while the adsorption capacities decreased. For the RB3R dye adsorption process, increasing CS dosage from 0.2 to 0.8 g/L increased the RB3R dye removal percentage from 58.6 to 69.9%, but decreased the adsorption capacity from 146.4 to

43.7 mg/g. Similarly, the RP4BN dye removal increased with the CS dosage from 43.6 to 76.9%, while the adsorption capacity decreased from 109.1 to 48.1 mg/g. Increasing the adsorbent dosage above 0.4 g/L slightly increased the removal percentages of RP4BN (Figure 7 (b)), but effectively increased it for RB3R removal (Figure 7 (a)). In addition, the adsorbent dosage showed a strong effect on the adsorption capacity of both dyes.



(a)



(b)

Figure 7. Effect of adsorbent dosage on the removal efficiencies and adsorption capacities in (a) RB3R and (b) RP4BN dye adsorption processes (Initial dye concentrations: 50 mg/L, time: 150 min, temperature: 25 °C)

Table 4 presents the adsorption capacities of some adsorbents prepared using chitosan in previous studies with the CS in dye removal processes. According to Table 4, CS has a moderate adsorption capacity compared to other studies in the literature.

Table 4. Adsorption capacities of adsorbents synthesized with chitosan in dye removal

Adsorbent	Dye	Adsorption capacity (mg g ⁻¹)	Reference
salicylaldehyde functionalized chitosan	Crystal violet	6.85	Parshi et al., 2019
	Rose Benga	15.26	
chitosan-Gelatin / zirconium (IV) selenophosphate nanocomposite	Methylene blue	10.46	Kaur and Jindal, 2019
CS	RB3R	146.4	Present study
	RP4BN	109.1	
photocatalytic flyash/TiO ₂ modified chitosan biopolymer composite	Congo red	163.51	Gajera et al., 2022
	Methylene blue	55.75	
chitosan-montmorillonite hydrogel beads	methyl green	303.21	Kurczewska, 2022
magnetic Fe ₃ O ₄ embedded chitosan-crosslinked-polyacrylamide composites	Sunset yellow	359.71	Jiang et al., 2022
MIL-53(Fe)/chitosan composite hydrogel spheres	Congo red	590.8	Jin et al., 2022
chitosan-based dual network composite hydrogel	Methylene blue	596.14	Wan et al., 2022

3.6. Effect of temperature and thermodynamics

The temperature effect on the RB3R and RP4BN dye removal processes was investigated at 25, 35, and 45 °C with 0.4 g/L adsorbent dosage at 50 ppm initial dye concentrations for 150 min. The equations given below are used to calculate thermodynamic parameters (Raghav and Kumar, 2018):

$$\ln K_d = \frac{\Delta S}{R} - \frac{\Delta H}{RT} \quad (7)$$

$$K_d = \frac{q_e}{C_e} \quad (8)$$

$$\Delta G = \Delta H - T\Delta S \quad (9)$$

where K_d ; adsorption equilibrium constant, ΔS ; entropy (J mol⁻¹K⁻¹), ΔH ; enthalpy (kJ mol⁻¹), ΔG ; Gibb's free energy (kJ mol⁻¹), R ; gas constant (8.314 J mol⁻¹ K⁻¹), T ; temperature (K) (Raghav and Kumar, 2018).

The Van't Hoff plot showing the relationship between temperature and equilibrium constant is shown in Figure 8. In addition, the thermodynamic parameters of both processes are given in Table 5 with the parameters of similar processes. According to Table 5, the positive enthalpy change values indicate the RB3R and RP4BN dye removal processes by the CS are endothermic (Rios-Donato et al., 2017). It is known that weak van der Waals forces are effective in bonding when the ΔH is below 25 kJ mol⁻¹ and strong chemical bonds are effective when it is in the range of 40-200 kJ mol⁻¹ (de Oliveira et al., 2023). $\Delta S > 0$ shows the processes that occur with an increase in disorder at the interface (Doke and Khan, 2013). According to the ΔS values in Table 5, a more disordered state at the interface can be mentioned for the RB3R adsorption process (93.38 J mol⁻¹K⁻¹) compared to the RP4BN process (72.23 J mol⁻¹K⁻¹). For both processes, negative ΔG values were found at the temperatures studied. The decrease in these values with increasing temperature

explains more effective dye removal at high temperatures (Batool et al., 2018).

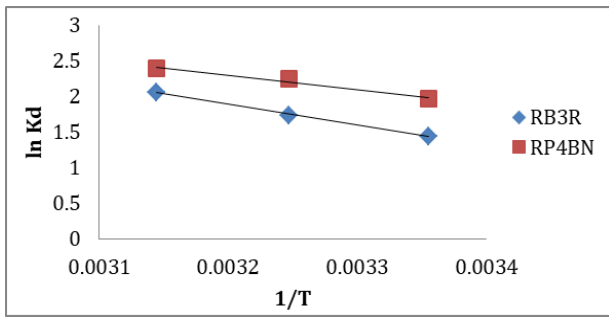


Figure 8. Van't Hoff plots of the RB3R and RP4BN dye adsorption processes

Table 5. Thermodynamic parameters of the RB3R and RP4BN dye adsorption processes and similar studies

Adsorbent	Dye	T (K)	ΔG^0 (kJ mol ⁻¹)	ΔH^0 (kJ mol ⁻¹)	ΔS^0 (J mol ⁻¹ K ⁻¹)	Ref.
chitosan composite of metal-organic framework	Methylene blue	298	9.203	-9.628	-63	Saeed et al., 2022
		308	9.834			
		318	10.466			
	Methyl orange	298	9.400	-19.588	-97	
		308	10.373			
		318	11.346			
polyethyleneimine-modified chitosan/Ce-UIO-66 composite	Methyl orange	303	-3.805	-15.954	-40.097	Chen et al., 2023
		313	-3.404			
		323	-3.003			
		333	-2.602			
		343	-2.201			
MIL-53(Fe)/chitosan composite hydrogel spheres	Congo red	298	-37.63	-5.60	-107.5	Jin et al., 2023
		308	-38.75			
		318	-39.79			
micro/nano MIL-88A (Fe, Al, Fe-Al)/chitosan composite sponge	MIL-88A (Fe-Al)/CS	298	-31.68	83.65	385.4	Zhao et al., 2023
		308	-34.06			
		318	-39.45			
	MIL-88A (Fe)/CS	298	-32.58	75.10	359.6	
		308	-34.51			
		318	-39.84			
	MIL-88A (Al)/CS	298	-32.93	79.34	374.9	
		308	-34.98			
		318	-40.50			
fibrous chitosan/sodium alginate composite foams	CSA1-1	298	-22.03	1.53	79.06	Zhao et al., 2021
		308	-22.82			
		318	-23.61			
	CSA1-5	298	-16.60	5.07	72.73	
		308	-17.33			
		318	-18.06			
citric acid-crosslinked Zn-MOF/chitosan composite	Methyl orange	298	-5.698	-33.448	-55.967	Niu et al., 2021
		308	-5.301			
		318	-4.653			
CS	RB3R	298	-3.55	24.27	93.38	Present study
		308	-4.48			
		318	-5.42			
	RP4BN	298	-4.93	16.59	72.23	
		308	-5.65			
		318	-6.37			

4. CONCLUSIONS

In the study, the usability of the spheres obtained by cross-linking chitosan and h-BN (CS) as an adsorbent was investigated. Also, the efficiency of h-BN as an adsorbent in adsorption processes is presented. The synthesized spheres were used to remove RB3R and RP4BN dyes from wastewater. According to pH effect studies, it was determined that the highest removals were obtained at pH 3 for the RB3R and RP4BN dye removal processes, as 62.8 and 74.2%, respectively. The equilibrium time of the processes was determined as 150 minutes. The pseudo-first-order kinetic model best explained the adsorption rates of the processes. The Freundlich isotherm model is best fitted to define the adsorption mechanisms for both dyes. ΔH values for RB3R and RP4BN dye adsorption processes were calculated as 24.27 and 16.59 kJ mol⁻¹, respectively and clarified that the processes were endothermic. For the RB3R and RP4BN dye removal processes, ΔS values were determined as 93.38 and 72.23 J mol⁻¹K⁻¹, respectively. Positive ΔS values indicate the processes that occur with an increase in disorder at the interface. Negative ΔG values show spontaneous adsorption for both dyes. As a result, the CS showed effectiveness as an adsorbent in RB3R and RP4BN dye adsorption processes.

Author Contributions

Conceptualization: S.D.; Investigation: S.D.; Material and Methodology: S.D., A.D.; Supervision: S.D.; Visualization: S.D.; Writing-Original Draft: S.D.; Writing-review & Editing: S.D., A.D.; Other: All authors have read and agreed to the published version of manuscript.

Conflict of Interest

The authors have no conflicts of interest to declare.

Funding

Bilecik Seyh Edebali University Scientific Research Projects Coordinator ship supported the study with the project code 2021-02.BŞEÜ.03-03.

REFERENCES

- Aditya Color Chem, <https://www.adityacolorchem.com/products/reactive-dyes.html>, (Accessed April 16, 2023)
- An, L., Gu, R., Zhong, B., Yu, Y., Zhang, J. (2022). Water-icing-triggered scalable and controllable exfoliation of hexagonal boron nitride nanosheets. *Cell Reports Physical Science*, 3(7), 100941. <https://doi.org/10.1016/j.xcrp.2022.100941>
- Artioli, Y. (2008). Adsorption, in: Jørgensen, S. E. and Fath, B. D. (Eds.), *Encyclopedia of Ecology*. Elsevier, Amsterdam, Netherlands, pp. 60-65. <https://doi.org/10.1016/B978-008045405-4.00252-4>
- Batool, F., Akbar, J., Iqbal, S., Noreen, S., Bukhari, S. N. A. (2018). Study of isothermal, kinetic, and thermodynamic parameters for adsorption of cadmium: an overview of linear and nonlinear approach and error analysis. *Bioinorganic chemistry and applications*, 2018. <https://doi.org/10.1155/2018/3463724>.
- Chen, B., Ding, L., Wang, Y., Zhang, Y. (2022). High efficient adsorption for thorium in aqueous solution using a novel tentacle-type chitosan-based aerogel: Adsorption behavior and mechanism. *International Journal of Biological Macromolecules*, 222, 1747-1757. <https://doi.org/10.1016/j.ijbiomac.2022.09.256>
- Chen, C., Wang, G., Beshiwork, B. A., Xu B., Lin B. (2022). Strain-tunable pure H⁻ conduction in one-atom-thick hexagonal boron nitride for high-energy-density fuel cells. *Chemical Engineering Journal*, 450, 138223. <https://doi.org/10.1016/j.cej.2022.138223>
- Chen, S., Tian, H., Mao, J., Ma, F., Zhang, M., Chen, F., Yang, P. (2022). Preparation and application of chitosan-based medical electrospun nanofibers. *International Journal of Biological Macromolecules*, 226, 410-422, 2022. <https://doi.org/10.1016/j.ijbiomac.2022.12.056>
- Chen, Z., Zhang, Z. B., Zeng, J., Zhang, Z. J., Ma, S., Tang, C. M., Xu, J. Q. (2023). Preparation of polyethyleneimine-modified chitosan/Ce-UIO-66 composite hydrogel for the adsorption of methyl orange. *Carbohydrate Polymers*, 299, 120079. <https://doi.org/10.1016/j.carbpol.2022.120079>
- Chouaybi, I., Ouassif, H., Bettach, M., Moujahid, E. M. (2022). Fast and high removal of acid red 97 dye from aqueous solution by adsorption onto a synthetic hydrocalumite: Structural characterization and retention mechanisms. *Inorganic Chemistry Communications*, 146, 110169. <https://doi.org/10.1016/j.inoche.2022.110169>
- Dandil, S., Sahbaz, D. A., Acikgoz, C. (2019). Adsorption of Cu (II) ions onto crosslinked chitosan/Waste Active Sludge Char (WASC) beads: Kinetic, equilibrium, and thermodynamic study. *International journal of biological macromolecules*, 136, 668-675. <https://doi.org/10.1016/j.ijbiomac.2019.06.063>
- de Oliveira, T. F., de Souza, C. P., Lopes-Moriyama, A. L., da Silva, M. L. P. (2023). In situ modification of MCM-41 using niobium and tantalum mixed oxide from columbite processing for methylene blue adsorption: Characterization, kinetic, isotherm, thermodynamic and mechanism study. *Materials Chemistry and Physics*, 294, 127011. <https://doi.org/10.1016/j.matchemphys.2022.127011>
- Doke, K. M., Khan, E. M. (2013). Adsorption thermodynamics to clean up wastewater; critical review. *Reviews in Environmental Science and Bio/Technology*, 12(1), 25-44. DOI 10.1007/s11157-012-9273-z
- Duan, Y. T., Yao, Y., Ameta, R. K. (2022). Removal and recovering of anionic and cationic dyes using Neem Leaf ash prepared at 250, 500 and 750° C: Analyzed by adsorption isotherm and physicochemical parameters. *Journal of Molecular Liquids*, 370, 121012. <https://doi.org/10.1016/j.molliq.2022.121012>

- Emco Dyestuff Pvt. Ltd., <https://www.emcochemicals.com/Dyes/Reactive-Dyes/Reactive-Dyes-VINYL-SULPHONE/Blue-3R> (Accessed April 16, 2023)
- Ewis, D., Ba-Abbad, M. M., Benamor, A., El-Naas, M. H. (2022). Adsorption of organic water pollutants by clays and clay minerals composites: A comprehensive review. *Applied Clay Science*, 229, 106686. <https://doi.org/10.1016/j.clay.2022.106686>
- Farouq, R. (2022). Coupling Adsorption-Photocatalytic Degradation of Methylene Blue and Maxilon Red. *Journal of Fluorescence*, 32(4), 1-8. <https://doi.org/10.1007/s10895-022-02934-1>
- Gajera, R., Patel, R. V., Yadav, A., Labhasetwar, P. K. (2022). Adsorption of cationic and anionic dyes on photocatalytic flyash/TiO₂ modified chitosan biopolymer composite. *Journal of Water Process Engineering*, 49, 102993. <https://doi.org/10.1016/j.jwpe.2022.102993>
- Hu, H., Xu, K. (2020). Physicochemical technologies for HRPs and risk control, in: Ren, H. and Zhang, X. (Eds.), *High-risk pollutants in wastewater*. Elsevier, Amsterdam, Netherlands, pp. 169-207. <https://doi.org/10.1016/B978-0-12-816448-8.00008-3>
- Jiang, R., Shen, T. T., Zhu, H. Y., Fu, Y. Q., Jiang, S. T., Li, J. B., Wang, J. L. (2022). Magnetic Fe₃O₄ embedded chitosan-crosslinked-polyacrylamide composites with enhanced removal of food dye: Characterization, adsorption and mechanism. *International Journal of Biological Macromolecules*, 227, 1234-1244. <https://doi.org/10.1016/j.ijbiomac.2022.11.310>
- Jin, Y., Li, Y., Du, Q., Chen, B., Chen, K., Zhang, Y., Wang, M., Sun, Y., Zhao, S., Jing, Z., Wang, Y. (2022). Efficient adsorption of Congo red by MIL-53 (Fe)/chitosan composite hydrogel spheres. *Microporous and Mesoporous Materials*, 348, 112404. <https://doi.org/10.1016/j.micromeso.2022.112404>
- Jin, Y., Li, Y., Du, Q., Chen, B., Chen, K., Zhang, Y., Wang, M., Sun, Y., Zhao, S., Jing, Z., Wang, J. (2023). Efficient adsorption of Congo red by MIL-53 (Fe)/chitosan composite hydrogel spheres. *Microporous and Mesoporous Materials*, 348, 112404. <https://doi.org/10.1016/j.micromeso.2022.112404>
- Kaur, K., Jindal, R. (2019). Comparative study on the behaviour of Chitosan-Gelatin based Hydrogel and nanocomposite ion exchanger synthesized under microwave conditions towards photocatalytic removal of cationic dyes. *Carbohydrate Polymers*, 207, 398-410. <https://doi.org/10.1016/j.carbpol.2018.12.002>
- Kurczewska, J. (2022). Chitosan-montmorillonite hydrogel beads for effective dye adsorption. *Journal of Water Process Engineering*, 48, 102928. <https://doi.org/10.1016/j.jwpe.2022.102928>
- Liyanage, D., Walpita, J. (2020). Organic pollutants from E-waste and their electrokinetic remediation. in: Prasad, M.N.V., Vithanage, M. and Borthakur, A. (Eds.), *Handbook of Electronic Waste Management*. Elsevier, Amsterdam, Netherlands, pp. 171-189.
- Loganathan, M., Raj, A. S., Murugesan, A., Kumar, P. S. (2022). Effective adsorption of crystal violet onto aromatic polyimides: Kinetics and isotherm studies. *Chemosphere*, 304, 135332. <https://doi.org/10.1016/j.chemosphere.2022.135332>
- Long, W., Yang, C., Wang, G., Hu, J. (2022). Effective adsorption of Hg (II) ions by new ethyleneimine polymer/ β -cyclodextrin crosslinked functionalized magnetic composite. *Arabian Journal of Chemistry*, 104439. <https://doi.org/10.1016/j.arabjc.2022.104439>
- Mahmoodi, N. M., Mokhtari-Shourijeh, Z. (2015). Preparation of PVA-chitosan blend nanofiber and its dye removal ability from colored wastewater. *Fibers and Polymers*, 16(9), 1861-1869. DOI 10.1007/s12221-015-5371-1
- Niu, C., Zhang, N., Hu, C., Zhang, C., Zhang, H., Xing, Y. (2021). Preparation of a novel citric acid-crosslinked Zn-MOF/chitosan composite and application in adsorption of chromium (VI) and methyl orange from aqueous solution. *Carbohydrate Polymers*, 258, 117644. <https://doi.org/10.1016/j.carbpol.2021.117644>
- Ojediran, J. O., Dada, A. O., Aniyi, S. O., David, R. O., Adewumi, A. D. (2021). Mechanism and isotherm modeling of effective adsorption of malachite green as endocrine disruptive dye using Acid Functionalized Maize Cob (AFMC). *Scientific reports*, 11(1), 1-15. | <https://doi.org/10.1038/s41598-021-00993-1>
- Parshi, N., Pan, D., Dhavle, V., Jana, B., Maity, S., Ganguly, J. (2019). Fabrication of lightweight and reusable salicylaldehyde functionalized chitosan as adsorbent for dye removal and its mechanism. *International journal of biological macromolecules*, 141, 626-635. <https://doi.org/10.1016/j.ijbiomac.2019.09.025>
- Pathania, D., Sharma, S., Singh, P. (2017). Removal of methylene blue by adsorption onto activated carbon developed from Ficus carica bast. *Arabian journal of chemistry*, 10, S1445-S1451. <https://doi.org/10.1016/j.arabjc.2013.04.021>
- Peng, R., Zhang, S., Yao, Y., Wang, J., Zhu, X., Jiang, R., Zhang, J., Zhang, W., Wang, C. (2022). MOFs meet electrospinning: new opportunities for water treatment. *Chemical Engineering Journal*, 453, 139669. <https://doi.org/10.1016/j.cej.2022.139669>
- Qasem, K. M., Khan, S., Chinnam, S., Saleh, H. A., Mantasha, I., Zeeshan, M., Manea, Y. K., Shahid, M. (2022). Sustainable fabrication of Co-MOF@ CNT nano-composite for efficient adsorption and removal of organic dyes and selective sensing of Cr (VI) in aqueous phase. *Materials Chemistry and Physics*,

- 291, 126748.
<https://doi.org/10.1016/j.matchemphys.2022.126748>
- Raghav, S., Kumar, D. (2018). Adsorption equilibrium, kinetics, and thermodynamic studies of fluoride adsorbed by tetrametallic oxide adsorbent. *Journal of Chemical & Engineering data*, 63(5), 1682-1697. <https://doi.org/10.1021/acs.jced.8b00024>
- Rios-Donato, N., Peña-Flores, A. M., Katime, I., Leyva-Ramos, R., Mendizábal, E. (2017). Kinetics and thermodynamics of adsorption of red dye 40 from acidic aqueous solutions onto a novel chitosan sulfate. *Afinidad*, 74(579), 214-220. <https://raco.cat/index.php/afinidad/article/view/328558/419163>
- Saeed, T., Naeem, A., Din, I. U., Farooq, M., Khan, I. W., Hamayun, M., Malik, T. (2022). Synthesis of chitosan composite of metal-organic framework for the adsorption of dyes; kinetic and thermodynamic approach. *Journal of Hazardous Materials*, 427, 127902. <https://doi.org/10.1016/j.jhazmat.2021.127902>
- Salim, N. A. A., Puteh, M. H., Khamidun, M. H., Fulazzaky, M. A., Abdullah, N. H., Yusoff, A. R. M., Zaini, M. A. A., Ahmad, N., Lazim, Z. M., Nuid, M. (2021). Interpretation of isotherm models for adsorption of ammonium onto granular activated carbon. *Biointerface Res. Appl. Chem*, 11, 9227-9241. <https://doi.org/10.33263/BRIAC112.92279241>
- Salimi, F., Tahmasobi, K., Karami, C., Jahangiri, A. (2017). Preparation of modified nano-SiO₂ by bismuth and iron as a novel remover of methylene blue from water solution. *Journal of the Mexican Chemical Society*, 61(3), 250-259. [chrome-extension://efaidnbmnnnibpcajpcglclefindmkaj/https://www.scielo.org.mx/pdf/jmcs/v61n3/1870-249X-jmcs-61-03-00250.pdf](https://www.scielo.org.mx/pdf/jmcs/v61n3/1870-249X-jmcs-61-03-00250.pdf)
- Tara, N., Sharma, A., Choudhry, A., Abdulla, N. K., Rathi, G., Khan, A. M., Chaudhry, S. A. (2021). Graphene, graphene oxide, and reduced graphene oxide-based materials: a comparative adsorption performance, in: Ahamad, A., Siddiqui, S.I. and Singh, P. (Eds.), *Contamination of Water*. Elsevier, Amsterdam, Netherlands, pp. 495-507. <https://doi.org/10.1016/B978-0-12-824058-8.00014-1>
- Verma, S., Dutta, R. K. (2020). Adsorptive Removal of Toxic Dyes Using Chitosan and Its Composites, in: Naushad, Mu., Lichtfouse, E. (Eds.), *Green Materials for Wastewater Treatment*. Springer, Berlin, Germany, pp. 223-255. DOI:10.1007/978-3-030-17724-9_10
- Wan, X., Rong, Z., Zhu, K., Wu, Y. (2022). Chitosan-based dual network composite hydrogel for efficient adsorption of methylene blue dye. *International Journal of Biological Macromolecules*, 222, 725-735. <https://doi.org/10.1016/j.ijbiomac.2022.09.213>
- Wang, H., Luo, W., Guo, R., Li, D., Xue B. (2022). Effective adsorption of Congo red dye by magnetic chitosan prepared by solvent-free ball milling. *Materials Chemistry and Physics*, 292, 126857. <https://doi.org/10.1016/j.matchemphys.2022.126857>
- Wong, S., Ghafar, N. A., Ngadi, N., Razmi, F. A., Inuwa, I. M., Mat, R., Amin, N. A. S. (2020). Effective removal of anionic textile dyes using adsorbent synthesized from coffee waste. *Scientific reports*, 10(1), 1-13. | <https://doi.org/10.1038/s41598-020-60021-6>
- Xu, K., Li, L., Huang, Z., Tian, Z., Li, H. (2022). Efficient adsorption of heavy metals from wastewater on nanocomposite beads prepared by chitosan and paper sludge. *Science of The Total Environment*, 846, 157399. <https://doi.org/10.1016/j.scitotenv.2022.157399>
- Yeo, J. Y. J., Khaerudini, D. S., Soetaredjo, F. E., Waworuntu, G. L., Ismadji, S., Putranto, A., Sunarso, J. (2023). Experimental and modelling study of adsorption isotherms of amoxicillin, ampicillin and doripenem on bentonite-chitosan composite. *South African Journal of Chemical Engineering*, 43, 38-45. <https://doi.org/10.1016/j.sajce.2022.09.013>
- Yun, J., Zhao, C., Li, X., Zhang, W., Liu, H., Liu, B. (2022). Rheological properties and early mechanical strength of oil-well cement modified by hybrid nano-silica and nano-hexagonal boron nitride. *Construction and Building Materials*, 356, 129291. <https://doi.org/10.1016/j.conbuildmat.2022.129291>
- Zaini, M. S. M., Arshad, M., Syed-Hassan, S. S. A. (2022). Adsorption Isotherm and Kinetic Study of Methane on Palm Kernel Shell-Derived Activated Carbon. *Journal of Bioresources and Bioproducts*, 8, 66-77. <https://doi.org/10.1016/j.jobab.2022.11.002>
- Zhao, S., Li, Y., Wang, M., Chen, B., Zhang, Y., Sun, Y., Chen, K., Du, Q., Wang, Y., Pi, X., Jing, Z., (2023). Efficient adsorption of Congo red by micro/nano MIL-88A (Fe, Al, Fe-Al)/chitosan composite sponge: Preparation, characterization, and adsorption mechanism. *International Journal of Biological Macromolecules*, 124157. <https://doi.org/10.1016/j.ijbiomac.2023.124157>
- Zhao, X., Wang, X., Lou, T. (2021). Preparation of fibrous chitosan/sodium alginate composite foams for the adsorption of cationic and anionic dyes. *Journal of Hazardous Materials*, 403, 124054. <https://doi.org/10.1016/j.jhazmat.2020.124054>

Automatic Detection of Water Surfaces Using K-means++ Clustering Algorithm with Landsat-9 and Sentinel-2 Images on the Google Earth Engine Platform

Osman Salih Yılmaz*¹

Abstract: Water is the most essential requirement for sustaining the life cycle on Earth. These resources are constantly dynamic due to anthropogenic and climatological effects. Therefore, management and consistent water policies are necessary to be followed for the proper management of water resources. Monitoring water resources is possible by accurately determining the water surface boundaries and determining the change in water surface areas. In this context, the normalized difference water index (NDWI) and modified normalized difference water index (MNDWI) were computed using JavaScript on the Google Earth Engine (GEE) through Landsat-9 and Sentinel-2 satellite images. Water pixels were extracted from other details using the K-means++ cluster algorithm based on the calculated indices. The water surfaces were determined using the Otsu thresholding method, which is the most preferred method for the NDWI and MNDWI indices calculated from the Sentinel images and was used as verification data. The K-means++ clustering algorithm yielded successful results in detecting water surfaces. In the two indices used, the NDWI index was found to be more successful than the MNDWI index. For Landsat-9 images, OA, Kappa, and F1-scores in the NDWI index were calculated as 99.72%, 0.994, and 99.57%, respectively. The overall accuracy (OA), Kappa, and F1-scores in the NDWI index for Sentinel-2 images were calculated as 99.39%, 0.986, and 99.04%, respectively. This study demonstrated that clustering algorithms can be successfully applied to automatically detect water surfaces.

Keywords: Remote sensing, Google Earth Engine, NDWI, MNDWI, K-means++, Terkos Lake.

¹**Address:** Manisa Celal Bayar University, Demirci Vocational School, 45900, Manisa, Türkiye.

***Corresponding author:** osmansalih.yilmaz@cbu.edu.tr

Citation: Yılmaz, O., S. (2023). Automatic detection of water surfaces using K-means++ clustering algorithm with Landsat-9 and Sentinel-2 images on the Google Earth Engine Platform. *Bilge International Journal of Science and Technology Research*, 7(2): 95-111.

1. INTRODUCTION

Detection of water surfaces is very important for hydrological processes and the ecosystem. It has become a necessity to monitor water resources that are under pressure due to climatic and anthropogenic effects (Hu et al., 2022). The extensive spread and continuous dynamics of surface waters make their monitoring difficult (Gao et al., 2012; Yılmaz et al., 2023). Nowadays, remote sensing (RS)-based approaches have been very practical in determining water surfaces (Khalid et al., 2021). Various spectral information recorded by satellites provides valuable information about the Earth's surface and water resources (Govender et al., 2007). Synthetic aperture radar (SAR), advanced very high-resolution radiometer (AVHRR), moderate resolution

imaging spectroradiometer (MODIS), and other optical image data are widely used for the detection of water surfaces. In recent years, the processing challenges associated with SAR images and the high cost of high-resolution optical imagery have made Landsat and Sentinel satellites unique resources for the detection and monitoring of surface waters, primarily due to their high temporal, spatial, and spectral resolutions (Cordeiro et al., 2021; Yılmaz et al., 2023). Furthermore, cloud computing systems have eliminated the data storage problem and facilitated the processing and storage of large volumes of satellite images, particularly in recent years. In this regard, Google Earth Engine (GEE), an RS platform, is very useful due to its simultaneous access to many free satellite platforms and its

ability to analyze large volumes of data (Nguyen et al., 2019; Pekel et al., 2016).

The physical properties of the environment surrounding water surfaces and the chemical properties of water cause changes in the electromagnetic spectrum (Elachi and Van Zyl, 2021). Therefore, various methods have been developed to extract water surfaces from other details. Supervised classification (Mahdianpari et al., 2017; Mansaray et al., 2019), unsupervised classification (Gao et al., 2012; S. Reis and Yilmaz, 2008; Zhang et al., 2018), spectral mixture analysis (SMA) (Feng et al., 2016), sub-pixel classification (Liu et al., 2020), water indices (Gao, 1996; Ji et al., 2009; McFeeters, 2013; Qiao et al., 2012; Yang et al., 2017), and clustering algorithms (Cordeiro et al., 2021) are the most commonly used radar and optical-based systems for detecting water surfaces. Each method used to determine water surfaces has its own advantages and disadvantages. Generally, classification techniques require user experience, but spectral indices are independent of user experience and can be used to differentiate water surfaces from other details. Various indices have been developed that aim to enhance water surfaces and suppress other details by utilizing the responses of bands to water and other details in the studies conducted.

The Normalized Difference Water Index (NDWI) suppresses terrestrial plant and soil properties while maximizing the reflection of water surface by using green and near-infrared (NIR) bands (McFeeters, 1996). In urban areas, the modified NDWI (MNDWI) has been proposed using the shortwave infrared (SWIR) band rather than the NIR band for calculating water surfaces (Xu, 2006). To minimize the mixing of water pixels with other pixels in shaded areas and shallow waters, the automatic water extraction indices (AWEI) has been proposed (Feyisa vd. 2014). The AWEI index is designed in two different forms: AWEI_{sh} for shaded areas and AWEI_{nsh} for non-shaded areas. In the resulting indices, each pixel has a gray value. Various thresholding methods are used to extract water surfaces from other details using these gray values. Some of these methods are manual thresholding, while others are automatic thresholding methods such as Otsu's and Canny edge detection (Donchyts et al., 2016; Gu et al., 2021; Rad et al., 2021).

There are various studies available for the detection of water surfaces. Tang et al. (2022) designed an adapted RF algorithm on the GEE platform using Landsat-7 (ETM+), Landsat-8 (OLI), and Sentinel-1 SAR images to detect water surfaces in the study area. The method achieved a water surface detection accuracy of 96.6% and a Kappa statistic of 0.931. Owusu (2022) developed the PyGEE-SWToolbox on the GEE platform and used Landsat, Sentinel-1, and Sentinel-2 images to detect water surfaces in Elephant Butte Lake, Hubbard Creek Reservoir, Clearwater Lake, and Neversink Reservoir in the United States. They utilized NDWI, MNDWI, AWEI, and dynamic surface water extend (DSWE) indices. The time series of water surface areas generated by PyGEE-SWToolbox yielded good results, with R² values ranging between 0.63 and 0.99 for Elephant Butte Lake, Hubbard Creek Reservoir, and Clearwater Lake, except for Neversink Reservoir, which had a maximum R² value of 0.52. Yilmaz (2023) examined the surface water

dynamics of lakes in the Lakes Region of Türkiye on the GEE platform from 1985 to 2022. Acigol, Aksehir, Beysehir, Burdur, Egirdir, Ilgin, Isikli, Karatas, Salda, and Yarisli lakes were analyzed using the NDWI index and the Otsu threshold method. Additionally, climate variables were used to analyze the changes in lake surfaces using the Mann-Kendall (MK) and Sen's slope statistical methods. The study found a decreasing trend in the surface areas of all lakes except Acigol. Cordeiro et al. (2021) proposed a machine learning approach for water extraction from a single image using optical high-resolution images that can be applied at a large scale. They utilized random subsampling and a Naïve Bayes classifier for generalization. Unlike other thresholding approaches that only use a single dimension, such as a water index, the proposed method aimed to analyze the applicability of combining different water indices and spectral bands within an unsupervised multidimensional hierarchical clustering. The study was conducted using Sentinel-2 images for 15 different water surfaces in France. They tested combinations of NDWI, MNDWI, Multi-band Water Index (MBWI), B8, and B12 bands and determined that the best two combinations were NDWI and B12. This study is highly valuable in terms of utilizing clustering algorithms for water surface detection. However, despite the various approaches used to identify water surfaces, studies related to clustering algorithms have not gained popularity (Cordeiro et al., 2021).

Therefore, the goal of this study is to detect water surfaces from water extraction indices calculated on optical images using a clustering algorithm instead of thresholding methods, which is different from other studies. For this purpose, NDWI and MNDWI were computed using Landsat-9 and Sentinel-2 images on the GEE platform. Water surfaces were determined using K-means++ clustering algorithm from the calculated NDWI and MNDWI indices. This study is quite valuable in understanding the success of clustering algorithms in determining water surfaces.

2. MATERIAL AND METHOD

2.1. Study Area

Terkos Lake, also called Duru Lake, is located within the boundaries of the Catalca district in the northern part of Istanbul. The lake, which has a coastline to the Black Sea, is situated between the Karaburun and Ormanlı regions (Bayram et al., 2013). Terkos Lake is approximately 40-50 km away from the city and has a surface area of approximately 25 km² (Kaya et al., 2019). With a water potential of 142,000,000 m³/year, Terkos Lake constitutes 30% of the freshwater reserves around Istanbul (Maktav et al., 2002). The location map of Terkos Lake, which is the subject of this study, is presented in Figure 1.

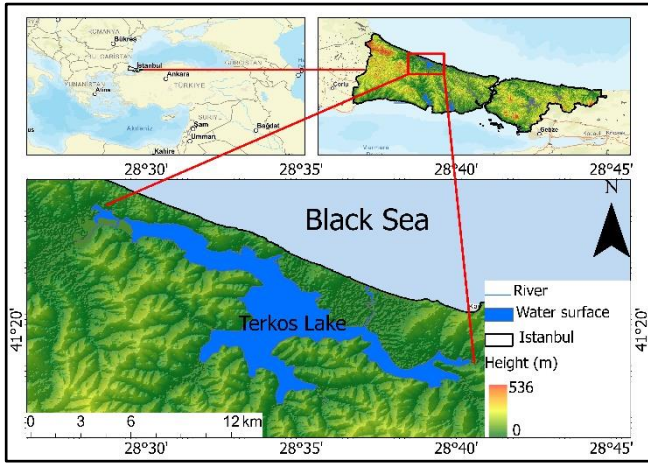


Figure 1. Study area

2.2. Data Used

In this study, images captured by Landsat-9's Operational Terrain Imager (OLI-2) and Sentinel-2's Multispectral Instrument (MSI) were used. Landsat-9 was jointly launched by the United States Geological Survey (USGS) and the National Aeronautics and Space Administration (NASA) on September 27, 2021, and operates at an altitude of 705 km. The satellite provides data with a spatial resolution of 30 m, a temporal resolution of 16 days, and a 14-bit radiometric resolution. The OLI-2 sensor captures multi-band images in the visible and mid-infrared wavelengths, and the Thermal Infrared Sensor (TIRS-2) spectrometer analyses ground temperatures. The satellite also improves its ability to detect changes in dark surfaces such as water and dense forests. (Bouslihim et al., 2022). In this study, Landsat-9 Collection 2 Tier 1 top-of-atmosphere (TOA) reflectance calibrated images were used in the GEE platform.

The Sentinel-2 satellites, which are a component of the European Commission's (EC) Copernicus program, consist of two groups, Sentinel-2A and Sentinel-2B. These satellites were launched on June 23, 2015, and March 7, 2017, respectively. They orbit at an altitude of roughly 786 km and provide a combined temporal resolution of 5 days. The MultiSpectral Instrument (MSI) has 13 spectral bands ranging from 10 to 60 m with a 12-bit radiometric resolution. In this research, Sentinel-2 level (L2A) images, which are calibrated for bottom-of-atmosphere (BOA) reflectance, were obtained from the GEE platform.

Spectral band information and resolutions of these images are given in Table 1.

Table 1. Features of Satellite Images (L9/S2A/S2B)

Spectral range	Wavelength	Spatial resolution
Blue (B2)	450-510/496.6/492.1	30/10
Green (B3)	530-590/560/559	30/10
Red (B4)	640-670/664.5/665	30/10
NIR (B5/B8)	850-880/835.1/833	30/10
SWIR-1 (B6/B11)	1,570-1,650/1,613.7/1,610.4	30/20
SWIR-2 (B7/B12)	2,110-2,290/2,202.4/2,185.7	30/20

2.3. Used Indices

The design of spectral water indices takes advantage of the ability of water to absorb energy in near-infrared (NIR) and shortwave infrared (SWIR) wavelengths. Spectral indices like NDWI and MNDWI enhance the contrast between water bodies and surrounding features, making them useful for mapping surface water using satellite imagery. These indices involve combining different spectral bands using mathematical operations, and a threshold value is applied to separate water from other features based on their spectral properties. MNDWI is especially effective at reducing noise from vegetation and soil, as well as in urban areas where there may be a lot of interference. In this study, NDWI and MNDWI indexes were computed using Equation 1 and 2 using Landsat and Sentinel images.

$$NDWI = (Green - NIR)/(Green + NIR) \tag{1}$$

$$MNDWI = (Green - SWIR1)/(Green + SWIR1) \tag{2}$$

where, the green band for Landsat-9 and Sentinel-2 images is represented by B3. The NIR band for Landsat-9 and Sentinel-2 is represented by B5 and B8, respectively. The SWIR band for Landsat-9 and Sentinel-2 is represented by B6 and B11, respectively.

2.4. K-means++ Clustering Algorithm

The k-means clustering algorithm was first suggested by MacQuen (1967) and developed by Lloyd (1982). The k-means clustering method presupposes knowledge of the number of clusters (k) and necessitates initial values for the cluster centers to be seeded to execute. The accuracy of the data assignment to clusters is heavily reliant on the initial seed values. In summary, k-means clustering is considerably influenced by the selection of initial seed values for cluster centers (Agarwal et al., 2012; Khan, 2012). The k-means++ algorithm evaluates the performance of the preliminary seed selection based on the sum of normalized squared differences between the data dimension and the cluster center for a cluster's members (Khan, 2012). In this study, the K-means++ algorithm running on the GEE platform was used (Arthur and Vassilvitskii, 2007). After several trials of different cluster numbers to extract water details via clustering, it was observed that the best result was obtained with three classes, and the cluster number was determined as three. One of the obtained three classes represents the water surface, while the others represent the non-water surface.

2.5. Accuracy Assessment

The accuracy of this study was evaluated using Overall Accuracy (OA), Kappa (κ) statistics, and F1-score. In this study, the Otsu's thresholding method was used to determine water surfaces for NDWI and MNDWI obtained from Sentinel-2 images, and this was used as the basis for evaluating the accuracy in this study (Figure.2). The Otsu thresholding method maximizes the intra-class variance in a bimodal histogram for any image and automatically extract water and non-water surfaces by determining an optimal threshold. This is a widely used technique. (Sekertekin,

2021). An error matrix has been created for accuracy evaluation by considering all pixels (933,337 pixels)

3. RESULTS

The accuracy assessment of the Landsat-9 (OLI-2) images used in the study is presented in Table 2 for the images obtained by NDWI, MNDWI, and the K-means++ clustering algorithm, while the images are shown in Figure 4. Overall, accuracy metrics were found to be above 90% based on the obtained using the K-means++ clustering algorithm for both the NDWI and MNDWI. Based on these results, it can be easily said that the K-means++ clustering algorithm utilized to both NDWI and MNDWI indices performed very successfully in extracting water surfaces. The maximum NDWI value obtained from the Landsat-9 image was calculated as 0.855 for water surfaces, while it was +1.000 for MNDWI. The K-means++ algorithm showed higher success in the NDWI image. The NDWI OA and F1-score were calculated as 99.72% and 99.57%, respectively, while these values were calculated as 97.37% and 95.87% in MNDWI. While the F1-score was 99.72% and 99.57%, respectively, these values were calculated as 97.37% and 95.87% in MNDWI.

Table 2. Accuracy assessment of the Landsat-9 (OLI-2) images

Indices	OA (%)	κ	F1-score (%)	Area (km ²)
NDWI	99.72	0.994	99.57	29.43
MNDWI	97.37	0.939	95.87	29.45

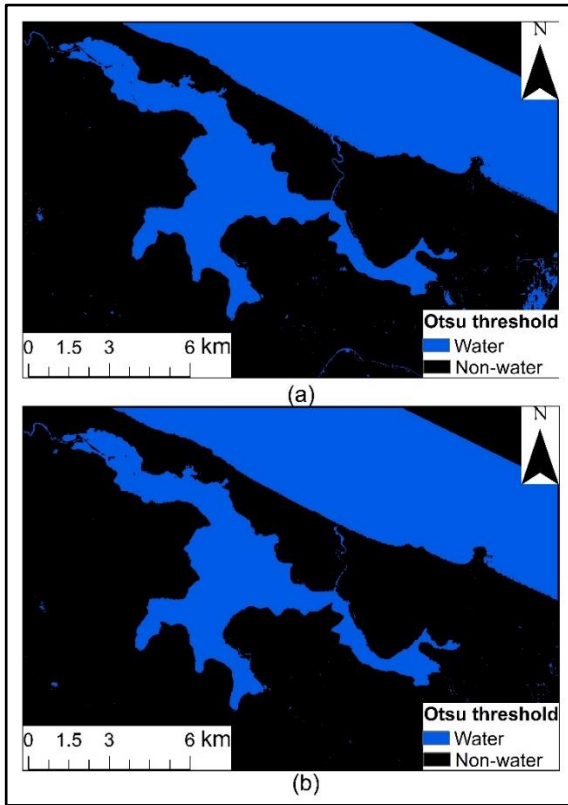


Figure 2. Water surfaces obtained using the Otsu threshold method: a) Sentinel-2 NDWI, b) Sentinel-2 MNDWI

The workflow of this study is shown in Figure 3.

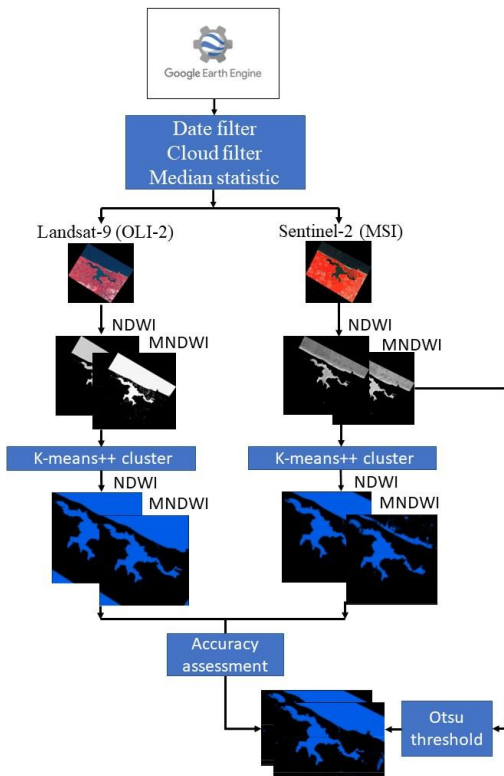


Figure 3. Workflow diagram

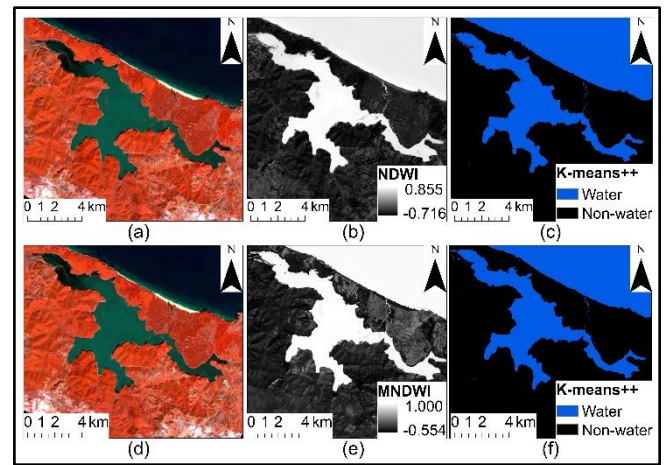


Figure 4. Landsat-9 images where NDWI and K-means++ algorithm were applied: a,d) Landsat-9 false color image, b) Landsat-9 NDWI, c) NDWI K-means++ cluster image, e) Landsat-9 MNDWI, f) MNDWI K-means++ cluster

Accuracy assessment of the Sentinel-2 (MSI) images used in the study is given in Table 3, and the images obtained with NDWI, MNDWI and K-means++ clustering algorithms are shown in Figure 5. The OA obtained with Sentinel-2 images is also calculated to be above 90%. This result shows that water surfaces were successfully detected using NDWI and MNDWI values calculated with Sentinel-2 images in a similar way. The maximum NDWI value obtained from the Sentinel-2 image was calculated as 0.767 for the water surface, while it was calculated as 0.802 for MNDWI. K-means++ algorithm also showed higher performance in the indices obtained from Sentinel-2 images. While the OA and

F1-score of NDWI were calculated as 99.39% and 99.04%, respectively, these values were calculated as 95.26% and 91.99% for MNDWI.

Table 3. Accuracy assessment of the Sentinel-2 (MSI) images

Indices	OA (%)	κ	F1-score (%)	Area (km ²)
NDWI	99.39	0.986	99.04	29.08
MNDWI	95.26	0.887	91.99	22.21

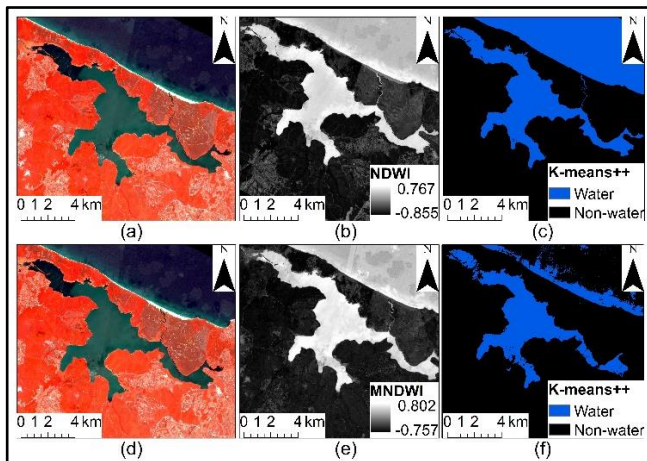


Figure 5. NDWI and K-means++ applied Sentinel-2 (MSI) images: a) Sentinel-2 false color image, b) Sentinel-2 NDWI, c) NDWI K-means++ cluster image, e) Sentinel-2 MNDWI, f) MNDWI K-means++ cluster

4. DISCUSSION AND CONCLUSIONS

Detecting, monitoring, and managing surface waters and water resources is a crucial task for water management. Remote sensing techniques are frequently preferred due to their effectiveness and cost-efficiency when compared to other methods. Recent advancements in satellite imagery, particularly in terms of temporal, spatial, and spectral resolutions, have further increased research in utilizing water surfaces for such tasks. As a result, various methods have been devised to identify water surfaces from satellite imagery.

In this study, water surfaces were extracted from other details using the K-means++ clustering algorithm based on NDWI and MNDWI indices using optical images on the GEE platform. Terkos Lake located within the boundaries of Istanbul province was selected for the study. In the accuracy assessment of the study, Sentinel images with higher resolution than Landsat images were used. Water surfaces were determined using the most preferred Otsu thresholding method for NDWI and MNDWI indices calculated from Sentinel images and used as verification data. The accuracy of the water surfaces obtained with the K-means++ method was evaluated by using all pixels for validation. When the results were evaluated, water surface accuracies obtained through clustering algorithms using both indices were quite successful with OA and F1-score values above 90%. In this study, it was observed that water surfaces obtained using

NDWI were more successful than water surface areas obtained using MNDWI. In many previous studies, many water extraction indices such as NDWI, MNDWI, AWEIsh, AWEInsh, NWI were used (Deng et al., 2020; Guo et al., 2017; Khalid et al., 2021; Rad et al., 2021; Sarp and Ozcelik, 2017; Sunder et al., 2017; Yue et al., 2020; Zhou et al., 2017). Similarly, automatic methods such as Otsu's threshold have been used to distinguish water and land in these indices (Babaei et al., 2021; Cordeiro et al., 2021; Guo et al., 2017; Rad et al., 2021; L. G. de M. Reis et al., 2021; Sekertekin, 2021). However, studies using clustering algorithms are very limited. In this study, water and land separation was easily accomplished using the K-means++ clustering method from NDWI and MNDWI water extraction indices used. Cordeiro et al. (2021) found that the use of clustering algorithms was quite successful in extracting water surfaces. They determined the κ value as 0.874 in their study. When compared with the κ values found in this study, it can be concluded that this study is successful.

This study is promising for automatically detecting water pixels on optical images without the need for auxiliary techniques or pre-trained data using clustering algorithms. However, more research is still needed to address misclassification issues in water surfaces such as clouds, snow, shadows, shallow waters, turbid waters, and green waters.

Ethics Committee Approval

N/A

Peer-review

Externally peer-reviewed.

Author Contributions

All process steps such as conceptualization, investigation, analysis, visualization, methodology and writing were written by Osman Salih Yılmaz. The author has read and agreed to the published version of manuscript.

Conflict of Interest

The authors have no conflicts of interest to declare.

Funding

The authors declared that this study has received no financial support.

REFERENCES

- Agarwal, S., Yadav, S., & Singh, K. (2012). Notice of Violation of IEEE Publication Principles: K-means versus k-means++ clustering technique. In 2012 Students Conference on Engineering and Systems, 1–6.
- Arthur, D., & Vassilvitskii, S. (2007). K-means++: The advantages of careful seeding In: Proceedings of the Eighteenth Annual ACM-SIAM Symposium on Discrete Algorithms. SODA'07, Society for Industrial and Applied Mathematics, 1027–1035, Philadelphia, PA, USA.
- Bayram, B., Seker, D. Z., Acar, U., Yuksel, Y., Guner, H. A. A., & Cetin, I. (2013). An integrated approach to

- temporal monitoring of the shoreline and basin of Terkos Lake. *Journal of Coastal Research*, 29(6), 1427–1435. <https://doi.org/10.2112/JCOASTRES-D-12-00084.1>
- Bouslihim, Y., Kharrou, M. H., Miftah, A., Attou, T., Bouchaou, L., & Chehbouni, A. (2022). Comparing Pan-sharpened Landsat-9 and Sentinel-2 for Land-Use Classification Using Machine Learning Classifiers. *Journal of Geovisualization and Spatial Analysis*, 6(2), 35.
- Cordeiro, M. C. R., Martinez, J. M., & Peña-Luque, S. (2021). Automatic water detection from multidimensional hierarchical clustering for Sentinel-2 images and a comparison with Level 2A processors. *Remote Sensing of Environment*, 253(November 2020). <https://doi.org/10.1016/j.rse.2020.112209>
- Donchyts, G., Schellekens, J., Winsemius, H., Eisemann, E., & van de Giesen, N. (2016). A 30 m resolution surfacewater mask including estimation of positional and thematic differences using landsat 8, SRTM and OPenStreetMap: A case study in the Murray-Darling basin, Australia. *Remote Sensing*, 8(5). <https://doi.org/10.3390/rs8050386>
- Elachi, C., & Van Zyl, J. J. (2021). *Introduction to the physics and techniques of remote sensing*. John Wiley & Sons.
- Feng, M., Sexton, J. O., Channan, S., & Townshend, J. R. (2016). A global, high-resolution (30-m) inland water body dataset for 2000: first results of a topographic–spectral classification algorithm. *International Journal of Digital Earth*, 9(2), 113–133. <https://doi.org/10.1080/17538947.2015.1026420>
- Feyisa, G. L., Meilby, H., Fensholt, R., & Proud, S. R. (2014). Automated Water Extraction Index: A new technique for surface water mapping using Landsat imagery. *Remote Sensing of Environment*, 140, 23–35. <https://doi.org/10.1016/j.rse.2013.08.029>
- Gao, B.-C. (1996). NDWI—A normalized difference water index for remote sensing of vegetation liquid water from space. *Remote Sensing of Environment*, 58(3), 257–266. [https://doi.org/10.1016/S0034-4257\(96\)00067-3](https://doi.org/10.1016/S0034-4257(96)00067-3)
- Gao, H., Birkett, C., & Lettenmaier, D. P. (2012). Global monitoring of large reservoir storage from satellite remote sensing. *Water Resources Research*, 48(9), 1–12. <https://doi.org/10.1029/2012WR012063>
- Govender, M., Chetty, K., & Bulcock, H. (2007). A review of hyperspectral remote sensing and its application in vegetation and water resource studies. *Water Sa*, 33(2), 145–151.
- Gu, Z., Zhang, Y., & Fan, H. (2021). Mapping inter- and intra-annual dynamics in water surface area of the Tonle Sap Lake with Landsat time-series and water level data. *Journal of Hydrology*, 601(July), 126644. <https://doi.org/10.1016/j.jhydrol.2021.126644>
- Hu, Q., Li, C., Wang, Z., Liu, Y., & Liu, W. (2022). Continuous Monitoring of the Surface Water Area in the Yellow River Basin during 1986–2019 Using Available Landsat Imagery and the Google Earth Engine. *ISPRS International Journal of Geo-Information*, 11(5), 305. <https://doi.org/10.3390/ijgi11050305>
- Ji, L., Zhang, L., & Wylie, B. (2009). Problems of Dynamic NDWI Threshold and Objectives of the Study The NDWI data derived from Landsat MSS, TM, and ETM (Jain et al. *Photogrammetric Engineering & Remote Sensing*, 75(11), 1307–1317. <https://doi.org/10.14358/PERS.75.11.1307>
- Kaya, H., Ertek, T. A., & Gazioğlu, C. (2019). Geomorphological Features of Terkos Lake and Surroundings. *International Journal of Environment and Geoinformatics (IJECEO)*, 6(2), 192–205. <https://doi.org/10.30897/ijegeo>
- Khalid, H. W., Khalil, R. M. Z., & Qureshi, M. A. (2021). Evaluating spectral indices for water bodies extraction in western Tibetan Plateau. *Egyptian Journal of Remote Sensing and Space Science*, 24(3), 619–634. <https://doi.org/10.1016/j.ejrs.2021.09.003>
- Khan, F. (2012). An initial seed selection algorithm for k-means clustering of georeferenced data to improve replicability of cluster assignments for mapping application. *Applied Soft Computing Journal*, 12(11), 3698–3700. <https://doi.org/10.1016/j.asoc.2012.07.021>
- Liu, C., Shi, J., Liu, X., Shi, Z., & Zhu, J. (2020). Subpixel mapping of surfacewater in the Tibetan Plateau with MODIS data. *Remote Sensing*, 12(7), 1–20. <https://doi.org/10.3390/rs12071154>
- Lloyd, S. (1982). Least squares quantization in PCM. *IEEE Transactions on Information Theory*, 28(2), 129–137.
- MacQueen, J. B. (1967). Some methods for classification and analysis of multivariate observation. *Proceedings of the 5th Berkley Symposium on Mathematical Statistics and Probability*, 281–297.
- Mahdianpari, M., Salehi, B., Mohammadimanesh, F., & Motagh, M. (2017). Random forest wetland classification using ALOS-2 L-band, RADARSAT-2 C-band, and TerraSAR-X imagery. *ISPRS Journal of Photogrammetry and Remote Sensing*, 130, 13–31. <https://doi.org/10.1016/j.isprsjprs.2017.05.010>
- Maktav, D., Sunar Erbek, F., & Kabdasli, S. (2002). Monitoring coastal erosion at the Black Sea coasts in Turkey using satellite data: A case study at the Lake Terkos, North-west Istanbul. *International Journal of Remote Sensing*, 23(19), 4115–4124. <https://doi.org/10.1080/01431160110115979>
- Mansaray, L. R., Wang, F., Huang, J., & Yang, L. (2019). Accuracies of support vector machine (SVM) and random forest (RF) in rice mapping with Sentinel-1A, Landsat-8 and Sentinel-2A datasets. *Geocarto International*, 0(0), 1–17. <https://doi.org/10.1080/10106049.2019.1568586>
- McFeeters. (1996). The use of the Normalized Difference Water Index. *International Journal of*

- Remote Sensing, 17(7), 1425–1432. <https://doi.org/10.1080/01431169608948714>
- McFeeters, S. K. (2013). Using the normalized difference water index (ndwi) within a geographic information system to detect swimming pools for mosquito abatement: A practical approach. *Remote Sensing*, 5(7), 3544–3561. <https://doi.org/10.3390/rs5073544>
- Nguyen, U. N. T., Pham, L. T. H., & Dang, T. D. (2019). An automatic water detection approach using Landsat 8 OLI and Google Earth Engine cloud computing to map lakes and reservoirs in New Zealand. *Environmental Monitoring and Assessment*, 191(4), 1–12. <https://doi.org/10.1007/s10661-019-7355-x>
- Owusu, C. (2022). PyGEE-SWToolbox : A Python Jupyter Notebook Toolbox for Interactive Surface Water Mapping and Analysis Using Google Earth Engine. *Sustainability*, 14, 2557.
- Pekel, J. F., Cottam, A., Gorelick, N., & Belward, A. S. (2016). High-resolution mapping of global surface water and its long-term changes. *Nature*, 540(7633), 418–422. <https://doi.org/10.1038/nature20584>
- Qiao, C., Luo, J., Sheng, Y., Shen, Z., Zhu, Z., & Ming, D. (2012). An Adaptive Water Extraction Method from Remote Sensing Image Based on NDWI. *Journal of the Indian Society of Remote Sensing*, 40(3), 421–433. <https://doi.org/10.1007/s12524-011-0162-7>
- Rad, A. M., Kreitler, J., & Sadegh, M. (2021). Augmented Normalized Difference Water Index for improved surface water monitoring. *Environmental Modelling and Software*, 140(March), 105030. <https://doi.org/10.1016/j.envsoft.2021.105030>
- Reis, S., & Yilmaz, H. M. (2008). Temporal monitoring of water level changes in Seyfe Lake using remote sensing. *Hydrological Processes*, 22(22), 4448–4454. <https://doi.org/10.1002/hyp.7047>
- Sekertekin, A. (2021). A Survey on Global Thresholding Methods for Mapping Open Water Body Using Sentinel-2 Satellite Imagery and Normalized Difference Water Index. *Archives of Computational Methods in Engineering*, 28(3), 1335–1347. <https://doi.org/10.1007/s11831-020-09416-2>
- Tang, H., Lu, S., Baig, M. H. A., Li, M., Fang, C., & Wang, Y. (2022). Large-Scale Surface Water Mapping Based on Landsat and Sentinel-1 Images. *Water (Switzerland)*, 14(9). <https://doi.org/10.3390/w14091454>
- Xu, H. (2006). Modification of normalised difference water index (NDWI) to enhance open water features in remotely sensed imagery. *International Journal of Remote Sensing*, 27(14), 3025–3033. <https://doi.org/10.1080/01431160600589179>
- Yang, X., Zhao, S., Qin, X., Zhao, N., & Liang, L. (2017). Mapping of urban surface water bodies from sentinel-2 MSI imagery at 10 m resolution via NDWI-based image sharpening. *Remote Sensing*, 9(6), 1–19. <https://doi.org/10.3390/rs9060596>
- Yilmaz, O. S. (2023). Spatiotemporal statistical analysis of water area changes with climatic variables using Google Earth Engine for Lakes Region in Türkiye. *Environmental Monitoring and Assessment*, 195(6), 735. <https://doi.org/10.1007/s10661-023-11327-1>
- Yilmaz, O. S., Gulgen, F., Balik Sanli, F., & Ates, A. M. (2023). The Performance Analysis of Different Water Indices and Algorithms Using Sentinel-2 and Landsat-8 Images in Determining Water Surface: Demirkopru Dam Case Study. *Arabian Journal for Science and Engineering*, 48, 7883–7903. <https://doi.org/10.1007/s13369-022-07583-x>
- Zhang, Y., Liu, X., Zhang, Y., Ling, X., & Huang, X. (2018). Automatic and unsupervised water body extraction based on spectral-spatial features using GF-1 satellite imagery. *IEEE Geoscience and Remote Sensing Letters*, 16(6), 927–931.

A Retrospective Study on Wild Animals Admitted to Animal Rescue and Rehabilitation Centres in Türkiye

Emrah Bozkaya^{1*}, Tamay Başağaç Gül²

Abstract: The main purpose of this study was to retrospectively reveal the rehabilitation numbers of wild animals admitted to rescue and rehabilitation centres in Türkiye between 2017 and 2021. It was also aimed to investigate the wild animals hospitalized in the centres under mammal, bird and reptile classes at the level of order and species, and to identify the deficiencies in wildlife rehabilitation and to make recommendations. The main material of the research was the data for the years 2017-2021 obtained from the Wildlife Information System-YABIS, a database of the Ministry of Agriculture and Forestry. As the method, numerical data on the species downloaded from YABIS were analysed. Accordingly, it was understood that a total of 35764 cases were admitted to all rescue centres across Türkiye. About 61% of these cases were treated and released into nature, about 34% died and about 5% were placed in zoos. While the Cetartiodactyla was the most affected order in mammals, the most admitted species in the centres was the Roe deer (*Capreolus capreolus*). In birds, the Columbiformes was the most affected order, the most admitted species in the centres was the Rock dove (*Columba livia*). In reptiles, the Testudinata was the most affected order, the most admitted species in the centres was the Mediterranean spur-thighed tortoise (*Testudo graeca*). The increase in the number of cases brought to rehabilitation centres between 2017-2021, excluding 2019, clearly showed the role of rescue and rehabilitation centres in protecting wild animals and providing sustainable wildlife.

Keywords: Rehabilitation, rescue centres, treatment, Türkiye, wild animal

¹**Address:** The Department of Veterinary History and Deontology, The Graduate School of Health Sciences, Ankara University, 06110, Ankara, Türkiye.

²**Address:** The Department of Veterinary History and Deontology, The Veterinary Faculty, Ankara University, 06110, Ankara, Türkiye.

***Corresponding author:** ebozkaya@ankara.edu.tr

Citation: Bozkaya, E., Başağaç Gül, R.T. (2023). A Retrospective Study on Wild Animals Admitted to Animal Rescue and Rehabilitation Centres in Türkiye. Bilge International Journal of Science and Technology Research, 7(2): 112-116.

1. INTRODUCTION

Wild animals, one of the main components of biodiversity, are at risk in many parts of the world due to threats such as the misuse of poison and illegal hunting, collisions with sheet glass and plastic in the form of windows and electricity power lines, a high density of human population, the impact of the exposure to roaming, stray and feral cats and dogs, climate change and wildfires, habitat fragmentation and loss (Van't Woudt, 1990; Elliott & Avery, 1991; Bevanger, 1998; Fahrig, 2003; Donazar et al., 2005; Klem, 2008; Sanderfoot et al., 2022). As in other countries, the biodiversity of Türkiye has been deteriorating due to rapid human population growth (about 2.5% per annum) and associated intensive or unwise use of natural resources and habitats (Kaya & Raynal, 2001). In this context, wildlife rehabilitation, which is defined as “the treatment and

temporary care of injured, diseased and displaced indigenous animals, and then the subsequent release of healthy animals to suitable habitats in the wild” (Miller, 2012), has become increasingly important.

Wild animal rehabilitation serves principal three main purposes. Firstly, it offers the opportunity to explore wildlife and surrounding more. Secondly, it might promote conservation efforts relating to endangered species. Finally, it provides the welfare requirements of an animal suffering from disease or injury or being orphaned (Vogelnest, 2008). So, the rescue and rehabilitation centres are key factors in the rehabilitation of wildlife for biodiversity conservation and whole ecosystem work.

Türkiye has been among the countries with rich biodiversity in the sense of the intersection of three phylogeographical

regions; Euro-Siberian, the Mediterranean, and Irano-Turanian (Davis et al., 1965). As it has important bird migration routes between the Middle East, Africa and Eastern Europe, and the richest flora among European and Near Eastern countries (Şekercioğlu et al., 2011; Eker et al., 2015), it has been like a small continent in terms of biodiversity (Kahraman et al., 2012). Considering the place of wild animals in this richness, animal rescue and rehabilitation centres were established for the care, treatment and rehabilitation of wild animals confiscated or delivered in accordance with international agreements and legal regulations to which Türkiye has been a party, or animals in need of care or treatment due to natural disasters, environmental problems and injuries. These facilities have been operated within the framework of protocols with the Ministry of Agriculture and Forestry, other public institutions and organizations, zoos or non-governmental organizations (Official Gazette of the Republic of Türkiye, 2004).

The main purpose of this study was to retrospectively present the rehabilitation numbers of wild animals admitted to rescue and rehabilitation centres in Türkiye between 2017 and 2021, to investigate the wild animals hospitalized in the centres under mammal, bird and reptile classes at the level of order and species, and to identify the deficiencies in wildlife rehabilitation and to make recommendations.

2. MATERIAL AND METHOD

The main material of the research was the data for the years 2017-2021 obtained from the Wildlife Information System-YABIS, a database of the Ministry of Agriculture and Forestry. YABIS includes data on the number of wild animals which are treated and released back to nature or placed into zoos, and the number of animals that died. Furthermore, it contains information on the species, dates and provinces where wild animals are rehabilitated. Official permission has been obtained from the Ministry of Agriculture and Forestry to use this data. In addition to YABIS data, previous literature related to the subject was also used.

In the first step, rehabilitation data from 2017 to 2021 were downloaded from the YABIS and species were classified as mammals, birds, and reptiles. Then, mammals, birds and reptiles were examined at the order level. The classification of the International Union for Conservation of Nature-IUCN² (IUCN, 2022) was taken as the basis while determining the orders to which the species belonged according to the taxonomic classification. Finally, the number of rehabilitated species under each order was determined for each year between 2017 and 2021.

3. RESULTS

The number of wild animal cases registered in YABIS (2017-2021) is given in Table 1. As seen in the Table, a total of 35764 cases of wild animals were admitted to all rescue centres across Türkiye.

Table 1. The number of wild animal cases registered in YABIS (2017-2021)

Year	Animals treated and released back to nature	Dead wild animals	Animals placed into zoos	Total
2017	976	553	172	1701
2018	3413	1643	315	5371
2019	2681	1780	194	4655
2020	6348	3149	399	9896
2021	8491	5024	626	14141
Total	21909	12149	1706	35764

A total number of 35764 registered to the database over five years were divided into 3 categories. The approximate percentage distribution of cases between 2017 and 2021 is given in Figure 1. As presented in the Figure, of 35764 total wild animal cases; 21909 wild animals were treated and released into nature, 12149 wild animals died and 1706 wild animals were placed into zoos.

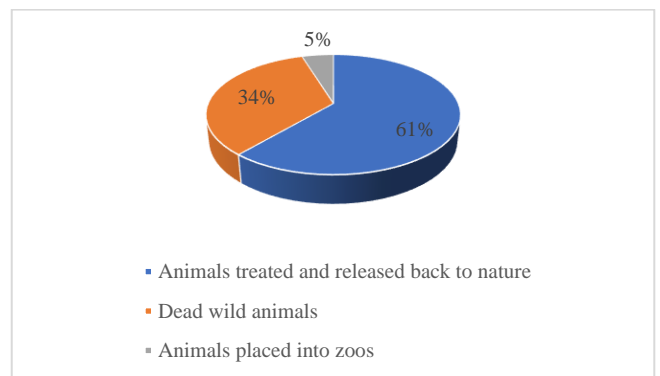


Figure 1. The approximate percentage distribution of wild animal cases between 2017 and 2021

When the total number of 35764 wild animals admitted to the animal rescue and rehabilitation centres from 2017 to 2021 was evaluated in terms of class, it was determined that 2535 of them were mammals, 32979 were birds and 250 were reptiles (Figure 2).

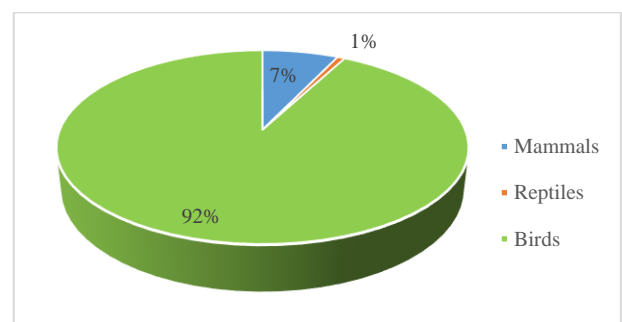


Figure 2. The percentage of taxonomic distribution of cases between 2017 and 2021

Among the taxa of mammals, the number of cases admitted to the centres is shown in Figure 3 in terms of order.

² The website of the IUCN Red List of Threatened Species was used for the taxonomic classification.

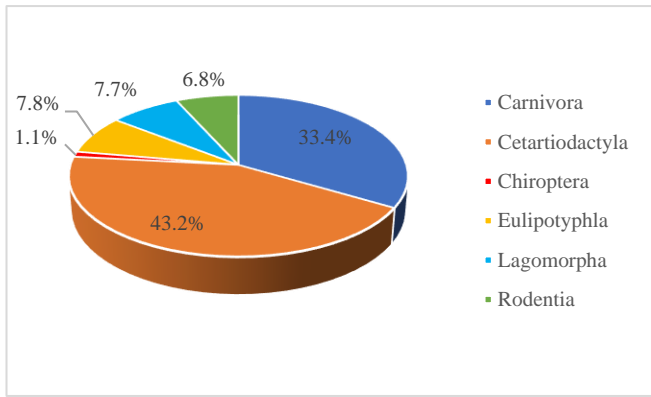


Figure 3. The number of mammal cases in terms of order between 2017 and 2021

Within mammals, Cetartiodactyla was the most affected order (43.2%), followed by Carnivora (33.4%), Eulipotyphla (7.8%), Lagomorpha (7.7%), Rodentia (6.8%) and Chiroptera (1.1%). The most frequently admitted two species to the centres were Roe deer (*Capreolus capreolus*) (47.1% of total mammals) and Red fox (*Vulpes vulpes*) (20.4% of total mammals).

Among the taxa of birds, the number of cases admitted to the centres is shown in Figure 4 in terms of order.

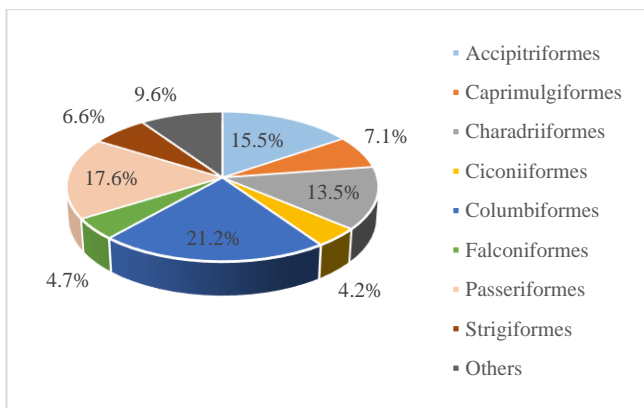


Figure 4. The number of bird cases in terms of order between 2017 and 2021

Within birds, Columbiformes was the most affected order (21.2%), followed by Passeriformes (17.6%), Accipitriformes (15.5%), Charadriiformes (13.5%), Caprimulgiformes (7.1%), Strigiformes (6.6%), Falconiformes (4.7%), Ciconiiformes (4.2%) and other least represented orders. The most frequently admitted five species to the centres were Rock dove (*Columba livia*) (14.29% of total birds), Yellow-legged gull (*Larus michahellis*) (7.94% of total birds), Common swift (*Apus apus*) (6.76% of total birds), Buzzard (*Buteo buteo*) (6.58% of total birds) and Long-legged buzzard (*Buteo rufinus*) (4.54% of total birds).

Among the taxa of reptiles, the number of cases admitted to the centres is shown in Figure 5 in terms of order.

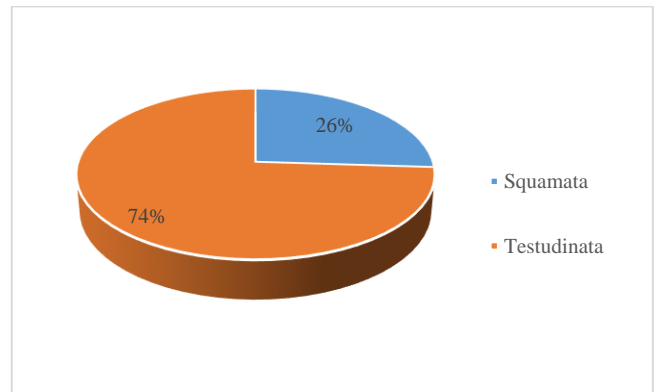


Figure 5. The number of reptile cases in terms of order between 2017 and 2021

Within reptiles, Testudinata was the most affected order (74%), followed by Squamata (26%). The most frequently admitted species to the centres was Mediterranean spur-thighed tortoise (*Testudo graeca*) (53.2% of total reptiles).

4. DISCUSSION and CONCLUSIONS

As of 2022, there were 11 animal rescue and rehabilitation centres in Türkiye, which were supported by the government and 7 of them were being operated by veterinary faculties within the scope of protocols with the Ministry of Agriculture and Forestry (Ministry of Agriculture and Forestry, 2022). In addition, other public institutions and organizations, zoos or non-governmental organizations also carry out rehabilitation activities within the scope of the protocol with the Ministry.

In this research, the increase in the number of cases admitted to rehabilitation centres between 2017 and 2021 by year, except for 2019, was clearly seen (Table 1). It is assumed that the reason for the decrease in the number of cases admitted to rehabilitation centres in 2019 was due to incomplete data entry into the database. The increase in the number of cases can be considered as one of the indicators of the increasing pressure on wildlife in Türkiye; however, it can be evaluated as a result of an increase in veterinary services regarding wild animals in recent years. Further studies are needed to definitively reveal the reason for this increase.

The total percentage entered to the database over five years was 61% in the category of “animals treated and released back to nature” (Figure 1). In a similar study conducted by Kandır and Aslan (2017), it was reported that the percentage of wild animals treated and released to nature in Türkiye between 2012 and 2015 was 50.18%. When the two researches are compared, the increase of approximately 10% in the releasing between 2017 and 2021 is clear evidence of Türkiye's success in treating wild animals and releasing them back to nature. However, the problems related to measuring the success of rehabilitated wild animals in Türkiye after they are released into the wild are one of the issues to be considered. In order to make sure that rehabilitated animals can survive in the wild and to evaluate the success of their post-release survival, they need to be tracked using methods such as radio-tracking, satellite tracking and bird-ringing (Grogan & Kelly, 2013). For this purpose, it is crucial to

systematically use satellite tracking tools in order to measure the survival success of the rehabilitated wild animals. There is no enough research indicating the success of post-release survival in Türkiye and it is important to encourage that kind of studies from the related institutions. Wildlife management should be connected with the four Rs: Rescue, rehabilitation, release, and research (Pyke & Szabo, 2018). Therefore, it should not be the sole purpose of treating and releasing wild animals into nature but monitoring and research should also be given importance to understand the biology of animals after release.

According to the cases admitted to the centres between 2017 and 2021, approximately 5% of wild animals had to be sent to zoos (Figure 1). Therefore, zoos can play an important role in terms of the keeping of the wild animals which they are unable to return to nature because of the health condition. Consequently, increasing the number of protocols on rehabilitation between veterinary faculties, NGOs, zoos and the Ministry will lead to a significant increase in the number of rehabilitated wild animals.

Considering the cases brought to the centres between 2017 and 2021, birds were the most affected taxonomic group, followed by mammals and fewer reptiles (Figure 2). A similar pattern was found in previous studies (Kandır & Aslan, 2017; Romero et al., 2019). The reason why birds were the most affected is because citizens may have encountered injured birds more frequently in urban areas.

Roe deer (*Capreolus capreolus*) and Rock dove (*Columba livia*) which were the most frequently admitted species to the centres within mammals and birds between 2017 and 2021 (Figure 3 and Figure 4) are listed according to IUCN data as Least Concern (LC) (Lovari, 2016; BirdLife International, 2019). Conversely, Mediterranean spur-thighed tortoise (*Testudo graeca*) which was the most frequently admitted species to the centres within reptiles between 2017 and 2021 (Figure 5) is listed according to IUCN data as Vulnerable (VU) (Tortoise & Freshwater Turtle Specialist Group, 1996).

Considering the limited financial resources and the shortage of trained manpower, the issue of rehabilitating non-endangered wild animals can be discussed as a separate ethical topic. However, it should be taken into account that according to Turkish regulation, every wild animal brought to rehabilitation centres must be treated, regardless of IUCN conservation status.

Besides, the domestication problem may occur as a result of the interaction of wild animals with humans during the rehabilitation process. Assessment of a rehabilitated wild animal's suitability for releasing should be carried out as soon as the treatment procedure is completed (Hall & Zoo, 2005). Therefore once animals have completed their treatment, they should be quickly released back into the environment from which they were rescued. When rehabilitated animals are released into the natural environment, the guide prepared by Species Survival Commission- SSC should be consulted (IUCN/SSC, 2013).

Orphaned wild animals found in nature and brought to the centres by the citizens for treatment are also an important

problem in Türkiye (Coşkun, 2020; Kandır & Tuğrul, 2020). Off-springs are unnecessarily taken from nature by sensitive citizens who think that animals need help. Hence, education and public awareness studies on people about what to do when they see a wild animal in nature should be enhanced by government and related NGOs.

The aim of this research was to form an insight on the rehabilitation of wild animals in Türkiye. In addition to this research, it is deemed necessary to carry out further studies on threat factors that affect wild animals over whole country. Consequently, wild animal rescue and rehabilitation centres can be seen as an indicator in point of detecting of unfavourable effects on nature stemmed from anthropogenic impacts and ecological changes. The rescue and rehabilitation centres play a key role in the protection of wild animals, which are an element of biological diversity, thus helping to ensure a sustainable wildlife. As a consequence, it is considered essential to increase the number of animal rescue and rehabilitation centres in Türkiye.

Acknowledgements

We would like to extend our sincere thanks to the Ministry of Agriculture and Forestry for providing the data for this research.

Ethics Committee Approval

N/A

Peer-review

Externally peer-reviewed.

Author Contributions

Conceptualization: E.B, R.T.B.G.; Investigation: E.B, R.T.B.G.; Material and Methodology: E.B, R.T.B.G.; Supervision: R.T.B.G.; Visualization: E.B.; Writing-Original Draft: E.B; Writing-review & Editing: R.T.B.G.; Other: All authors have read and agreed to the published version of manuscript.

Conflict of Interest

The authors have no conflicts of interest to declare.

Funding

The authors declared that this study has received no financial support.

REFERENCES

- Bevanger, K. (1998). Biological and conservation aspects of bird mortality caused by electricity power lines: a review. *Biological Conservation*, 86, 67-76.
- BirdLife International. (2019). *Columba livia* (amended version of 2016 assessment). The IUCN Red List of Threatened Species 2019: e.T22690066A155493121. <https://www.iucnredlist.org/species/22690066/155493121>
- Coşkun, G. (2020). Yardıma Muhtaç Yaban Hayvanlarının Rehabilitasyonu ve Doğaya Salınması: Antalya Örneği [Yüksek Lisans Tezi, Akdeniz Üniversitesi]. 2020.

- Davis, P. H., Cullen, J., & Coode, M. J. E. (Eds.). (1965). *Flora of Turkey and the East Aegean Islands* (Vol. 1).
- Donazar, J. A., Gangoso, L., Forero, M. G., & J., J. (2005). Presence, richness and extinction of birds of prey in the Mediterranean and Macaronesian islands. *Journal of Biogeography* 32, 1701- 1713.
- Eker, İ., Vural, M., & Aslan, S. (2015). Ankara İli'nin Damarlı bitki çeşitliliği ve korumada öncelikli taksonları [Research Article]. *Bağbahçe Bilim Dergisi*, 2(3), 57-114. <https://doi.org/https://dergipark.org.tr/tr/pub/bagbahce/issue/53948/727582>
- Elliott, G., & Avery, M. (1991). A review of reports of buzzard persecution 1975–1989. *Bird Study*, 38(1), 52-56.
- Fahrig, L. (2003). Effects of Habitat Fragmentation on Biodiversity. *Annual Review of Ecology, Evolution, and Systematics*, 34, 487-515.
- Grogan, A., & Kelly, A. (2013). A review of RSPCA research into wildlife rehabilitation. *Veterinary Record*, 172(8), 211-211.
- Hall, E., & Zoo, T. (2005). Release Considerations for Rehabilitated Wildlife National Wildlife Rehabilitation Conference,
- IUCN. (2022). The IUCN Red List of Threatened Species. Retrieved 18 Nisan from <https://www.iucnredlist.org/search>
- IUCN/SSC. (2013). Guidelines for Reintroductions and Other Conservation Translocations. Retrieved 14.12.2022 from <https://portals.iucn.org/library/efiles/documents/2013-009.pdf>
- Kahraman, A., Onder, M., & Ceyhan, E. (2012). The importance of bioconservation and biodiversity in Turkey. *International Journal of Bioscience, Biochemistry and Bioinformatics*, 2(2), 95-99.
- Kandır, E., & Aslan, A. (2017). An investigation on releasing treated wild animals into the nature in Turkey. *Applied Ecology and Environmental Research*, 15(4), 1757-1763.
- Kandır, E. H., & Tuğrul, G. (2020). A retrospective study on wild orphan animals in Afyon Kocatepe University wildlife rescue rehabilitation, training, practice and research center (AKUREM). *Kocatepe Veterinary Journal*, 13(3), 272-280.
- Kaya, Z., & Raynal, D. J. (2001). Biodiversity and conservation of Turkish forests. *Biological Conservation*, 97(2), 131-141.
- Klem, D. (2008). Avian Mortly at Windows: The Second Largest Human Source of Bird Mortality on Earth. *Proceedings of the Fourth International Partners in Flight Conference: Tundra to Tropics*,
- Lovari, S., Herrero, J., Masseti, M., Ambarli, H., Lorenzini, R. & Giannatos, G. (2016). *Capreolus capreolus*. The IUCN Red List of Threatened Species 2016: e.T42395A22161386. <https://www.iucnredlist.org/species/42395/22161386>
- Miller, E. A. (Ed.). (2012). *Minimum standards for wildlife rehabilitation* (4th edition ed.). National Wildlife Rehabilitators Association.
- Ministry of Agriculture and Forestry. (2022). 7 Bin 784 Yaban Hayvanı Tedavi Edilerek Doğaya Bırakıldı. <https://www.tarimorman.gov.tr/Haber/5454/7-Bin-784-Yaban-Hayvani-Tedavi-Edilerek-Dogaya-Birakildi>
- Official Gazette of the Republic of Türkiye. (2004). Regulation on the Establishment, Management and Inspection of Game and Wild Animal Breeding Sites and Stations and Rescue Centers. <https://mevzuat.gov.tr/mevzuat?MevzuatNo=7209&MevzuatTur=7&MevzuatTertip=5>
- Pyke, G. H., & Szabo, J. K. (2018). Conservation and the 4 Rs, which are rescue, rehabilitation, release, and research. *Conservation Biology*, 32(1), 50-59.
- Romero, F., Espinoza, A., Sallaberry-Pincheira, N., & Napolitano, C. (2019). A five-year retrospective study on patterns of casuistry and insights on the current status of wildlife rescue and rehabilitation centers in Chile. *Revista chilena de historia natural*, 92(1), 1-10.
- Sanderfoot, O., Bassing, S., Brusa, J., Emmet, R., Gillman, S., Swift, K., & Gardner, B. (2022). A review of the effects of wildfire smoke on the health and behavior of wildlife. *Environmental Research Letters*, 16(12), 123003.
- Şekercioğlu, Ç. H., Anderson, S., Akçay, E., Bilgin, R., Can, Ö. E., Semiz, G., Tavşanoğlu, Ç., Yokeş, M. B., Soyumert, A., & Ipekdal, K. (2011). Turkey's globally important biodiversity in crisis. *Biological Conservation*, 144(12), 2752-2769.
- Tortoise & Freshwater Turtle Specialist Group. (1996). *Testudo graeca*. The IUCN Red List of Threatened Species 1996: e.T21646A9305693. <https://www.iucnredlist.org/species/21646/9305693>
- Van't Woudt, B. D. (1990). Roaming, stray, and feral domestic cats and dogs as wildlife problems. *Proceedings of the Vertebrate Pest Conference*,
- Vogelnest, L. (2008). Veterinary considerations for the rescue, treatment, rehabilitation and release of wildlife. *Medicine of Australian mammals*, 1-12.

Use of Spinning Roller in Cylindrical Densification; Spring back in Black Poplar, Larch and Cedar of Lebanon after Densification

Zafer Kaya^{1*}, Sait Dündar Sofuoğlu²

Abstract: Wood materials have been the solution to many needs throughout history due to their unique positive properties. By improving the properties of wood materials, their areas of use can be expanded and ensured that they are preferred. The densification process is one of the studies carried out to improve wood material properties. With densification, the physical and mechanical properties of the wood material can be improved. There are many different methods used for densifying wood materials. While the densification process brings many positive properties to the wood material, an undesirable situation such as spring-back after the process is the negative side of the densification process. In this study, black poplar (*Populus nigra* L.), larch (*Pinus nigra* Arnold) and cedar of Lebanon (*Cedrus libani* A.Rich.) trees were shaped into cylinders on a lathe. After that, densification processes were carried out on the lathe machine using the spinning roller designed and manufactured for this purpose. Densification processes were carried out at 0.081, 0.121, and 0.202 mm/rev feed, at 200 and 400 rev/min, and 0.5 and 1 mm densification depths. The spring-back rates after densification in three different types of cylindrical wood materials were investigated. Theoretical and experimental spring-back amounts of test specimens whose surfaces were densified under different densification conditions were interpreted. When evaluated in general, the highest densification rate was obtained in black poplar wood species, 0.081 mm/rotate feed, 200 rpm spindle speed and 1 mm depth of densification. The lowest spring-back ratio was obtained in larch wood species, 0.121 mm/rotate feed, 400 rpm spindle speed and 1 mm depth of densification. The highest densification percentage was obtained in black poplar wood species, and the lowest in larch wood species. The lowest percentage of spring-back was obtained in the larch wood species and the highest in the black poplar wood species.

Keywords: Cedar, densification, larch, poplar, spinning roller, spring back

¹**Address:** Kutahya Dumlupinar University, Simav Vocational School, Kutahya/Türkiye

²**Address:** Kutahya Dumlupinar University, Simav Technology Faculty, Wood Works
Industrial Engineering Kutahya/Türkiye

***Corresponding author:** zafer.kaya@dpu.edu.tr

Citation: Kaya, Z., Sofuoğlu, S.D. (2023). Use of spinning roller in cylindrical densification; Spring back in black poplar, larch and cedar of Lebanon after densification. Bilge International Journal of Science and Technology Research, 7(2): 117-127.

1. INTRODUCTION

Wood material has been used in many areas throughout history to meet human needs. Today, with the rapid increase in population, wood material, which is one of the natural resources, has started to be insufficient. This situation reveals the need to use the resources available more efficiently.

Numerous studies aim to use wood material efficiently, minimise its negative aspects, and further develop its positive properties. Densification, which is one of the processes for these purposes, is generally applied to low-

density wood species. Densification using temperature and pressure in an open system known as Thermo-Mechanical (TM) and densification using temperature, pressure and steam in a closed system called Thermo-Hygro-Mechanical (THM). In addition, there is densification made by temperature and pressure after pre-softening with steam, called Viscoelastic-Thermal-Compression (VTC) (Senol and Budakci, 2019; Kaya and Sofuoğlu, 2023). And there are also methods, such as densification using temperature, pressure and vibration, called Thermo-Vibro-Mechanical (TVM) By densification, dimensional stability, hygroscopicity, durability and mechanical properties improve

(Welzbacher et al., 2008). On the other hand, it is stated that the densified wood material has a more homogeneous structure depending on the densification ratio (applied pressure) (Blomberg, et al., 2005).

Since the densification of wood material increases its mechanical properties and hardness, many attempts have been made to develop a suitable process in this regard. In the process of densification with compression of the wood material, the cell wall of the material collapses and the void volume is reduced (Kutnar et al., 2009; Pelit, 2014; Pelit and Sonmez, 2015, Sofuoglu, 2022; Sofuoglu et al., 2023; Tosun and Sofuoglu, 2021; Tosun and Sofuoglu, 2023a; Tosun and Sofuoglu, 2023b). Using wood material by increasing density can be an option compared to other materials (Blomberg and Persson, 2004; Pelit et al., 2014).

The density of wood material is mechanical (Rautkari, 2012) and machining (Lin et al., 2006; Malkocoglu, 2007; Malkocoglu and Ozdemir, 2006; Pinkowski et al., 2018; Sofuoglu et al., 2023; Zhong et al., 2013) significantly affect its properties. When examined in general, hardness, mechanical and physical properties increase, surface roughness and wettability decrease and occurrence of spring back as a negative situation may be seen, contingent on the increase in density in compressed densified wood species. In addition, another disadvantage caused by the densification process in the wood material is that deformations such as cracking, fracture, and breaking can occur in the cell wall of the densified wood material under normal atmospheric conditions (Rautkari et al., 2010).

The biggest problem encountered in densified wood materials is that they tend to return to their initial dimensions due to the spring-back feature that occurs immediately after densification. This situation occurs more when the wood material is used in places where it may be exposed to moisture or contact with water (Pelit, 2014). There are many studies to eliminate or minimize the spring-back, which is one of the negative aspects of the surface densification process. In some of these studies, the effect of additional methods applied before and after densification on spring-back was investigated. One of these methods is heat treatment (Skyba et al., 2009; Tenorio et al. 2021; Li et al., 2013; Fu et al., 2016; Laine et al., 2016; Esteves et al., 2017). It is known that the spring-back is also eliminated by the effect of temperature and steam (Kunar and Sernek, 2007; Pelit, 2014; Rautkari et al., 2010; Li et al., 2017). Heat treatment applied after the densification is more effective in reducing spring-back recovery than before (Esteves et al., 2017). Heat treatment reduces spring-back and improves wood stability and durability (Esteves and Pereira, 2009). However, most had less success in reducing spring-back in the densified wood. Previous work dealing with the combined-hydrothermo-mechanical treatment showed great reduction in the densified poplar wood spring-back (Hajhassani et al., 2018).

In other studies, wood veneers under the effect of heat, steam and pressure after recovery (Cloutier et al., 2008; Fang et al., 2012), effect of ionic liquid or organic superbase pre-treatment on the elastic spring-back and Brinell hardness of surface-densified wood (Neyses et al., 2020), Examined that reducing the spring-back of surface densified solid Scots pine wood by hydrothermal post-treatment (Laine et al., 2013). When wood is re-moisture, the spring-back is one of the main problems of compressed wood. These authors proposed three mechanisms to avoid spring-back. Prevent the wood from being re-softened by changing the hygroscopicity of the cell, form covalent crosslinks between the wood components in the deformed state or release the elastic stresses and strains created during compression (Esteves et al., 2017). The spring-back effect, which is one of the main problems associated with the densification process, can be eliminated by steaming or heating, which can induce permanent fixation of the compressive deformation (Kutnar and Sernek, 2007). As the densification temperature and heat treatment temperature increase, the spring-back decreases. The densification time has little or no effect on the spring-back (Li et al., 2013). Another study examined densified wood impregnated with phenol resin for reduced spring-back (Schwarzkopf, 2021).

Some studies on the subject have shown that due to their dimensional stability and high density, densified wood veneers treated by the oil-heat treatment process show good potential for appearance products (Fang et al., 2011). The spring-back of densified samples was further significantly decreased following surface polymerization with glycerol and maleic anhydride (68% lower than the non-polymerized ones) (Yahyaee et al., 2022). Impregnation with phenol resin can significantly reduce the spring-back of compressed deformation. According to the results of the study with the Continuous Surface Densification of Wood method; spring-back of the densified cells occurred after the soaking-drying cycles but was considerably lower than in the other densification studies performed under static conditions. It was suggested that the lowered spring-back was a consequence of the specific process conditions, i.e., a combination of pre-wetting by spraying water onto the surface and a long pre-heating period before the compressive force was applied.

After densification, it is possible to talk about two types of spring-back. The first of these is sudden spring-back, which is triggered by the release of internal stresses that occur in the material when the press table is opened. The other is the air-dry spring-back that occurs when the material reaches a constant weight at 20°C and 65% relative humidity.

The literature shows that; The spring-back effect in densified wood materials and coatings was investigated and evaluated in press-compressed materials. Studies have been carried out to reduce this effect. However, no case determination was found regarding the spring-back effect in the densification processes applied to cylindrical materials.

This study, it is aimed to expand the usage area of wood material in the woodworking and furniture industry. Densification processes contribute to this situation. However, with the method used in the study, the spring-back effect is not known in cylindrical densified materials.

With this study, the densification process was performed using a new method. It is planned to determine the spring-back condition, which can be seen as a measure of the success of the densification of cylindrical materials. With the determination of this situation, the ground will be prepared for the studies that can be done to prevent the spring-back condition.

2. MATERIAL AND METHOD

In the present experiments, black poplar (*Populus nigra* L.), larch (*Pinus nigra* Arnold) and cedar of Lebanon (*Cedrus libani* A.Rich.) wood species were used. Wood species commonly used and grown in Turkey. Conditioning of samples was carried out at temperatures of 20 ± 2 °C and 65 ± 5 °C, with relative humidity to moisture content (MC) of about 12%. The density of wood species at 12% humidity was specified as poplar 340 kg/m^3 , larch 650 kg/m^3 , cedar of Lebanon 500 kg/m^3 (ISO 13061 2014; ISO 13061-2 2014).

The test specimens were first cut in $2 \times 2 \times 30$ cm dimensions. After this process, the test specimens were cylindrical on the lathe machine until their average diameter was 1.9 cm. By using a grooving insert, 5 sections of equal length were formed on the test specimens with an average diameter of 1.9 cm. 3 of these sections are used for the implementation of the experimental parameters and 2 are the control sections (Figure 1).

The prepared test specimens were kept in an air-conditioned cabinet at 20 ± 2 °C and $65 \pm 5\%$ relative humidity until their weight was stable. The aim here is to ensure that the moisture content reaches $12 \pm 2\%$ before densification (Figure 2). The densification parameters and levels used in the experiments were determined as in Table 1 and experiments were conducted.

The experimental application of the study (Schematic representation for surface densification process) is given in Figure 3. Figure 4 shows the measurement of specimens with a caliper before and after densification.

Table 1. Assignment of levels to factors (parameters used in the densification of black poplar, larch, and cedar of Lebanon)

Parameters	Level 1	Level 2	Level 3
Wood species	Black poplar	Larch	Cedar of Lebanon
Feed (mm/rotate)	0.081	0.121	0.202
Spindle speed (rpm)	200	400	
Depth of dens. (mm)	0.5	1	



Figure 1. Test specimens before densification



Figure 2. The position of the experimental specimens in the air-conditioned cabinet

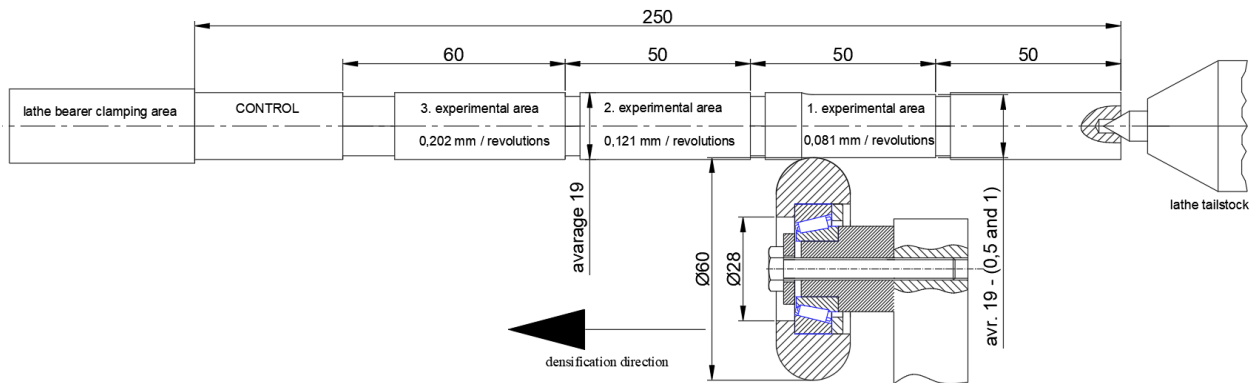


Figure 3. Schematic representation for surface densification process



Figure 4. Measurement of test specimens' diameters with the caliper.

The spinning roller, designed and manufactured for the densification process, is formed by bringing together seven pieces. The material of the main roller element, which performs the press function from these parts, is steel in DIN EN AISI 1.0402 C22 – 1020 standard. After this part is brought to its final shape by a turning machine, it was hardened by heat treatment. This part is supported by a tapered roller bearing perpendicular to the turning axis of the wood material to be densified and capable of meeting the forces that will occur in the direction of the densification axis. The standard number of this bearing is 302/30202-A. The other parts in the assembly set and the prismatic part connected to the tool post of the lathe was produced by using non-hardened steel materials in DIN EN AISI 1.0402 C22-1020 standard. The M6 bolt that connects the parts is supplied as standard. This assembled set was used for densification operations by connecting to the tool post on the lathe (Figure 5).



Figure 5. Densification of cylindrical parts with a spinning roller.

Densification processes were carried out on the TOS GALANTA SUIL 40A lathe seen in Figure 6. This lathe is in Kütahya Dumlupınar University, Simav Technology Faculty, Mechanical Engineering Department Laboratories.



Figure 6. TOS GALANTA SUIL 40A lathe.

Determining Compression Ratio

The density of wood materials is important because it directly affects their mechanical properties. The material densities obtained after the densification process are directly proportional to the compression ratio. The main item examined in this study is the detection of

instantaneous spring-back due to densification processes.

First of all, the necessary environmental conditions were created for all test samples to be at 12% humidity before and during the densification process. For this, the test specimens, which were kept in the climatized cabinet until they reached a constant weight at 20 °C and 65% relative humidity, were subjected to the densification process as soon as they were received from the climatized cabinet. Just before starting the densification process, the initial diameters (*tk*) of cylindrical wood materials were measured from 4 different points using a digital caliper with ±0.01 mm precision, and the arithmetic average of the measured diameters was taken. After the densification process, the diameters of the densified sections (*tilk*) were measured from 4 different points using the same digital caliper and the arithmetic average of these diameters was taken. While densifying the cylindrical wood material, two different diameter reductions, 0.5 mm, and 1 mm were aimed as test parameters. To observe the achievability of these aims, the theoretical % compression ratios were calculated for 0.5 mm in equation 1 (*Teo.SO_{0.5}* (%)), and for 1 mm diameter reduction in equation 2 (*Teo.SO₁* (%)). In Equation 3, experimental % compression ratios were calculated depending on the diameter changes before and after densification. The difference between the

theoretical and experimental % compression ratios is the % spring-back amount calculated using equation 4.

$$Teo.SO_{0.5} (\%) = \frac{(tk - (tk - 0.5))}{(tk - 0.5)} \times 100 \tag{1}$$

$$Teo.SO_1 (\%) = \frac{(tk - (tk - 1))}{(tk - 1)} \times 100 \tag{2}$$

$$Exp.SO (\%) = \frac{(tk - tilk)}{tilk} \times 100 \tag{3}$$

$$Spring - back_{0.5} (\%) = Exp.SO (\%) - Teo.SO_{0.5} (\%) \tag{4}$$

Spring - back₁ (%) = Exp.SO (%) - Teo.SO₁ (%)
Teo.SO_{0.5} (%); theoretical % compression ratios for 0.5 mm, *tk*; initial diameter of test specimen, 0.5 mm and 1 mm; test parameters, *Teo.SO₁* (%); theoretical % compression ratios for 1 mm, *Exp.SO* (%); experimental % compression ratios in every test condition, *tilk*; diameters obtained as a result of experiments, Spring - back_{0.5} (%) and Spring - back₁ (%); Spring-back percentages for 0.5 mm and 0.1 mm.

3. RESULTS AND DISCUSSION

Theoretical (targeted) densification under densification conditions, densification, and spring-back percentages obtained at the end of the test results are given in Table 2.

Table 2. Theoretical densification, experimental densification and spring-back percentages obtained according to densification conditions.

Material	Process N.	Feed (mm/rotate)	Feed (mm/min)	Spindle speed (rpm)	Dept. of dens. (mm)	Theoretical compression ratio (%)	Experimental compression ratio (%)	Spring-back (%)
Black poplar	1	0.081	16.2	200	0.5	2.85	1.75	-1.10
	2	0.081	16.2	200	1	5.63	2.79	-2.84
	3	0.081	32.4	400	0.5	2.78	0.84	-1.94
	4	0.081	32.4	400	1	5.57	2.67	-2.90
	5	0.121	24.2	200	0.5	2.85	1.63	-1.22
	6	0.121	24.2	200	1	5.63	2.29	-3.34
	7	0.121	48.4	400	0.5	2.78	0.67	-2.11
	8	0.121	48.4	400	1	5.57	2.30	-3.27
	9	0.202	40.4	200	0.5	2.85	1.92	-0.93
	10	0.202	40.4	200	1	5.63	2.27	-3.36
	11	0.202	80.8	400	0.5	2.78	0.84	-1.94
	12	0.202	80.8	400	1	5.57	2.62	-2.96
Larch	1	0.081	16.2	200	0.5	2.88	0.81	-2.07
	2	0.081	16.2	200	1	5.75	1.66	-4.09
	3	0.081	32.4	400	0.5	2.86	0.24	-2.62
	4	0.081	32.4	400	1	5.99	1.01	-4.98
	5	0.121	24.2	200	0.5	2.88	0.88	-1.99
	6	0.121	24.2	200	1	5.75	1.57	-4.19
	7	0.121	48.4	400	0.5	2.86	0.20	-2.66

Cedar of Lebanon	8	0.121	48.4	400	1	5.99	0.89	-5.10
	9	0.202	40.4	200	0.5	2.88	1.02	-1.86
	10	0.202	40.4	200	1	5.75	1.68	-4.07
	11	0.202	80.8	400	0.5	2.86	0.86	-2.00
	12	0.202	80.8	400	1	5.98	1.00	-4.98
	1	0.081	16.2	200	0.5	2.71	1.43	-1.28
	2	0.081	16.2	200	1	6.38	1.65	-4.74
	3	0.081	32.4	400	0.5	2.73	1.18	-1.55
	4	0.081	32.4	400	1	5.61	2.65	-2.96
	5	0.121	24.2	200	0.5	2.71	1.16	-1.55
	6	0.121	24.2	200	1	6.38	1.21	-5.17
	7	0.121	48.4	400	0.5	2.73	0.89	-1.84
8	0.121	48.4	400	1	5.61	1.67	-3.94	
9	0.202	40.4	200	0.5	2.71	1.14	-1.57	
10	0.202	40.4	200	1	6.38	1.21	-5.17	
11	0.202	80.8	400	0.5	2.73	0.98	-1.75	
12	0.202	80.8	400	1	5.61	1.58	-4.03	

Experimental and theoretical % compression ratios according to the densification processes for Figure 7 poplar wood type, Figure 8 larch wood type, and Figure 9 cedar wood type are given graphically.

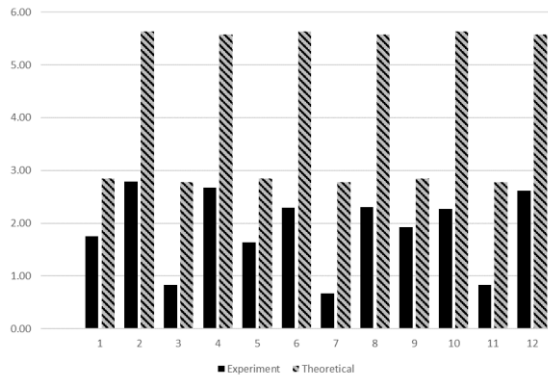


Figure 7. Experimental and theoretical % compression ratios according to the densification processes of the poplar wood.

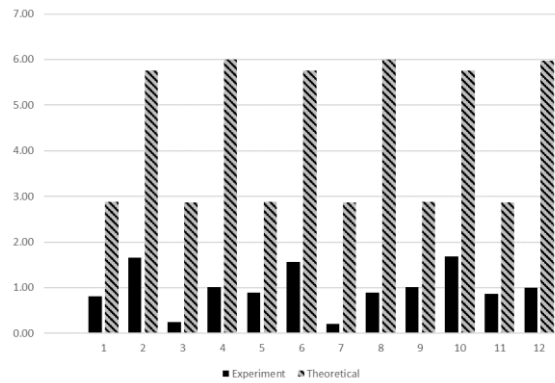


Figure 8. Experimental and theoretical % compression ratios according to the densification processes of the larch wood.

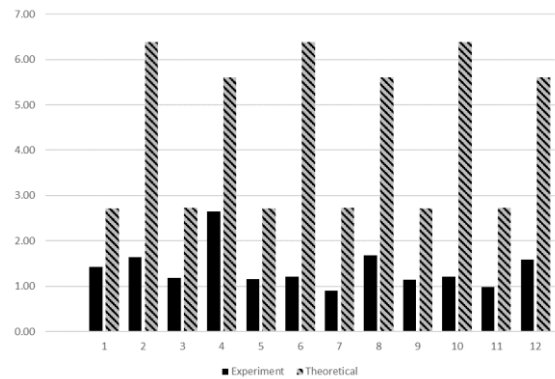


Figure 9. Experimental and theoretical % compression ratios according to the densification processes of the cedar wood.

As can be seen from the graphics, spring-back effect occurs after densification. It has been determined by experimental studies in the literature that the spring-back effect is a condition seen after densification (Pelit et. al., 2014; Tenario et. al., 2021; Laine et. al., 2016; Kariz et. al., 2017). It has been stated that the density increase obtained by compressing the wood material depends on the characteristics of the wood species, the spring-back effect, and the level of compression by the applied densification method (Rautkari, 2012; Pelit et al. 2015). The results of the variance analysis are given for densification in Table 3 and for spring-back in Table 4.

Table 3. Analysis of variance for densification

Source	DF	Adj SS	Adj MS	F-Value	P-Value
Wood species	2	4.8445	2.4223	16.24	0.000
Feed (mm/rotate)	2	0.4598	0.2299	1.54	0.231
Spindle speed (rpm)	1	0.6889	0.6889	4.62	0.040
Depth of dens. (mm)	1	5.6644	5.6644	37.98	0.000
Error	29	4.3253	0.1491		
Total	35	15.9830			

According to the results of analysis of variance for densification, the effects of wood species ($P=0.000<0.05$) and spindle speed ($P=0.040<0.05$) and depth of densification ($P=0.000<0.05$) were found significant at 95% confidence level. Feed ($P=0.231>0.05$) has no statistical effect (Table 3).

Table 4. Analysis of variance for spring-back

Source	DF	Adj SS	Adj MS	F-Value	P-Value
Wood species	2	6.8129	3.4064	11.26	0.000
Feed (mm/rotate)	2	0.4571	0.2286	0.76	0.479
Spindle speed (rpm)	1	0.2483	0.2483	0.82	0.372
Depth of dens. (mm)	1	44.6892	44.6892	147.71	0.000
Error	29	8.7737	0.3025		
Total	35	60.9813			

According to the results of analysis of variance for spring-back, the effect of wood species ($P=0.000<0.05$) and depth of densification ($P=0.000<0.05$) were found significant at 95% confidence level. Feed ($P=0.479<0.05$) and spindle speed ($P=0.372<0.05$) have no statistically significant effect (Table 4).

The main effect graph for the densification percentage is given in Figure 10. The highest densification percentage was obtained in black poplar wood species, and the lowest densification percentage was obtained in larch wood species.

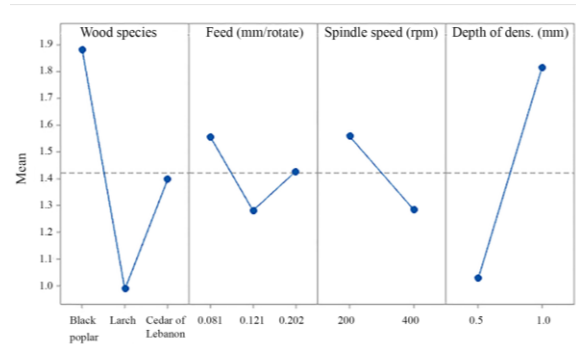


Figure 10. Main effect plot for densification

While the highest densification percentage was obtained at 0.081 mm/rotate feed, a decrease occurred at 0.121 mm/rotate with an increase in the feed value. And it rose again at the highest feed value of 0.202 mm/rotate. However, this value is around an average densification value. The highest densification value was obtained at 200 rpm spindle speed and 1 mm depth of densification. When evaluated in general, the highest densification was obtained in Black poplar wood species, 0.081 mm/rotate feed, 200 rpm spindle speed, and 1 mm depth of densification. When the interaction plot for densification is examined in Figure 11, it is seen that the highest densification occurs at 1 mm depth of densification for all wood species.

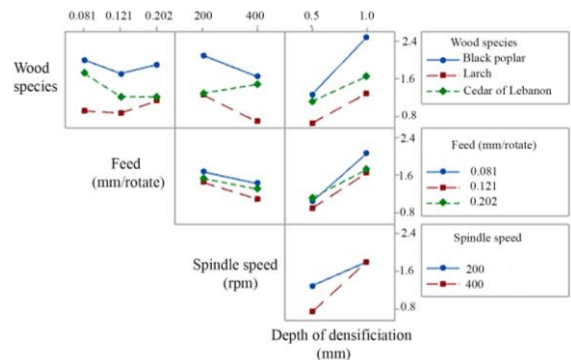


Figure 11. Interaction plot for densification

It is seen that the difference between 0.5 and 1 mm in terms of the densification percentage of poplar wood is high, while this difference is obtained close to each other in larch and cedar wood. The interaction of depth of densification in both feed and two spindle speed values occurred similarly in different wood species. Spindle speed showed similar interaction at different feed values. On the other hand, when the interaction between spindle speed and wood species was examined, the highest densification was obtained at 200 rpm in poplar and larch wood species. Although close to each other in Cedar, the highest value occurred at 400 rpm. The interaction between the feed and wood species is similar in all three wood types.

In Figure 12, the main effect graph for the spring-back percentage is given.

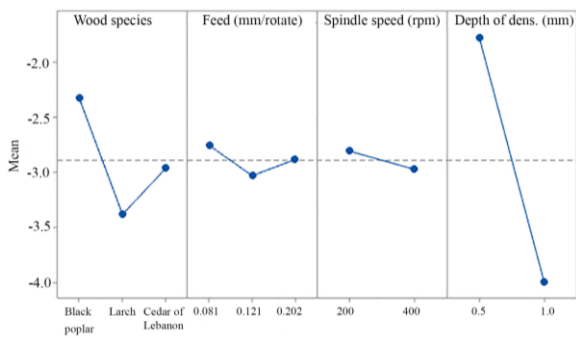


Figure 12. Main effect plot for spring-back

The highest spring-back percentage was obtained in the poplar wood species, and the lowest spring-back percentage was obtained in the larch wood species. The highest percentage of spring-back was obtained in 0.081 mm/rotate feed. With the increase of the feed value, a decrease of 0.121 mm/rotate occurred and increased again at the highest value of 0.202. However, this increase has not been too much. In fact, this change was not found to be significant at the 95% confidence level according to the result of the analysis of variance. The lowest percentage of spring-back was obtained at 400 rpm spindle speed and 1 mm depth of densification. When evaluated in general, the lowest percentage of spring-back was obtained in larch wood species, 0.121 mm/rotate feed, 400 rpm spindle speed, and 1 mm depth of densification.

When the interaction plot for spring-back is examined in Figure 13, it is seen that the lowest percentage of spring-back occurs at a 1 mm depth of densification for all wood species. The interaction of depth of densification in both feed and two spindle speed values occurred similarly in different wood species.

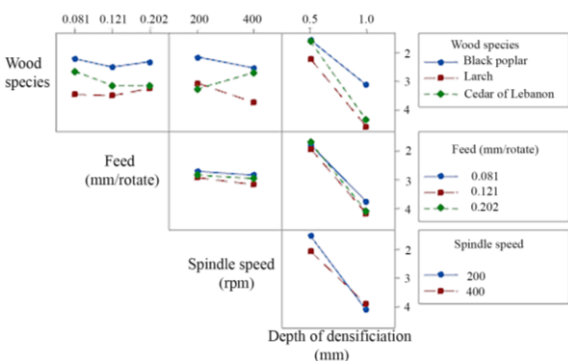


Figure 13. Interaction plot for spring-back

Spindle speed showed similar interaction in different feed values and the spring-back effect occurred close to each other in both feed values. However, when the interaction between spindle speed and wood species was examined, the lowest spring-back effect was obtained at 400 rpm in poplar and larch woods, while the lowest value occurred at 200 rpm in cedar woods, although they were close to each other. In terms of spring-back effect, the percentage of spring-back was very close to each other in larch and cedar woods at 200 rpm, and poplar and cedar woods at 400 rpm. The interaction between

the feed and wood species is similar in all three wood types. With the increase in feed, there was a decrease in the spring-back percentage first, and then there was an increase again.

When the literature is examined, it has been tried to reduce the spring-back effect by steaming or heating, which can induce permanent fixation of the compressive deformation (Kutnar and Sernek, 2007).

4. CONCLUSIONS

In this study, black poplar (*Populus nigra* L.), larch (*Pinus nigra* Arnold), and cedar of Lebanon (*Cedrus libani* A.Rich.) wood species were selected as experimental materials. The surfaces of the cylindrical test specimens were densified by changing various densification parameters with the spinning roller on the lathe, and the densification and spring-back percentages were evaluated. The obtained results can be summarized as follows.

- The effects of wood species, spindle speed and depth of densification were significant for densification percentage. The effect of the feed is not significant.
- The effect of wood type and depth of densification was significant in terms of spring-back. The feed and spindle speed effect is not significant.
- When evaluated in general, the highest densification percentage was obtained in black poplar wood, 0.081 mm/rotate feed, 200 rpm spindle speed and 1 mm depth of densification.
- When evaluated in general, the lowest percentage of spring-back was obtained in larch wood species, 0.121 mm/rotate feed, 400 rpm spindle speed and 1 mm depth of densification.
- The highest densification percentage was obtained in the black poplar wood, and the lowest densification percentage was obtained in the larch wood.
- The lowest spring-back percentage was obtained in the larch wood species, and the highest spring-back percentage was obtained in the black poplar wood species.
- The highest percentage of densification and the lowest spring-back occurred at a 1 mm depth of densification for all wood species.

Ethics Committee Approval

N/A

Peer-review

Externally peer-reviewed.

Author Contributions

Conceptualization: Z.K., S.D.S.; Investigation: S.D.S.; Material and Methodology: Z.K., S.D.S.; Supervision: S.D.S.; Visualization: Z.K., S.D.S.; Writing-Original Draft: Z.K., S.D.S.; Writing-review & Editing: Z.K., S.D.S.

Conflict of Interest

The authors have no conflicts of interest to declare.

Funding

The authors declared that this study has received no financial support.

REFERENCES

- Blomberg, J., Persson, B., (2004). Plastic deformation in small clear pieces of Scots pine (*Pinus sylvestris*) during densification with the CaLignum process. *J Wood Sci*, 50(4), 307–314. <https://doi.org/10.1007/s10086-003-0566-2>
- Blomberg, J., Persson, B., Blomberg, A. (2005). Effects of semi-isostatic densification of wood on the variation in strength properties with density. *Wood Science and Technology*, 39, 339-350. <https://doi.org/10.1007/s00226-005-0290-8>
- Cloutier, A., Fang, C., Mariotti, N., Koubaa, A., Blanchet, P. (2008). Densification of wood veneers under the effect of heat, steam and pressure. In *Proceedings of the 51st International Convention of Society of Wood Science and Technology*.
- Esteves, B., Pereira, H., (2009). Wood modification by heat treatment: A review. *BioResources*, 4(1), 370-404. <https://doi.org/10.15376/biores.4.1.370-404>
- Esteves, B., Ribeiro, F., Cruz-Lopes, L., Ferreira, J., Domingos, I., Duarte, M., Nunes, L., (2017). Densification and heat treatment of maritime pine wood. *Wood Research*, 62(3), 373-388.
- Fang, C. H., Cloutier, A., Blanchet, P., Koubaa, A., Mariotti, N., (2011). Densification of wood veneers combined with oil-heat treatment. Part I: Dimensional stability. *BioResources*, 6(1), 373-385.
- Fang, C. H., Mariotti, N., Cloutier, A., Koubaa, A., Blanchet, P., (2012). Densification of wood veneers by compression combined with heat and steam. *European Journal of Wood and Wood Products*, 70(1), 155. <https://doi.org/10.1007/s00107-011-0524-4>
- Fu, Q., Cloutier, A., Laghdir, A. (2016). Optimization of the thermo-hydrromechanical (THM) process for sugar maple wood densification. *BioResources*, 11(4), 8844-8859. <https://doi.org/10.15376/biores.11.4.8844-8859>
- Hajihassani, R., Mohebby, B., Najafi, S. K., Navi, P. (2018). Influence of combined hygro-thermo-mechanical treatment on technical characteristics of poplar wood. *Maderas. Ciencia y tecnología*, 20(1), 117-128. <http://dx.doi.org/10.4067/S0718-221X2018005011001>
- ISO 13061 (2014). Wood - Determination of moisture content for physical and mechanical tests, International Organization for Standardization, Geneva, Switzerland.
- ISO 13061-2 (2014). Wood - Determination of density for physical and mechanical tests, International Organization for Standardization, Geneva, Switzerland.
- Kariz, M., Kuzman, M. K., Sernek, M., Hughes, M., Rautkari, L., Kamke, F. A., Kutnar, A. (2017). Influence of temperature of thermal treatment on surface densification of spruce. *European Journal of Wood and Wood Products*, 75, 113-123. <https://doi.org/10.1007/s00107-016-1052-z>
- Kaya, Z., Sofuoğlu, S.D. (2023). Use of spinning roller in cylindrical densification; change in hardness, brightness, and surface roughness in solid wood (Larch) after densification. *Furniture and Wooden Material Research Journal*, 6 (1), 14-25. <https://doi.org/10.33725/mamad.1260723>
- Kutnar A., Kamke F. A., Sernek M., (2009). Density profile and morphology of viscoelastic thermal compressed wood. *Wood Science and Technology*, 43(1-2), 57-68. <https://doi.org/10.1007/s00226-008-0198-1>
- Kutnar, A., Šernek, M. (2007). Densification of wood. *Zbornik gozdarstva in lesarstva*, (82), 53-62.
- Laine, K., Rautkari, L., R., Hughes, M., Kutnar, A., (2013). Reducing the set-recovery of surface densified solid Scots pine wood by hydrothermal post-treatment. *European Journal of Wood and Wood Products*, 71(1), 17-23. <https://doi.org/10.1007/s00107-012-0647-2>
- Laine, K., Segerholm, K., Wälinder, M., Rautkari, L., Hughes, M. (2016). Wood densification and thermal modification: hardness, set-recovery and micromorphology. *Wood science and technology*, 50, 883-894. <https://doi.org/10.1007/s00226-016-0835-z>
- Li, T., Cai, J. B., Zhou, D. G. (2013). Optimization of the Combined Modification Process of Thermo-Mechanical Densification and Heat Treatment on Chinese Fir Wood. *BioResources*, 8(4), 5279-5288

- Li, T., Cai, J. B., Avramidis, S., Cheng, D. L., Wålinder, M. E., Zhou, D.G., (2017). Effect of conditioning history on the characterization of hardness of thermo-mechanical densified and heat treated poplar wood. *Holzforschung*, 71(6), 515-520. <https://doi.org/10.1515/hf-2016-0178>
- Lin, R.J.T.; Van Houts, J.; Bhattacharyya, D. (2006). Machinability investigation of medium-density fibreboard. *Holzforschung*, 60(1), 71–77. <https://doi.org/10.1515/HF.2006.013>
- Malkocoglu, A. (2007). Machining properties and surface roughness of various wood species planed in different conditions. *Build Environ*, 42(7), 2562–2567. <https://doi.org/10.1016/j.buildenv.2006.08.028>
- Malkocoglu, A., Ozdemir, T. (2006). The machining properties of some hardwoods and softwoods naturally grown in Eastern Black Sea Region of Turkey. *J Mater Process Technol*, 173(3), 315–320. <https://doi.org/10.1016/j.jmatprotec.2005.09.031>
- Matthew Schwarzkopf (2021). Densified wood impregnated with phenol resin for reduced set-recovery. *Wood Material Science & Engineering*, 16(1), 35-41. <https://doi.org/10.1080/17480272.2020.1729236>
- Neyses, B., Karlsson, O., Sandberg, D. (2020). The effect of ionic liquid and superbase pre-treatment on the spring-back, set-recovery and Brinell hardness of surface-densified Scots pine. *Holzforschung*, 74(3), 303-312. <https://doi.org/10.1515/hf-2019-0158>
- Pelit, H., (2014). The effects of densification and heat treatment to finishing process with some technological properties of eastern beech and scots pine. PhD thesis, Gazi University, Ankara-Türkiye
- Pelit, H., Sönmez, A., (2015). The Effect of Thermo-Mechanical Densification and Heat Treatment on Some Physical Properties of Eastern Beech (*Fagus orientalis* L.) wood. *Duzce University Journal of Science and Technology*, 3(1), 1-14.
- Pelit, H., Sonmez, A., Budakci, M. (2014). Effects of ThermoWood process combined with thermo-mechanical densification on some physical properties of scots pine (*Pinus sylvestris* L.). *BioResources*, 9(3) 4552-4567. <https://doi.org/10.15376/biores.9.3.4552-4567>
- Pelit, H., Sonmez, A., M. Budakci, M. (2015). Effects of thermomechanical densification and heat treatment on density and Brinell hardness of Scots pine (*Pinus sylvestris* L.) and Eastern beech (*Fagus orientalis* L.). *BioResources*, 10(2), 3097-3111. <https://doi.org/10.15376/biores.10.2.3097-3111>
- Pinkowski, G., Szymański, W., Krauss, A., Stefanowski, S. (2018). Effect of sharpness angle and feeding speed on the surface roughness during milling of various wood species. *BioResources*, 13(3), 6952-6962. <https://doi.org/10.15376/biores.13.3.6952-6962>
- Rautkari, L. (2012). Surface modification of solid wood using different techniques. Aalto University, Finland, PhD Thesis.
- Rautkari, L., Properzi, M., Pichelin, F., Hughes, M., (2010). Properties and set-recovery of surface densified Norway spruce and European beech. *Wood Science and Technology*, 44(4), 679-691. <https://doi.org/10.1007/s00226-009-0291-0>
- Senol, S.; Budakci, M. (2019). Effect of Thermo-Vibro-Mechanic® densification process on the gloss and hardness values of some wood materials. *BioResources*, 14(4), 9611–9627. <https://doi.org/10.15376/biores.14.4.9611-9627>
- Skyba, O., Schwarze, F. W. M. R., Niemz, P. (2009). Physical and mechanical properties of thermo-hygro-mechanically (THM) - densified wood. *Wood Research*, 54(2), 1-18.
- Sofuoglu S.D., Tosun, M., Atilgan, A. (2023). Determination of the machining characteristics of Uludağ fir (*Abies nordmanniana* Mattf.) densified by compressing. *Wood Material Science & Engineering*, 18(3), 841-851. <https://doi.org/10.1080/17480272.2022.2080586>
- Sofuoglu, S.D. (2022). Effect of thermo-mechanical densification on brightness and hardness in wood. *Turkish Journal of Engineering Research and Education*, 1(1), 15-19.
- Tenorio, C., Moya, R., Navarro-Mora, A. (2021). Flooring characteristics of thermo-mechanical densified wood from three hardwood tropical species in Costa Rica. *Maderas. Ciencia y tecnología*, 23. <https://doi.org/10.4067/S0718-221X2021000100416>
- Tosun, M., Sofuoglu, S.D. (2023). The use of an artificial neural network for predicting the machining characterizing of wood materials densified by compressing. *Bilge International Journal of Science and Technology Research*, 7(1), 55-62. <https://doi.org/10.30516/bilgesci.1110376>
- Tosun, M., Sofuoglu, S.D. (2021). Studies of densification of wood material by compression. *Furniture and Wooden Material Research Journal*, 4(1), 91-102.
- Tosun, M., Sofuoglu, S.D. (2023). Determination of processing characteristics of wood materials densified by compressing. *Maderas-Cienc Tecnol*, 25. Retrieved from <https://revistas.ubiobio.cl/index.php/MCT/articloe/view/5821>

- Welzbacher, C. R., Wehsener, J., Rapp, A. O., Haller, P. (2008). Thermo-mechanical densification combined with thermal modification of Norway spruce (*Picea abies* Karst.) in industrial scale– Dimensional stability and durability aspects. *Holz als Roh-und Werkstoff*, 1(66), 39-49. [https://doi.org/ 10.1007/s00107-007-0198-0](https://doi.org/10.1007/s00107-007-0198-0)
- Yahyae, S. M. H., Dastoorian, F., Ghorbani, M., Zabihzadeh, S. M. (2022). Combined effect of organosolv delignification/polymerization on the set recovery of densified poplar wood. *European Journal of Wood and Wood Products*, 1-9. <https://doi.org/10.1007/s00107-021-01756-5>
- Zhong, Z.W., Hiziroglu, S.; Chan, C.T.M. (2013). Measurement of the surface roughness of wood based materials used in furniture manufacture. *Measurement*, 46(4), 1482–1487. <https://doi.org/10.1016/j.measurement.2012.11.041>

Prediction of Turkish Constitutional Court Decisions with Explainable Artificial Intelligence

Tülay Turan ^{1*}, Ecir Uğur Küçüksille ², Nazan Kemaloğlu Alagöz ³

Abstract: Using artificial intelligence in law is a topic that has attracted attention in recent years. This study aims to classify the case decisions taken by the Constitutional Court of the Republic of Turkey. For this purpose, open-access data published by the Constitutional Court of the Republic of Turkey on the website of the Decisions Information Bank were used in this research. KNN (K-Nearest Neighbors Algorithm), SVM (Support Vector Machine), DT (Decision Tree), RF (Random Forest), and XGBoost (Extreme Gradient Boosting) machine learning (ML) algorithms are used. Precision, Recall, F1-Score, and Accuracy metrics were used to compare the results of these models. As a result of the evaluation showed that the XGBoost model gave the best results with 93.84% Accuracy, 93% Precision, 93% Recall, and 93% F1-Score. It is important that the model result is not only good but also transparent and interpretable. Therefore, in this article, using the SHAP (SHapley Additive exPlanations) method, one of the explainable artificial intelligence techniques, the features that affect the classification of case results are explained. The study is the first study carried out in our country to use explainable artificial intelligence techniques in predicting court decisions in the Republic of Turkey with artificial intelligence.

Keywords: Explainable Artificial Intelligence, Turkish Constitutional Court, Legal Judgment Prediction, SHAP, XGBoost.

¹**Address:** Süleyman Demirel University, Institute of Science, Computer Engineering, Isparta, Türkiye

²**Address:** Süleyman Demirel University, Department of Computer Engineering, Isparta, Türkiye

³**Address:** Isparta University of Applied Science, Department of Computer Technologies, Isparta, Türkiye

***Corresponding author:** tulayturan@mehmetakif.edu.tr

Citation: Turan, T., Küçüksille, E. U., Kemaloğlu Alagöz, N. (2023). Prediction of Turkish Constitutional Court Decisions with Explainable Artificial Intelligence. Bilge International Journal of Science and Technology Research, 7(2): 128-141.




1. INTRODUCTION

Along with big data, artificial intelligence (AI) technology, which has developed rapidly in recent years, appears with various work examples in many sectors. In the literature review, it is seen that the application diversity is high in fields such as education (Roll and Wylie 2016; Knox 2020; Chen et al., 2020; Meço and Çoştu 2022), defense (Bistrion and Piotrowski 2021), health (Yu et al., 2018; Jiang et al., 2017; Turan et al., 2022), trade (Di Vaio et al., 2020; Loureiro et al., 2021) and engineering (Goertzel and Pennachin 2007). It has been observed that the application diversity in the field could be higher. In this context, the development of AI solutions in the field of law is seen as an area that attracts the attention of scientists and needs a lot of new work.

When the studies in the field of law are examined, it is seen that it has developed in parallel with the development of natural language processing, a sub-branch of AI. It has been reported that AI solutions have been developed under the sub-titles of litigation decision prediction (Zhong et al., 2018; Long et al., 2019), document analysis (Zadgaonkar and Agrawal 2021), legal assistance (Socatiyanurak et al., 2021), contract creation, and review (Antos and Nadhamuni 2021; Labin and Segal 2021) on legal documents. Making models, analyzing, and producing results using case decision data from these titles is called Legal Judgment Prediction (LJP). LJP practices are an important field of application as it quickly concludes case decisions, works without the need for rest periods that people need, do not show emotionality in the decisions it takes, and offer

recommendations. Niklaus et al., reported in their study that there are approximately 24 million cases per 17,000 judges in India and approximately 1.6 million cases on only five charges in Brazil (Niklaus et al., 2022). The duration of conclusion of these cases will inevitably be prolonged. LJP practices provide various benefits for law firms, clients, and legal professionals as a solution to this problem. These benefits are shown in Table 1.

Table 1: Benefits of LJP

 Law Firm	<p>Thanks to the LJP, they can predict the outcome of the cases they defend, improve their defense case and increase their winning rate (Velez and Kim 2017).</p>
 Client	<p>Thanks to LJP, they can get an estimate of the outcome of the case they want to file before applying to any law firm. If the result is that they cannot win the case, they will not incur any costs because they will not apply to the law firm (Stevenson and Wagoner 2015).</p>
 Court	<p>The workload of judges and courts will be reduced as faster solutions are achieved in less time with LJP (Ma et al., 2021).</p>

The diversity of the data source is important in developing LJP applications. The Ministry of Justice of the Republic of Turkey has decided that in the "Human Rights Action Plan" published in April 2021, all court decisions in Turkey will be digitized and made accessible.¹ In the literature review, Chinese and English LJP practices were used by using open access court decisions shared by the European Court of Human Rights (Aletras et al., 2016; Kaur and Bozic 2019; Collenette et al., 2020), Supreme People's Court of China (Yan et al., 2019; Yang et al., 2020; Gan et al., 2022) and Supreme Court of the United States (Strickson and Iglesia, 2020). The development of Turkish legal datasets and LJP applications is still in its infancy, and it is seen that there are only two studies (Sert et al., 2021; Mumcuoğlu et al., 2021). In this context, it is aimed to create a new Turkish data set as a first step in the research and to contribute to Turkish LJP studies.

The Constitutional Court of Turkey shares the decisions of norm review, individual application, supreme Court and political parties as open access on the "Decisions Information Bank" website. This study uses individual application court decisions shared by the Turkish Constitutional Court for a new Turkish legal dataset. Personal application decisions consist of approximately 10,000 lawsuits filed by individuals for alleged human rights violations since 2012. When the contents of the lawsuits are examined, it is seen that lawsuits have been filed for 24 fundamental rights and freedoms guaranteed by the Turkish Constitution. These lawsuits are based on "Violation, No Violation, Clearly Unfounded, Lack of

Constitutional and Personal Importance, Non-Exhaustion of Recourses, Refusal of Application, Rejection, Objection to Administrative Rejection, No Place for Review, Incompetence in Terms of Person, Incompetence in Terms of Subject" for the relevant fundamental rights and freedoms. It is concluded with 15 different results, including "Incompetence of the Court, Time-Out of Time, Incompetence in terms of Place, Incompetence in terms of Time." The study aims to predict the result of "Violation" / "No Violation" from these results, and the data set was created accordingly.

Explainability is one of the important topics to be addressed while developing LJP applications. Classification models used in LJP applications can make decisions that are not easy to interpret with their non-linear and complex structures, and it is not known exactly how they reach the result. These results obtained by the models are defined as the black box (Mumford et al., 2021; Xu 2022). Explainable Artificial Intelligence (XAI) provides techniques to understand better and explain our model's results (Gunning and Aha 2019; Gunning et al., 2019). Thus, AI results defined as black box are converted into white box results. Disclosure of LJP model results is also important for legal professionals and clients awaiting explanations for why certain decisions were made. In this study, the results obtained by machine learning (ML) models are plotted using the SHAPley Additive exPlanations (SHAP) method, one of the XAI techniques. Thus, the features that affect the model results are presented clearly and visually.

The contributions of this article to the literature are as follows.

1. Taking large volumes of legal data and automating the process of generating structured information and rules will reduce the time it takes for legal professionals to review hundreds of case documents and materials.
2. It will successfully expand the analysis of the case and help legal professionals reach the decision's conclusions faster.
3. It is the first study carried out in the country to explain the court decisions of the Republic of Turkey with XAI techniques.
4. Sharing a new publicly available Turkish legal dataset will significantly contribute to developing Turkish LJP practices.

2. RELATED WORK

Predicting the legal consequences of cases depends on many factors, such as evidence, witnesses, judges, opinions, and previous court decisions. Legal professionals try to predict a case's outcome using their experience, knowledge, professional judgment, and other cognitive skills, and for this, they have to review large amounts of data. Today, Lex Machina, Premonition Analytics, and Ravel Law have developed LJP software. These softwares draw attention with accelerating information access, optimizing time management, and successful forecasting results.

When the LJP studies in the world and our country are examined, it has been seen that the diversity of legal data

¹ <https://insanhaklarieylemplani.adalet.gov.tr/>

sets is not enough. Therefore, the scientists who work first start to develop applications by creating a legal data set. Xiao et al., revealed the first Chinese LJP dataset, CAIL2018. They created the data set using the decisions shared by the Supreme People's Court of China. Also, they pointed out that the transmitted data set was the largest LJP data set ever (Xiao et al., 2018). Chalkidis et al., (2019) stated that they created a data set in English using the decisions shared by the European Court of Human Rights. Their study stated whether the lawsuits' results are infringed or not by binary classification and multi-label classification. Niklaus et al., (2021) stated that they created a multilingual (German, French, and Italian) data set using the decisions shared by the Federal Supreme Court of Switzerland. They used BERT-based methods to develop models. In additionally, they stated that the Hierarchical BERT model with a Macro-F1-Score of 70% showed the best performance. Long et al., first created a Chinese dataset for automatic judgment estimation. In additionally, they propose AutoJudge, a new LRC model that captures complex semantics in their work. They reported that they obtained better estimation results with the AutoJudge model compared to many advanced models (Long et al., 2019). Guo et al., (2021) created the dataset they used in their studies from the Chinese referee document network page. In their work, they propose a new method called ModTen based on tensor models. They showed that their results were better than those obtained with the classification methods. Li et al., (2019) developed models with MANN, one of the deep neural network methods, using the Chinese dataset CAIL2018 in their study. Also, they compared the model they developed with the SVM, GRU, Bi-GRU, HAN, and TOPJUDGE models. As a result, they stated that the MANN model achieved the best results. Katz et al., (2017) created a data set using English decisions shared by the United States Supreme Court. The model they developed gave an accuracy rate of 70.2%. The studies of Mumcuoğlu et al., (2021) were available in the literature as the first comprehensive study of NLP for the Turkish legal system. In their studies, they classified deep learning methods using Decision Trees, Random Forests, Support Vector Machines and the decisions of the Constitutional Court and Supreme Court. Sert et al., (2021) have developed estimation models for “violation” or “non-violation” of Constitutional Court decisions. As a result of their studies, they achieved 90% success with MLP. The open-access court information used by the current LJP studies in the literature as the data source is shown in Table 2.

Table 2 Data Sources of LJP Articles

Year	Article	Dataset Source
2021	Using Artificial Intelligence to Predict Decisions of the Turkish Constitutional Court (Sert et al., 2021)	Constitutional Court of Turkey
2021	Natural language processing in law: Prediction of outcomes in the higher courts of Turkey (Mumcuoğlu et al., 2021)	Constitutional Court of Turkey
2018	Caill2018: A large-scale legal dataset for judgment Prediction (Xiao et al., 2018)	Supreme People's Court of China
2019	Neural legal judgment prediction in English (Chalkidis et al., 2019)	European Court of Human Rights
2021	Swiss-judgment-prediction: a multilingual legal judgment prediction benchmark (Niklaus et al., 2021)	Federal Supreme Court of Switzerland
2019	Automatic judgment prediction via legal reading comprehension (Long et al., 2019)	Supreme People's Court of China
2021	TenLa: an approach based on controllable tensor decomposition and optimized lasso regression for judgment prediction of legal cases (Guo et al., 2021)	Supreme People's Court of China
2019	Mann: A multichannel attentive neural network for legal judgment Prediction (Li et al., 2019)	Supreme People's Court of China
2017	A general approach for predicting the behavior of the Supreme Court of the United States (Katz et al., 2017)	Supreme Court of the United States
2019	Convolutional Neural Network-based Automatic Prediction of Judgments of the European Court of Human Rights (Kaur and Bozic 2019)	European Court of Human Rights
2016	Predicting judicial decisions of the European Court of Human Rights: A natural language processing perspective (Aletas et al., 2016)	European Court of Human Rights
2020	An Explainable Approach to Deducing Outcomes in European Court of Human Rights Cases Using ADFs (Collenette et al., 2020)	European Court of Human Rights
2022	Exploiting Contrastive Learning and Numerical Evidence for Improving Confusing Legal Judgment Prediction (Gan et al., 2022)	Supreme People's Court of China
2019	Law article prediction based on deep learning (Yan et al., 2019)	Supreme People's Court of China
2020	Leniency to those who confess? Predicting the Legal Judgement via Multi-Modal Analysis (Yang et al., 2020)	Supreme People's Court of China
2020	Legal judgment prediction for UK courts (Strickson and Iglesia 2020)	Supreme Court of the USA
2022	ClassActionPrediction: A Challenging Benchmark for Legal Judgment Prediction of Class Action Cases in the US (Semo et al., 2022)	Supreme Court of the USA

The comparative use of XAI in LJP applications is a new topic, and there are few study examples in the literature. Gorski et al., used the Grad-CAM image processing technique to make it explicable in legal texts. Gorski et al., (2020) of the DistilBERT expression with an accuracy of 85% of the best performance from the models they developed in their studies. Gorski and Ramakrishna (2021) stated in their studies that they explain legal texts with explainable methods such as Grad-CAM, LIME, and SHAP. They evaluated the results they obtained by contacting protective lawyers.

3. MATERIAL AND METHOD

3.1. Dataset

The data set was created from the individual application decisions shared by the Constitutional Court of the Republic of Turkey on the Decisions Information Bank website. When the transmitted cases are examined, it is seen that they were opened for 24 fundamental rights and freedoms guaranteed by the Turkish Constitution and were concluded with 15 different results. This study aims to predict the result of "Violation" and "No Violation" of fundamental rights and freedoms. For this purpose, all decisions with the result of "Violation" and "No Violation" have been obtained from the web page. When the cases taken were examined, it was seen that there were no exemplary decisions for some rights and freedoms. Table 3 shows the data set content of the study.

Table 3 Dataset Content

No	Right Freedom	Violation	No Violation
1	Right to Fair Trial (Penalty)	60	60
2	Right to Fair Trial (Law)	60	60
3	Right to Fair Trial (Administration)	60	60
4	Prohibition of Discrimination	3	3
5	Individual Application Right	0	0
6	Freedom of Religion and Conscience	1	1
7	Education right	3	3
8	Effective Right to Apply	2	2
9	Right to Request Review of the Provision	0	0
10	Freedom of expression	50	50
11	Excluded Rights	0	0
12	Right to Personal Freedom and Security	80	80
13	Abuse Ban	60	60
14	The right to protection of material and spiritual property	50	50
15	Freehold	80	80
16	Freedom of association	10	10
17	Protection of private and family life right	55	55
18	The right to vote, be elected, and engage in political activity	4	4
19	The legality of crimes and punishments principles	2	2

20	The right to organize meetings and demonstration marches	20	20
21	Right to life	50	50
22	Prohibition of forced labor and drudgery	0	0
23	Other Rights	0	0
24	Union Right	0	0
Total		650	650
Overall Total		1300	

When the decisions were examined, it was seen that they consisted of six main parts. These sections are the subject of the application, the application process, the events and facts, the relevant law, the examination, and the law and judgment section, respectively. To determine of these sections would be the independent variable and the dependent variable for the models, interviews were held with the lawyers. As a result, it has been decided to designate the "Examination and Justification" section as the "independent variable" and the "Provision" section as the "dependent variable." The dataset created for this study has been published on GitHub and can be accessed at <https://github.com/tulayturan/KararListesi>.

3.2. K-Nearest Neighbors (KNN)

The KNN algorithm is based on the logic of calculating the distance of the unknown data from other data and including it in the nearest class (Nikam, 2015). Euclidean, Manhattan, or Minkowski methods are used to calculate the distance measure (Shahid et al., 2009; Singh et al., 2013)

Euclidean distance calculation is calculated as given in Equation 1.

$$\sqrt{\sum_{i=1}^n (x_i - y_i)^2} \tag{1}$$

Manhattan distance calculation is calculated as given in Equation 2.

$$\sum_{i=1}^n |x_i - y_i| \tag{2}$$

Minkowski distance calculation is calculated as given in Equation 3.

$$\left(\sum_{i=1}^n (|x_i - y_i|^q) \right)^{1/q} \tag{3}$$

The n value in the equations can be defined as "no of dimensions," the x value as "datapoint from the dataset," and the y value as "new data point (to be predicted)."

3.3. Support Vector Machine (SVM)

SVM is an algorithm that properly separates data from two or more classes (Ghosh et al., 2019). The separation of

classes is determined by decision boundaries or hyperplanes (Somvanshi et al., 2016). In Figure 1, a red hyperplane and hyperplanes belonging to each class separate the two classes from each other. The region between +1 and -1 is called Margin. The wider the margin value, the better it classifies two or more classes (Brereton and Lloyd, 2010).

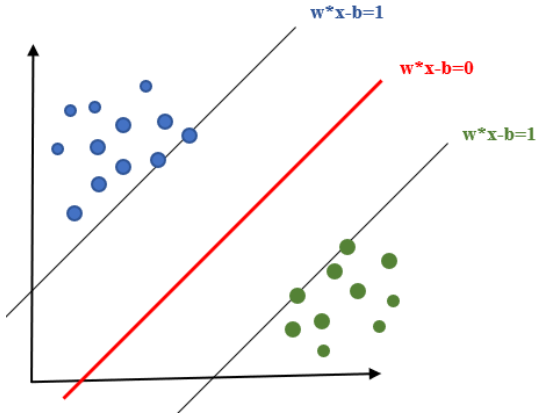


Figure 1. Class Separation with SVM

In Figure 1;
 The $w^*x-b=1$ hyperplane and each data represent the class members labeled 1.
 The $w^*x-b=-1$ hyperplane and any data below it represents class members labeled -1.

3.4. Random Forest (RF)

The RF classifier is based on evaluating the predictions produced by multiple decision trees (Rokach, 2016). Observations for trees are determined by the Bagging method, and the variables are determined by the Random Subspace method. RF uses Gini as the feature selection measure, and Gini calculus is calculated as given in Eq. 4.

$$\sum_{j \neq i} \sum (f(C_i, T)/|T|)(f(C_j, T)/|T|) \tag{4}$$

An unexpected situation is selected for the T training set in the equation, and whether the selected value belongs to the Ci class is calculated.

3.5. Decision Tree (DT)

The first cells of the decision trees are called Root Nodes (Fletcher and Islam, 2019). There are nodes and leaves under the root. The root node is decided in decision trees by calculating Gini or Entropy values (Nanfack et al., 2022). Calculating the Gini value is shown in Equation 5, and the calculation of the Entropy value is shown in Equation 6.

$$Gini = 1 - \sum_j p_j^2 \tag{5}$$

$$Entropy = - \sum_{j=1}^c p_j \log_2(p_j) \tag{6}$$

p_j is the probability of occurrence of class j. It is calculated for each class, and the sum of the squares of the results is subtracted. The Gini value gets a result between 0 and 1, and the closer the result is to 0, the better the discrimination.

3.6. XGBoost

XGBoost is an ML algorithm proposed by Chen and Guestrin (2016). Boosting Tree algorithms are based on a decision tree known as a classification and regression tree (CART) (Dong et al., 2020).

The advantage of XGboost is that it supports linear classifiers and performs second-order Taylor expansion of the cost function to make the results more accurate. The loss function score used in the XGBoost algorithm and the solution of the weights are expressed as follows (Jiang et al., 2020).

$$w_j^* = - \frac{\sum g_i}{\sum h_i + \lambda} \tag{7}$$

$$obj^* = - \frac{1}{2} \sum_{j=1}^T \frac{(\sum g_i)^2}{\sum h_i + \lambda} + \lambda.T \tag{8}$$

In the equation, obj^* represents the score of the loss function. The smaller the score, the better the structure of the tree. w^*j represents the solution of the weights.

3.7. Model Evaluation Metrics

In this study, Confusion Matrix, Accuracy, Sensitivity, Precision, and Recall calculation methods were used to evaluate the performance success of the models. A confusion Matrix is an analysis tool that shows the extent to which a classifier can classify different class labels. In this study, the data set has 2 class labels and will be 2k*2 in size, as shown in Confusion Matrix Figure 2.

		ACTUAL	
		Negative	Positive
PREDICTION	Negative	True Negative (TN)	False Negative (FN)
	Positive	False Positive (FP)	True Positive (TP)

Figure 2. Confusion Matrix

Accuracy, Sensitivity, Precision, and Recall calculations of the models can be made using the Confusion Matrix values.

The Accuracy value is calculated as shown in Equation 9.

$$Accuracy = \frac{TP + TN}{TP + FP + TN + FN} \tag{9}$$

The sensitivity value is calculated as shown in Equation 10.

$$\text{Sensitivity} = \frac{TP}{TP + FN} \quad (10)$$

The precision value is calculated as shown in Equation 11.

$$\text{Precision} = \frac{TP}{TP + FP} \quad (11)$$

The Recall value is calculated as shown in Equation 12.

$$\text{Recall} = \frac{TP}{TP + FN} \quad (12)$$

3.8. Hyperparameter Tuning

Hyperparameters are parameters determined initially before the learning process starts in a machine learning model. The values of these parameters do not change when the learning process is over. Learning Rate, Epoch, etc., parameters can be given as examples.

Hyperparameter values given by default in machine learning models do not guarantee the best performance (Schratz et al., 2019). Therefore, the determination of hyperparameter values can greatly affect the model's performance (Mantodan et al., 2016). A large amount of hyperparameters in the models makes it almost impossible to adjust these values manually. For this reason, many hyperparameter tune methods are available and used in the literature. The most used methods are GridSearch and RandomSearch.

GridSearch creates a new model by trying all possible combinations from the given collection of values for each hyperparameter and returns the hyperparameter combination that provides the highest accuracy. The problem with this method is the process takes a long time when there are too many hyperparameters and values to try, and this causes the technique to run very slowly.

In the RandomSearch method, N combinations determined from each hyperparameter value collection are randomly selected and return the hyperparameter combination that provides the highest accuracy. With this method, a search can be made much faster and with an accuracy close to GridSearch.

3.9. Explainable Artificial Intelligence (XAI)

Today, where technological developments are advancing at a dizzying pace, AI; is used in many points that directly affect human life, such as health, autonomous vehicles, and military areas. Parallel to these developments, the fact that the mechanism used by AI in making decisions (black box) is not known exactly causes questions about reliability, transparency, bias, and fairness. In light of all this information, XAI can be defined as a field consisting of tools, techniques, and algorithms that can produce human-explainable explanations of AI decisions (Das and Rad, 2020). XAI is divided into different groups according to various approaches.

XAI scope is divided into local and global, depending on whether you understand the model from a local instance or as a whole. Local XAI focuses on disclosure on a single

data basis and creates a description for each data. In Global XAI, the model is tried to be explained as a whole (Anders et al., 2021; Spinner et al., 2019). Local Interpretable Model-Agnostic Explanations (LIME) (Ribeiro et al., 2016) and SHapley Additive exPlanations (SHAP) (Lundberg and Lee 2017) methods can be given as examples for Local XAI. For Global XAI, Class Model Visualization [80] and Spectral Relevance Analysis (SpRAy) (Lapuschkin et al., 2019) methods can be given as examples. At this point, LIME and SHAP can also be used for global XAI.

BackProb and Perturbation, depending on the algorithmic approach used, whether it focuses on the input sample or the model parameters. BackProb XAI's description depends on the gradients propagating back from the prediction layer to the input layer. In Perturbation XAI, however, the explanation depends on random or carefully chosen changes in properties in the input data (Nie et al., 2018; Lin et al., 2020; Ivanovs et al., 2021). For BackProb XAI, DeConvolutional Nets (Zeiler and Fergus, 2014) and SpRAy methods can be given as examples. For Perturbation, XAI, LIME, and SHAP methods can be given as examples.

XAI is divided into two depending on integration into a particular model and can be applied to the desired model in general. In Intrinsic XAI, explainability resides in the synergy architecture and cannot be transferred to other architectures. In Post-Hoc XAI, however, the algorithm does not depend on the model architecture and can be pre-trained neural networks (Weber and Wermter 2020; Tritscher et al., 2020; Kenny et al., 2021, Colaner 2021). Neural Additive Models (Agarwal et al., 2020) and Bayes Rule Lists (Letham et al., 2015) are examples of Intrinsic XAI. For Post-Hoc XAI, LIME and SHAP can be given as examples. Besides, Automatic Concept-based Explanations (Ghorbani et al., 2019) are one of the Post-Hoc methods.

3.10. SHapley Additive exPlanations (SHAP)

SHAP is a game theory-based method used to describe the performance of a machine learning model. In SHAP, an output model is defined as a linear sum of input variables (Mangalathu et al., 2020). SHAP is defined as a model-independent interpretability method because it can derive post-hoc explanations for the predictions of any classification model by associating inputs with output (Tideman et al., 2021).

Equation 13, which explains the importance of the i feature as a Shapley value, is given below (Rodríguez-Pérez and Bajorath 2020).

$$\phi_i = \frac{1}{|N|!} \sum_{S \subseteq N \setminus \{i\}} |S|! (|N| - |S| - 1)! [f(S \cup \{i\}) - f(S)] \quad (13)$$

Here $f(S)$ is the model's output, and N is the set of all features. In the equation, the Shapley value of the feature i expresses the mean of the contributions in all possible permutations of a feature set. In this method, features are added to the set separately. The model output change shows that variable's relevance.

4. RESULTS

The developed system consists of 5 parts. In the first stage, the content of the Turkish legal data set was passed through the data preprocessing steps. In the second stage, the vector space model of each word was created with the tf-idf (Term Frequency - Inverse Document Frequency) method. The supervised learning model classification techniques KNN, SVM, DT, RF, XGBoost, and LJP models were developed in the third stage. In the fourth stage, the classification performances of the models were compared with precision, recall, F1-score, and accuracy evaluation metrics. In the last section, the XGBoost model, which achieved the best result with an accuracy rate of 93.07%, is explained with SHAP plot techniques. The developed system diagram is given in Figure 3.

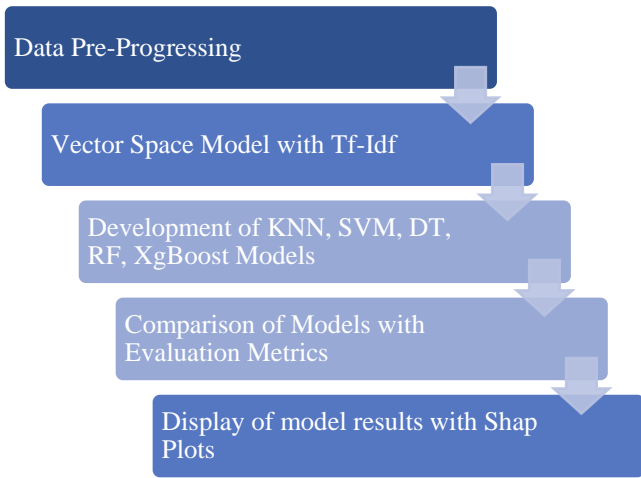


Figure 3 Developed System Diagram

Data preprocessing can be defined as the operations performed on the data set before AI models are developed. It is an important step in applications developed with natural language processing. Data preprocessing, transformation, deletion of duplicate data, and editing of noisy, incomplete, or contradictory data are performed on the data. As a result of this process, the model performance increases. The data preprocessing steps performed on the data in the study are shown in Figure 4.

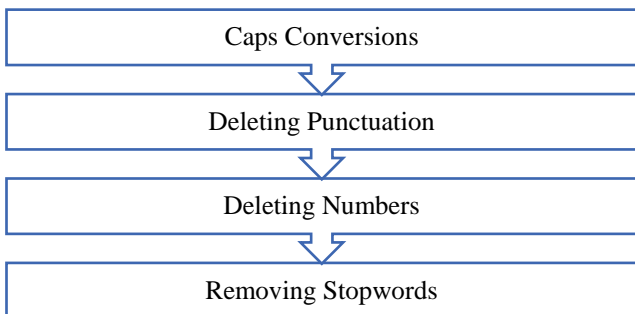


Figure 4. Data Preprocessing Steps

After the data preprocessing step, the vector space model of each word was created with the tf-idf method. The tf-idf method is used in the digitization of the text. Each text is an

MxN vector of available words. The document term matrix is formed by superimposing the vectors. This matrix consists of M texts and N terms. If terms are mentioned in the text, the weight value of that term will be different from "0". Tf-idf looks at the frequency of the related term in the text "Tf" and its importance in the text "idf."

While calculating the Tf text frequency value, the ratio of the number of terms in the sentence to the total number of words is considered. Eq.14 shows the calculation method.

$$tf(t, d) = \frac{f_{t,d}}{\sum t' \in d f_{t',d}} \tag{14}$$

- d : Document
- t : Relative Frequency of Term

When calculating the Idf importance value, it is the logarithm of the total number of sentences, the ratio of the selected term to the total number of sentences in all sentences. Eq. 15 shows the calculation method.

$$idf = (t, D) = \log \frac{N}{|\{d \in D : t \in d\}|} \tag{15}$$

After calculating the tf and idf values, the tf-idf value of each word is obtained by multiplying the two values found. Eq. 16 shows the calculation method.

$$tfidf = (t, d, D) = tf(t, d).idf(t, D) \tag{16}$$

The data for which the vector space model was created was divided into an 80% training set and a 20% test set by the Holdout method in model validation methods. As a result, of the 1300 case texts in the data set, 1040 were used for training and 260 for evaluation.

In the third stage of the study, models were developed with KNN, SVM, DT, RF, and XGBoost. Hyperparameter optimization was performed on the models to obtain the best accuracy result. The GridSearchCv object in the scikit-learn library is used for this. With GridSearchCv, separate models were established for the model's hyperparameter values desired to be tested, and the hyperparameter values that gave the most successful results were determined. The hyperparameter values that provide the best accuracy result for the models are shown in Table 4.

Table 4 Hyperparameter results of models

Models	HyperParameters	Value
K-Neaest Neighbors Model	n_neighbors	8
	p(metric)	Manhattan
	c	3
Support Vector Machines Model	kernel	rbf
	max_features	8
	min_samples_split	5
Random Forest Model	n_estimators	100
	criterion	Gini
Decision Tree Model	max_depth	3
	min_samples_split	2
	learning_rate	0.1

max_depth	3
n_estimators	500
subsample	0.6

After the hyperparameter optimization, the final models were established, and the classification performances of the models were compared with the precision, recall, F1-score, and accuracy evaluation criteria. As a result of the assessment showed that the XGBoost model gave the best results with 93.84% Average Accuracy, 93% Precision, 93% Recall, and 93% F1-Score. The performance values of the KNN, SVM, DT, RF, and XGBoost models are shown in Table 5.

Table 5 Model Performance Values

Model	Class	Precision	Recall	F1-Score	Accuracy
KNN Model	No violation (0)	0.80	0.92	0.86	90.76
	Violation (1)	0.93	0.83	0.88	
	Mean/Total	0.87	0.88	0.87	
SVM Model	No violation (0)	0.84	0.94	0.88	89.61
	Violation (1)	0.95	0.87	0.91	
	Mean/Total	0.89	0.90	0.90	
DT Model	No violation (0)	0.83	0.89	0.86	88.07
	Violation (1)	0.92	0.87	0.89	
	Mean/Total	0.87	0.88	0.88	
RF Model	No violation (0)	0.81	0.95	0.87	90
	Violation (1)	0.95	0.84	0.89	
	Mean/Total	0.88	0.89	0.88	
XGBoost Model	No violation (0)	0.90	0.94	0.92	93.84
	Violation (1)	0.95	0.93	0.94	
	Mean/Total	0.93	0.93	0.93	

Classification estimation successes of the models are also shown in Figure 5 with ROC (Receiver Operating Characteristic) curves.

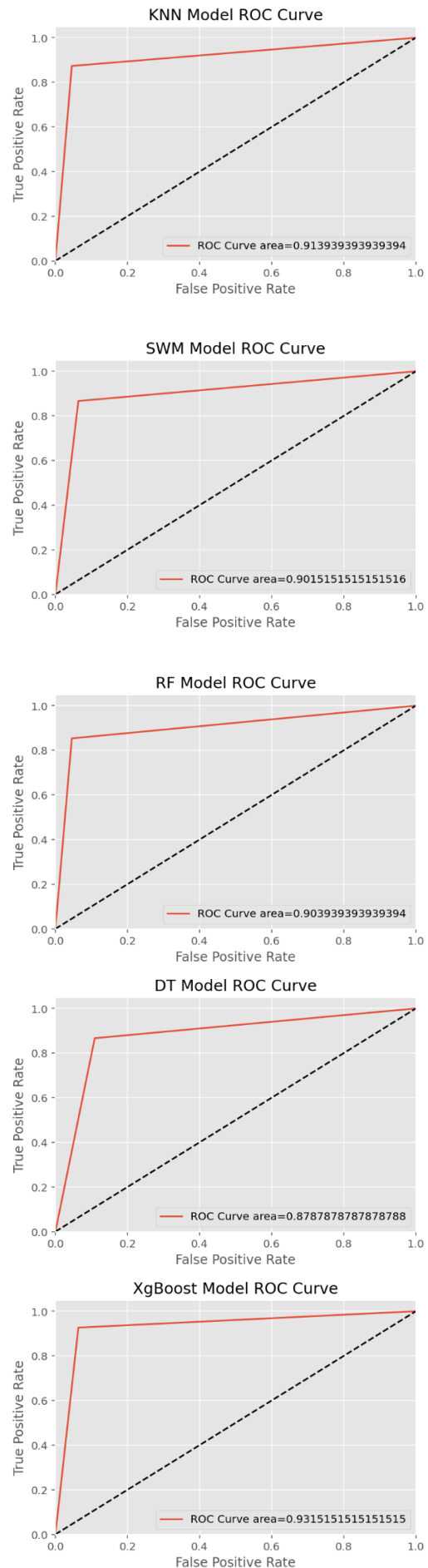


Figure 5. ROC Curve Area

XGBoost, where the best prediction result is obtained in our LJP application, is a tree-based complex machine learning algorithm. Although it provides very high success, the results cannot be interpreted directly. In this study, using the SHAP method, one of the XAI techniques, the variables that affect the classification of the case decisions of the XGBoost model are explained with graphics. The waterfall plot shows the variables that push the model output from the baseline to the predicted model output. In the graph, variables that make the forecast higher are shown with a positive (red) contribution value, and variables that push the forecast down are shown with a negative (blue) contribution value. Figure 6 shows how much each variable affects the estimation result for the first case decision. This is also the result of the local interpretability of the initial decision. In the figure, it is seen that the variable "kararında" is the variable that most affects the $f(x)$ value with the positive value of "+1.64". It is seen that the bars in the graph are mostly red and have positive values. Accordingly, the variables increase the SHAP value for the first case decision. As a result, since the $f(x)$ value moves away from $E[f(x)]$ value positively, it is seen that the case may result in "Violation" for the first case decision.

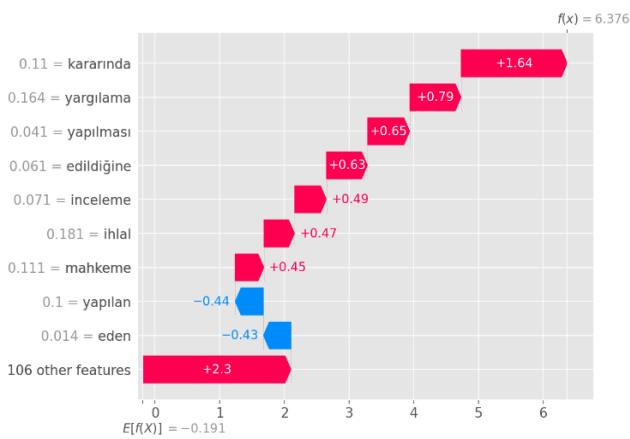


Figure 6. Waterfall Plot for First Case Decision

The force plot in Figure 7 is one of the local interpretability plots that show how variables contribute to the model's prediction. The graph shows the variables that contributed the most to the initial lawsuit decision and their marginal contributions, similar to the Waterfall graph. It is seen that the bars in the graph are mostly red and have positive values. As a result, the case may result in a "Violation" for the first case decision.

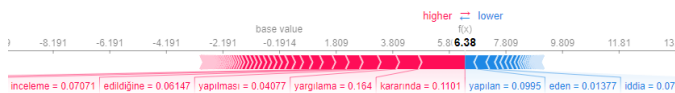


Figure 7. Force Plot for First Case Decision

The bar graph clearly shows the effects of the variables on the model output, thanks to its simple appearance. Figure 8 shows how much each variable affects the estimation result for the 100th example of the case decisions. In the graph, it is seen that the variable "edilmedigine" is the variable that

affects the $f(x)$ value the most, with the negative value of "-1.5". It is seen that the bars in the graph are mostly blue and have negative values. Accordingly, for the 100th case decision sample, the variables decrease the SHAP value. As a result, since the $f(x)$ value deviates from the $E[f(x)]$ value in a negative direction, it is seen that the case for the 100th case decision may result in "No Violation."

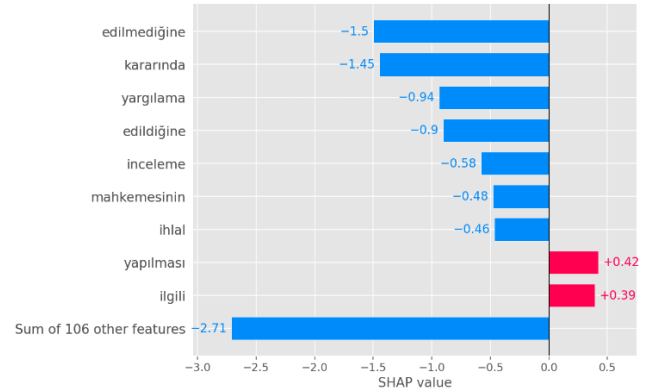


Figure 8 Bar Chart for Centenary Verdict

Beeswarm and Summary plot charts are used to explain the importance of the variables and their contribution to the model on the whole data set. The global interpretability of the model trained with XGBoost in this study is shown in Figure 9 and Figure 10. Each graph dot represents a case decision, while the X-axis shows the SHAP values. When the examine the results obtained in both graphs, it is seen that the variable "kararında" makes the most marginal contribution to the estimates. It is also seen that with the increase of this variable value, the SHAP value also increases. As a result of this, it is seen that the probability that the case will result in "Violation" increases.

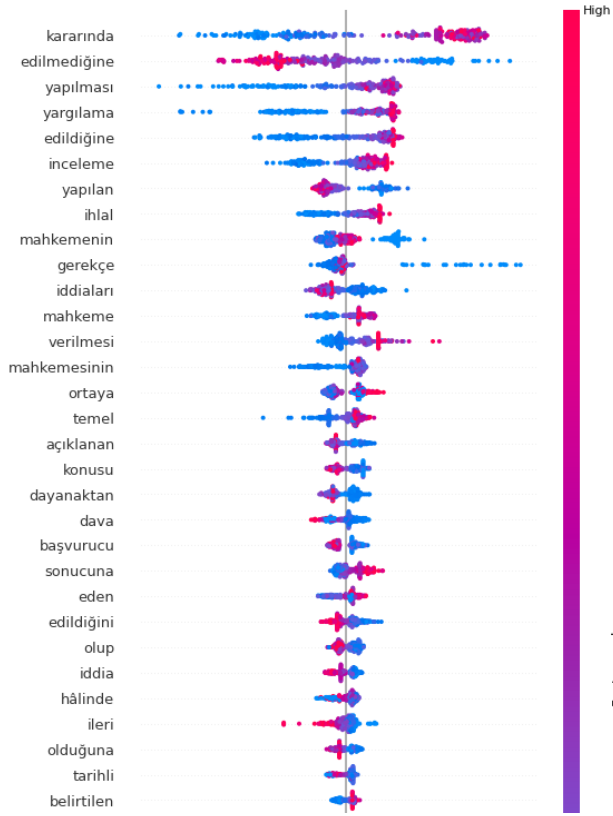


Figure 9. Beeswarm Plot

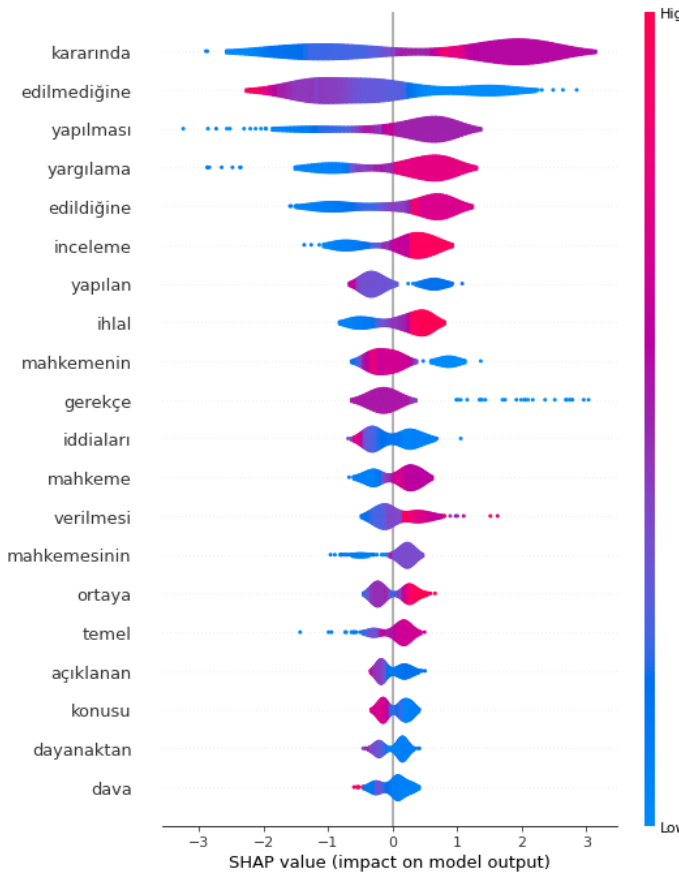


Figure 10. Summary Plot

The last SHAP chart used in the study is the Heatmap plot shown in Figure 11. This graph shows the global interpretability of the trained model. In the graph, the X-axis represents the decision examples, and the y-axis represents the variables. The $f(x)$ curve at the top of the graph is the model estimates of the samples. To the right of the graph are the SHAP values encoded in the color scale. According to the graph, the word "kararında" is the most important variable, and each decision's impact value is shown.

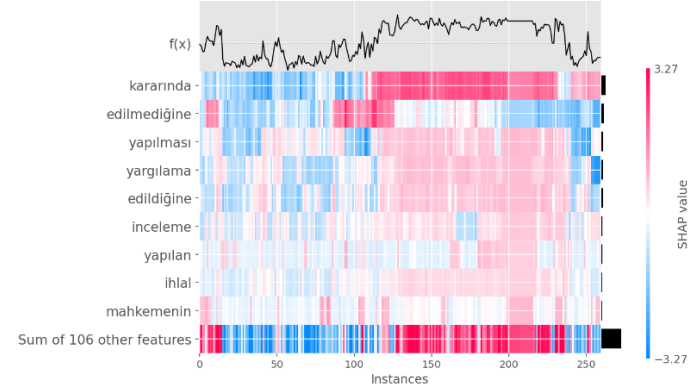


Figure 11. Heatmap Plot

5. DISCUSSION AND CONCLUSIONS

With the LJP applications developed due to the combination of artificial intelligence and legal data, some studies have started a new process in the legal sector. Litigation decisions that take a long time can be concluded quickly, the workload of the legal staff will be alleviated, and they can produce logical, clear results because they do not show emotionality in the decisions. With this study, the Turkish LJP application, which has very few working examples in Turkey, has been developed. The results of the Turkish Constitutional Court case decisions were estimated using the KNN, SVM, DT RF, and XGBoost algorithms. Among the developed models, the XGBoost model achieved the best prediction result with an accuracy rate of 93.07%. The results of the XGBoost model were made more transparent and interpretable by using the SHAP plots techniques such as Waterfall plot, Force plot, Beeswarm plot, Summary plot, Bar plot, and Heatmap plot. According to the results obtained, it was seen that SHAP values produced consistent results. As a result, end-users trust the models and that the decisions are fair and reliable. The AI models, prediction success rates, and the methods used by the Turkish LJP applications in the developed study and the literature are compared in Table 6. Accordingly, it is seen that the study stands out with its success rate and the XAI methods it uses.

Table 6 Comparison of Turkish LJP Studies

Year	Article	Court	Machine Learning Models	Research Handbook on Big Data Law, ed. Vogl, R., 467-481, Edward Elgar Publishing. XAI Plots
2021	Predicting Turkish Constitutional Court Decisions using Artificial Intelligence (Sert et al., 2021)	Constitutional Court of Turkey	MLP	Elstron, M., Piotrowski, Z. (2021). Artificial intelligence applications in military systems and their influence on sense of security of citizens. <i>None</i> , Electronics, 10(7), 871.
2021	Using natural language processing to predict decisions in Turkey's higher courts (Mumcuoğlu et al., 2021)	Constitutional Court of Turkey	DT RF SWM	Brereton, R.G., Lloyd, G.R. (2010). Support vector machines for classification and regression. <i>None</i> , Analysts, 135(2), 230-267.
2022	This study	Constitutional Court of Turkey	DL KNN SWM DT RF XGBoost	Chalkidis, I., Androutsopoulos, I., Aletras, N. (2019). Neural legal judgment prediction in English. arXiv preprint arXiv:1906.02059. Bar Plot Chen, L., Chen, P., Lin, Z. (2020). Artificial intelligence in education: A review. <i>None</i> , Ieee Access, 8, 75264-75278. Summary Plot Chen, T., Guestrin, C. (2016). Xgboost: A scalable tree boosting system. In: Proceedings of the 22nd acm sigkdd international conference on knowledge discovery and data mining, 785-794, Association for Computing Machinery, New York, United States. Besswarm Plot Heatmap Plot

The study is the first in Turkey to explain the model results using SHAP graphics, one of the XAI techniques. The new Turkish law data set has been brought to the literature with the study. In future studies, models with different AI algorithms can be built on the data set, applications can be developed, and Turkish LJP studies can be contributed.

Ethics Committee Approval

N/A

Peer-review

Externally peer-reviewed.

Author Contributions

All authors have read and agreed to the published version of manuscript.

Conflict of Interest

The authors have no conflicts of interest to declare.

Funding

The authors declared that this study has received no financial support.

REFERENCES

Agarwal, R., Melnick, L., Frosst, N., Zhang, X., Lengerich, B., Caruana, R., & Hinton, G. E. (2021). Neural additive models: Interpretable machine learning with neural nets. *Advances in Neural Information Processing Systems*, 34, 4699-4711.

Altreas, N., Tsarapatsanis, D., Preotiuc-Pietro, D., & Lampos, V. (2016). Predicting judicial decisions of the European Court of Human Rights: a Natural Language Processing perspective. *PeerJ Comput Sci.*

Anders, C. J., Neumann, D., Samek, W., Müller, K. R., & Lapuschkin, S. (2021). Software for dataset-wide XAI: from local explanations to global insights with Zennit, CoRelAy, and ViRelAy. arXiv preprint arXiv:2106.13200.

Antos, A., Nadhamuni, N. (2021). Practical guide to artificial intelligence and contract review. In:

Chen, T., Guestrin, C. (2016). Xgboost: A scalable tree boosting system. In: Proceedings of the 22nd acm sigkdd international conference on knowledge discovery and data mining, 785-794, Association for Computing Machinery, New York, United States.

Colaner, N. (2021). Is explainable artificial intelligence intrinsically valuable? *AI & SOCIETY*, 37, 231-238.

Collenette, J., Atkinson, K., Bench-Capon, T. J. (2020). An Explainable Approach to Deducing Outcomes in European Court of Human Rights Cases Using ADFs, In: COMMA, ed. Prakken, H., Bistarelli, S. and Santini, F., 21-32, IOS Press.

Das, A., Rad, P. (2020). Opportunities and challenges in explainable artificial intelligence (xai): A survey. arXiv preprint arXiv:2006.11371.

Di Vaio, A., Palladino, R., Hassan, R., Escobar, O. (2020). Artificial intelligence and business models in the sustainable development goals perspective: A systematic literature review. *Journal of Business Research*, 121, 283-314.

Dong, W., Huang, Y., Lehane, B., Ma, G. (2020). XGBoost algorithm-based prediction of concrete electrical resistivity for structural health monitoring. *Automation in Construction*, 114, 103155.

Doshi-Velez, F., Kim, B. (2017). Towards a rigorous science of interpretable machine learning. arXiv preprint arXiv:1702.08608.

Fletcher, S., Islam, M. Z. (2019). Decision tree classification with differential privacy: A survey. *ACM Computing Surveys (CSUR)*, 52(4), 1-33.

Gan, L., Li, B., Kuang, K., Yang, Y., & Wu, F. (2022). Exploiting Contrastive Learning and Numerical Evidence for Improving Confusing Legal Judgment Prediction. arXiv preprint arXiv:2211.08238.

Ghorbani, A., Wexler, J., Zou, J. Y., Kim, B. (2019). Towards automatic concept-based explanations. *Advances in Neural Information Processing Systems*, 32.

- Ghosh, S., Dasgupta, A., Swetapadma, A. (2019). A study on support vector machine based linear and non-linear pattern classification. In: 2019 International Conference on Intelligent Sustainable Systems (ICISS) (pp. 24-28). IEEE.
- Goertzel, B., Pennachin, C. (2007). The Novamente artificial intelligence engine. *Artificial general intelligence*, 63-129.
- Górski, Ł., Ramakrishna, S. (2021, June). Explainable artificial intelligence, lawyer's perspective. In: Proceedings of the Eighteenth International Conference on Artificial Intelligence and Law (pp. 60-68).
- Gorski, L., Ramakrishna, S., Nowosielski, J. M. (2020). Towards grad-cam based explainability in a legal text processing pipeline. *arXiv preprint arXiv:2012.09603*.
- Gunning, D., Aha, D. (2019). DARPA's explainable artificial intelligence (XAI) program. *AI magazine*, 40(2), 44-58.
- Gunning, D., Stefik, M., Choi, J., Miller, T., Stumpf, S., Yang, G. Z. (2019). XAI—Explainable artificial intelligence. *Science robotics*, 4(37).
- Guo, X., Zhang, H., Ye, L., Li, S. (2021). TenLa: an approach based on controllable tensor decomposition and optimized lasso regression for judgement prediction of legal cases. *Applied Intelligence*, 51, 2233-2252.
- Ivanovs, M., Kadikis, R., Ozols, K. (2021). Perturbation-based methods for explaining deep neural networks: A survey. *Pattern Recognition Letters*, 150, 228-234.
- Jiang, F., Jiang, Y., Zhi, H., Dong, Y., Li, H., Ma, S., Wang, Y. (2017). Artificial intelligence in healthcare: past, present and future. *Stroke and vascular neurology*, 2(4).
- Jiang, H., He, Z., Ye, G., Zhang, H. (2020). Network intrusion detection based on PSO-XGBoost model. *IEEE Access*, 8, 58392-58401.
- Katz, D. M., Bommarito, M. J., Blackman, J. (2017). A general approach for predicting the behavior of the Supreme Court of the United States. *PloS one*, 12(4).
- Kaur, A., Bozic, B. (2019). Convolutional Neural Network-based Automatic Prediction of Judgments of the European Court of Human Rights. In: AICS, pp 458-469
- Kenny, E. M., Ford, C., Quinn, M., Keane, M. T. (2021). Explaining black-box classifiers using post-hoc explanations-by-example: The effect of explanations and error-rates in XAI user studies. *Artificial Intelligence*, 294, 103459.
- Knox, J. (2020). Artificial intelligence and education in China. *Learning, Media and Technology*, 45(3), 298-311.
- Labin, S., Segal, U. (2021). AI-driven contract review: A product development journey. In *Research Handbook on Big Data Law*, 454-466, Edward Elgar Publishing.
- Lapuschkin, S., Wäldchen, S., Binder, A., Montavon, G., Samek, W., Müller, K. R. (2019). Unmasking Clever Hans predictors and assessing what machines really learn. *Nature communications*, 10(1), 1096.
- Letham, B., Rudin, C., McCormick, T. H., Madigan, D. (2012). Building interpretable classifiers with rules using Bayesian analysis. Department of Statistics Technical Report tr609, University of Washington, 9(3), 1350-1371.
- Li, S., Zhang, H., Ye, L., Guo, X., Fang, B. (2019). Mann: A multichannel attentive neural network for legal judgment prediction. *IEEE Access*, 7, 151144-151155.
- Lin, Y. S., Lee, W. C., Celik, Z. B. (2021). What do you see? Evaluation of explainable artificial intelligence (XAI) interpretability through neural backdoors. In: Proceedings of the 27th ACM SIGKDD Conference on Knowledge Discovery & Data Mining (pp. 1027-1035).
- Long, S., Tu, C., Liu, Z., Sun, M. (2019). Automatic judgment prediction via legal reading comprehension. In: Chinese Computational Linguistics: 18th China National Conference, 558-572, Springer International Publishing.
- Loureiro, S. M. C., Guerreiro, J., Tussyadiah, I. (2021). Artificial intelligence in business: State of the art and future research agenda. *Journal of business research*, 129, 911-926.
- Lundberg, SM., Lee, SI. (2017). A unified approach to interpreting model predictions. In: Proceedings of the 31st international conference on neural information processing systems, 30, 4768-4777.
- Ma, L., Zhang, Y., Wang, T., Liu, X., Ye, W., Sun, C., Zhang, S. (2021). Legal judgment prediction with multi-stage case representation learning in the real court setting. In Proceedings of the 44th International ACM SIGIR Conference on Research and Development in Information Retrieval (pp. 993-1002).
- Mangalathu, S., Hwang, S. H., Jeon, J. S. (2020). Failure mode and effects analysis of RC members based on machine-learning-based SHapley Additive exPlanations (SHAP) approach. *Engineering Structures*, 219, 110927.
- Mantovani, R. G., Horváth, T., Cerri, R., Vanschoren, J., De Carvalho, A. C. (2016, October). Hyperparameter tuning of a decision tree induction algorithm. In: 2016 5th Brazilian Conference on Intelligent Systems (BRACIS) (pp. 37-42). IEEE.
- Meço, G., Çoştu, F. (2022). Eğitimde Yapay Zekânın Kullanılması: Betimsel İçerik Analizi Çalışması. *Karadeniz Teknik Üniversitesi Sosyal Bilimler Enstitüsü Sosyal Bilimler Dergisi*, 12(23), 171-193.
- Mumcuoğlu, E., Öztürk, C. E., Ozaktas, H. M., Koç, A. (2021). Natural language processing in law:

- Prediction of outcomes in the higher courts of Turkey. *Information Processing & Management*, 58(5), 102684.
- Mumford, J., Atkinson, K., Bench-Capon, T. (2021). Machine learning and legal argument. In: *CEUR Workshop Proceedings (Vol. 2937, pp. 47-56)*.
- Nanfack, G., Temple, P., Fréney, B. (2022). Constraint Enforcement on Decision Trees: A Survey. *ACM Computing Surveys (CSUR)*, 54(10s), 1-36.
- Nie, W., Zhang, Y., Patel, A. (2018). A theoretical explanation for perplexing behaviors of backpropagation-based visualizations. In: *International Conference on Machine Learning*, PMLR, 3809-3818.
- Nikam, SS. (2015). A comparative study of classification techniques in data mining algorithms. *Oriental Journal of Computer Science and Technology*, 8(1), 13-19.
- Niklaus, J., Chalkidis, I., Stürmer, M. (2021). Swiss-judgment-prediction: A multilingual legal judgment prediction benchmark. *arXiv preprint arXiv:2110.00806*.
- Niklaus, J., Stürmer, M., Chalkidis, I. (2022). An Empirical Study on Cross-X Transfer for Legal Judgment Prediction. *arXiv preprint arXiv:2209.12325*.
- Ribeiro, M. T., Singh, S., Guestrin, C. (2016). Model-agnostic interpretability of machine learning. *arXiv preprint arXiv:1606.05386*.
- Rodríguez-Pérez, R., Bajorath, J. (2020). Interpretation of machine learning models using shapley values: application to compound potency and multi-target activity predictions. *Journal of computer-aided molecular design*, 34, 1013-1026.
- Rokach, L. (2016). Decision forest: Twenty years of research. *Information Fusion*, 27, 111-125.
- Roll, I., Wylie, R. (2016). Evolution and revolution in artificial intelligence in education. *International Journal of Artificial Intelligence in Education*, 26, 582-599.
- Schratz, P., Muenchow, J., Iturritxa, E., Richter, J., Brenning, A. (2019). Hyperparameter tuning and performance assessment of statistical and machine-learning algorithms using spatial data. *Ecological Modelling*, 406, 109-120.
- Semo, G., Bernsohn, D., Hagag, B., Hayat, G., Niklaus, J. (2022). ClassActionPrediction: A Challenging Benchmark for Legal Judgment Prediction of Class Action Cases in the US. *arXiv preprint arXiv:2211.00582*.
- Sert, M. F., Yıldırım, E., Haşlak, İ. (2022). Using artificial intelligence to predict decisions of the Turkish constitutional court. *Social Science Computer Review*, 40(6), 1416-1435.
- Shahid, R., Bertazzon, S., Knudtson, M. L., Ghali, W. A. (2009). Comparison of distance measures in spatial analytical modeling for health service planning. *BMC health services research*, 9(1), 1-14.
- Simonyan, K., Vedaldi, A., Zisserman, A. (2013). Deep inside convolutional networks: Visualising image classification models and saliency maps. *arXiv preprint arXiv:1312.6034*.
- Singh, A., Yadav, A., Rana, A. (2013). K-means with Three different Distance Metrics. *International Journal of Computer Applications*, 67(10), 13-17.
- Socatiyanurak, V., Klangpornkun, N., Munthuli, A., Phienphanich, P., Kovudhikulrungsri, L., Saksakulkunakorn, N., Tantibundhit, C. (2021). Law-u: Legal guidance through artificial intelligence chatbot for sexual violence victims and survivors. *IEEE Access*, 9, 131440-131461.
- Somvanshi, M., Chavan, P., Tambade, S., Shinde, S. V. (2016, August). A review of machine learning techniques using decision tree and support vector machine. In *2016 international conference on computing communication control and automation (ICCUBEA) (pp. 1-7)*. IEEE.
- Spinner, T., Schlegel, U., Schäfer, H., El-Assady, M. (2019). explAIner: A visual analytics framework for interactive and explainable machine learning. *IEEE transactions on visualization and computer graphics*, 26(1), 1064-1074.
- Stevenson, D., Wagoner, N. J. (2015). Bargaining in the shadow of big data. *Fla. L. Rev.*, 67, 1337.
- Strickson, B., De La Iglesia, B. (2020, March). Legal judgement prediction for uk courts. In *Proceedings of the 3rd International Conference on Information Science and Systems (pp. 204-209)*.
- Tideman, L. E., Migas, L. G., Djambazova, K. V., Patterson, N. H., Caprioli, R. M., Spraggins, J. M., Van de Plas, R. (2021). Automated biomarker candidate discovery in imaging mass spectrometry data through spatially localized Shapley additive explanations. *Analytica Chimica Acta*, 1177, 338522.
- Tritscher, J., Ring, M., Schlr, D., Hettlinger, L., & Hotho, A. (2020). Evaluation of post-hoc XAI approaches through synthetic tabular data. In *Foundations of Intelligent Systems: 25th International Symposium, ISMIS 2020, Graz, Austria, September 23–25, 2020, Proceedings (pp. 422-430)*. Springer International Publishing.
- Turan. T., Turan, G., Köse, U. (2022). Uyarlamalı Ağ Tabanlı Bulanık Mantık Çıkarım Sistemi ve Yapay Sinir Ağları ile Türkiye'deki COVID-19 Vefat Sayısının Tahmin Edilmesi. *Bilişim Teknolojileri Dergisi* 15(2), 97-105.
- Weber, T., Wermter, S. (2020). Integrating intrinsic and extrinsic explainability: The relevance of understanding neural networks for human-robot interaction. *arXiv preprint arXiv:2010.04602*.

- Xiao, C., Zhong, H., Guo, Z., Tu, C., Liu, Z., Sun, M., Xu, J. (2018). Cail2018: A large-scale legal dataset for judgment prediction. arXiv preprint arXiv:1807.02478.
- Xu, Z. (2022). Human judges in the era of artificial intelligence: challenges and opportunities. *Applied Artificial Intelligence*, 36(1), 2013652.
- Yan, G., Li, Y., Shen, S., Zhang, S., Liu, J. (2019, July). Law article prediction based on deep learning. In 2019 IEEE 19th International Conference on Software Quality, Reliability and Security Companion (QRS-C) (pp. 281-284). IEEE.
- Yang, L., Zeng, J., Peng, T., Luo, X., Zhang, J., Lin, H. (2020, October). Leniency to those who confess. Predicting the Legal Judgement via Multi-Modal Analysis. In Proceedings of the 2020 International Conference on Multimodal Interaction (pp. 645-649).
- Yu, K. H., Beam, A. L., Kohane, I. S. (2018). Artificial intelligence in healthcare. *Nature biomedical engineering*, 2(10), 719-731.
- Zadgaonkar, A. V., Agrawal, A. J. (2021). An overview of information extraction techniques for legal document analysis and processing. *International Journal of Electrical & Computer Engineering* (2088-8708), 11(6).
- Zeiler, M. D., Fergus, R. (2014). Visualizing and understanding convolutional networks. In *Computer Vision—ECCV 2014: 13th European Conference, Zurich, Switzerland, September 6-12, 2014, Proceedings, Part I 13* (pp. 818-833). Springer International Publishing.
- Zhong, H., Guo, Z., Tu, C., Xiao, C., Liu, Z., Sun, M. (2018). Legal judgment prediction via topological learning. In Proceedings of the 2018 conference on empirical methods in natural language processing (pp. 3540-3549).

Modeling of *E. coli* Inactivation from Solutions using GInaFiT via Hybrid Electrode Connected Electro-Disinfection Process

Murat Solak^{1*} , Rüya Tekin Karaköse² 

Abstract: *E. coli* (*Escherichia coli*) is a bacterium found in human and animal intestines. These bacteria, which can enter the bloodstream through as anyway as the environment or food, can cause many diseases such as diarrhea, respiratory problems, and blood/urinary tract infections, especially in humans. Therefore, these bacteria have to be removed from drinking water sources by some inactivation methods. Conventional methods such as chlorination, ozonation, and UV inactivation methods are effective. But the development of techniques that do not require the transportation and storage of chemicals and do not produce negative by-products and are cost-effective on the basis of environmental engineering studies. In this study, the inactivation effectiveness of a hybrid electrode-connected electrochemical process as a new approach on *E. coli* was investigated. The connection system was experienced with Al/SS/SS as Anode/Cathode/Anode electrode. Simultaneously electrocoagulation (EC) and electrooxidation (EO) mechanism works together in this electrode connection system. The inactivation coefficients were determined by the GInaFiT (Geeraerd and Van Impe Inactivation Model Fitting Tool) modeling tool, which is a Microsoft Excel add-on and the model was statistically well fitted with Double-Weibull. 4D degradation of *E. coli* was achieved as 21 minutes at a current density of 0.3 A and an optical density (O.D.) of 0.21. It has been determined that hybrid electrode-connected electro-disinfection process is an effective approach for the *E. coli* inactivation.

Keywords: Electro-disinfection, *E. coli*, inactivation models, hybrid electrode, Double Weibull.

*¹**Address:** Düzce University, Faculty of Engineering, Department of Environmental Engineering, Düzce/Türkiye

²**Address:** Düzce University, Graduate School of Natural and Applied Sciences, Department of Environmental Engineering Düzce/Türkiye

Corresponding author: muratsolak@duzce.edu.tr

Citation: Solak M., Tekin Köse, R. (2023). Modeling of *E. coli* Inactivation from Solutions using GInaFiT via Hybrid Electrode-Connected Electro-Disinfection Process. Bilge International Journal of Science and Technology Research, 7(2): 142-155.

1. INTRODUCTION

One of the most basic needs for people and all other living things to continue their vital activities is clean drinking and utility water. For this reason, clean water supply, water treatment, and water recovery will be the most important research topics for all countries today and in the future.

Drinking and using water must comply with the minimum standards determined by each country. Physical, chemical, organic, inorganic and bacteriological parameters are used in the evaluation of water quality. Total coliform and fecal

coliform parameters are generally used in the evaluation of bacteriological contamination in water. One of the markers of bacteriological contamination in waters as a pathogenic microorganism is *E. coli* (*Escherichia coli*), a Gram (-) member of the Enterobacteriaceae family. *E. coli* is a subgroup of fecal coliform. A general distribution diagram of bacteriological indicators and *E. coli* in water is shown in Figure 1. (W.S. Dep. of Health Division of Env. Health Office of Drinking Water).

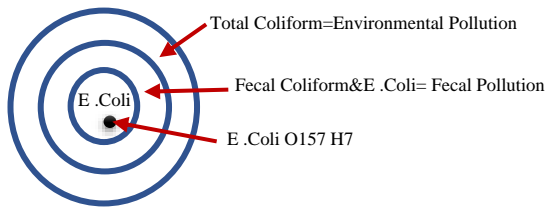


Figure 1. General distribution chart of *E. coli*

The usage of electrochemical processes has increased in recent years due to the convenience of operating/investment costs, ease of operation and alternative treatment processes to conventional processes. Electrochemical processes can simultaneously remove many pollutants such as chemical oxygen demand (COD) (Solak et al., 2023 a and b), suspended solid (SS), color, and heavy metals. To remove pathogenic microorganisms, chemical processes such as Cl_2 (Fiorentino et al., 2021), O_3 (Taoran Liu et al., 2019), physical processes such as ultraviolet (UV) (Fiorentino et al., 2021) or their hybrid configurations and advanced filtration techniques such as membrane filtration processes (Saleh et al., 2021) are used.

Electrochemical processes, which have recently been used and developed as environmentally friendly, are accepted as promising methods for pathogen removal from water (Feng et al., 2004; Delaedt et al., 2008; Li et al., 2011). Electrochemical technologies include disinfection types such as electrosorption (Matsunaga et al., 2000), and electrophoresis (Rowan et al., 2001). In addition, electrochemical processes have been successfully applied in the inactivation of different organisms (bacteria, viruses and microalgae) (Li et al., 2011). Bacterial inactivation of *E. coli* and *Legionellapneumophila* occurs effectively in various studies where electrochemical processes are applied. (Delaedt et al., 2008; Feng et al., 2004; Diao et al., 2004; Liv et al., 2004; Patermarakis and Fountoukidis 1990). *E. coli* is effectively removed by the EC process, which is one of the electrochemical processes. The most commonly used electrode types in these processes are Aluminum (Al) and Iron (Fe) electrodes as they are cheap and easy to supply (Haydar and Aziz, 2009; Mohammed and Sivakumar, 2009; Holt et al., 2005). The EO process is a subsection of electrochemical processes in which insoluble electrodes such as TiO_2 , Ti/RuO_2 , SS, and BBD are generally used. This process is effective for the degradation of organic pollutants (Diaz et al., 2011) and bacteriological pathogens (Isidro et al., 2020).

To determine the mechanism and the efficacy of the inactivation processes some predictive models are used. These models are also grouped as primary, secondary, and tertiary models. Primary models track a microorganism's reaction to a single set of circumstances throughout time. The response might be either direct or indirect indicators of microbial population density or metabolic products. Secondary models define how primary model parameters vary in response to one or more environmental or cultural elements (for example, atmosphere, pH, temperature, etc.). Tertiary models are computer-based adaptations of primary and secondary models (Whiting and Buchanan, 1993). In the study, a tertiary model was preferred to model the *E. coli*

inactivation of the hybrid electrode-connected electro-disinfection process with the GInaFiT modeling program, which is a Microsoft Excel add-on.

Real-life applications show that there is no single treatment method that can perform a complete, efficient and cost-effective disinfection process in accordance with the literature. The aim of the study is to develop a new approach to the hybrid electrode connected electro disinfection process, to determine the effective applied current, to determine the inactivation capability of pathogenic microorganisms and to determine which model fits the *E. coli* inactivation with hybrid electrochemical technique.

2. MATERIAL and METHOD

2.1. Preparation of *E. coli* suspension

In the study, the water that was electrochemically disinfected was prepared synthetically with sterile water. *E. coli* (ATCC 25922) was prepared from lyophilized strains as specified by the ATCC. The resulting biomass was used to create cellular suspensions at appropriate bacterial densities in sterile electrolytic solutions. 3N NaCl (Merck) was used to provide electrochemical conductivity, and 0.1 N HCl and 0.1 N NaOH were used to neutralize water.

2.2. Electro-disinfection Experimental Studies

A water-cooled reactor with a volume of 0.5 L, made of plexiglass, was used in the removal of *E. coli* from wastewater employing electro-disinfection process. The reactor internal dimensions were 8x8x11cm. 0.45 L water was used in each experiment. Anode/Aluminum (Al)/(+), Cathode/Stainless Steel (SS)/(-), Anode/Stainless Steel (SS)/(+) electrodes with approximately 80 cm² active surface area were used in the electro-disinfection process. (Figure 2). Electrode dimensions were 10cmx4cm; The dimensions that react in water were 5cmx4cm.

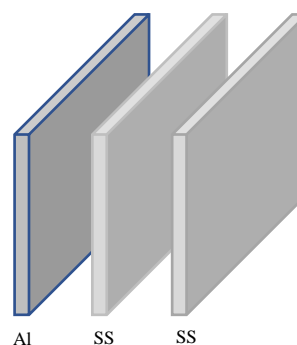


Figure 2. Hybrid connection of electrodes

The experimental design is given in Figure 3. The reaction was started after the electrodes, which were prepared synthetically and whose absorbance at 600 nm was determined, were washed with HCl on the wastewater surfaces of which the number of colonies was determined, and placed in the reactor. During the reaction, the sample was mixed with a magnetic stirrer at 300 rpm. The temperature, which was measured continuously during the reaction, was

kept at room temperature by the water-cooling system outside the reactor. In the first stage, the variation of *E. coli* inactivation with time was observed at constant *E. coli* and current densities. The effect of the current on constant *E. coli* concentration was determined.

The opacity of a bacterial solution which is called optical density (OD600) of the *E. coli* was analyzed by using a Hach DR6000 spectrophotometer at a 600 nm wavelength. The initial and residual number of *E. coli* in the wastewater was determined by counting.

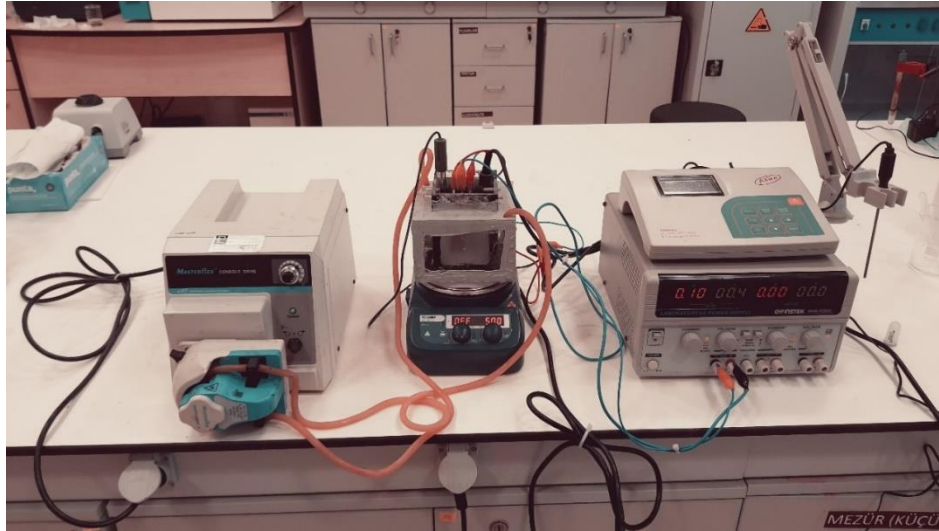


Figure 3. Experimental set-up of electro-disinfection

2.3. Determination of Inactivation Coefficient

Inactivation curves corresponding to the experimental data were performed using the Microsoft Excel add-in tool GInaFiT, developed by Geeraerd (Geeraerd ve Van Impe Inactivation Fitting Tool). With GInaFiT, the change of bacterial cells (log CFU/ml) damaged by disinfection methods over time is determined by various microbial inactivation models. Models used: Log-linear, Log-linear + shoulder, Log-linear + tail, Log-linear + shoulder + tail,

Weibull, Weibull + tail, Double Weibull, Biphasic Model and Biphasic + shoulder. In addition, model parameters such as the inactivation coefficient in the GInaFiT program provide information on various subjects such as the resistance of bacterial cells to stress, residual cell concentration and purification efficiency. Inactivation models' equations and coefficients are given in Table 1.

Table 1. Inactivation models' equations and coefficients

Model	Equations	Coefficients	Reference
Log-linear	$N = N_0 \cdot \exp(-k_{max} \cdot t)$	k_{max}	Bigelow and Esty 1920
Log-linear shoulder	$N = N_0 \cdot \exp(-k \cdot t) \cdot (\exp(k \cdot SI)) / (1 + (\exp(k \cdot SI) - 1) \cdot \exp(-k \cdot t))$	k, SI	Geeraerd et al., 2000
Log-linear tail	$N = (N_0 - N_{res}) \cdot \exp(-k \cdot t) + N_{res}$	k, N_{res}	Geeraerd et al., 2000
Log-linear shoulder+tail	$N = (N_0 - N_{res}) \cdot \exp(-k \cdot t) \cdot ((\exp(k \cdot SI)) / (1 + (\exp(k \cdot SI) - 1) \cdot \exp(-k \cdot t))) + N_{res}$	k, N_{res}, SI	Geeraerd et al., 2000
Weibull	$N/N_0 = 10^{-((\frac{t}{a})^n)}$	a, n	Mafart et al., 2002.
Weibull fixed p	$N/N_0 = 10^{-((\frac{t}{b})^p)}$	p	Mafart et al., 2002.
Weibull+tail	$N = (N_0 - N_{res}) \cdot 10^{-((\frac{t}{a})^n)} + N_{res}$	a, n, N_{res}	Albert and Mafart 2005.
Double Weibull	$N(t) = \left(\frac{N_0}{(1 + 10^a)} \right) \cdot \left(10^{-((\frac{t}{a_1})^{n_1 + a}} + 10^{-((\frac{t}{a_2})^{n_2}}) \right)$	a_1, a_2, n_1, n_2, a	Coroller et al. 2006.
Biphasic	$N = N_0 \cdot (f \cdot \exp(-k_1 \cdot t) + (1 - f) \cdot \exp(-k_2 \cdot t))$	f, k_1, k_2	Cerf et al, 1977.
Biphasic + shoulder	$\log_{10}(N) = \log_{10}(N_0) + \frac{\log_{10}(f \cdot \exp(-k_1 \cdot t) \cdot \exp(k_1 \cdot SI))}{1 + (\exp(k_1 \cdot SI) - 1) \cdot \exp(-k_1 \cdot t)} \cdot \left(1 - f \cdot \exp(-k_2 \cdot t) \cdot \frac{\exp(k_2 \cdot SI)}{1 + (\exp(k_1 \cdot SI) - 1) \cdot \exp(-k_1 \cdot t)} \right) \cdot \exp(-k_1 \cdot t)^{(k_2/k_1)}$	f, k_2, k_2, SI	Geeraerd et al., 2006.

N: microbial population at any time; N_0 : initial microbial population; k: specific inactivation coefficient; N_{res} : residual population density; Sl: shoulder length; a: scale parameter;

n: shape parameter; k_1 and k_2 : specific inactivation rates of the two subpopulations; f: fraction of the initial population in a less resistant subpopulation.

2.4. Equations

In microbial inactivation studies, logarithmic removal efficiency is calculated by Equation 1.

$$\log \text{removal} = -\log_{10}(N_0/N_t) \quad \text{Eq. 1}$$

N_0 = initial concentration of *E. coli* (CFU/mL), N_t = *E. coli* concentration at time t (CFU/mL)

The current density was calculated by Equation 2.

$$J = I/A \quad \text{Eq. 2.}$$

Here; J: Current density, A/m², I: current (Ampere), A: Active surface area, cm².

3. RESULTS and DISCUSSION

3.1. Experimental Results

0.1 A (1.25 mA/cm²), 0.2 A (2.5 mA/cm² and 0.3 A (3.75 mA/cm²) current was applied to the Al/SS/SS connected electrochemical process. The experimental results of the study are given in Table 2. Initial number of *E. coli* was varied from 54.10⁶ to 56.10⁶. When 0.1 A current was applied to the water, 4D degradation of *E. coli* was achieved in >30 minutes, and in a 0.2 A was applied current >38 minutes. In a 0.3 A applied current, 4D was achieved at a minute of 21. The inactivation effectiveness of the process was increased with the increase of applied current.

Table 2. Experimental results

Time (min.)	0.1 A (1.25 mA/cm ²)			0.2 A (2.5 mA/cm ²)			0.3 A (3.75 mA/cm ²)		
	<i>E. coli</i> Number	Log N/No	R.E. (%)	<i>E. coli</i> Number	Log N/No	R.E. (%)	<i>E. coli</i> Number	Log N/No	R.E. (%)
0	54000000	0	0	56000000	0	0	56000000	0	0
2	52000000	-0.01639	3.703704	38000000	-0.1684	32.14286	54000000	-0.01579	3.571429
4	50000000	-0.03342	7.407407	31000000	-0.25683	44.64286	48000000	-0.06695	14.28571
6	48000000	-0.05115	11.11111	29000000	-0.28579	48.21429	14900000	-0.575	73.39286
8	47000000	-0.0603	12.96296	12500000	-0.65128	77.67857	12700000	-0.64438	77.32143
10	32500000	-0.22051	39.81481	10000000	-0.74819	82.14286	5400000	-1.01579	90.35714
12	32300000	-0.22319	40.18519	5100000	-1.04062	90.89286	4000000	-1.14613	92.85714
14	19800000	-0.43573	63.33333	4200000	-1.12494	92.5	3600000	-1.19189	93.57143
16	11300000	-0.67932	79.07407	4000000	-1.14613	92.85714	1400000	-1.60206	97.5
18	11100000	-0.68707	79.44444	3500000	-1.20412	93.75	1340000	-1.62108	97.60714
20	8600000	-0.7979	84.07407	2400000	-1.36798	95.71429	1190000	-2.5	97.875
22	8400000	-0.80811	84.44444	1700000	-1.51774	96.96429	190	-5.46943	99.99966
24	7500000	-0.85733	86.11111	1250000	-1.65128	97.76786			
26	6300000	-0.93305	88.33333	220000	-2.40577	99.60714			
28	5900000	-0.96154	89.07407	50000	-3.04922	99.91071			
30	1480000	-1.56213	97.25926	28000	-3.30103	99.95			
32	1340000	-1.60529	97.51852	0		100			
34	1210000	-1.64961	97.75926						
36	1190000	-1.65685	97.7963						
38	230000	-2.3067	99.57407						
40	30000	-3.25527	99.94444						

3.2. Optical Density of the *E. coli* Colony

0.1 A (1.25 mA/cm²), 0.2 A (2.5 mA/cm²) and 0.3 A (3.75 mA/cm²) current was applied to the Al/SS/SS connected electrochemical process. The absorbance values (Optical Density₆₀₀-OD₆₀₀) are given in Table 3. The density of a cell suspension (Optical Density) is related to the number of

cells, and optical density is employed to assess this density. With the use of this measurement, it will be possible to estimate how the decrease in *E. coli* cells has affected the media's opacity. (Kourdali et al., 2018).

Table 3. The optical density of *E. coli*

	Applied Current		
	0.1 A (1.25 mA/cm ²)	0.2 A (2.5 mA/cm ²)	0.3 A (3.75 mA/cm ²)
Time (min.)	Abs (600nm)	Abs (600nm)	Abs (600nm)
0	0.512	0.530	0.530
2	0.510	0.523	0.514
4	0.504	0.512	0.509
6	0.503	0.489	0.494
8	0.501	0.481	0.472
10	0.496	0.439	0.429
12	0.492	0.381	0.332
14	0.489	0.369	0.325
16	0.484	0.352	0.283
18	0.473	0.351	0.258
20	0.444	0.300	0.200
22	0.434	0.248	0.145
24	0.377	0.168	
26	0.346	0.142	
28	0.300	0.134	
30	0.287	0.092	
32	0.239	0.085	
34	0.228		
36	0.207		
38	0.146		
40	0.111		

OD₆₀₀ values for different applied current values are given in Figure 4. As it is seen in Figure 4 that OD₆₀₀ values of *E. coli* inactivation were almost the same for all applied current values at a time of 0 to 8 min. After 8 min. inactivation effect of 0.1 A current was less effective than 0.2 A and 0.3 A. 4D

inactivation of *E. coli* was determined at a time of 21 min. The increase of current increases the *E. coli* inactivation. It is thought that applying a 0.4 A current can present a shorter time 4D inactivation opportunity.

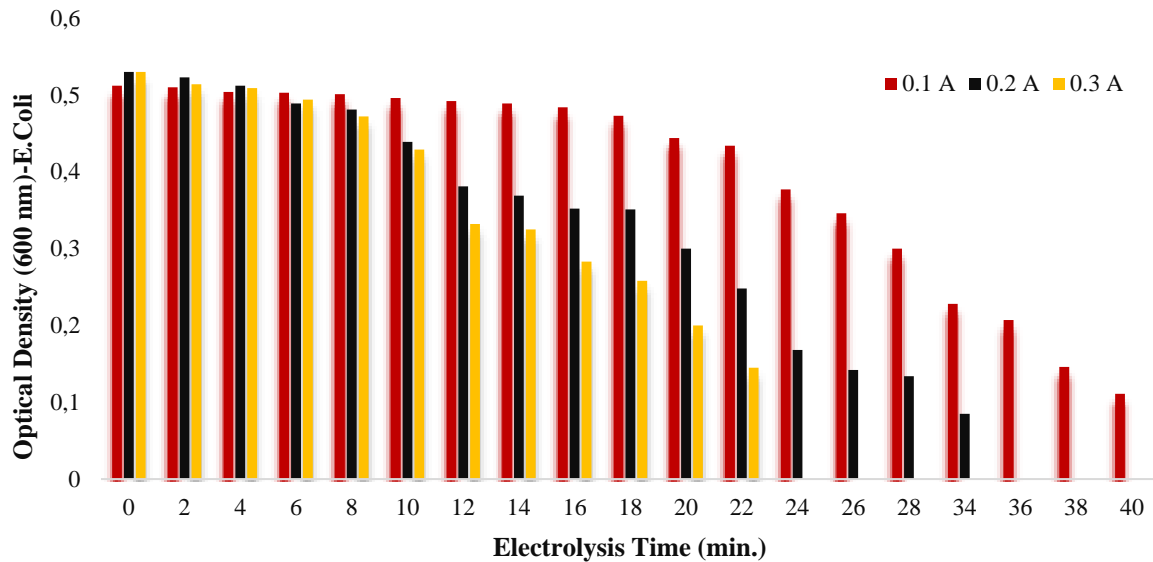


Figure 4. OD 600 Values for 0.1 A, 0.2 A and 0.3 A

Outlet concentration of *t* versus electrolysis time is given in Figure 5.



Figure 5. Outlet Concentration of *E. coli* versus electrolysis time (for 0.3 A)

3.3. Data Modeling of *E. coli* Inactivation Kinetics

The GInaFit was used to determine the inactivation model of the electro-disinfection process. GInaFit is an add-in Excel component (<https://cit.kuleuven.be/biotec>) that was released by Geeraerd et al. (2015). This programme can be applied by selecting the time versus $\log N/N_0$. Then the GInaFit plugin is selected (Figure 6) and the desired model is created with the help of the plugin (Figure 7). With this plugin, statistical

parameters such as coefficient of determination (R^2), adjusted R^2 , sum of squares of error (SSE), sum of squares of mean error (MSE), root mean square error (RMSE), experimental and estimated values, and 2D graphs can be obtained (Figure 8). The significance of the models and parameters is evaluated by these statistical parameters.

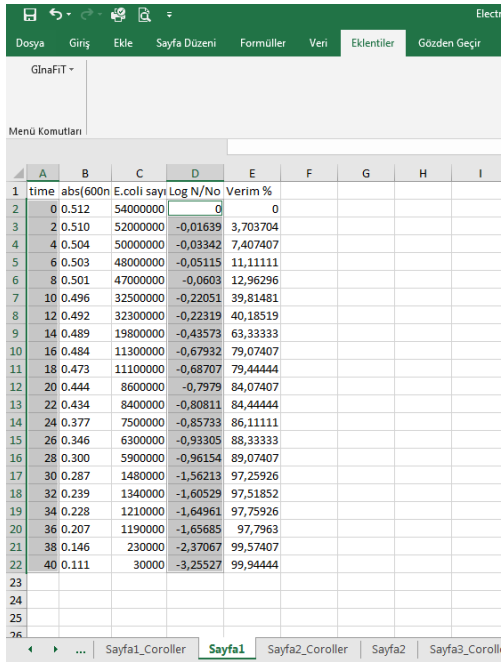


Figure 6. Selecting the time versus log N/N₀

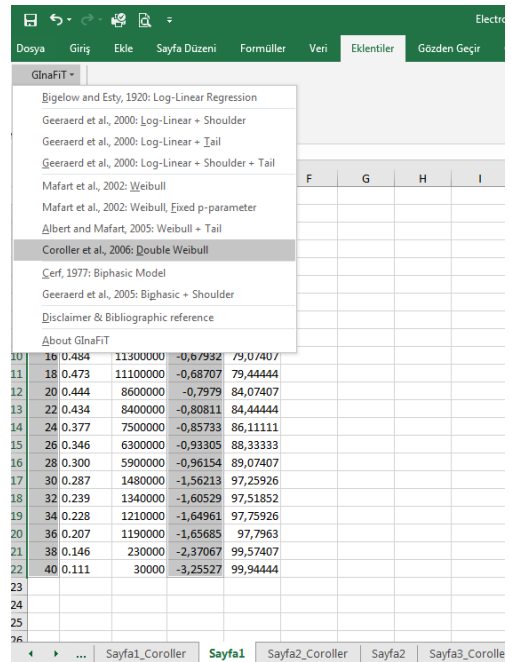


Figure 7. Selecting the model

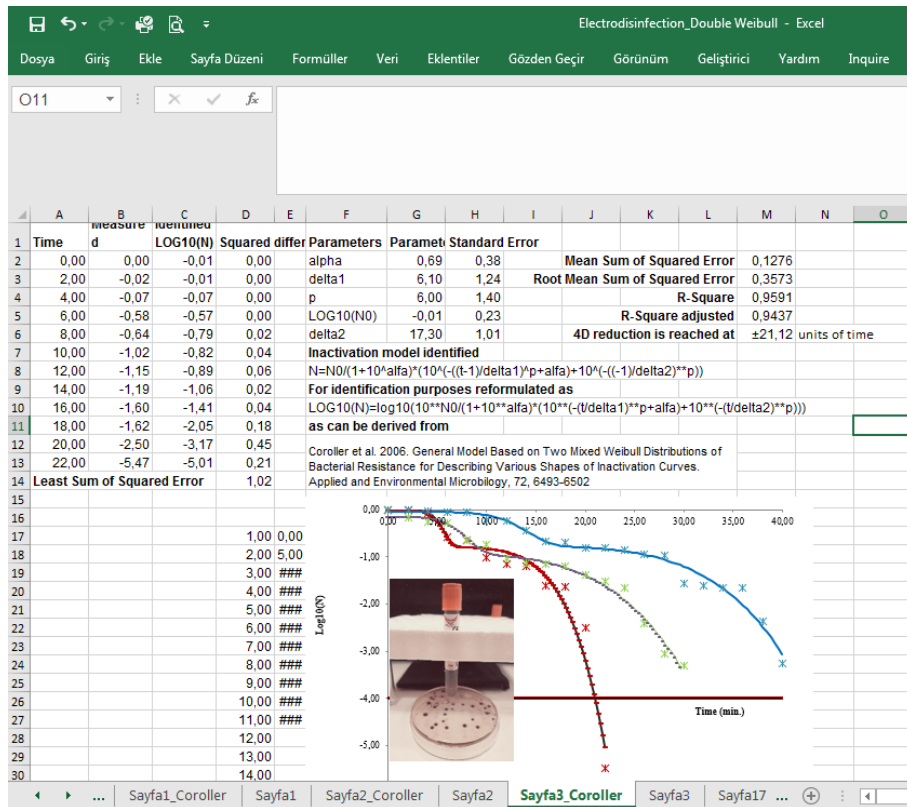


Figure 8. Evaluation of model results of the GlnaFIT

Modeling kinetic parameters of *E. coli* under different current densities is given in Table 4.

Table 4. Inactivation models and coefficients

Model	Current (A)	R ²	R ² _{adj}	a	b	kmax	c	Log ₁₀ (N ₀)	c				
Log-linear	0.1	0.86	0.85	0.1116	0.3341	0.15	0.01	0.39	0.14				
	0.2	0.90	0.89	0.1025	0.3201	0.22	0.02	0.22	0.15				
	0.3	0.71	0.68	0.7354	0.8576	0.40	0.08	0.61	0.47				
	Current (A)	R ²	R ² _{adj}	a	b	kmax	c	Log ₁₀ (N ₀)	c	Sl	c	4D reduction is reached at	
Log-linear shoulder	0.1	0.92	0.91	0.0681	0.2611	0.24	0.03	-0.10	0.11	16.65	2.65		
	0.2	0.93	0.92	0.0814	0.2852	0.30	0.04	-0.21	0.16	9.18	2.66		
	0.3	0.87	0.84	0.3721	0.6100	2.36	0.60	-0.71	0.20	17.65	0.85	21.56	
	Current (A)	R ²	R ² _{adj}	a	b	kmax	c	Log ₁₀ (N ₀)	c	Log ₁₀ (N _{res})	c		
Log-linear tail	0.1	0.86	0.84	0.1178	0.3433	0.15	0.02	0.39	0.17	-13.35	> 70.10 ⁶		
	0.2	0.90	0.88	0.1103	0.3322	0.22	0.03	0.22	0.18	-15.03	> 10.10 ¹¹		
	0.3	0.82	0.90	0.7052	0.6397	0.40	0.12	0.61	0.54	-14.75	> 41.10 ¹⁰		
	Current (A)	R ²	R ² _{adj}	a	b	kmax	c	Log ₁₀ (N ₀)	c	Log ₁₀ (N _{res})	c	Sl	c
Shoulder tail	0.1	0.92	0.90	0.0722	0.2686	0.24	0.06	-0.10	0.12	-33.89		16.65	3.26
	0.2	0.93	0.91	0.0881	0.2969	0.30	0.07	-0.21	0.18	-33.42		9.18	3.33
	0.3	0.87	0.82	0.4186	0.6470	2.36	1.33	-0.71	0.22	-17.56	> 44.10 ¹¹	17.65	1.13
	Current (A)	R ²	R ² _{adj}	a	b	delta	c	Log ₁₀ (N ₀)	c	p	c	4D reduction is reached at	
Weibull	0.1	0.94	0.93	0.0493	0.2221	27.08	1.52	-0.11	0.09	2.48	0.35		
	0.2	0.95	0.94	0.0573	0.2394	17.91	1.53	-0.26	0.12	2.06	0.33		
	0.3	0.89	0.86	0.3192	0.5650	15.88	1.24	-0.53	0.23	4.89	1.21	±21.12	
	Current (A)	R ²	R ² _{adj}	a	b	delta	c	Log ₁₀ (N ₀)	c	p	c		
Weibull fixed	0.1	0.91	0.89	0.1076	0.3280	10.49	3.09	0.20	0.26	1.02	0.24		
	0.2	0.86	0.85	0.1151	0.3393	15.89	4.55	0.37	0.24	1.02	0.26		
	0.3	0.71	0.64	0.8064	0.8980	5.85	4.71	0.59	0.76	1.02	0.55		

	Current (A)	R ²	R ² _{adj}	a	b	delta	c	Log ₁₀ (N ₀)	c	p	c	Log ₁₀ (N _{res})	c		
Weibull tail	0.1	0.94	0.93	0.0522	0.2285	27.08	1.60	-0.11	0.10	2.48	0.56	-12.23	16.10 ⁸		
	0.2	0.95	0.94	0.0621	0.2492	17.91	1.70	-0.26	0.14	2.06	0.51	-13.38	95.10 ⁸		
	0.3	0.92	0.89	0.2577	0.5077	17.41	1.16	6.60	3.15	-0.54	0.20	-15.48	36.10 ⁹		
	Current (A)	R ²	R ² _{adj}	a	b	Alpha	c	Delta 1	c	P	c	Log ₁₀ (N ₀)	c	Delta 2	c
Double Weibull	0.1	0.98	0.98	0.14	0.019	0.70	0.14	8.97	0.9	4.22	0.59	-0.14	0.08	24.11	0.84
	0.2	0.97	0.97	0.15	0.022	0.61	0.13	15.34	1.14	5.7	0.84	-0.04	0.07	34.52	0.83
	0.3	0.96	0.94	0.36	0.13	0.69	0.38	6.1	1.24	6	1.4	0.01	0.23	17.30	1.01
	Current (A)	R ²	R ² _{adj}	a	b	f	c	Log ₁₀ (N ₀)	c	kmax1	c	kmax2	c		
Biphasic	0.1	0.86	0.83	0.1248	0.3532	0.8475	90.10 ¹³	0.39	0.15	0.15	-	0.15	-		
	0.2	0.90	0.88	0.1195	0.3457	0.8722		0.22	-	0.22	-	0.22	-		
	0.3	0.71	0.60	0.9192	0.9588	0.7763	19.10 ¹⁴	0.61	0.54	0.40	-	0.40	-		
	Current (A)	R ²	R ² _{adj}	a	b	f	c	Log ₁₀ (N ₀)	c	kmax1	c	kmax2	c	Sl	
Biphasic shoulder	0.1	0.92	0.90	0.0767	0.2769	1.0000	-	-0.10	-	0.24	-	0.24	-	16.65	
	0.2	0.93	0.90	0.0962	0.3101	1.0000	-	-0.21	-	0.30	-	0.30	-	9.18	
	0.3	0.87	0.79	0.4784	0.6917	1.0000	-	-0.71	-	2.36	-	2.36	-	17.65	

c: Standart Error

A log-linear equation, which is based on the idea that there is a negative and linear relationship between cell count and deadly treatment/inactivation rate, is the most fundamental method for describing the inactivation kinetics (Bevilacqua et al., 2015). R^2 , and adjusted R^2 were checked to determine the adequacy of the models. The R^2 value of the Log-linear model for 0.1 A, 0.2 A and 0.3 A was determined as 0.86, 0.9 and 0.71, respectively, while R^2_{adj} values were 0.85, 0.89 and 0.68, respectively. The 2D plot of the Log-linear inactivation model is given in Figure 9a. The term "log-linear shoulder model" describes first-order inactivation kinetics that have the shoulder parameter added (Geeraerd et al. 2000). R^2 values of the Log-linear shoulder model for 0.1 A, 0.2 A and 0.3 A were determined as 0.92, 0.93 and 0.87, respectively, while R^2_{adj} values were 0.91, 0.92 and 0.84, respectively. Figure 9b shows the log-linear shoulder inactivation model of *E. coli*. Log-linear tail model refers to conventional first-order inactivation kinetics with an added tail parameter (Geeraerd et al. 2000). R^2 values of the Log-linear tail model for 0.1 A, 0.2 A and 0.3 A were determined as 0.86, 0.90 and 0.82, respectively, while R^2_{adj} values were 0.84, 0.88 and 0.90, respectively. But the minimum value that may be measured is less than $\text{Log}_{10}(N_{res})$. For this data, a model with tailing is implausible, and the findings do not fit the model. Log-linear shoulder tail model refers to conventional first-order inactivation kinetics with an added shoulder and tail parameter (Geeraerd et al. 2000). R^2 values of Log linear shoulder tail model for 0.1 A, 0.2 A and 0.3 A were determined as 0.92, 0.93 and 0.87, respectively, while R^2_{adj} values were 0.90, 0.91 and 0.82, respectively. $\text{Log}_{10}(N_{res})$, however, is lower than the smallest measured value. For this data, a model with tailing is implausible, and the findings do not fit the model.

The Biphasic model assumes an initially large subpopulation that is more susceptible to stress (smoother steady decline) and a smaller subpopulation that is more resistant to stress (smoother steady decline) (Cerf et al., 1977). R^2 values of Biphasic model for 0.1 A, 0.2 A and 0.3 A were determined as 0.86, 0.90 and 0.71, respectively, while R^2_{adj} values were 0.83, 0.88 and 0.60, respectively. However, the parameter estimate for k_{max1} equals k_{max2} perfectly. This shows that the biphasic model is unlikely to fit the facts in this case. R^2 values of the Biphasic shoulder model for 0.1 A, 0.2 A and 0.3 A were determined as 0.92, 0.93 and 0.87, respectively, while R^2_{adj} values were 0.90, 0.90 and 0.79, respectively. The parameter estimates for k_{max1} and k_{max2} are identical. This shows that the biphasic model is unlikely to fit the facts in this case.

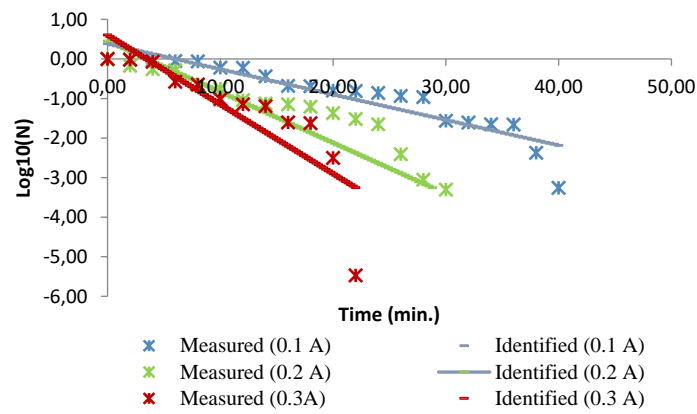
R^2 values of the Weibull model for 0.1 A, 0.2 A and 0.3 A were determined as 0.94, 0.95 and 0.89, respectively, while R^2_{adj} values were 0.93, 0.94 and 0.86, respectively. Figure 9c presents the Weibull inactivation model. R^2 values of Weibull fixed p model for 0.1 A, 0.2 A and 0.3 A were determined as 0.91, 0.86 and 0.71, respectively, while R^2_{adj} values were 0.89, 0.85 and 0.64, respectively. The 2D plot of the Weibull fixed p model is given in Figure 9d. R^2 values of the Weibull tail model for 0.1 A, 0.2 A and 0.3 A were determined as 0.94, 0.95 and 0.92, respectively, while R^2_{adj} values were 0.93, 0.94 and 0.89, respectively. But, the minimum value that may be measured is less than $\text{Log}_{10}(N_{res})$. For this data, a model with tailing is unlikely

for these data. The Double Weibull model assumes that in the first wave, there is a large subpopulation more sensitive to stress, while in the second wave, there is a small subpopulation that is more resistant to stress (Coroller et al., 2006). R^2 values of the Double Weibull model for 0.1 A, 0.2 A and 0.3 A were determined as 0.98, 0.97 and 0.96, respectively, while R^2_{adj} values were 0.98, 0.97 and 0.94, respectively. Figure 9e shows the Double Weibull inactivation model. The Double Weibull model had a high signal, which is thought to explain the electro-disinfection process for *E. coli* inactivation.

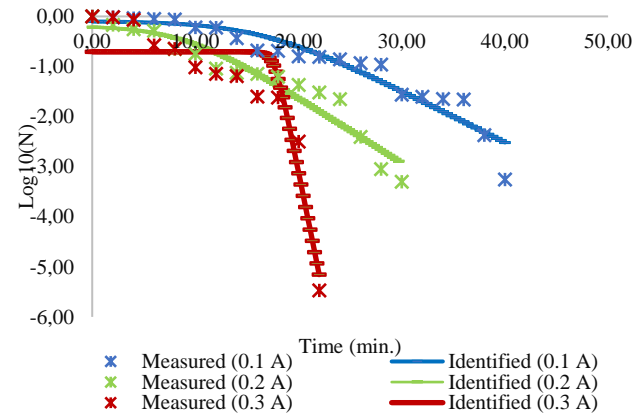
2D Plots of inactivation models are given in Table 2. The mean square error (RMSE) and coefficient of determination (R^2) parameters were used to evaluate the fit of the model. Finally, with the mathematical kinetic models in GInaFit, the model that will explain the hybrid electrode-connected electro-disinfection process and the *E. coli* removal model was chosen. It was observed that the inactivation curves obtained in the study fit with the Double Weibull model. In order to determine the effective current value, the time required for the microbial population to decrease by 4 log (t4D) was determined together with the Double Weibull model. This model was built on the assumption that the population is comprised into two subpopulations with varying stress resistances, and that the inactivation kinetics of both subpopulations follow a Weibull distribution (Coroller et al., 2006). In a study, Double Weibull model was obtained for the *E. coli* inactivation as present study (Hwang et al., 2019).

In the study, a hybrid electrode system was used. In this system, both EC process and EO processes work together. Accordingly, the mechanisms of both electrochemical methods are effective in the reactor. It has been reported that *E. coli* inactivation by electrochemical disinfection process using Pt as anode electrode occurs by two different mechanisms including direct oxidation on the electrode surface and indirect oxidation due to hydroxyl radicals (Jeong et al., 2007). Inactivation by EC process has both direct and indirect effects. Electric field application produces a direct effect. The indirect impact, on the other hand, is caused by microorganisms coming into contact with oxidants produced by water electrolysis and anode dissolution (Droguet et al., 2001; Li et al., 2004, Drees et al., 2003; Ghernaout et al., 2008). All these considerations lead to the hypothesis that the use of a hybrid electrode coupling system should be highly effective in *E. coli* inactivation. In the study, it was observed that *E. coli* inactivation was realized effectively.

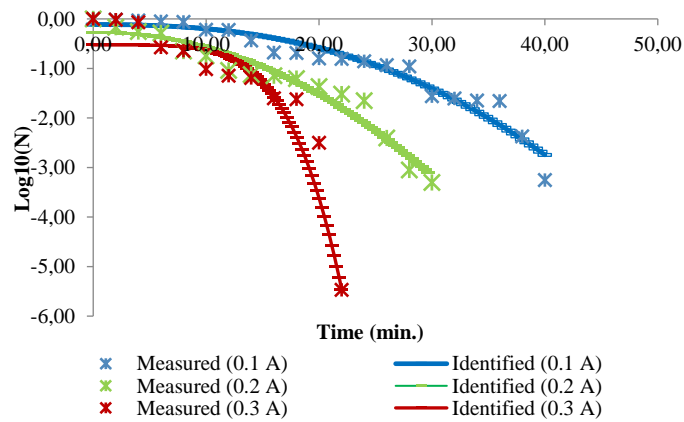
Table 2 D Plots of Inactivation Models



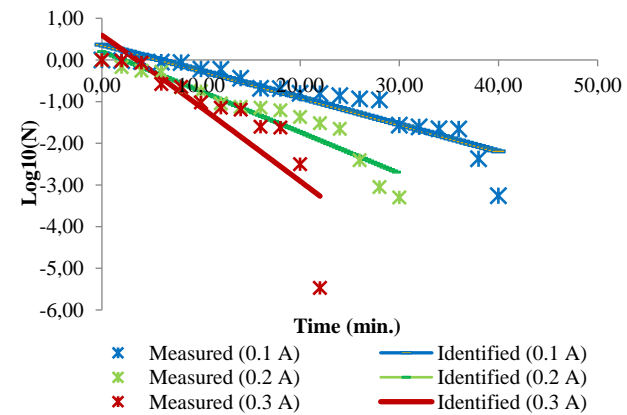
a) Log linear



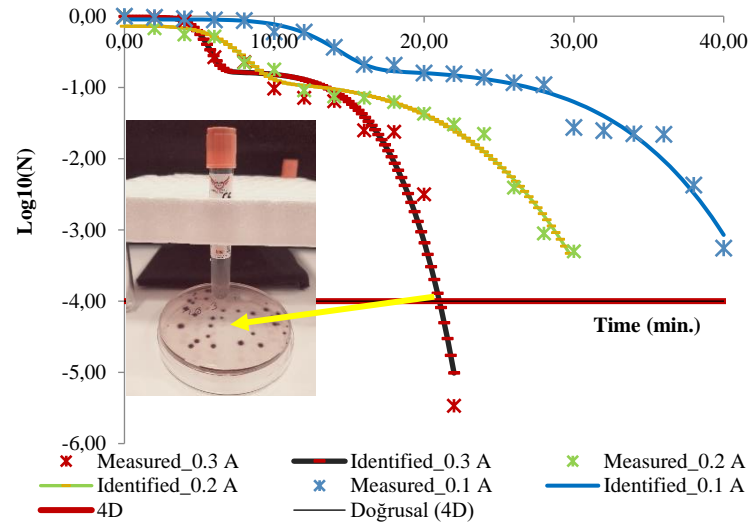
b) Log linear shoulder



c) Weibull



d) Weibull fix p



- * Log linear tail
- * Log linear shoulder+tail
- * Weibull+tail
- ** Biphasic
- ** Biphasic + shoulder

* Log10(Nres) is less than the minimal measured value. Model with tailing is unlikely for these data.

** The parameter estimate for kmax1 is exactly equal to kmax2. This indicates that the biphasic model is unlikely for these data.

e) Double Weibull

Figure 9. 2D Plots of Inactivation models

4.CONCLUSION

E. coli is a parameter that should be evaluated bacteriologically, especially for drinking water. Since it is a pathogenic microorganism, its removal from drinking water is very important. In this study, the inactivation efficiency of *E. coli* with the electro-disinfection process using a hybrid electrode connection system, which is a new approach, and the inactivation kinetics of *E. coli* were determined. The increase in applied current also shows its significant efficiency in terms of *E. coli* cell inactivation and disintegration (OD₆₀₀). At an applied current of 0.1 A and 0.2 A, 4D inactivation of *E. coli* could not be reached. At an applied current of 0.3 A, 4D degradation of *E. coli* was occurred at an electrolysis time of 21.12 min. It has been determined that the inactivation model was compatible with the Double Weibull model. As a result, a hybrid electrode connected electro-disinfection process could be a reliable approach and a significant alternative to conventional methods for *E. coli* inactivation from water/wastewater.

Ethics Committee Approval

N/A

Peer-review

Externally peer-reviewed.

Author Contributions

Conceptualization: M.S.; Investigation: M.S., R.T.K.; Material and Methodology: M.S., R.T.K; Supervision: M.S., R.T.K; Visualization: M.S.; Writing-Original Draft: M.S.; Writing-review & Editing: M.S.; Other: All authors have read and agreed to the published version of manuscript.

Conflict of Interest

The authors have no conflicts of interest to declare.

Funding

The authors declared that this study has received no financial support.

REFERENCES

- Albert, I., Mafart P. (2005). A modified Weibull model for bacterial inactivation. *International Journal of Food Microbiology*, 100, 197-211.
- Bevilacqua, A., Speranza, B., Sinigaglia, M. and Corbo, M.R. (2015). A focus on the death kinetics in predictive microbiology: Benefits and limits of the most Important models and some tools dealing with their application in foods. *Foods*, 4, 565-580.
- Bigelow W.D., Esty, J.R. (1920). The thermal death point in relation to typical thermophilic organisms. *Journal of Infectious Diseases*, 27, 602.
- Cerf O. (1977). Tailing of survival curves of bacterial spores. *Journal of Applied Bacteriology*, 42, 1-19.
- Coroller, L., Leguerinel, I., Mettler, E., Savy, N. Mafart P. (2006). General Model Based on Two Mixed Weibull Distributions of Bacterial Resistance for Describing Various Shapes of Inactivation Curves. *Applied and Environmental Microbiology*, 72, 10, 6493-6502.
- Delaedt, Y., Daneels, A., Declerck, P., Behets, J., Ryckeboer, J., Peters, E., Ollevier, F. (2008). The impact of electrochemical disinfection on *Escherichia coli* and *Legionella pneumophila* in tap water. *Microbiol. Res.* 163, 192–199.
- Diao, H.F., Li, X.Y., Gu, J.D., Shi, H.C., Xie, Z.M. (2004). Electron microscopic investigation of the bactericidal action of electrochemical disinfection in comparison with chlorination, ozonation and Fenton reaction. *Process Biochem.* 39, 1421–1426.
- Díaz, V., Ibáñez, R. Gómez, P. Urriaga, A.M., Ortiz, I. (2011). Kinetics of electro-oxidation of ammonia-N, nitrites and COD from a recirculating aquaculture saline water system using BDD anodes. *Water Research*, 45, 1, 125-134.
- Drees, K.P., Abbaszadegan M., Maier, R.M. (2003) Comparative electrochemical inactivation of bacteria and bacteriophage, *Water Res.*, 37 2291–2300.
- Drogui, P., Elmaleh, S., Rumeau, M., Bernard C., Rambaud, A. (2001). Oxidising and disinfecting by hydrogen peroxide produced in a two-electrode cell, *Water Res.*, 35(13) 3235–3241.
- Feng, C., Suzuki, K., Zhao, S., Sugiura, N., Shimada, S., Maekawa, T. (2004). Water disinfection by electrochemical treatment. *Bioresour. Technol.* 94, 21–25.
- Fiorentino A., G. Lofrano, R. Cucciniello, M. Carotenutoa, O. Mottac, A. Protoa, L. Rizzod. (2021). Disinfection of roof harvested rainwater inoculated with *E. coli* and *Enterococcus* and post-treatment bacterial regrowth: Conventional vs solar driven advanced oxidation processes *Science of the Total Environment*, 801, 149763.
- Geeraerd, A.H., Herremans, C.H., Van Impe, J.F. (2000). Structural model requirements to describe microbial inactivation during a mild heat treatment. *International Journal of Food Microbiology*, 59(3), 185-209.
- Geeraerd, A.H., Valdramidis, V.P., Van Impe, J.F. (2006). GInaFiT, a freeware tool to assess non-log-linear microbial survivor curves. *International Journal of Food Microbiology*, Volume 102, Issue 1, Pages 95-105.
- Gheraout, D., Badis, A., Kellil, A., Gheraout, B., (2008). Application of electrocoagulation in *Escherichia coli* culture and two surface waters. *Desalination*, 219, 118-125.
- Haydar S., Aziz J. A. (2009). Coagulation–Flocculation Studies of Tannery Wastewater Using Combination of Alum with Cationic and Anionic Polymers, *Journal of Hazardous Materials*, 168 (2–3), 1035–1040.
- Hee-Jeong H., Ji-Hyun S., Chanmin J., Chan-Ick C., Myong-Soo C. (2019). Analysis of bacterial inactivation by intense pulsed light using a double-Weibull survival model *Innovative Food Science and Emerging Technologies* 56, 102185.

- Holt P.K., Barton, G.W., Mitchell, C.A. (2005). The Future for Electrocoagulation as a Localised Water Treatment Technology, *Chemosphere*, 59 (3), 55–367.
- Isidro, J., Brackemeyer, D., Sáez, C., Llanos, J., Lobato, J. Cañizares, P., Matthée, T. Rodrigo, M.A. (2020). Electro-disinfection with BDD-electrodes featuring PEM technology, *Separation and Purification Technology*, 248, 1, 117081.
- Jeong, J., Kim, J.Y, Cho, M., Choi, W., Yoon, J., (2007). Inactivation of *Escherichia coli* in the electrochemical disinfection process using a Pt anode. *Chemosphere* 67, 652–659.
- Kourdali, S., Badisa, A., Boucherita, A., Boudjema, K., Saibaa, A. (2018). Electrochemical disinfection of bacterial contamination: Effectiveness and modeling study of *E. coli* inactivation by electro-Fenton, electro-peroxicoagulation and electrocoagulation, *Journal of Environmental Management*, 226, 106–119.
- Li, H., Zuo, X., Ni, J., (2011). Comparison of electrochemical method with ozonation, chlorination and monochloramination in drinking water disinfection, *Electrochimica Acta*, 56, 27, 9789-9796.
- Li, M., Qu J.-H., Peng, Y.-Z. (2004). Sterilization of *E. coli* cells by the application of pulsed magnetic field, *J. Environ. Sci.*, 16(2), 348–352.
- Mafart, P., Couvert, O., Gaillard S., Leguerinel, I. (2002). On calculating sterility in thermal preservation methods: application of the Weibull frequency distribution model. *International Journal of Food Microbiology*, 72, 107-113.
- Matsunaga, T., Okochi, M., Takahashi, M., Nakayama, T., Wake, H., Nakamura, N. (2000). TiN electrode reactor for disinfection of drinking water. *Water Res.* 34, 3117–3122.
- Mohammed M.E., Sivakumar M. (2009). Review of Pollutants Removed by Electrocoagulation and Electrocoagulation/Flotation Processes. *Journal of Environmental Management*, 90 (5), 1663-1679.
- Patermarakis, G., Fountoukidis, E. (1990). Disinfection of water by electrochemical treatment. *WaterRes.* 24, 1491–1496.
- Rowan, N.J., MacGregor, S.J., Anderson, J.G., Cameron, D., Farish, O., (2001). Inactivation of *Mycobacterium paratuberculosis* by pulsed electric fields. *Appl. Environ. Microbiol.* 67, 2833–2836.
- Saleh, M., Gonca, S., Isik Z., Ozay, Y., Harputlu, E., Ozdemir S., Yalvac, M., Ocaoglu, K., Dizge, N. (2021) Preparation of ZnO nanorods or SiO₂ nanoparticles grafted onto basalt ceramic membrane and the use for *E. coli* removal from water. *Ceramics International* 47, 27710–27717.
- Solak M. (2023). Cost-Effective Processes for Denim Production Wastewater: Dual Criterial Optimization of Techno-Economical Parameters by RSM and Minimization of Energy Consumption of Photo Assisted Fenton Processes via Direct Photovoltaic Solar Panel Integration. *Processes*, 11, 1903.
- Solak, M., (2023). Technoeconomic Analysis of Hybrid Advanced-Oxidation Processes for the Treatment of Ultrafiltration Filtrate Wastewaters, a Byprocess of Yeast Production, *Journal of Environmental Engineering*, 149, 10.
- Taoran Liu, Dan Wang, Han Liu, Wei Zhao, Wei Wang, Lei Shao. (2019). Rotating packed bed as a novel disinfection contactor for the inactivation of *E. coli* by ozone, *Chemosphere* 214, 695-701.
- Washington State Department of Health Division of Environmental Health Office of Drinking Water <https://www.doh.wa.gov/portals/1/documents/pubs/331-181.pdf>
- Whiting, R., Buchanan, R., (1993). A classification of models in predictive microbiology. *Food Microbiology*, 10(2), 175-177.

Biometric Personal Classification with Deep Learning Using EMG Signals

Bekir Bilgin^{1*}, Mehmet İsmail Gürsoy², Ahmet Alkan¹

Abstract: Biometric person recognition systems are becoming increasingly important due to their use in places requiring high security. Since it includes the physical and behavioral characteristics of people, the iris structure, which is a traditional person recognition system, is more secure than methods such as fingerprints or speech. In this study, a deep learning-based person classification/recognition model is proposed. The Gesture Recognition and Biometrics ElectroMyogram (GrabMyo) dataset from the open access PhysioNet database was used. With the 28-channel EMG device, 10 people were asked to make a fist movement with their hand. During the fist movement, data were recorded with the EMG device from the arm and wrist for 5 seconds with a sampling frequency of 2048. The Empirical Mode Decomposition (EMD) method was chosen to determine the spectral properties of EMG signals. With the EMD method, 4 IMF signal vectors were obtained from the high frequency components of the EMG signals. The classification performance effect of the feature vector is increased by using statistical methods for each IMF signal vector. Feature vectors are classified with CNN and LSTM methods from deep learning algorithms. Accuracy, Precision, Sensitivity and F-Score parameters were used to determine the performance of the developed model. An accuracy value of 95.57% was obtained in the model developed with the CNN method. In the LSTM method, the accuracy value was 93.88%. It is explained that the deep learning model proposed in this study can be effectively used as a biometric person recognition system for person recognition or classification problems with the EMG signals obtained during the fist movement. In addition, it is predicted that the proposed model can be used effectively in the design of future person recognition systems.

Keywords: EMG, Personal Classification, Empirical Mode Decomposition, CNN, LSTM.

^{1,3}**Address:** Kahramanmaraş Sütcü İmam University, Electrical Electronics Engineering Department, Kahramanmaraş/Turkiye

²**Address:** Adiyaman University, Electrical and Energy Department, Adiyaman/Turkiye

***Corresponding author:** bekirbilgin0202@gmail.com

Citation: Bilgin, B., Gürsoy, M. İ., Alkan, A. (2023). Biometric Personal Classification with Deep Learning Using EMG Signals. Bilge International Journal of Science and Technology Research, 7(2): 156-161.

1. INTRODUCTION

Electromyography (EMG) is a test used to measure the electrical activity of muscles. When muscles contract, muscle fibres produce electrical signals. By measuring these signals, EMG can give information about how well the muscles are working and whether the nerves are sending signals to the muscles. (Phinyomark et al., 2011; Shin et al., 2017) "Electro" means muscles and "myography" means measuring the activity of muscles. EMG works by recording the electrical signals that muscles in the body produce during their contraction. Muscles are controlled by nerves, and nerves transmit electrical signals to the muscles from the brain, making them move. EMG records the electrical signals obtained from these muscles using small metal

electrodes called electrodes. Electrodes are placed on the skin surface and detect the electrical activity from the muscles. They are used for many diseases, especially Peripheral neuropathy, Muscular dystrophy, Myoclonus, Shivering, Amyotrophic lateral sclerosis (ALS), Polymyositis, Rheumatoid arthritis, Muscle injuries. EMG is performed by a neurologist or physical therapist (Shioji et al., 2018; Taşar, 2022; Venugopalan et al., 2015).

Person recognition systems are technologies used to authenticate, recognize or classify a person. These systems perform the recognition process using a person's unique physical or behavioural characteristics. There are different types of person recognition systems used to recognize people. Biometric Identification Systems is the process of

authenticating or recognizing people using their unique physical or behavioural characteristics (Fan et al., 2022; Kim & Pan, 2017). Individuals are recognized using different biometric features such as fingerprint recognition, face recognition, iris recognition, retinal scan, finger vein, hand geometry, voice recognition and gait biometrics (Morikawa et al., 2019).

Face Recognition Systems, Face recognition systems are a type of biometric recognition that performs authentication or recognition using people's faces. Face recognition classifies or matches people using the unique features and structures of the face. **Fingerprint Recognition Systems,** Fingerprint recognition is authentication or recognition using the fingerprints of people. Fingerprints are different for each person, thanks to the unique patterns on the outer surface of the fingers. **Voice Recognition Systems:** Voice recognition systems perform authentication or recognition processes using people's voices. Persons are recognized using their speaking styles, tones, and other vocal features. **Retinal Scanning Systems:** Retinal scanning is a type of biometric recognition used in person recognition using unique vascular patterns in the retinal layer of the eye. **Finger Vein Recognition Systems,** Finger vein recognition is authentication or recognition using vein patterns on the inner surface of the fingers. **Hand Geometry Recognition Systems** classify people using features such as hand geometry, the general shape of the hand, and the lengths of the fingers (Gui et al., 2019; Kim et al., 2021; Lu et al., 2020).

Person identification systems are used in security, access control, fraud prevention, person identification and other applications. However, it is important that these systems are implemented with ethical and confidentiality issues in mind (Jamaluddin et al., 2023; Kang et al., 2023). Appropriate measures should be taken to ensure the security of personal data and prevent misuse. There are very few studies of person identification/classification using EMG signals in the literature. For person classification problems, machine learning algorithms are generally used together with the method of determining the spectral properties of EMG signals. A feature vector can be obtained by methods such as the Fast Fourier Transform (FFT), DWT, EWT. It can be classified by methods such as Artificial Neural Network (ANN) (Shin et al., 2017), Support Vector Machines (SVM) (Raurale et al., 2021; Shin et al., 2017), Multi-Layer Perception (MLP) (A. Raurale et al., 2020; Raurale et al., 2021), Decision Tree (DT) (Ramírez-Arias et al., 2022).

Kim et al. (Kim & Pan, 2017) proposed a person classification study using EMG signals of different wrist and hand movements and SVM and kNN algorithms. In his study, he achieved 86.66% accuracy. Raurale et al. (Raurale et al., 2021) proposed EMG signals of eight different arm movement activities from five volunteers for person classification. Accuracy values were 90.2% with the DT method, 91.6% with the MLP method, 91.3% with the SVM method and 91.7% with the ANN method. Shin et al. (Shin et al., 2017) obtained 87.1% accuracy in person classification problems with EMG signals using the SVM algorithm. Shioji et al. (Shioji et al., 2017) obtained an average accuracy of 94.5% with the proposed method using the CNN model. The aim of this article is to look into the capabilities of sEMG

signals, electrical signals produced by various muscle actions. This study also explores how well the EMD approach can identify people. The suggested methodology is anticipated to significantly improve issues with biometric person recognition.

2. MATERIAL AND METHOD

In this study, the feature vector of EMG signals was found by using the EMD method and statistical parameters. A person recognition/classification model has been developed with CNN and LSTM methods, which are deep learning algorithms.

2.1. Dataset

In this study, the Gesture Recognition and Biometrics ElectroMyogram (GrabMyo) dataset from the open-access PhysioNet database was used (Pradhan et al., 2022). A personal recognition model was developed (Fig.1). Data were recorded with the EMG device for 5 seconds at a sampling frequency of 2048 Hz (Figure 3). Each person repeated the fist movement of the hand seven times.

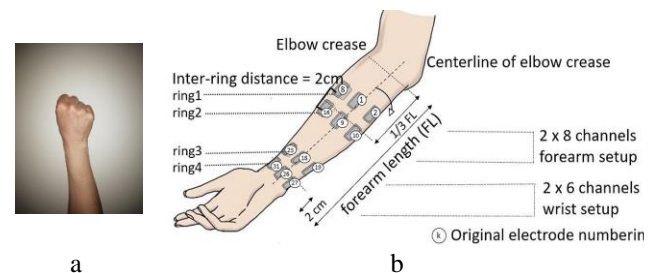


Figure 1. (a) Fist gesture of the hand, (b) EMG measurement regions

The data obtained from each channel was divided into 500 ms (1024 samples) windows and 4 level IMF components were analysed by EMD method.

2.2. Feature Extraction

Huang et al. The Empirical Mode Decomposition (EMD) method proposed by (Huang et al., 1998) is a method developed to analyse nonlinear signals (Mishra et al., 2016). It is a method that can be decomposed into frequency subcomponents (IMF) when applied to complex signals with the EMD method. It is used in the analysis of biomedical signals because it preserves the characteristics of the input signal after decomposition into sub-bands (Huang et al., 1998).

In this study, 4 levels of IMF components were obtained in the EMD method applied to the EMG input signal. The highest frequency components IMF0, IMF1, IMF2 and IMF3 levels were used to create the feature vector (Fig.2).

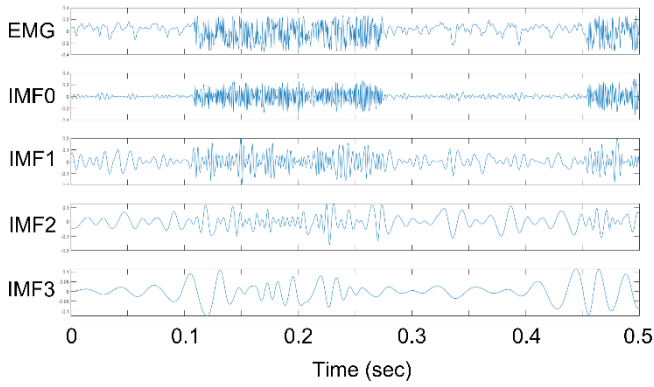


Figure 2. Four IMFs levels of EMD

In biometric person classification problems, the properties of time and frequency components in EMG signals affect the success of the model(Khan et al., 2020). The feature vector to be obtained will be determined by the EMD method with 4 IMF components whose dimensions are the same as the input signal. Seven statistical methods were chosen to characterize the frequency behaviour of signals in the IMF components(Albaqami et al., 2021; Gaso et al., 2021).

1. The mean of the absolute value of each IMF signal

$$\mu = \frac{1}{N} \sum_{i=1}^N |y_i|$$

2. Standard deviation of each IMF signal,

$$\delta = \sqrt{\frac{1}{N} \sum_{i=1}^N ((y_i - \mu))^2}$$

3. The skewness of each IMF signal,

$$\phi = \sqrt{\frac{1}{N} \sum_{i=1}^N \frac{(y_i - \mu)^3}{\delta^3}}$$

4. Kurtosis of each IMF signal

$$\phi = \sqrt{\frac{1}{N} \sum_{i=1}^N \frac{(y_i - \mu)^4}{\delta^4}}$$

5. The median of each IMF signal

$$Median = \begin{cases} \frac{(N + 1)}{2}, & \text{When } N \text{ is odd} \\ \frac{N}{2} + \frac{(N + 1)}{2}, & \text{When } N \text{ is even} \end{cases}$$

6. RMS values of each IMF signal

$$RMS = \sqrt{\frac{1}{N} \sum_{i=1}^N y_i^2}$$

7. The ratio of the average absolute values of the coefficients of the adjacent IMF signal

$$X = \frac{\sum_{i=1}^N |y_i|}{\sum_{i=1}^N |z_i|}$$

3. RESULTS

The model developed in this study was implemented in the Python programming language and in the Spyder editor. Deep learning algorithms were implemented using Tensorflow and Keras libraries.

Data were collected with the bio-armband sensor placed on the wrists and arms of 10 different volunteers by making a fist movement of the hand. The obtained data were separated into 4 different frequency sub-bands with the EMD algorithm and a feature vector was obtained with statistical methods. Classification was done with CNN and LSTM methods, which are deep learning algorithms. 85% of the dataset was used as training data and 15% as test data.

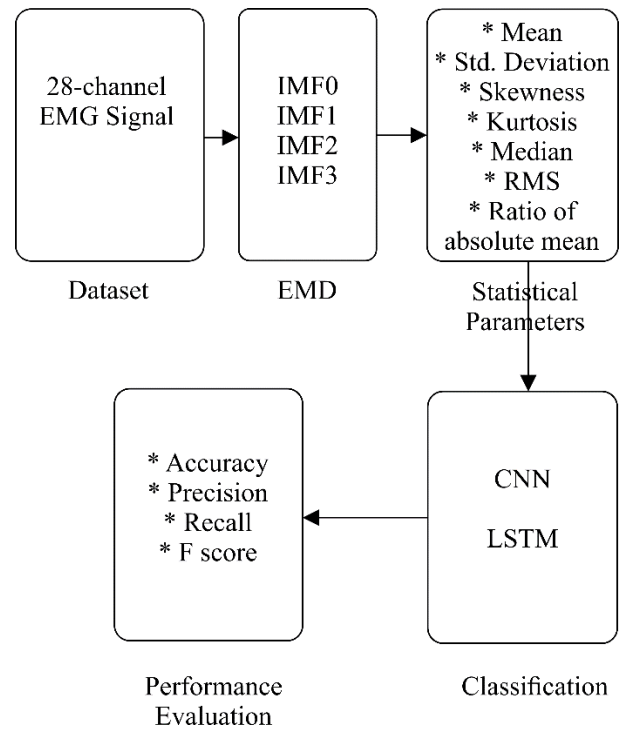


Figure 3. Architecture of the personal classification method

The classification model of the feature vector obtained by EMD and statistical parameters with CNN and LSTM deep learning algorithms is shown in Figure 3.

With the 28-channel EMG device, 10 different volunteers made fist movements for 5 s, and EMG signals were obtained with the bio-armband sensor. The data set was created by repeating the fist movement of each volunteer hand 7 times. Signals were collected with a sampling frequency of 2048 Hz.

The signals obtained from each volunteer were divided into 500 ms (1024 samples) long windows and analysed. The highest 4 level IMF coefficients of the input signal were calculated with the EMD method. In order to characterize the properties of these coefficients, the Mean, Standard

deviation, Skewness, Kurtosis, Median, RMS and Ratio of absolute mean values of each IMF vector were calculated and a feature vector was obtained to classify with CNN and LSTM methods from deep learning algorithms.

The resulting feature vector was first classified by the CNN method. The CNN algorithm generally consists of three main layers. The first layer, the Convolutional layer, forms the main layer of the model. The main task of the first layer is to calculate the features from the input data. The second layer pooling layer performs less computation by reducing the number of parameters used in the model. The third layer, Fully-connected layer, is used to connect each neuron in the previous layer to the next layer.

In the model developed with the CNN method, 2 convolution layers and 3 fully-connected layers are used. In the output layer, the softmax function is chosen as the activation function and ADAM is chosen as the optimization function of the model.

In order to compare the results obtained with the CNN model, the second classification method was classified with the LSTM algorithm. The LSTM algorithm is a special type of RNN model developed by Hochreiter & Schmidhubert at the end of 1990, which is applied for the analysis of sequential data.

In the LSTM model, each block consists of three layers: forget input and output. The forget layer uses the sigmoid function to decide which of the input signals to delete. In the second layer, the input signals are updated using the sigmoid and tanh functions. By using the tanh function in the output layer, it provides learning by the model in a way that minimizes the difference between the training values and the output values.

In the LSTM model implemented in this study, the LSTM layer consisting of 100 blocks was first created. 2 Dense layers (1st Dense layer 60 neurons, 2nd Dense layer 30 neurons) were used to transfer information between layers. In the last layer, the output values of each class were obtained with the softmax function used in multiple classification problems.

In this study, accuracy, precision, sensitivity and F-score parameters were used to evaluate the classification performance of the feature vector obtained by the EMD method.

Table 1. Model performance for personal classification

	CNN	LSTM
Accuracy	%95,57	%93,88
Precision	%95,65	%94,15
Sensitivity (Recall)	%95,57	%93,82
F-Score	%95,58	%93,86

After running 100 iterations with the CNN algorithm and 200 iterations with the LSTM algorithm, the accuracy, precision, sensitivity and F-score values are shown in Table 1. In the proposed method, it is seen that CNN and LSTM methods make classification with high accuracy. However, with the CNN method, higher classification performance was obtained with an accuracy rate of 95.57%.

4. DISCUSSION AND CONCLUSIONS

In this study, a nonlinear model was developed for person classification problems by using the EMG signals obtained with the fist movement of the hand. In both proposed models, person classification can be made with high accuracy. In Table.2, it is seen that higher accuracy was obtained than the related studies.

In the biometric person classification model, the physiological EMG signals that occur in the wrist and arm muscles during the voluntary behavioural fist movement of the individuals are non-reproducible. Since both behavioural and physiological features are used in person recognition with EMG signals, it provides much higher security than existing traditional methods.

Table 2. Personal classification comparison experiment

Reference	Classification method	Account of pattern	Accuracy
Shin et al. (Shin et al., 2021)	SVM (Cubic)	5	%87,1
Khan et al. (Khan et al., 2020)	SVM kNN DT	10	%95,3
Shioji et al. (Shioji et al., 2017)	CNN	3	%94,6
Li et al. (Li et al., 2020)	SVM	10	%98,2
Raurale et al (Raurale et al., 2021)	DT	5	%90,2
	MLP		%91,6
	SVM		%91,3
	RBF-NN		%91,7
Morikava et al (Morikawa et al., 2019)	CNN	6	%47,6
Ryohei Shioji et al. (Shioji et al., 2018)	CNN	8	%94,6
Proposed	CNN	10	%95,57
	LSTM		%93,88

The model developed in this study will provide safer access with the use of banks, military zones, R&D centres and places requiring high security. It can be said that EMG, which is a safer person recognition method than traditional methods such as face recognition and iris recognition, will be safer by using electrical signals and behavioural and physiological features.

Ethics Committee Approval

N/A

Author Contributions

All authors have read and agreed to the published version of manuscript.

Conflict of Interest

The authors have no conflicts of interest to declare.

Funding

The authors declared that this study has received no financial support.

REFERENCES

- A. Raurale, S., McAllister, J., & Del Rincon, J. M. (2020). Real-Time Embedded EMG Signal Analysis for Wrist-Hand Pose Identification. *IEEE Transactions on Signal Processing*, 68, 2713–2723. <https://doi.org/10.1109/TSP.2020.2985299>
- Albaqami, H., Hassan, G. M., Subasi, A., & Datta, A. (2021). Automatic detection of abnormal EEG signals using wavelet feature extraction and gradient boosting decision tree. *Biomedical Signal Processing and Control*, 70, 102957. <https://doi.org/10.1016/J.BSPC.2021.102957>
- Fan, J., Jiang, X., Liu, X., Zhao, X., Ye, X., Dai, C., Akay, M., & Chen, W. (2022). Cancelable HD-SEM Biometric Identification via Deep Feature Learning. *IEEE Journal of Biomedical and Health Informatics*, 26(4), 1782–1793. <https://doi.org/10.1109/JBHI.2021.3115784>
- Gaso, M. S., Cankurt, S., & Subasi, A. (2021). Electromyography Signal Classification Using Deep Learning. 2021 16th International Conference on Electronics Computer and Computation, ICECCO 2021. <https://doi.org/10.1109/ICECCO53203.2021.9663803>
- Gui, Q., Ruiz-Blondet, M. V., Laszlo, S., & Jin, Z. (2019). A survey on brain biometrics. *ACM Computing Surveys*, 51(6). <https://doi.org/10.1145/3230632>
- Huang, N. E., Shen, Z., Long, S. R., Wu, M. C., Snin, H. H., Zheng, Q., Yen, N. C., Tung, C. C., & Liu, H. H. (1998). The empirical mode decomposition and the Hubert spectrum for nonlinear and non-stationary time series analysis. *Proceedings of the Royal Society A: Mathematical, Physical and Engineering Sciences*, 454(1971), 903–995. <https://doi.org/10.1098/rspa.1998.0193>
- Jamaluddin, F. N., Ibrahim, F., & Ahmad, S. A. (2023). A New Approach to Noninvasive-Prolonged Fatigue Identification Based on Surface EMG Time-Frequency and Wavelet Features. *Journal of Healthcare Engineering*, 2023, 13–16. <https://doi.org/10.1155/2023/1951165>
- Kang, P., Jiang, S., & Shull, P. B. (2023). Synthetic EMG Based on Adversarial Style Transfer can Effectively Attack Biometric-based Personal Identification Models. *IEEE TRANSACTIONS ON NEURAL SYSTEMS AND REHABILITATION ENGINEERING*, 31, 2022.10.14.512221. <https://doi.org/10.1109/TNSRE.2023.3303316>
- Khan, M. U., Choudry, Z. A., Aziz, S., Naqvi, S. Z. H., Aymin, A., & Imtiaz, M. A. (2020). Biometric Authentication based on EMG Signals of Speech. 2nd International Conference on Electrical, Communication and Computer Engineering, ICECCE 2020, June, 2–6. <https://doi.org/10.1109/ICECCE49384.2020.9179354>
- Kim, J. S., Kim, M. G., & Pan, S. B. (2021). Two-step biometrics using electromyogram signal based on convolutional neural network-long short-term memory networks. *Applied Sciences (Switzerland)*, 11(15). <https://doi.org/10.3390/app11156824>
- Kim, J. S., & Pan, S. B. (2017). A Study on EMG-based Biometrics. *Journal of Internet Services and Information Security (JISIS)*, 7(2), 19–31. <https://doi.org/http://dx.doi.org/10.22667/JISIS.2017.05.31.019>
- Li, Q., Dong, P., & Zheng, J. (2020). Enhancing the security of pattern unlock with surface emg-based biometrics. *Applied Sciences (Switzerland)*, 10(2). <https://doi.org/10.3390/app10020541>
- Lu, L., Mao, J., Wang, W., Ding, G., & Zhang, Z. (2020). A Study of Personal Recognition Method Based on EMG Signal. *IEEE Transactions on Biomedical Circuits and Systems*, 14(4), 681–691. <https://doi.org/10.1109/TBCAS.2020.3005148>
- Mishra, V. K., Bajaj, V., Kumar, A., & Singh, G. K. (2016). Analysis of ALS and normal EMG signals based on empirical mode decomposition. *IET Science, Measurement and Technology*, 10(8), 963–971. <https://doi.org/10.1049/iet-smt.2016.0208>
- Morikawa, S., Ito, S. I., Ito, M., & Fukumi, M. (2019). Personal authentication by lips EMG using dry electrode and CNN. 2018 IEEE International Conference on Internet of Things and Intelligence System, IOTAIS 2018, 180–183. <https://doi.org/10.1109/IOTAIS.2018.8600859>
- Phinyomark, A., Limsakul, C., & Phukpattaranont, P. (2011). Application of wavelet analysis in EMG feature extraction for pattern classification. *Measurement Science Review*, 11(2), 45–52. <https://doi.org/10.2478/v10048-011-0009-y>
- Pradhan, A., He, J., & Jiang, N. (2022). Multi-day dataset of forearm and wrist electromyogram for hand gesture

- recognition and biometrics. *Scientific Data*, 9(1), 1–10. <https://doi.org/10.1038/s41597-022-01836-y>
- Ramírez-Arias, F. J., García-Guerrero, E. E., Tlelo-Cuautle, E., Colores-Vargas, J. M., García-Canseco, E., López-Bonilla, O. R., Galindo-Aldana, G. M., & Inzunza-González, E. (2022). Evaluation of Machine Learning Algorithms for Classification of EEG Signals. *Technologies*, 10(4), 79. <https://doi.org/10.3390/technologies10040079>
- Raurale, S. A., McAllister, J., & Rincon, J. M. Del. (2021). EMG Biometric Systems Based on Different Wrist-Hand Movements. *IEEE Access*, 9, 12256–12266. <https://doi.org/10.1109/ACCESS.2021.3050704>
- Shin, S., Jung, J., & Kim, Y. T. (2017). A study of an EMG-based authentication algorithm using an artificial neural network. *Proceedings of IEEE Sensors*, 2017-Decem, 1–3. <https://doi.org/10.1109/ICSENS.2017.8234158>
- Shin, S., Kang, M., Jung, J., & Kim, Y. T. (2021). Development of miniaturized wearable wristband type surface emg measurement system for biometric authentication. *Electronics (Switzerland)*, 10(8). <https://doi.org/10.3390/electronics10080923>
- Shioji, R., Ito, S. I., Ito, M., & Fukumi, M. (2018). Personal authentication and hand motion recognition based on wrist EMG analysis by a convolutional neural network. 2018 Joint 10th International Conference on Soft Computing and Intelligent Systems and 19th International Symposium on Advanced Intelligent Systems, SCIS-ISIS 2018, 1172–1176. <https://doi.org/10.1109/SCIS-ISIS.2018.00184>
- Shioji, R., Ito, S., Ito, M., & Fukumi, M. (2017). Personal Authentication Based on Wrist EMG Analysis by a Convolutional Neural Network. 5th IAE International Conference on Intelligent Systems and Image Processing, 12–18. <https://doi.org/10.12792/icip2017.006>
- Taşar, B. (2022). Deep-BBiIdNet: Behavioral Biometric Identification Method Using Forearm Electromyography Signal. *Arabian Journal for Science and Engineering*. <https://doi.org/10.1007/s13369-022-06909-z>
- Venugopalan, S., Juefei-Xu, F., Cowley, B., & Savvides, M. (2015). Electromyograph and keystroke dynamics for spoof-resistant biometric authentication. *IEEE Computer Society Conference on Computer Vision and Pattern Recognition Workshops*, 2015-Octob, 109–118. <https://doi.org/10.1109/CVPRW.2015.7301326>

Perception of Yachts by Non-Owners

Murat Aydın^{1*}

Abstract: Yachts are vessels built for especially recreational cruises or racing using sails or engines. These types of vessels are built for private use or charter activities and are generally associated with wealth, luxury, better living conditions, society, and of course remarkable expenses while operating. In literature, there are limited studies concerned with the yachts in terms of their perceptions. This study tried to figure out the perceptions of yachts by non-owners. A face-to-face survey consisting of 28 questions (yes/no, priority order, and Likert scale) was performed for 251 participants. According to the results, the yacht was perceived as a luxury vessel that shows better living rather than necessity. Furthermore, the length of the yacht, especially when the super or mega-yachts were considered, was interpreted as an indicator that shows the social belonging and economic purchasing power of the surveyed people. Composite is the lesser-known construction material that attendees preferred while steel and wood are the first two. The Interior of the yacht attracts more attention than the exterior while imported materials or goods are the prominent choice for interiors. Functionality and safety were identified as two of the main properties of the yacht.

Keywords: Consumer, behaviour, boat, socio-economics.

¹Address: Isparta University of Applied Sciences, Keçiborlu Vocational School, Isparta/Türkiye

***Corresponding author:** murataydin@isparta.edu.tr

Citation: Aydın, M. (2023). Perception of Yachts by Non-Owners. Bilge International Journal of Science and Technology Research, 7(2): 162-171.

1. INTRODUCTION

Yachts are vessels built not only for cruising but also for entertainment or racing. The term yacht was initially used to address the sailing world but then extended to cover motorboats which are being used for pleasure cruises (Fricke and Bronsart, 2012). There is an interchangeable use of the terms for yacht and boat, but size and luxury are assumed as the distinctive factors for the yachts. However, boatbuilding dates back to 4500 years (Köküöz and Örs, 1995), and the history of yachting starts from the 17th century and can be divided into two; the first period (from the beginning of 1600 to 1815) and the modern era (up to time) (Clark, 1903). And technological developments are unveiled as the door to a new age through the transformation of building technologies and used materials, tools, equipment, etc.

Nowadays, vehicles are essential not only for individuals but also for commercial activities. But luxury is one of the key factors for consumers who are willing to have unique products. From past to present, luxury is associated not only with vehicles but also with everything that can be bought. And the yacht is one of these vehicle types purchased by customers who generally have high purchasing power. According to Aydın (2012) yachts, especially semi or custom

super or mega yachts are the peaks for the luxury of the high-end sector. Custom-built yachts are generally constructed by the demand and are user-centered, designed to fulfill the needs and lifestyle of the users (Ergul, 2017). Customization is a reflection of lifestyle, and custom-built yachts express the social standing, aesthetics, and dignity of the owners (Changxue et al., 2012) in terms of wealth. Design, consumer, preference, and rational choice in consuming theory, admiration, necessity, purchasing power, channelization or tendency, and production restraints can be assumed as the main factors that form the reflection. Also, the effects of these factors on the life cycle of a final product can be considered another issue that influences the environment.

Purchasing power does not mean that the consumers must buy the vessel because renting or chartering a yacht is the fundamental in business activity of post-production in this high-end sector. And, according to Blundel and Thatcher (2005) chartering or renting sector became a global partner that shapes the nature of demand because of an increase in disposable income, a decrease in the cost of airfare, desirable exchange rates in destinations, activity-based vacations, etc. Furthermore, yacht clubs are another important party that provide involving opportunities for non-yacht owners to this

culture and potential of sharing awareness. But whether is owned or rented, using such a vehicle expresses meanings to the community. And, wealth and luxury are the main associations of these vessels as Tokol (2010, 2013) says. Also, Dear and Kemp (2005) and Simpson and Weiner (2001) stated that yachts are being used by the “important person” for pleasure while cruising. Khufu, the ancient ship that dates to 2500 BC, is one of the best examples that express “important person” and power not only in the social and economic but also political manner.

Kan and Nas (2014) evaluated the effect of various factors on the purchase decision for motor or sailing yachts. And, according to the results, speed, width, and comfort are the first three factors for purchasing a motor yacht. On the other hand, width, comfort, and safety are for purchasing a sailing yacht. Furthermore, personal characteristics, product properties, and sociocultural effects are assumed as some of the variables that define the yacht type while making a purchase decision.

Yachts are specific vehicles for some individuals. Design, durability, comfort, speed, size, types, costs, etc. for the construction, and wealth and sense of belonging for the society are some of the prominent factors for the yachting world. However, the fact is that what normal people think about these factors and so on. Therefore, this study tried to figure out the perception of yachts by the non-owners in terms of yacht type, the relationship between the product and person, construction material, priorities for functionality, comfort, aesthetic, safety, durability, interior or exterior designs, and such common-sense such as purchasing power, length, operational costs, the effect of society or popular culture. Furthermore, it’s thought that the results of this study might provide some comparative data in the field of yachting.

2. MATERIAL and METHOD

To evaluate the perception of the yachts, a questionnaire, by face-to-face method, was performed with randomly selected people who have never owned a boat or a yacht and had undergraduate or upper-level education. Furthermore, the target population of the study did not consist of businessmen or entrepreneurs. They can be assumed as middle income when their professions were taken into consideration. However, the income of the surveyed people was not asked in the survey. The survey was performed in the city of Isparta which has 421766 (Turkish Statistical Institute, 2020) habitats for the year 2015. The percentage of the survey sample was 95 %. Eq. 1 (Yamane, 2001) was used to determine the sample size. Eventually, sample size (n) was determined as around 250.

$$n = (Z^2 \times N \times P \times Q) \div (N \times D^2 + Z^2 \times P \times Q) \quad (1)$$

Where; Z is the confidence coefficient (1.96 for $\alpha = 95\%$), N is the population size, P is the confidence level (95 %), Q is (1-P), and D is the confidence interval or margin of error (2.7 %).

The questionnaire, presented in the appendix, consisted of multiple-choice, five points Likert scale, and priority

questions (total of 28) to figure out the perceptions of the population. The applicants’ interest in yachts was evaluated by asking about the yacht types, construction materials, and priorities for functionality, comfort, aesthetics, safety, and durability. Besides, the following 14 main investigations (MI) were evaluated by the population.

- MI-1: Are the yachts luxury vessels?
- MI-2: Is yacht ownership a necessity?
- MI-3: Yacht ownership is an indicator of better living conditions.
- MI-4: Yacht ownership means a more comfortable life.
- MI-5: You must have high purchasing power for yacht ownership.
- MI-6: The length of the yacht means more recreation space.
- MI-7: More the length more the guest entertainment
- MI-8: Purchasing price and operational costs increase with the increase in length.
- MI-9: There is a direct relation between the length and purchasing power.
- MI-10: There is a direct relation between the length of a yacht and social belonging.
- MI-11: Do social surroundings, fairs, etc. organizations cause cognitive channelization on yacht ownership?
- MI-12: Fashion and popular culture have effects on yacht ownership.
- MI-13: Fashion is dominated by people who have high purchasing power.
- MI-14: Yachts are generally owned by males but are effectively used by females.

Before performing the survey, a pilot application was done to enhance the apprehensibility by correcting or rearranging the questions. Eventually, a total of 251 surveys were performed and descriptive statistics were presented to figure out the main investigations using graphs and tables.

3. RESULTS and DISCUSSION

The gender of the subject groups was almost equal (49 % male and 51 % female) and 82.1 % of them stated that they would like to have a boat. However, 17.9 % of the subjects stated that they want neither a boat nor a floatage. As seen in Figure 1, sailing (21.5 %), motor (20.7 %), and catamaran (15.5 %) were the top three types of the yacht that desired to have.

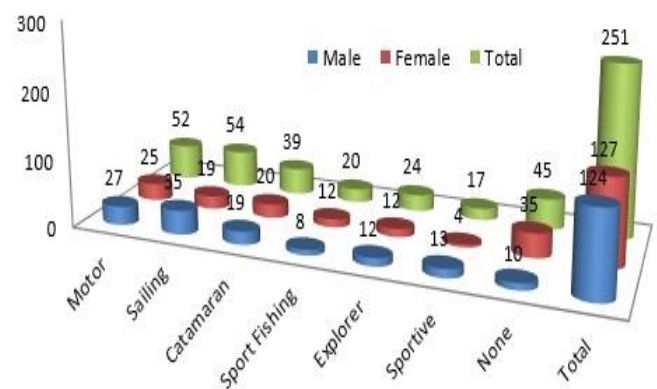


Figure 1. Frequencies for the Desired Yacht Types

According to Solomon (2019) self-concept (Product supports to form of user identity), nostalgia (products serve as a connection with a past self), interdependence (products are part of the owners' daily routines), and love (strong emotional bonds elicited by a product) are some of the relationship types that a person might have with a product. As seen in Figure 2, the order of the four different consumer types of subjects was defined according to this relationship: interdependence (38.2 %), self-concept (31.9 %), nostalgia (17.5 %), and love (10.8 %). Four of the subjects (1.6 %), among those who do not want any, did not specify their properties. Furthermore, the yacht preferences of the subjects in terms of consumer types are presented in Figure 2. The motor (41.7 %), sailing (28.7 %), sailing (45.4 %), and motor (29.6 %) yachts were the top choices of the consumer types, respectively. Sailing and motor yacht preferences of the subjects who identified themselves as nostalgic and interdependent were meaningful due to today's conditions.

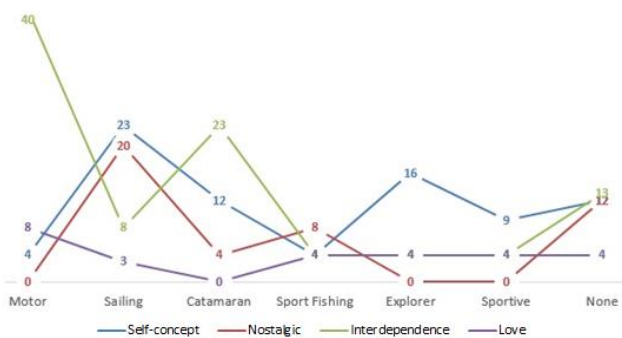


Figure 2. Consumer types and their yacht type preferences (Frequencies)

Steel, wood, aluminum, and composites are the main yacht building materials. Construction of a yacht can be done by the standalone or a mixture of these materials. Choosing the proper material is a crucial issue not only for structural purposes but also for performance by reducing the weight, cost, practicability, availability, etc. But, in this study, building material was not asked in this manner; just it was intended to figure out the attitude of subjects. Subjects were asked “Is yacht building material important for you? If yes please make the order of priority”, and 167 (66.5 %) of 251 subjects stated that yes, it is, and as seen in Table 1, steel and wood are the foremost choices. Furthermore, the distribution of the preferences for building materials according to gender is presented in the table. Also, 80 and 4 of 251 subjects marked the “no” option and did not present an opinion, respectively. It is thought that composite is not a well-known material by an ordinary human being. However, when the education level of the subjects was taken into consideration, it was thought that they would hear it in any conversation. Anyhow, perception of robustness and awareness may be some of the main motives for preferring steel and wood as top choices, respectively.

Wood, before BC to today, is being used for a great variety of purposes such as nutrition, housing, heating, transportation, consumer goods, and art or craft. And, the ancient vessel, Khufu, is one of the oldest and best examples of this. As stated in the study performed by El Hadidi (2005), the great majority of the vessel was constructed using Cedrus

libani wood. According to Wegner (2017) long-life and durability properties of cedar were taken into for the construction of royal funerary boats. Furthermore, edge-joinery with Mortise-Tenon joint technique was used for the construction of the Khufu hull planks, and planks from coniferous species swell around Tenon for a tighter fit when the wood is wet (Mark, 2014). And, this enhances the structural durability. As it is understood, wood is a traditional construction material in boat building, and with advances in nowadays technologies, the physical and mechanical properties of solid wood material can be improved by some modification methods. Also, the natural or engineered growth of trees provides sustainable and renewable construction material for different industries such as boat-building. Furthermore, engineered wood products such as plywood are of great interest in construction. Anyhow, they still have some disadvantages for the devastating environment such as marine and need to be protected. Ultraviolet (UV) is one of them and Ulay and Çakıcıer (2017) evaluated the effects of UV on varnished Iroko and Ashwoods that were used for boat construction. Furthermore, Ulay et al., (2016a) mentioned some significant issues for yacht interior production. Apart from solid wood used for interior production, composite materials will get a significant share in the future of marine construction due to the lightness, ease of production, durability, and strength properties (Koci, 2017) even if they have some major restrictions. Furthermore, carbo-epoxy resin, developed for aviation purposes, is used to build transoceanic racing yachts (Baley et al., 2014).

Table 1. Order of the construction material preferences

No	Material	Priority preferences ((Male+Female)xPoint)				Total Points
		1st (4 P*)	2nd (3 P)	3rd (2 P)	4th (1 P)	
1	Steel	(47+36)x4*	(28+28)x3	(8+16)x2	(12+0)x1	560
2	Wood	(40+32)x4	(4+16)x3	(43+16)x2	(8+12)x1	486
3	Aluminum	(0+4)x4	(36+16)x3	(26+28)x2	(33+28)x1	341
4	Composite	(8+8)x4	(27+16)x3	(18+18)x2	(42+36)x1	339

Note: P* means Points.

As in other vehicles, there are two main focuses of interest of yachts; interior and exterior. However, a great majority of yachts are white even if they have stunning exterior styles. Besides, the exterior of a yacht is particularly related to seaworthiness instead of consumer demand. On the contrary, except for the structural requirements, living spaces, and their arrangement require not only the customer demands but also conceptualization of the spaces according to budget, perception of the volume, anthropometry, and materials. According to Özer and Tokol (2021) forming the structure of the interior space of a yacht is directly related to interior equipment. Furthermore, material choices can be limited due to the regulation of the construction activity. The selection of interior decorative material and furniture is touchy because the interior of a yacht is one of the most time-spent places. Moreover, Aydın (2015) figured out that the design phase of a yacht plays a critical role in the material selection for the interior and provides significant contributions to the local supplier if the domestic goods are chosen. It is because; around 79 % of the firms located in the Marmara region manufacture order-type custom-design interiors (Aydın and Koç, 2015). However, achievements in yacht building and

interior production were not similarly repeated for luxury yacht interior design (Aydın and Yılmaz Aydın, 2016).

According to Campolongo (2017) recreating the family or home atmosphere was the topmost aim of yacht interior design for the beginning of the 20th century. Furthermore, traditional wooden interiors reflected the prestige of these boats. As seen in Figure 3, the interior of the yachts was indicated as the first priority (50.2 %) and women (54.8 %) paid more attention to interior priority.

As seen in Figure 3, 60.2 % of the subjects stated that they would choose imported fittings, equipment, and accessories. This fact may be due to the perception of the import products in Turkey because they are assumed as highly valued and prestigious not only for a yacht but also for other industrial products by marketing tactics (Gürler, 2013). In support of this, activities such as conceptual, structural, interior, and exterior designs, building, interior production, materials, and equipment or tools in the yacht building industry are dominated by a few leading industrialized countries (Aydın and Yılmaz Aydın, 2019).

As seen in Figure 3, the great majority (84 %) of the subjects expressed that admiration for the yachts arises from individual psychology. Admiration in the communal-sociological was 12.8 % while 3.2 % were hesitant.

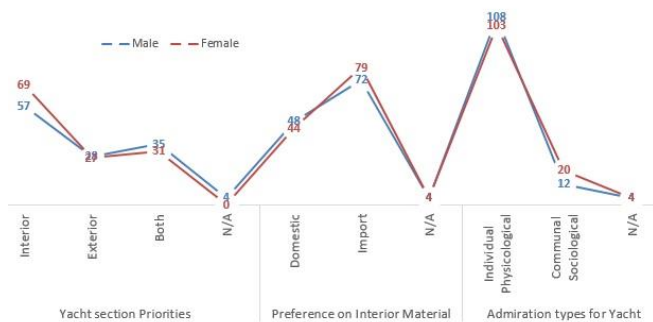


Figure 3. Priority for the interior or exterior, the choice of interior materials or goods, the formation of yacht applause (Frequencies)

Priority for the functionality, comfort, and aesthetics in the interior was evaluated by 127 of 251 subjects who stated that the interior of the yacht is precedence. According to results seen in Figure 4, functionality is placed on the top by 305 points while comfort was second by slightly lower points. In the yacht-building industry, the type of yacht may play a critical role in functionality. For example, functionality is at the forefront in sailing yachts due to hull geometry. On the contrary, comfort is at the forefront in motor yachts due to the relatively big spaces provided by hull design. Flush decks, cramped cabins, and small wet areas with low-height ceilings are some of the essential factors for uncomfortable interiors of sailing yachts (Felek, 2020). However, according to Kan and Nas (2014), speed and comfort are some of the main factors for choosing a motor yacht, but comfort is the common factor for choosing both motor and sailing yachts.

Ergonomics or human factors engineering, function, shape, and material which form the basis of design concepts are the most important design criteria that influence the relationship of the equipment with the area they are in and the user they

serve (Özer and Tokol, 2021). Meunier and Fogg (2009) reported that comfort, high-quality interior, and performance are related to design. Furthermore, the number of hulls is another important factor that influences the handling, performance, and spatial comfort of a yacht and this is an essential factor that affects the user or owner's expectations and preferences (Tokol, 2020). Considering the noise and vibration damping tools and materials is another key factor in the design phase to provide more comfortable interiors not only for the motor but also for sailing and other types of yachts (Aydın et al., 2016). However, both functionality and comfort are also related to the budget. Furthermore, according to Kan and Nas (2014) cost is another important factor for sailing yacht owners. And, when the choices of the subjects (21.5 % sailing and 20.7 % motor yachts) were taken into consideration, the order of the choices became meaningful.

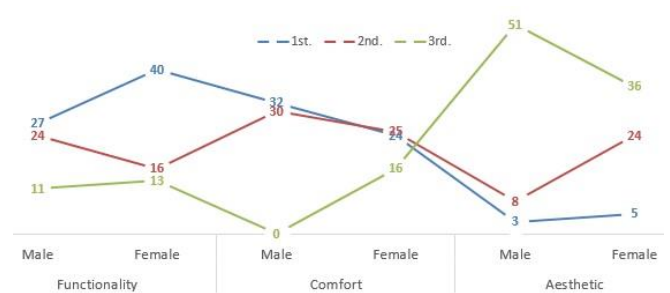


Figure 4. Priority for the functionality, comfort, and aesthetic in the interior of a yacht in terms of gender (Frequencies)

Priorities for the safety, durability, functionality, and aesthetics in yacht preferences according to gender are presented in Figure 5. Outfitting, comfort, and safety are the determinants for a floating living space or vessel (Göksel, 2006) and safety was the supreme preference factor with 890 points and followed by durability (688 points), functionality (495), and aesthetics (397). It's thought that perceptual reasoning may play a critical role in establishing a relationship between safety and steel which was expressed as the first choice for the construction material of a yacht. Therefore, choosing safety as the first choice was reasonable.

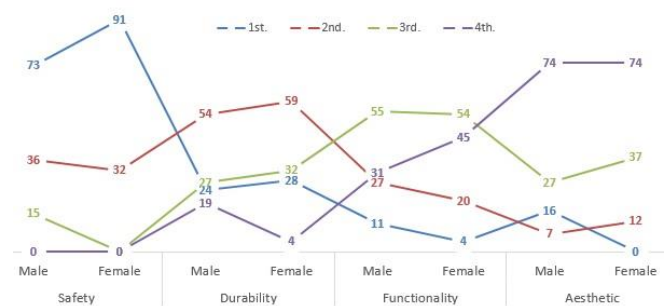


Figure 5. Priority for the safety, durability, functionality, and aesthetics in yacht preference in terms of gender (Frequencies)

Turkey has lots of attractive tourism destinations due to its geographic and climatic properties. Turkish coastline (over eight thousand km) offers safe and unique blue voyages not

only for foreign visitors but also for domestic tourists. Providing sufficient and quality conditions for the yachting is important for providing foreign currency inflow when the nature of the yachting is taken into consideration. However, there were only 83 marinas in Turkey by the end of the year 2018 while around 5000 were in Europe (DTO, 2019). Progress from the beginning of 2000 was significant because there were only 25. However, according to Öztürk et al. (2013) the main problem in Turkish marinas is excess capacity due to lack of required marina. Another important factor besides the capacity is that such societies seek prestigious marinas. More than half (53.8 %) of the subjects stated that marinas in Turkey are insufficient in terms of capacity while 25.9 % of them were neutral. However, this query requires knowledge not only about the capacity and properties of the marinas but also the size and number of the registered domestic and visiting vessels. Furthermore, this issue is not directly related to the perception of yachts and should be evaluated by another study. Anyhow, facilities especially in the Aegean and Mediterranean region in Turkey are top class and safe both for the vessels and tourists but must be supported by at least the same quality individual or public marinas. Furthermore, the new or planned expansion of ports and marinas for the Sea of Marmara and Black Sea coastlines may help to transform Turkish yachting into a major destination for tourism (Sariisik et al., 2011). As Ioannidis (2019) expressed; yachting tourism provides pronounced contributions to the local and state economy through the coastal lines. Out of providing tourism activities

by Yachting, another important contribution to the economic field is the building activities by the main and supporting industries. To improve the contributions to all partners, the perception and accessibility of such vessels must be changed and widened to middle-income families, respectively. Therefore, ownership of serial production yachts should be encouraged due to relatively low purchasing and operational costs. For example, Ulay et al., (2016b) compared the interior production properties for traditional and computer aided manufacturing.

Yachts are associated with lux and wealth (Tokol, 2010, 2013), and according to results of 1st and 5th MIs seen in Table 2, 95.6 % and 68.2 % of the subjects agreed that the yachts are luxury vessels, and in such a high-end sector, purchasing a yacht requires high income, respectively. However, there are typical differences between the serial and semi-custom or custom yachts, and particularly custom-built yachts are assumed as a wealth indicator. Anyhow, owners of serial productions such as Ferretti, Azimut, and Beneteau take part in a certain social class or society (Gürler, 2013). Even if the majority of the subjects agree on high purchasing power is required to own a yacht, a considerable amount of the subjects (30.2 %) disagreed with this expression. Furthermore, reasons for disagreeing are presented in Figure 6. Anyhow, the fact is that ownership of a luxury and large yacht requires high purchasing power.

Table 2. Main investigations for the non-owners’ perceptions of yachts (frequencies for 5 points likert scale)

Main Investigations (MI)	Definitely Agree	Agree	Neutral	Disagree	Definitely Disagree
1-Are the yachts luxury vessels?	137 (54.6)*	103 (41)	11 (4.4)	-	-
2-Is yacht ownership a necessity?	4 (1.6)	12 (4.8)	43 (17.1)	115 (45.8)	77 (30.7)
3-Yacht ownership is an indicator of better living conditions.	99 (39.4)	89 (35.5)	28 (11.2)	28 (11.2)	7 (2.8)
4-Yacht ownership means a more comfortable life.	67 (26.7)	93 (37.1)	36 (14.3)	31 (12.3)	24 (9.6)
5-You must have high purchasing power for yacht ownership	90 (35.9)	81 (32.3)	4 (1.6)	44 (17.5)	32 (12.7)
6-Length of the yacht means more recreation space	44 (17.5)	73 (29.1)	75 (29.9)	35 (13.9)	24 (9.6)
7-More the length more the guest entertainment	49 (19.5)	82 (32.7)	52 (20.7)	37 (14.7)	31 (12.4)
8-Purchasing price and operational costs increase with the increase in length	109 (43.4)	119 (47.4)	15 (6)	6 (2.4)	2 (0.8)
9-There is a direct relation between the length and purchasing power	118 (47)	117 (46.6)	4 (1.6)	9 (3.6)	3 (1.2)
10-There is a direct relation between the length of a yacht and social belonging	86 (34.3)	122 (48.6)	24 (9.6)	14 (5.6)	5 (2)
11-Do social surroundings, fairs, etc. organizations cause cognitive channelization on yacht ownership?	24 (9.6)	36 (14.3)	67 (26.7)	79 (31.5)	45 (17.9)
12-Fashion and popular culture have effects on yacht ownership	83 (33.1)	131 (52.2)	25 (9.9)	8 (3.2)	4 (1.6)
13-Fashion is dominated by people who have high purchasing power.	56 (22.3)	108 (43)	55 (21.6)	18 (7.2)	14 (5.6)
14-Yachts are generally owned by males but are effectively used by females.	84 (33.5)	94 (37.4)	52 (20.7)	14 (5.6)	7 (2.8)

* % percentages.

It is obvious that yachts, particularly custom-built ones, are not one of the vital or basic needs, and subjects (76.5 %) did not agree with the 2nd MI as expected. However, the role of an owned product cannot be limited to vitality and functionality or making life easier because it represents the owner's reflections in terms of social, cultural, psychological, and economic manner.

Better living conditions vary from person to person in terms of expectations that are affected by physiology, sociology, and economic factors. As seen in the 3rd MI, the majority of subjects (76.4 %) agreed that yacht ownership is a better living indicator.

In general, comfort is related to what you have and who you are. Therefore, having a yacht would enable the owner to feel free from the terrestrial dependence and sense the oceanic feeling onboard. As seen in the results of the 4th MI, the majority of the subjects (63.8 %) agreed that yacht ownership means a more comfortable life.

In most cases, dimension is the key element for planning the spaces. Therefore, arranging the indoor and outdoor spaces depends on the dimension. As indicated with the 6th MI was agreed by 46.6 %, and this approximation is valid for lots of people.

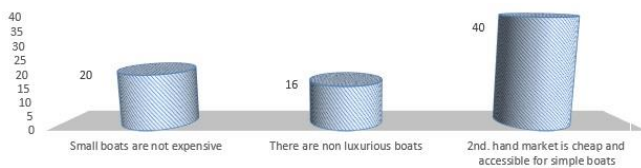


Figure 6. Frequencies for the reasons for disagreeing on the 5th MI

Privately owned or used boats sought to copy a home environment (Campolongo, 2017), and yacht owners tend to reflect their home interior in the yachts to show their social status even while they are on the sea (Lynn, 2010). This reflection can be vice versa for example inspiration of a costly yacht idea to a hotel design (Tara, 2007). Furthermore, according to 10th MI (82.9 %), social belonging or extent of reflection was directly related to the length of a yacht. This relation may be due to an increase in spaces and the ability to accommodate plenty of guests by the increase in length and deck number. Regarding this, increases in the spaces may provide more entertainment areas, and the results of the 7th MI (52.2 %) underpin the positive effect of length. However, the most affecting factor on the price of a mega yacht is the length, and deck number has little effect on the overall cost (Akyürek, 2013).

According to the result of the 8th MI (90.8 %), subjects agreed that not only the purchasing price but also operational costs increase with the increase in yacht length. Apart from the individually used boats, the employment of a captain and or crew is required for most of the yachts. Furthermore, crew expenditure is around 30-40 % of the operational cost of a yacht, and as a rule, the operational cost is 10 % of the purchase price of a yacht (Newing, 2013). Therefore, if the

purchasing price increase, then the operational costs increase due to 10 % generality.

According to the result of the 9th MI seen in Table 2, 93.6 % of subjects agree with relationship between length and purchasing power. Furthermore, the increase in cost is exponential instead of linear for each meter of any custom-built yacht (Perignon, 2008). However, the cost of each meter of 134 meters yacht built by Fincantieri was not reported as exponential due to the 2M USD for each meter (Alessandra, 2007).

According to the result seen in Table 2, the 11th MI statement was not appreciated by almost half of the subjects. However, reading or watching media and visiting boat shows were reported as some of the factors that have influences on the decision for purchasing a boat (Mills and Hughes, 2014). Furthermore, socio-cultural criteria such as preferring to buy the objects around a person may provide acceptance by the community to feel psycho-sociologically secure (Baykal, 2006). According to Kuentzel and Heberlein (1997) there is a sequential interaction for owning a boat. At first, friends or relatives introduce sailing to a person, and gaining confidence following to successful experience with cruising may result in purchasing a boat. Therefore, yacht clubs also may play a critical role in boat ownership. However, a significant percentage of the subject, who can turn the scales, were hesitant and they might agree with the above literature if only the cognitive channelization of the social surrounding was asked.

In today's era of communication, everything happens publicly due to sharing over social media. This is one of the most up-to-date and effective ways of influencing the surroundings. Furthermore, popular culture and fashion bombardments make an impression in perceptive advertising that causes a demonstration effect. As a result of perceptual filtering due to social concern, the instinct of possession may rise. In furtherance, the influence of fashion and popular culture on yacht ownership is approved by a majority of subjects (85.3 %) seen in the 12th MI. However, one of the most common facts seen in modern communities is the steering the social life by relatively few but dominant communities who have high income (Chung and Cox, 1998). According to the result seen in the 13th MI (65,3 %), the majority of the subjects agree on the "Fashion is dominated by people who have high purchasing power" expression.

The engagement of women in every part of life is on the increase with the increase in attending working life and technological developments. Apart from public transport vehicles, driving private vehicles by the woman became widespread day by day. Furthermore, such vehicles are relatively easy to access for a large segment of the population. However, high-end vehicles such as yachts (particularly luxury ones) may be excluded. In this sense, around 70.9 % of the subjects agreed on the 14th MI (Yachts are generally owned by males but are effectively used by females), and this may make sense when the wealthy businesswoman or leading characters of the societies is excluded. Furthermore, such vessels may have spiritual meanings such as fertility of soil and female fecundity as expressed by Kobyliński and Rabięga (2018). Apart from

these exceptions, just taking a seat for an excursion may be the context of yachting because as reported in a survey performed by Market Solution Pty. Ltd. (2012), sailing is predominantly a man's sport and it's required to be wealthy to deal with it. Because of the deep-rooted yet dehistoricized somatic codes, sailing has been assumed as a male-dominated special interest (Schmitt et al. 2020). To prove participation of the woman in yachting should be proved by performing a further study evaluating the owner-shipping, chartering, skippering, or just attending the cruises or sports activities.

The luxury yacht industry, especially for mega yachts, has an anti-cyclic and insensitive nature to the negative effects of the global economic crisis (Merendino, 2013, 2014). Owners of the yachts are entrepreneurs or industrialists that have high incomes instead of a member of the royalty or Silicon Valley (Kranz, 2008). Purchasing a custom or semi-custom yacht is a way of differentiation among society instead of choosing an existing vessel. For example, mass production is an efficient and effective way the production of less costly vessels due to standardization but customization of the design in the super or mega-yacht industry is the way for adding value (Van der Harst, 2020). Again, purchasing power is the dominant factor that shapes the behavior of customers. However, not only the budget but also limitations such as time, and extent or scope define the nature of demand. An increase in purchasing power is one of the main factors that cause increases in demand for larger, faster, and more comfortable yachts. Thus, small and simple yachts became large and more technologically developed than ever before (Fricke and Bronsart, 2012). However, physical and physiological comforts are associated with volume arrangement. Furthermore, lighting, sight, the shape of volume, and color choice not only define physiological comfort but also visual comfort (Di Nicolantonio et al., 2015). Eventually, the interior of a 45 m yacht can be as much as 65 m with an effective design and a proper layout (Rover, 2010). The functional design may allow effective use of limited spaces to some extent, but more spaces provided by enlargement and increasing the decks of a yacht mean more entertainment or functional spaces such as a gym, sun deck, tender stowage, helipad, etc.

4. CONCLUSIONS

In this study perception of yachts by the non-owners was evaluated by the face-to-face survey method. Sailing, motor, and catamaran yachts are the top three types that subjects were willing to have. Steel and wood, traditional materials, are assumed as the primary sources for the yacht building. And safety was the first out of the durability, functionality, and aesthetic factors for yacht perception. Therefore, it can be thought that there was a consistent approach between the material and reliability. Furthermore, functionality was one step ahead of comfort. This can be due to size and cost relation and when the small yachts are taken into consideration functionality can be at the forefront. The size of a yacht influences the recreational and accommodation spaces, building and operational costs, and social belonging. Accordingly, as subjects agreed size matters for yacht ownership.

The Interior of the yacht and import products for the interior was prioritized by the subjects against exterior and domestic products, respectively. This can be considered a threat to the local industry, but it should be regarded as an opportunity to design and manufacture new appliances or products for yacht interiors. Furthermore, to increase interest in yachts and yachting, and provide economic contributions to all partners, interrelated parties should be kept in touch to ensure appropriate conditions.

Expect the 2nd and 11th, the acceptance levels of the MIs were remarkable. Therefore, yachts are luxury vessels but having one is not vital. Yachts are assumed as an indicator of comfortable and better living conditions, but you have to cover the expenses even if they are anchored.

The order of the consumer types of the subjects was interdependence, self-concept, nostalgia, and love in terms of the product-person relationship. Subjects' interests in yachts form individual/physiological ways instead of communal/sociological ones. This expression was moderately supported by the result of the 11th MI because around half of the subjects did not agree with the influences of the surroundings, fair, etc. on the yacht owner-shipping.

This study was performed with a small number of participants who live in the Mediterranean region of Turkey. Therefore, it's important to remark that the results of this study may not be representative of the non-owning community as a whole. Moreover, further studies performed in other regions of Turkey may be useful to reflect the overall perception of the Turkish community.

Ethics Committee Approval

N/A

Peer-review

Externally peer-reviewed.

Author Contributions

Conceptualization: M.A.; Investigation: M.A.; Material and Methodology: M.A.; Supervision: M.A.; Visualization: M.A.; Writing-Original Draft: M.A.; Writing-review & Editing: M.A.; Other: Author has read and agreed to the published version of manuscript.

Conflict of Interest

The author has no conflicts of interest to declare.

Funding

The author declared that this study has received no financial support.

REFERENCES

- Akyürek, E. (2013). Pricing of mega yachts. MSc Thesis, Istanbul Bilgi University.
- Alessandra, I. (2007). Building the mega yacht. *WWD*, 193(108), 57.
- Aydın, M. (2012). The structural analysis of Turkish yacht furniture manufacturing sector in Marmara Region. MSc Thesis. Istanbul University.

- Aydın, M. (2015). Effects of yacht interior design on material selection in Turkey. *Selçuk Teknik Online, UMDK* 2015, 350–368.
- Aydın, M., Koç, K.H. (2015). A fieldwork on yacht furniture manufacturing and problems that firms encountered. *Selçuk Teknik Online, UMDK-2015*, 251–268.
- Aydın, M., Yılmaz Aydın, T. (2016). A research on the interior design of yachts built in Turkey. *Tasarım Kuram*, 12(21), 61–77.
- Aydın, M., Yılmaz Aydın, T. (2019). Is Turkey really a global competitor in yacht building industry? *The Online Journal of Science and Technology*, 9(200–208).
- Aydın, M., Yılmaz Aydın, T., Güntekin, E. (2016). Noise and vibration damping for yacht interior. *Muğla Journal of Science and Technology*, 2(2), 166–170.
- Baley, C., Lan, M., Davies, P., Cartié, D. (2014). Porosity in ocean racing yacht composites: A review. *Applied Composite Materials*, 22(1), 13–28.
- Baykal, H.H. (2006). The role of industrial design in passenger boat building: Concept design of a ferry for marine urban transportation in İzmir bay as a case. MSc Thesis, İzmir Institute of Technology.
- Blundel, R., Thatcher, M. (2005). Contrasting local responses to globalization: The case of volume yacht manufacturing in Europe. *Entrepreneurship and Regional Development*, 17(6), 405–429.
- Campolongo, M. (2017). House and yacht: The aesthetics of the interior as a link between different sectors. *The Design Journal*, 20(sup1), S209–S218.
- Changxue, P., Shuai, M., Jin, X. (2012). Analysis on the yacht interior outfitting modular partition design method. *Proceedings of the 9th International Conference on Innovation and Management, Wuhan*, pp. 1.
- Chung, K.H., Cox, R.K. (1998). Consumer behavior and superstardom. *Journal of Socio-Economics*, 27(2), 263–270.
- Clark, A.H. (1903). *The History of Yachting*. G.P. Putnam's Sons, New York.
- Dear, I., Kemp, P. (2005). A'dan Z'ye Yelkende Denizcilik Terimleri Sözlüğü. Kropi Yayınları, İstanbul.
- Di Nicolantonio, M., Di Bucchianico, G., Camplone, S., Vallicelli, A. (2015). The visual pleasantness in yacht design: natural lighting, views and interior colours. *Theoretical Issues in Ergonomics Science*, 16(4), 399–411.
- DTO. (2019). *Maritime Sector Report*. Chamber of Shipping, Istanbul, 329 pp.
- El Hadidi, N.M.N. (2005). The Cheops boat: 50 years later. *Proceedings of the International Conference of Conservation of Historic Wooden Structures, Italy*, pp. 452--457.
- Ergul, E. (2017). An evaluation of furniture making methods for yachts. *American Journal of Mechanical and Industrial Engineering*, 2(6), 205–211.
- Felek, S.Ö. 2020. Parametric sailing yacht exterior and interior design, *Tasarım Kuram*, 16(29):1-15.
- Fricke, W., Bronsart, R. (2012). Yacht design, *Proceedings of the 18th International Ship and Offshore Structures Congress, Germany*, pp. 319.
- Göksel, M.A. 2006. Cross boundaries of interior architecture discipline in nautical design and evaluation of it's interdisciplinary aspects, Doctor of Arts Thesis, Mimar Sinan Fine Arts University, İstanbul, 222 p.
- Gürler, A. (2013). A comparative study on the yacht building industry: The role of design strategy and management in the development of the yacht building industry in the World and Turkey. MSc Thesis, İstanbul Technical University.
- Ioannidis, S.A.K. (2019). An overview of yachting tourism and its role in the development of coastal areas of Croatia, *Journal of Hospitality and Tourism Issues*, 1(1), 30-43.
- Kan, N., Nas, S. (2014). Yacht type preference in yacht purchase decision: A case study through yacht owners at IC Cesme marina, *Dokuz Eylül University Maritime Faculty Journal*, 6(2), 49-69.
- Kobyliński, Z., Rabiega, K. (2018). The symbolic role of boats and ships in pagan and Christian Medieval Northern Europe, *Archaeologica Hereditas*, 13, 197–218.
- Koci, M. (2017). Stress analysis of composite materials used for yacht production through solid work simulation. *European Journal of Economics and Business Studies*, 9(1), 107.
- Köküöz, A.N., Örs, K. (1995). Yüzyıllara yayılan gelenek: Ahşap tekne yapımı. *Bilim ve Teknik*, 333, 30–37.
- Kranz, P. (2008). Measuring wealth by the foot. http://www.nytimes.com/2008/03/16/business/16drop.html?_r=2&position=andref=busiand (accessed 11 June 2013)
- Kuentzel, W.F., Heberlein, T.A. (1997). Social status, self-development, and the process of sailing specialization. *Journal of Leisure Research*, 29(3), 300–319.
- Lynn, B.M. (2010). *Luxury yacht interiors, 1870-1920 as a reflection of gilded age social status*. Ph.D. Dissertation, The Ohio State University.
- Mark, S. (2014). Ship- and boatbuilding in Ancient Egypt. In Selin, H. (Ed.), *Encyclopaedia of the History of Science, Technology, and Medicine in Non-Western Cultures*, Springer, pp. 1–14.
- Market Solutions. (2012). *Women and Girls in Sailing; A Survey of Non Sailors*. <https://cdn.revolutionise.com.au/cups/wgs/files/eyad55ysbtmkakrn.pdf> (accessed 3 July 2020)

- Merendino, A. (2013). Luxury yacht market and the anti-cyclical industry: An empirical comparison among the worldwide leaders in Italian shipyards. *The Macrotheme Review*, 2(4), 27–48.
- Merendino, A. (2014). Mega yacht, Italian leadership and financial crisis. empirical evidence on how Italian leading companies in mega yacht sector overcome the crisis. *European Scientific Journal*, 10(28), 9–35.
- Meunier, M., Fogg, R. (2009). Challenges associated with design and build of composite sailing super yachts. *Proceedings of the International Conference - Design, Construction and Operation of Super and Mega Yachts, Italy*, pp. 105–113.
- Mills, S., Hughes, E. (2014). *Boat owners survey 2013/14*. London.
- Newing, R. (2013). Yacht designs balance cost and luxury. <http://www.ft.com/cms/s/0/55cd5792-d124-11e2-be7b-00144feab7de.html> (accessed 14 April 2015)
- Özer, P., Tokol, T. (2021). Effect of ergonomics, function, form and material on equipment in yachts. *IDA: International Design and Art Journal*, 3(1), 117-131.
- Öztürk, E., Mesci, M., Kılınç, İ. (2013). The effect of innovation activities on business performance: an evaluation of yacht harbours. *Journal of Entrepreneurship and Development*, 8(2), 97–118.
- Perignon, L. (2008). *The (super) Yachting Index (1st ed.)*. Camper and Nicholson's International. N.Y.
- Rover, C. D. (2010). Yachting needs efficiency upgrade. *Holland Shipbuilding*, 59(3), 65–67.
- Sarişik, M., Turkay, O., Akova, O. (2011). How to manage yacht tourism in Turkey: A swot analysis and related strategies. *Procedia - Social and Behavioral Sciences*, 24, 1014–1025. <https://doi.org/10.1016/j.sbspro.2011.09.041>
- Schmitt, A., Atencio, M., Sempé, G. (2020). If I'm sailing with a girl, I get identified as a 'marshmallow': Gendered practices of school sport sailing in Western France and California. *International Review for the Sociology of Sport*, 1-19.
- Simpson, J.A., Weiner, S.C.E. (2001). *The Oxford English Dictionary*. Oxford Press, Oxford.
- Solomon, M. R. (2019). *Consumer Behavior: Buying, Having, and Being*. Essex: Pearson.
- Tara, M. (2007). Yacht chic. *Hospitality Design*, 29(2), 98–103.
- Tokol, H.T. (2010). Yacht interior design. TMMOB Chamber of Interior Architects Publication *Interior Architect Journal*. p.98.
- Tokol, H.T. (2013). The relationship between life, space, and equipment on transoceanic long-distance sailing cruising yachts. *Dissertation, Mimar Sinan Fine Arts University*.
- Tokol, H.T. (2020). A comparison of monohull and twin-hulled (catamaran) interior yacht designs, *International Journal of Interdisciplinary and Intercultural Art*, 5(11), 59-84.
- Turkish Statistical Institute (2020). Provincial populations by years, TUIK Institutional (tuik.gov.tr), (Accessed September 22, 2021)
- Ulay, G., Çakıcıer, N. (2017). The impact of accelerated aging (QUV) process on protective layer applied to wood specie used in yacht and boat manufacturing. *Journal of Advanced Technology Sciences*, 6(3), 212–218.
- Ulay, G., Cakicier, N., Koç, K.H. (2016a). The importance of yacht furniture and its construction needs. *Selçuk Technical Online*, (UMK 2015), 1055-1075.
- Ulay, G., Çakıcıer, N., Koç, K.H. (2016b). The use of CNC machines in yacht furniture production and encountered difficulties. *Selçuk Technical*, 1(1), 1033-1054.
- Van der Harst, S. (2020). Scale-To-Order-An engineering lead time reduction strategy for yachts. MSc. Thesis, Delft University of Technology.
- Wegner, J. (2017). A royal boat burial and watercraft tableau of Egypt's 12th dynasty (c.1850 BCE) at South Abydos. *International Journal of Nautical Archaeology*, 46(1), 5–30. <https://doi.org/10.1111/1095-9270.12203>
- Yamane, T. (2001). *Basic Sampling Methods*. Ankara: Literatür Publishing.

Appendix 1: Survey Form



1. Nasıl bir tüketicisiniz? **1. What is your Consumer Type?**
 Benlik kavramı bağlılığı olan, kullanıcı kimliği olan
 Self-concept (Product supports to form a user identity)
 Nostaljik bağlılığı olan, geçmişe bağlı
 Nostalgic (products serve as a connection with a past self)
 Günlük rutinin bir parçası
 Interdependence (products are part of the owners' daily routines)
 Tutkulu
 Love (strong emotional bonds elicited by product)

2. Nasıl bir yata sahipsiniz? **2. Which type yacht you have?**
 Yatım yok
 None
 motoryat
 Motor
 yelkenli
 Sail
 katamaran
 Catamaran
 sportif balıkçı
 Sportive fishing
 keşif tipi
 Explorer
 sportif
 Sportive

3. Yat sahibi değilseniz nasıl bir yata sahip olmak istiyorsunuz? **3. If you have not a yacht, which type you wish to have?**
 Motoryat
 None
 Yelkenli
 Motor
 Katamaran
 Sail
 Sportif Balıkçı
 Catamaran
 Keşif Tipi
 Sportive fishing
 Sportif
 Explorer
 İstemiyorum
 Sportive
 None

4. Yat sahipliği sizin için daha fazla konfor ifade etmektedir. **4. Yacht ownership means more comfort for you**
 Kesinlikle Katılmıyorum Katılmıyorum Kararsızım Katılmıyorum Kesinlikle Katılmıyorum

 Exactly agree Agree Neutral Disagree Exactly disagree

5. Yatın boyu sizin için daha fazla eğlence alanı demektir. **5. More the length more the entertainment area**
 Kesinlikle Katılmıyorum Katılmıyorum Kararsızım Katılmıyorum Kesinlikle Katılmıyorum

 Exactly agree Agree Neutral Disagree Exactly disagree

6. Yatın boyu sizin için daha fazla misafir barındırma anlamına gelmektedir. **6. More the length more the cabin**
 Kesinlikle Katılmıyorum Katılmıyorum Kararsızım Katılmıyorum Kesinlikle Katılmıyorum

 Exactly agree Agree Neutral Disagree Exactly disagree

7. Yatın boyu sizin için maliyet demek (daha büyük yat daha fazla maliyet) **7. Length is related to the cost**
 Kesinlikle Katılmıyorum Katılmıyorum Kararsızım Katılmıyorum Kesinlikle Katılmıyorum

 Exactly agree Agree Neutral Disagree Exactly disagree

8. Yatın boyu sizin için sosyal aidiyet ifade etmektedir (daha büyük daha güçlü aidiyet) **8. Length means social belonging**
 Kesinlikle Katılmıyorum Katılmıyorum Kararsızım Katılmıyorum Kesinlikle Katılmıyorum

 Exactly agree Agree Neutral Disagree Exactly disagree

9. Yatın boyu sizin için ekonomik güç göstergesidir (daha büyük daha fazla ekonomik güç) **9. Length is an expression for wealth**
 Kesinlikle Katılmıyorum Katılmıyorum Kararsızım Katılmıyorum Kesinlikle Katılmıyorum

 Exactly agree Agree Neutral Disagree Exactly disagree

10. Yat inşa malzemesi sizin için önemlidir? **10. Is construction material important for you?**
 Evet
 Yes
 Hayır
 No

11. **11. If your answer is yes for 10th question, please order the following using 1 to 5**
 11. Onuncu soruya cevabınız evet ise aşağıdaki malzemeleri 1'den başlayarak önem sırasına koyunuz
 Ahşap **Wood**
 Çelik **Steel**
 Alüminyum **Aluminum**
 Kompozit **Composite**

12. İç mekanda kullanılacak malzemelerde tercihiniz nedir? **12. What is your choice for interior materials?**
 Yerli Ürünler
 Domestic
 İthal Ürünler
 Imported

13. Türkiye'deki marinaları yeterli buluyor musunuz? **13. Are the marinas in Turkey sufficient?**
 Evet
 Yes
 Hayır
 No

1

2

14. Yatlara karşı beğeninizin nasıl oluşmaktadır **14. How your admiration forms for the yachts?**
 Bireysel / Psikolojik
 Individual/Physicological
 Toplumsal / Sosyolojik
 Communal/Sociological

15. Sizin için yatın hangi bölümü önceliklidir? **15. Which section of the yacht is important for you?**
 İç mekânı
 Interior
 Dış görünüşü
 Exterior

16. Sizin için iç mekân öncelikli ise aşağıdakileri 1, 2 ve 3 şeklinde öncelik sırasına koyunuz. **16. If the interior is more important than the exterior please order the followings by 1 to 3**
 Fonksiyonel bir iç mekân
 Functionality
 Konforlu bir iç mekân
 Comfort
 Estetik bir iç mekân
 Aesthetic

17. Yat sahipliği sizin için bir ihtiyaç mıdır? **17. Is yacht ownership a necessity?**
 Kesinlikle Evet Evet Kararsızım Hayır Kesinlikle Hayır

 Exactly agree Agree Neutral Disagree Exactly disagree

18. Yat sizin için bir lüks araç mıdır? **18. Is the yacht a luxury vessel?**
 Kesinlikle Evet Evet Kararsızım Hayır Kesinlikle Hayır

 Exactly agree Agree Neutral Disagree Exactly disagree

19. Yat sahipliği daha iyi yaşamın göstergesidir **19. Yacht ownership is the expression of better living?**
 Kesinlikle Evet Evet Kararsızım Hayır Kesinlikle Hayır

 Exactly agree Agree Neutral Disagree Exactly disagree

20. **20. What is the order of the following factors for the yacht preference? 1 for highest priority**
 20. Sizin için yat tercihinde aşağıdakilerin önceliği nasıldır? 1'den başlayarak sıralayınız.
 Fonksiyonellik **Functionality**
 Güvenlik - Emniyet **Safety**
 Dayanıklılık **Durability**
 Estetik **Aesthetic**

21. Yat sahibi olmak için alım gücünün yüksek olması gereklidir. **21. You have to high income or purchasing power for yacht ownership**
 Kesinlikle Evet Evet Kararsızım Hayır Kesinlikle Hayır

 Exactly agree Agree Neutral Disagree Exactly disagree

22. Üstteki soruya hayır cevabı verdilerse gerekçesi nedir? **22. If your answer is No for the 21th question please specify the reason(s)**
 Küçük teknelerin çok pahalı olması
 Small boats or yachts are not expensive
 Lüks olmayan teknelerin de var olması
 There are non-luxurious yachts
 İkinci el teknelerin ucuz ve ulaşılabılır olması
 Second hands cheap and accessible
 Operasyonel masrafların küçük yatlarda çok yüksek olması
 Operational cost are not high for small yachts
 Sigorta maliyetinin küçük ve lüks olmayan yatlarda çok yüksek olması
 Assurance costs are not high for small and non-luxurious yachts

23. Girişimci ya da sanayicisiniz? **23. Are you entrepreneur or industrialist?**
 Evet
 Yes
 Hayır
 No

24. **24. Do your surroundings, fairs, etc. channelize your sense for yacht ownership?**
 24. Yat sahibi olma çevreniz, fuarlar vb. algınızda yönlendirmelere neden oluyor mu?
 Kesinlikle Evet Evet Kararsızım Hayır Kesinlikle Hayır

 Exactly agree Agree Neutral Disagree Exactly disagree

25. Moda ve popüler kültürün yat sahipliğinde etkisi vardır. **25. Trends and popular culture have influences on the yacht ownership?**
 Kesinlikle Evet Evet Kararsızım Hayır Kesinlikle Hayır

 Exactly agree Agree Neutral Disagree Exactly disagree

26. Yatlar genelde erkekler tarafından alınan fakat bayanlar tarafından etkin bir biçimde kullanılan araçlardır. **26. Yachts are the vessels generally owned by the males but effectively used by females**
 Kesinlikle Evet Evet Kararsızım Hayır Kesinlikle Hayır

 Exactly agree Agree Neutral Disagree Exactly disagree

27. **27. Fashion is formed according to the physiological behavior of people who have high purchasing power**
 27. Moda ekonomik alım gücü yüksek kişilerin psikolojik davranışlarına göre şekillenir.
 Kesinlikle Evet Evet Kararsızım Hayır Kesinlikle Hayır

 Exactly agree Agree Neutral Disagree Exactly disagree

28. Cinsiyetiniz **28. Gender**
 Erkek
 Male
 Bayan
 Female

3

4

Effects of Contamination Agent for Tissue Culture Applications of *Bacopa monnieri*

Onur Sinan Türkmen^{1,2*}, Zeynep Karaceylan², Melike Küçük^{1,2*},
Refika Ceyda Beram³

Abstract: Biocides and plant protection products have been used in plant tissue culture sterilization procedures since they have broad spectrum, are inexpensive and resistant to autoclave process. This study aim was to determine the effects of two contamination agents on tissue culture conditions. MS medium was supplied with 0.5mg/L 6-benzylaminopurine and 0.1 mg/L indole-3-butyric acid as media. PPM (Plant Preservative Mixture) and Contaminacide and their three dosages (0, 3 and 6 ml/L) were used for maintaining tissue culture aseptic conditions. After plant explant were sow, vessel lids were remained open for three days under climate room conditions. Contamination rate and plant growth parameters were measured. Contamination did not occur in all dosages of Contaminacide and 6 ml/L PPM, although preservation-free and 3ml/L PPM-added media were contaminated. In conclusion 3ml/L Contaminacide added media were superior in terms of less preservation chemical cost, contamination rate, plant height, fresh and dry weight ($p \leq 0.05$).

Keywords: Sterilization, micropropagation, fungi, bacteria, PPM, Contaminacide

¹**Address:** Canakkale Onsekiz Mart University, Faculty of Agriculture, Field Crops Department, Çanakkale Türkiye

²**Address:** Margeht Biotechnology Inc. Çanakkale Teknopark Sarıcaeli Köyü 17100 Çanakkale Türkiye

³**Address:** Pamukkale University, Faculty of Science, Biology Department, Kınıklı, 20070 Denizli, Türkiye

***Corresponding author:** onurturkmen@comu.edu.tr

Citation: Türkmen, O. S., Karaceylan, Z., Küçük, M., Beram, R. C. (2023). Effects of Contamination Agent for Tissue Culture Applications of *Bacopa monnieri*. Bilge International Journal of Science and Technology Research, 7(2): 172-176.

1. INTRODUCTION

Sterilization processes are very important for tissue culture methods and reproduction procedures. Tissue culture methods and propagation stages are the most important problems of protection against fungal and bacterial infection (Reddy et al., 2021). Inhaled air contains significant microbial load due to humidity and temperature factors. These factors tend to multiply when suitable conditions are provided (Hanif, 2021). Rich sugar sources, high humidity and ideal growth conditions from the energy opening in the tissue culture medium cause a rapid proliferation of aerobic contamination factors.

Contamination losses are between %3 and %15 for each subculture stage even in strict sterile tissue culture laboratory (Boxus and Terzi, 1987). Plant tissue culture media are suitable for the growth of many fungi, yeasts and bacteria (Agrios, 1990). Because media for plant tissue culture are very similar to fungal media. Plant deaths occur due to some

phytotoxic metabolites produced by fungi growth such as *Aspergillus*, *Alternaria* and *Penicillium* (Xu et al., 2021). It

is also known that bacterial species with fermentative metabolism have pathogenicity mechanisms like fungi and yeasts (Leifert et al., 1989b).

Infected tissue culture vessels and in vitro plants die very quickly, especially since airborne microorganisms' reproduction and spread rates of occur faster than plants. If the infectious factors are not controlled, it is possible to quickly become infected with laminar flow, air conditioners and all plants in the laboratory (Kowalik and Grodek, 2002).

Sterilization and disinfection processes are applied to prevent contamination under tissue culture conditions. The purpose of using sterilization agent is to destroy the contaminant, not to prevent the life of the plant to which it is applied and not to cause somaclonal variation. The preferred sterilization method should be inexpensive, broad-spectrum, and the tissue should remain stable in different cultural

applications. The most used sterilization methods in tissue culture laboratories are heat, chemical sterilization and filtration methods. Steam sterilization method is widely used in the sterilization of nutrient media containers, nutrient media contents, metal equipment such as forceps, scalpels, and glassware. Hepafilters and injector/pipette tip hepafilters used in sterilization of sterile cabin and laboratory air are commonly used tissue culture sterilization methods. UV used in sterile cabinet sterilization and gamma sterilization ray sterilization methods used in sterilization of some disposable instruments can be given as examples. Bleach and ethanol are the most commonly chemicals in the surface sterilization of plant parts (Ahloowalia et al., 2004). The reason why these two chemicals are more preferred in tissue culture applications is one of the most preferred methods due to the wide range of infection agents it prevents, being economical and common usage area.

The high price of antibiotics, the possibility of agents to develop resistance to antibiotics and their specific fields of action narrows the area of use. The high price of silver chloride or the negative effects of mercury chloride on the environment and human health also limit the use of these chemicals. Therefore, the use of plant protection products or biocides in tissue culture applications is becoming widespread. In plant tissue culture studies, contamination agents are added to prevent the proliferation of unwanted microorganisms such as bacteria and fungi from contamination by microorganisms. PPM (Plant preservative mixture), the most common contamination agent, is a solution developed to protect plant material from infection by microorganisms.

Prospectus indicates that PPM contains 0.1305% 5-Chloro-2-methyl-3(2H)-isothiazolone and 0.0459% 2-methyl-3(2H)-isothiazolone. It is recommended that the storage must be at 4°C and usage dose of the product is 0.5-2.0 ml PPM per liter. It has been stated that the mechanism of action of PPM is both biocidal (>2ml/L medium) and biostatic (<2ml/L medium) and protection occurs by targeting the basic enzymes in the Krebs cycle and Electron Transport Chain. It is stated that the addition of 5-20 ml/L PPM to the growing medium is appropriate, and the effect of PPM will decrease when exposed to high concentrations of bacteria. It is stated in the user manual of Contaminacide that it is recommended to use 2-9 mL/L, and it contains non-ionic active substance, deionized water and Tween20.

B. monnieri plant extract widely contains different secondary metabolites, including saponins, alcohols, steroids, alkaloids, glycosides, sterol glycosides, phenylethanoid glycosides, sugars, some amino acids, flavonoids, and cucurbitaceous (Chakravarty et al., 2002; Rauf et al., 2013; Bhandari et al., 2007). Bacopacid, one of the bioactive components of *B. monnieri*, is known to protect the brain against oxidative damage and age-related cognitive deterioration (Saraf et al., 2011, Mukherjee et al., 2011). *B. monnieri* has a variety of bioactive compounds that are being investigated for therapeutic uses. *B. monnieri* extract is used to modulate neuropathological pathways involved in brain function and neuroprotection. Active ingredients from *B. monnieri* have been indicated to show possible therapeutic intervention against Parkinson's and Alzheimer's diseases.

There are many studies investigating the effect of PPM, which is widely used in plant tissue culture (Compton and Koch, 2001; Digonzelli, et. al., 2005; Gu et. al., 2022; Miyazaki, et. al., 2010). However, there is no study has been found on literature with using Contaminacide on plant tissue culture investigation.

In this study, it was carried out to examine the effects of two contamination agents used in tissue culture applications on contamination formation and plant growth to prevent contamination factors during the propagation of *Bocopa monnieri* under tissue culture conditions.

2. MATERIAL AND METHOD

The study was carried out in tissue culture laboratory conditions at Çanakkale Onsekiz Mart University, Agriculture Faculty, Department of Field Crops. The plant species *Bacopa monnieri* used as plant material was obtained from the collection of Margeht Biotechnology Inc. As the growing conditions, 24 °C 3.000 lux lighting and 16/8 hours light/dark photoperiod conditions were set. B5vitamin, 30g/L sucrose, 8g/L agar, 0.5mg/L 6-benzylaminopurine and 0.1mg/L indole-3-butyric acid were added Murashige and Skoog nutrient media. Contamination agents were added to the nutrient media before pH 5.7 adjusted with KOH and media autoclaved under 121°C, 1.0 bar pressure and 20 minutes long. Study was carried out in three replications according to the randomized blocks experimental design, replication number set as 3 and 9 plants were placed in each container. Two different 3-6 mg/L application doses of two different contamination agents, PPM and Contaminacide, were applied as a treatment, and medium without the addition of contamination agent was used as the control group. PPM (Plant Preservative Mixture) and Contaminacide and their three dosages (0, 3 and 6 ml/L) were used for maintaining tissue culture aseptic conditions. *Bacopa monnieri* was used as plant material and contamination rate and plant growth parameters were measured. The PPM product of Plant Cell Technology company was supplied as cold chain through Turkey Distributor Bee Biotechnology. The Contaminacide was obtained from Margeht Biotechnology Inc.

After the solidification of the medium, apical shoots of *Bocopa monnieri* 1.5 cm long were placed in the nutrient medium under a sterile cabinet and the lids of the nutrient medium were left open for 3 days in 24°C temperatures and 16/8h photoperiod climate room conditions. At the end of the 3rd day, the lids of the nutrient medium containers were closed. At the end of the 35th day following the explant sowing in the nutrient medium, the plant height, fresh and dry weight measurements were noted with the containers in which the infectious agent grew. The data were subjected to variance analysis with the GLM command in the SAS package program (SAS Institute, 1999).

3.RESULTS

This study was carried out to keep the lids of two different contamination agents added to the nutrient medium under *in vitro* tissue culture conditions completely open for three days, to keep the nutrient medium sterile and to examine the effects on the growth of *Bocopa monnieri*. Deathly contamination occurred in the control and the medium with 3 ml/L PPM added groups at the end of the 35th day (Figure

1). The investigated parameters were plant height, fresh weight and dry weight, and the highest application was 2.43 cm, 54.45 mg and 25.14 mg in 3 ml/l Contaminacide added nutrient medium, respectively (Table 1). It was determined that there was no significant difference between 6 ml/L dose of PPM and Contaminacide contamination agents in terms of plant height and wet weight parameters, and 6 ml/L Contaminacide application was more effective than PPM in terms of dry weight.

Table 1. Results on the effects of PPM and Contaminacide contamination agents applied at two different doses on some parameters.

	Control	Contaminacide		PPM	
		3 ml/L	6ml/L	3ml/L	6ml/L
Plant length (cm)	0.00 C	2.43 A	1.64 B	0.00 C	1.65 B
Fresh weight (mg)	0.00 C	54.45A	49.99 AB	0.00 C	45.60 B
Dry weight (mg)	0.00 C	25.14A	11.00 B	0.00 C	10.22 C

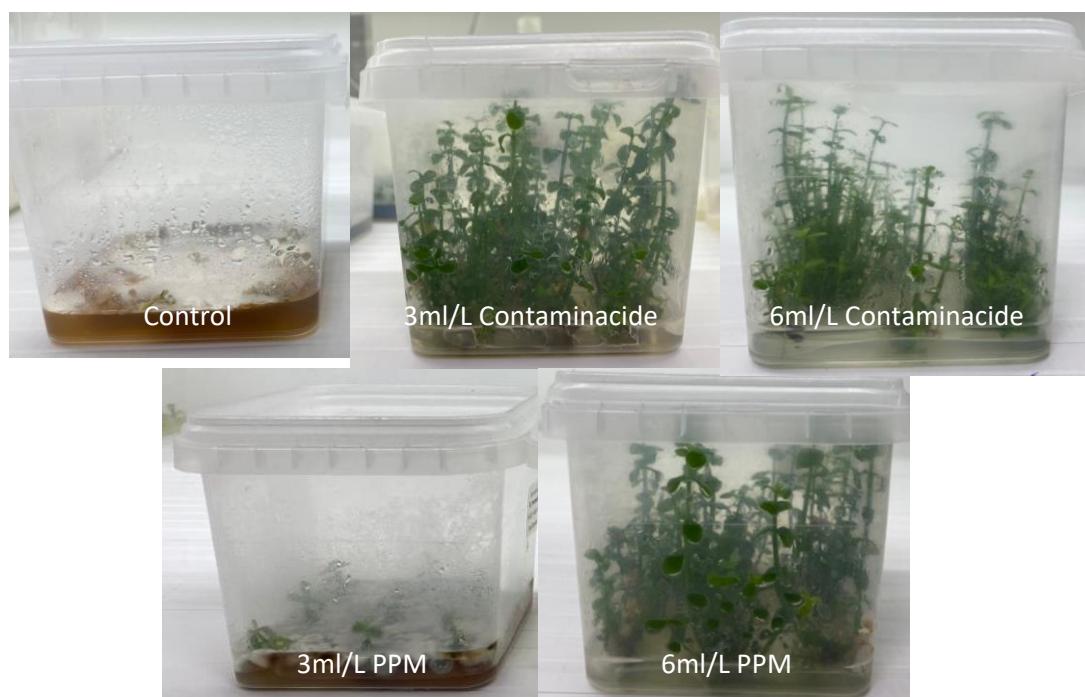


Figure 1. Control and two different contamination agent and dosages application results in *B. monnieri*

4. DISCUSSION

In related studies, PPM has been tested in various plant explants at various concentrations and it has been reported that some plants have a positive effect, while some have no positive effect (Compton and Koch, 2001; Digonzelli, et. al., 2005; Gu et. al., 2022; Miyazaki, et. al., 2010). It has been reported that PPM, which is used at different doses to control *Pseudomonas* contamination in sugar cane, inhibits bacterial growth, on the other hand, it does not have an inhibitory effect on length, fresh weight and cluster number (Digonzelli, et. al., 2005).

PPM applied at concentrations of 0.5 to 4.0 ml/L on chrysanthemum, European birch and rhododendron leaf

explants had a very low effect on the percentage of shoot-forming explants and the number of shoots developed per explant in birch and rhododendron. It has been determined that it has a significant negative effect in terms of the number of shoots (George and Tripepi, 2001).

To evaluate the phytotoxicity of PPM in the meristematic tissues of epiphytic orchids, *Dendrobium thyrsiflorum* Rchb.f. (1875) in a study using seeds and seedlings, it was reported that when 0.1% PPM was added to the medium, it did not show an observable growth inhibitory effect on protocorm, shoot or root development. However, it has been reported that PPM supplementation above 0.2% has a negative effect on *D. thyrsiflorum* explants, and that at high

PPM concentrations, root tissues of young in vitro seedlings were damaged (Chanh et. al., 2023).

The effect of PPM was investigated in four different (*Juglans regia* L.) walnut cultivars grown in tissue culture medium. One-year-old shoots of walnut cultivars were taken into DKW medium with and without PPM. Adding 0.2% v/v PPM to the starting medium reduced the number of contaminated explants from an average of 67.8% to 37.3% and increased the percentage of green shoots from 2.2% to 12.6% for all cultivars. After rinsing the explants in 5.0% v/v PPM and then inoculating in medium containing 0.2% v/v PPM, 21.7% of clean shoots were obtained. These shoots were indexed on 523 detection media and 87.5% were reported to be bacteria-free (Kushnarenko, 2022).

Carica papaya cv. Three treatments were performed on PPM taken from posterior Prabhath explants for endogenous contaminant control. Axillary shoot tips (1.0-1.5 cm) were treated with 5% (T1) PPM for 4 hours, 50% (T2) for 10 minutes, and 100% (T3) for 10 minutes. It was observed that no application yielded positive results because explants succumbed to microbial contamination (80% in T1) or phytotoxicity effect/contamination (90% in T2 and 95% in T3) at the end of 4-6 weeks. Another experiment using a multi-step surface sterilization treatment (carbendazim-cetrimide-HgCl₂) followed by culturing in papaya growth medium supplemented with 0.05% PPM showed 35% significant bacterial contamination compared to 40% in the control. The results indicated the prevalence of several PPM-tolerant endophytic bacteria in papaya and most of them survive in the MS-based environment, and this should be considered when using PPM for contamination management (Thomas et. al., 2017).

Two different immersion sterilization procedures were applied of the *Miscanthus* spp. genotype under plant tissue culture conditions with and without PPM. In the PPM study, explants obtained from two adult plants with accession numbers PI 668371 and PI 668375 on contamination were placed in MS medium with 1 mL/L PPM. At the end of the study, aseptic applications showed no difference in the percentage of bacterial and fungal contamination and the percentage of explant survival. It was observed that there was less bacterial contamination (28%) with the addition of PPM compared to its absence. For percentage of fungal contamination, it was stated that PPM had no significant effect on plant PI 668371 and a lower percentage of fungal contamination (16%) was found in PI 668375 accession. It has been emphasized that PPM may be an effective agent to prevent bacterial contamination in in vitro cultures of *Miscanthus* spp. and fungal contamination in the accession of PI 668375 (Ledo et. al., 2019).

5. CONCLUSION

In plant tissue culture applications, sugar added to the nutrient medium as a carbon source makes the nutrient medium particularly susceptible to bacterial and fungal contamination. The risk of contamination of the tissue culture medium is very high because the bacterial spores or fungal hyphae are invisible even if effort is made. Some contaminants can be stored in the vascular bundles for very

long time due to their endophyte properties and their emergence time may occur even after a few subcultures. In this case, systemic contamination agents play a very important role against vascular microorganisms.

In this study, it was carried out to determine the effects of 3 and 6 ml/L PPM and Contaminacide added to the MS medium and the effects of the containers without preservatives on the protection from contamination and plant growth due to the exposure time for three days. While all the media without preservatives and 3 ml/L PPM added were contaminated, there was no contamination in the environment containing the product named Contaminacide with 3 ml/L addition, on the other hand, it was concluded that in vitro plantlets were superior to other applications in terms of plant height, fresh and dry weight ($p < 0.05$).

This study is the first study on the contamination agent named Contaminacide, and it is predicted that it would be beneficial to apply the product at different doses and test it on different plants.

Ethics Committee Approval

N/A

Peer-review

Externally peer-reviewed.

Conflict of Interest

The authors have no conflicts of interest to declare.

Funding

The authors declared that this study has received no financial support.

REFERENCES

- Agrios, G. N., (1990). Plant Pathology, Academic Press, London, U.K.
- Ahloowalia, B. S., Prakash, J., Savangikar, V. A., Savangikar, C. (2004). Plant tissue culture. Low cost options for tissue culture technology in developing countries, 3-10, International Atomic Energy Agency, Vienna, Austria.
- Bhandari, P., Kumar, N., Singh, B., Kaul, V. K., (2007). Cucurbitacins from *Bacopa monnieri*. Phytochemistry, 68(9), 1248-1254.
- Boxus, P. H., Terzi, J. M., (1987). Big losses due to bacterial contamination can be avoided in mass propagation scheme. Acta Horticulturae 212: 91-93.
- Chakravarty, A.K., Sarkar, T., Nakane, T., Kawahara, N., Masuda, K., (2002). New phenylethanoid glycosides from *Bacopa monnieri*. Chemical and Pharmaceutical Bulletin, 50(12), 1616-1618.
- Chanh, T. T., Huy, N. T., Ha, N. T., Le, K., Hoang, N. H., (2023). Effects of plant preservative mixture™ on *In vitro* germination of *Dendrobium thyrsiflorum* Rchb.f. and its application in orchid conservation. The Korean Society of Plant Biotechnology, 50:108-114.

- Compton, M. E., Koch, J. M., (2001). Influence of plant preservative mixture (PPM)TM on adventitious organogenesis in melon, petunia, and tobacco *In vitro* Cellular & Developmental Biology-Plant, 37, 259-261.
- Digoncelli, P., Diaz, L., Carrizo De Bellone, S., (2005). Use of PPM (Plant Preservative Mixture) to control bacterial contaminants in the multiplication *In vitro* of sugarcane. *Revista de la Facultad de Agronomía*, 22(1): 23-33. ISSN 0378-7818.
- George, M. W., Tripepi, R. R., (2001). Plant Preservative MixtureTM Can Affect Shoot Regeneration from Leaf Explants of *Chrysanthemum*, European Birch, and *Rhododendron*. Plant Science Division, Department of Plant, Soils and Entomological Sciences, University of Idaho, Moscow, Hortscience, 36(4): 768-769.
- Hanif, Z., (2021). Analysis of bacterial loads in Houston indoor air thesis Presented in Partial Fulfillment of the Requirements for the Master of Science Degree in the Graduate School of Texas Southern University B.S, M.S. Texas Southern University.
- Kowalik, M., Grodek, M., (2002). Effect of Fungicides on the Growth of Fungi Isolated from *In vitro* Propagated Fruit-Bearing Plants *Plant Protection Science*, 38(Special Issue 2): 329–331.
- Kushnarenko, S., Aralbayeva, M., Rymkhanova, N., Reed, B. M., (2022). Initiation pretreatment with Plant Preservative MixtureTM increases the percentage of aseptic walnut shoots. *In vitro* Cellular & Developmental Biology-Plant Tissue Culture, 58, 964–971.
- Ledo, A. de S., Amaral, A. L. do., Jenderek, M. M., Harrison, M., Manter, D. K., (2019). Sterilization procedures and Plant Preservative Mixture on *In vitro* establishment of *Miscanthus sinensis* Andersson *Plant Cell Culture & Micropropagation*, 15(2): 27-32.
- Leifert, C., Morris, C. E., Waites, W. M., (2014). Ecology of Microbial Saprophytes and Pathogens in Tissue Culture and Field-Grown Plants: Reasons for Contamination Problems *In vitro*. *Critical Reviews in Plant Sciences*, 13(2): 139-183.
- Leifert, C., Waites, W. M., Camotta, H., and Nicholas, J. R., (1989b). *Lactobacillus plantarum*, a deleterious contaminant of plant tissue culture. *Journal of Applied Bacteriology*, 67: 363-370.
- Miyazaki, J., Tan, B. H., Errington, S. G., (2010). Eradication of endophytic bacteria via treatment for axillary buds of *Petunia hybrida* using Plant Preservative Mixture (PPMTM). *Plant Cell, Tissue and Organ Culture*, 102, 365–372.
- Mukherjee, S, Dugad, S, Bhandare. R, Pawar, N., Jagtap, S., Pawar, P. K., Kulkarni, O., (2011). Evaluation of comparative free-radical quenching potential of Brahmi (*Bacopa monnieri*) and Mandookparni (*Centella asiatica*). *An International Quarterly Journal of Research in Ayurveda*, 32, 258–264.
- Murashige, T., Skoog, F., (1962). A revised medium for rapid growth and bioassays with tobacco tissue cultures. *Physiologia Plantarum*, 15: 473–497.
- Rauf, K., Subhan, F., Al-Othman, A., Khan, I., Zarrelli, A., Shah, M., (2013). Pre-clinical profile of bacopasides from *Bacopa monnieri* (BM) as an emerging class of therapeutics for management of chronic pains. *Current Medicinal Chemistry*, 20(8): 1028-1037.
- Reddy, J., Ramesh, B. S., Praveena, V., Noronha, S., Nayak, S. P., Beena N., (2021). The Fungal and Bacterial Contaminations In Plant Tissue Culture Growth Media. *International Journal of Scientific & Engineering Research*, 12, 1.
- Saraf, M. K, Prabhakar, S, Khanduja, K. L, Anand, A., (2011). *Bacopa monnieri* attenuates scopolamine-induced impairment of spatial memory in mice. *Evidence-based Complementary and Alternative Medicine*, 236186.
- SAS Institute, (1999). SAS V8 User Manual, Cary, NC.
- Thomas, P., Agrawal, M., Bharathkumar, C. B., (2017). Use of Plant Preservative MixtureTM for establishing *In vitro* cultures from field plants: Experience with papaya reveals several PPMTM tolerant endophytic bacteria. *Plant Cell Rep.*, 36(11): 1717-1730.
- Xu, D., Xue M., Shen Z., Jia X., Hou X., Lai D., Zhou, L., (2021). Phytotoxic Secondary Metabolites from Fungi. *Toxins (Basel)*, 13(4): 1-65.

City and Brain Analogy: a Sample for Conservative Versus Adaptive Phenotypical Vision of a Genotypical Heritage

Ozgu Hafizoğlu¹, Kader Reyhan²

Abstract: Historical urban settlements and traditional structures are significant indicators and substantial values that document the past ways of life. From a contextual perspective, the preservation of these values and the revitalization of architectural heritage are like sustaining through the conservation of the integrated and continuous culture tied to the past just like a human brain does. This study encompasses all dimensions of a strategic model to conservation versus adaptation examining their interaction with historical building remnants through old-new compatibility. In this study, first; following the architectural assessment of each monumental structure, their spatial, formal, functional, and structural relationships are examined to grow the essences and values for a new vision of the city. Second, the advantages and disadvantages of the conservation approach are critiqued in comparison to adaptive renovation of the city heritages. The preservation of the physical characteristics of Vienna Gasometer monumental structures while renovation of the functions of the space within this framework reflect not only Europe's industrial, historical, and social evolution but also hold significance in terms of safeguarding socio-economic and cultural values. Furthermore, they contribute to shaping contemporary notions of conservation while adapting them to the vision of the new era operating the city as a brain.

Keywords: Analogy, Conservation, Adaptation, Heritage, Vision, Vienna Gasometers, Adaptive Industrial Heritage Reuse, City and Brain

¹**Address:** Pamukkale University, Faculty of Architecture and Design, Denizli/Türkiye.

²**Address:** Osmangazi University, Faculty of Architecture, Eskişehir/ Türkiye.

***Corresponding author:** drozgu@gmail.com

Citation: Hafizoglu, O., Reyhan, K. (2023). City and Brain Analogy: a Sample for Conservative Versus Adaptive Phenotypical Vision of a Genotypical Heritage. 21. Yüzyılda Fen ve Teknik Dergisi, 7(2): 177-186.

1. INTRODUCTION

Industrial heritage can be defined as physical structures, machinery, spaces, or documents that bear the historical traces of industrial developments and production activities (Madran and Kılınc, 2007; Douet, 2013). This type of heritage is often regarded as an important source for understanding and remembering past industrial processes, technologies, and societal changes. Industrial heritage can be found across a broad spectrum, spanning from pre-industrial periods to modern industrial eras. This heritage may encompass industrial facilities such as factories, mines, railways, warehouse buildings, bridges, gasometers, among others. Additionally, photographs, maps, documents, and other archival materials representing the documentation of industrial processes and lifestyles are also considered part of industrial heritage (Tekeli, 2001; TICCIH, 2023).

The conservation and restoration of industrial heritage aim to transmit the industrial culture of the past to future generations. At the same time, these types of areas offering

tourism and educational opportunities hold economic and cultural values.

Adaptive reuse of industrial heritage buildings means adapting these structures to new and different uses beyond their original industrial purposes. This approach combines the conservation of historical buildings with meeting the needs of modern society, thus promoting sustainability and increasing their value. Reuse projects can serve both cultural heritage conservation and provide economic, social, and environmental benefits (Mériai & Kulikov, 2021).

The main purpose and goal of preservation is to safeguard visual, aesthetic, environmental, historical, and architectural values, as well as cultural characteristics. These evaluative efforts, which are essential to be developed within the context of conservation approaches, aim to provide perspectives that establish the framework and general principles for the conservation and adaptive reusing of industrial heritage. Furthermore, this work intends to propose architectural assessments within the scope of

conservation, offering insights into the steps to be taken before making intervention decisions regarding historic structures and buildings within the framework of conservation approaches.

The content of the study consists of providing a general approach to the subject, conservation approaches within the settlement areas where the structures are located, the historical processes of the buildings, architectural analyses of each building both in relation to the whole and within their individual contexts, and finally, an overall assessment, presented in sequence.

The selection of the Simmering district and the Gasometer structures located on the outskirts of Austria for the subject matter is driven by the significance of the conservation decision in the context of the region. When considering the potential for new developments in the area, its adaptability for transformation, and the architectural features, scale, and location of the buildings, the decision to conserve becomes inevitable. Additionally, the Gasometer structures reflect an important turning point in Europe's historical and social development, emphasizing the conservation of socio-economic and cultural values in the context of physical characteristics and representing contemporary conservation practices and approaches. Due to their significant historical and social value, the Gasometer group of buildings falls within the scope of conservation. The group of structures is not only a symbol for Vienna but also holds an important place in the overall cityscape due to its dimensional scale and location throughout the city, thus considered to possess true monumental value. In this sense, the need for conservation in terms of its historical exterior appearance in Vienna is unquestionable. From this perspective, this study holds a significant framework for the examination of conservation approaches in general.

2. MATERIAL AND METHOD

Four monumental Gasometer structures located in the Simmering district on the outskirts of Austria serve as the sample for this study. The methodology employed in the study comprises the description of the chosen construction site and its characteristics, an examination of the general preservation approach associated with the site, an exploration of the intended use of the structure, an assessment of the structure's previous condition, an investigation of the transformations the structure underwent throughout its historical evolution (the reasons necessitating these transformations), an evaluation of the structure's current (present-day) condition, and the analysis of data concerning the site's and structure's general characteristics. These analyses are then subject to evaluation and discussion.

It is expected that the method applied in the assessments will contribute to the development of a systematic approach that allows for the creation of a framework reflecting the value of historical buildings in relation to their historical and architectural features, in connection with newly designed structures and functions. The analyses in the study are based on visually emphasizing the architectural characteristics of monumental structures and ranking them in order of importance.

In this study, the examination of the relationships between the city and architectural values through the analogy of a brain-like model is emphasized for its developmental significance at the urban scale. Below, in Figure 1, the abstract diagram of the brain model, resembling the Gasometers and the city, is depicted. The core, connections, and outer layer have been visualized based on an analogy between architectural and biological connections, proposing a new perspective across different layers of thought and strategy.



Figure 1. The brain's tri-layers: brainstem in red, axonal linkage in yellow, and new cortex in blue.

3. RESULTS

3.1. The Gasometer structures and their surroundings

In the 19th century, gas production was of great importance in terms of street lighting and the interior illumination of prestigious buildings. Gas production in Vienna began precisely in the year 1829. The Vienna city council signed an agreement with the Imperial-Continental Gas Association in London to supply gas to the city. In fact, the name of the "Guglgasse" street in Fuenfhaus is derived from the fact that this area was where the British company operated and supplied gas to many parts of the city.

Upon the completion of construction, project leader Franz Kapaun stated that the architecture of the Gasometer buildings would exert an authoritative influence on the system of future large industrial complex structures built with similar simple systems. Indeed, the four Gasometer structures have become significant symbols of Vienna's industrial age. In terms of architectural details, they exist as a reminder of 19th-century traditions in industrial construction. As a group consisting of four buildings, these structures have the unique distinction of being singular in Europe.

The Gasometer buildings, units serving urban gas production, were constructed between 1896 and 1899. During this period, Vienna was home to approximately two million people. In this era characterized by industrialization, Vienna's residential areas coexisted with growing and expanding commercial and industrial sectors (Wehdorn, 2000; Enichlmair, et al., 2005). Initially, the Gasometer structures were gas containers used for lighting streets and homes. Over time, new technical equipment and facilities were added during their use, but the external shell of the building remained unchanged. In 1985, the Gasometer buildings were closed (Schwarz, 2000).

The area where the Gasometer structures were established is the Simmering district, which is a quiet corner of Vienna. It is located approximately 10 minutes away from the city

center and in the middle of the city and the "Wien-Schwechat" airport, which is located outside the city (see Figure 2). The buildings have dimensions that can be easily perceived from a distance. In terms of its location and characteristics (transportation system, infrastructure, ample space for development), this area is considered a region open to development (see Figure 3). This area allows for new urban development in the formation of the city center. When its historical essence and symbolic value in the city's history are added, it can be characterized as an area with special opportunities that can lead the development axis to shift to this region and transform it into a commercial center (see Figure 4). Therefore, around the Gasometer structures, extensive office and business centers, entertainment, and shopping centers have been designed to spearhead transformation.



Figure 2. The overall view of the Gasometer structures, planned in conjunction with their immediate surroundings (Himmelb(I)au C., 2003, photo: Peter Korrak).

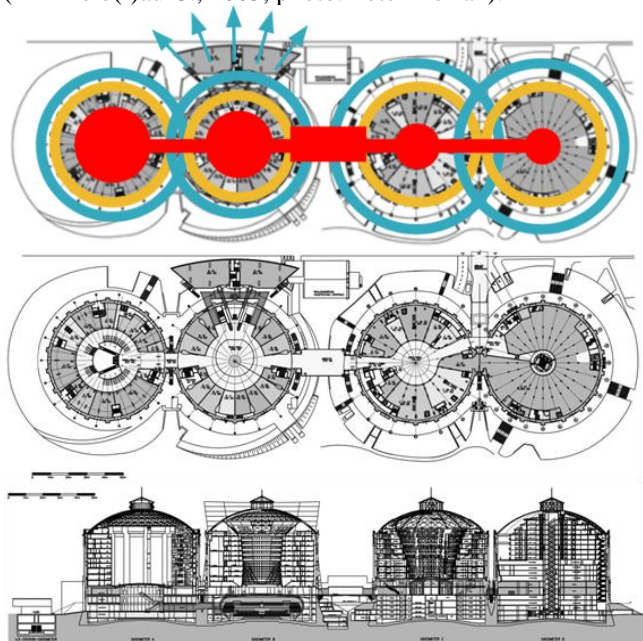


Figure 3. Ground floor plan and longitudinal section; plan and section drawings illustrating the spatial uses and the horizontal to vertical relationship of the Gasometer structures (www.gasometer.org, June 2005).

The structures were situated longitudinally on a site of approximately 300,000 m², adjacent to the Austria-Hungary railway. This arrangement facilitated the optimal transportation of coal, a necessary component for gas production. The four Gasometer structures were designed as part of an entire production complex, with variations in color and voids in the flat brick walls attempting to introduce dynamism while also striving to create a unity across all the buildings.



Figure 4. The silhouette view of the four conserved Gasometer structures with preserved exteriors, creating a self-contained city center (www.gasometer.org, June 2005).

These four monumental gas containers are the visual focal point of the entire complex. They are arranged in a row with a brick wall structure and grouped in pairs. These structures, resting on a cylindrical base, have a height of 64.9 m. Their dome-shaped top covers provide a cross-section diameter of 43.5 m and 13.33 m height arch. In each structure, a brick wall is placed on a concrete foundation that is 1.7 m deep, forming water tanks with a height of 12 m and an inner diameter of 62.8 m. This wall tapers upward to 1.65 m from a base section of 5.4 m. Above this, the wall continues upward to create the actual gas containers, tapering from 1.6 m to 0.9 m. The dome-shaped top cover spans 63.6 m. This iron-framed structure is placed on wooden cushions within zinc sheets (see Figure 5).



Figure 5. Layout arrangement within Gasometer Building A in transparent blocks (www.gasometer.org, June 2005).

Inside the structures with brick-covered exteriors, there were gas storage tanks made of steel. Each tank had a diameter of approximately 62.85 m and its widest internal height was about 72.5 m.

Within each Gasometer structure, there are container boilers made of iron, with a height of 33.6 m, placed inside a water-filled tank. These boilers are nested within each other and consist of three cylindrical sections with diameters of 58.2 m, 59.1 m, and 60 m. For control and maintenance purposes, there are iron stairs and galleries surrounding the inner part of the Gasometer structures' outer walls. To facilitate repairs on the interior of the roof, a mechanism with movable platforms has been installed. The rails of the moving mechanism, attached to one side of the roof, are integrated into the base of the roof. Between these two pairs of Gasometer structures, the pressure regulator structure that was responsible for conveying and distributing gas to the city still stands.

3.2. Gasometer Project: Conservation and adaptive reuse approach.

The Gasometer project is a redevelopment initiative that imbues new meanings (functional, structural, spatial) into four historical industrial monuments that were no longer in use. Each Gasometer building has been assigned distinct and complementary functions, creating an independent yet interdependent monumental integrity. These assigned functions were evaluated within an effort seeking answers to three significant themes reflecting the city's architectural character: residential structures, monumental conservation, and urban planning.

The fundamental approach to preserving monumental architecture within the city is based not so much on the architectural values of the buildings but on the symbolic value they bring to the city. The symbolic value in these structures lies in their representation of the city's infrastructure development. In order to preserve this symbolic value, only the external facades of the buildings were conserved, while internally, a self-contained urban center was constructed. In other words, the facades were preserved as the shell of the new structure, thereby delineating the boundaries of the city center. Strategically located to intercept the main artery coming from the city center, the Gasometer structures, constructed using modern building techniques and materials, serve as a symbolic curtain denoting the presence of the new development. Pedestrian bridges were established to gather people from the city's main artery and direct them into the Gasometer structures, thus establishing a connection between the city and the redevelopment.

The height, dimensions, and character of the Gasometer structures have served as a determining factor in shaping and guiding new architectural forms. While preserving and perpetuating the existing character, they establish the theme of the new construction, with their defining quality central to the formation. Therefore, in terms of construction and illumination, the relationship between old and new has been achieved through the intermediary buffer space created.

The concept of the Gasometer project carries a distinctive feature symbolizing the dynamic transformation of Vienna's iconic architecture within the realm of contemporary life. While monuments undergo transformation within their inner

core, the outward reflection of this transformation has been achieved through modern designs integrated into the monumental structures (Blüscher, et. al., 2000) This suggests that the renewal of the buildings might have been symbolically expressed through an outward manifestation.

Each of the four Gasometers has been individually designed by different architects, following distinct concepts and architectural projects. The creation of functions (event halls, shopping centers, etc.) to meet the requirements of urban life, along with their interconnections, and the development of various types of office and residential units associated with these functions, make it feel like a central hub catering to diverse needs has been established.

4. DISCUSSION AND CONCLUSIONS

4.1. DISCUSSION

As a former imperial city, Vienna, in addition to its historical and cultural significance, distinguishes itself from other cities by consciously developing and modernizing while simultaneously preserving certain values and character.

In the nineteenth century, it was a common approach to use the forms and styles of historical buildings in industrial structures. Gas containers and production facilities often featured a design reminiscent of medieval churches and other central structures. They were characterized by their appearance, which included rounded arches and arched windows.

Today, the four Gasometer buildings have undergone significant alterations and have been adapted to incorporate the latest advancements in complex technology and innovations. The complex, which suffered damage during World War II, was restored. However, with the advent of natural gas methods, the buildings became redundant. On June 14, 1985, Gasometer No. 2 was decommissioned, followed by the others on May 20, 1986.

Even before being decommissioned, they had been placed under protection by the Federal Monument Agency. Gasometer B has been converted into an exhibition space open for visitors. In accordance with preservation regulations, the Vienna City Gas Co. decided to carry out further renovations in 1987. Today, these structures serve as a reminder of the architectural encasing of functional structures of the past.

4.1.1. The general concept and design approach of the Gasometer project

Determining the heights between reinforced concrete layers, establishing their relationship with the old historic walls, and constructing pedestrian bridges between the two structures required attention to construction speed, accuracy, and safety. The harmony between the old and new buildings was carefully considered in terms of elevation transitions. Along the walls of each cylindrical structure, multi-story new units were constructed, and their upper parts were gradually stepped, aiming to maximize the flow of light into the spaces.

This gasometer project, where the impact of natural light on the design is maximized, stands out as a work in which the historic wall defines the project's perimeter and is reflected in the spatial organization. In the overall approach, the flow of daylight into the spaces has been achieved by either retreating the lower-level spaces through historic wall windows and gaps left between the wall and the new structures, or by creating setbacks on the upper floors, where the new structures lean against the historic wall, and setbacks form terraces and reverse conical shapes with transparent roofs (Figure 6). To facilitate this spatial arrangement and ensure the functionality of circulation spaces, horizontal setbacks and vertical circulation elements have been inserted between mass units. As a result, the passage of light to the inner courtyard is provided both through the transparent roof and the lateral vertical circulation units. Placing symmetrical plan schemes within the circular perimeter form serves this purpose and ensures continuity in transitions between repeating units. The horizontal placement of circulation units has been carried out to maximize the use of natural light and prevent monotony.

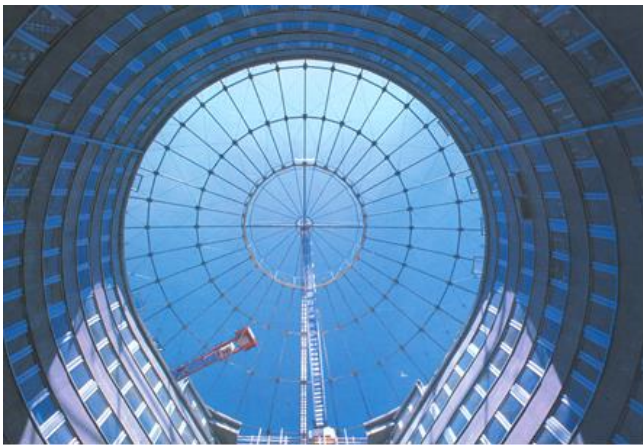


Figure 6. The view of Gasometer B structure's transparent roof (Himmelb(I)au C., 2003, photo: Toni Rappersberger).

These structures, along with the city formation known as UN City and the Millennium Tower in their vicinity, add a modern skyline to the city center, defining the urban landscape of Danube City.

Thanks to its robust infrastructure, the intersection of a fast transit route connecting to the city center via U3 and a motorway directly linked to the airport, these structures, especially Gazometre B, have become the meeting point and the liveliest space, akin to Austria's bank (Schwarz, 2000). Of course, it is undeniable that the decision made during the transformation of these historical structures also holds a significant place in terms of the functions assigned.

Establishing the relationship between the structures occurs at the elevation level, with Gazometre a directing the main circulation area leading from the subway, while in Gazometre B, it extends towards the newly constructed structure outside the shell. In the case of C and D structures, bridges constructed outside connect the two buildings, directing towards the exterior space.

The most prominent structure from the north is a new building connecting new to historic structure with a significant gap added in between. In Gasometer B, the foyer of the Concert Hall created within the structure is connected in a way that accommodates the metro entrance in Gasometer A, and the foyer is directly linked to the metro entrance. Vertical circulation elements (stairs, ramps, and elevators) have been integrated between the metro entrance level in A and the circulation level, shaping the continuity of circulation and transitions between elevations (Figure 7).

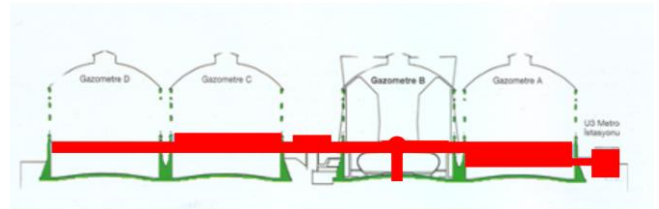


Figure 7. Section diagram illustrating the horizontal circulation relationship of the Gasometer structures (Himmelb(I)au C., 2003).

Gasometer A

French architect Jean Nouvel aimed to create a different spatial arrangement and a unique appearance concerning the old-new relationship while designing the interior of Gasometer A without accentuating the building's massive effect within his concept. To achieve this goal, he divided the interior into blocks, adding a third dimension to create a different spatial layout and maintain harmony between the old exterior walls of the gasometers and the new structures. Maximizing the use of available natural light while preserving the synergy or unity between the old gasometer walls and the new construction was a crucial aspect of the design.

In this context, the lower levels of the building feature a reinforced concrete structure, while the upper levels, where offices and residences are located, exhibit a dominant use of steel and glass, as shown in Figure 8. The choice and application of reflective materials effectively facilitate the flow of light into the spaces. Creating openings between the outer wall surfaces of these blocks and introducing vertical elements for the new units, despite limited space, can be regarded as a method employed in the project's design to maximize the quality of living.

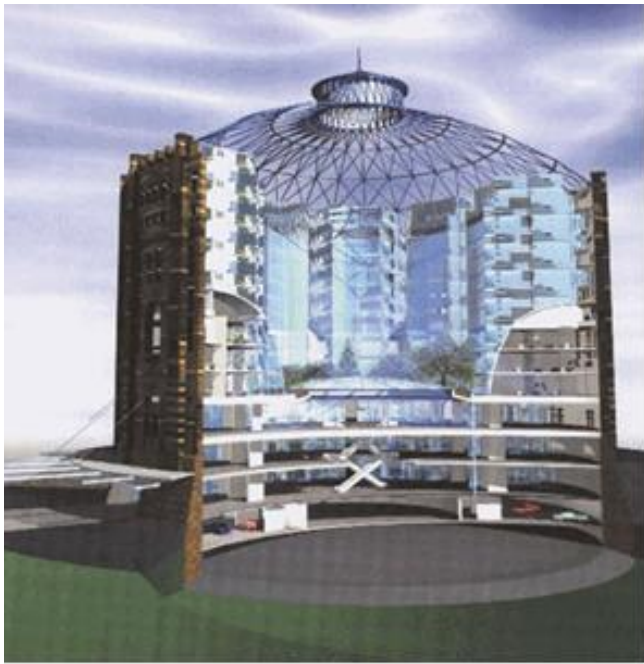


Figure 8. Sectional view of the three-dimensional model of Gazometre A structure (www.gasometer.org, June 2005).

Gasometer B

Gasometer B structure, along with its shield-like additional construction, has been designed with an understanding of form that evokes the street-building relationship within the city. The preserved walls and the inner courtyard created in the central space are structural elements that determine the lighting system of the historical structure (Figure 9). The shield-like structure, much like the new cortex of a brain, serves as a display of innovation, fulfilling its visionary role both physically and functionally, and structurally. In this context, the brain's gray matter can be likened to the gasometers' interiors, while the spirals inside them and the central parts can be seen as the core of the brain that directs the entire spinal cord.

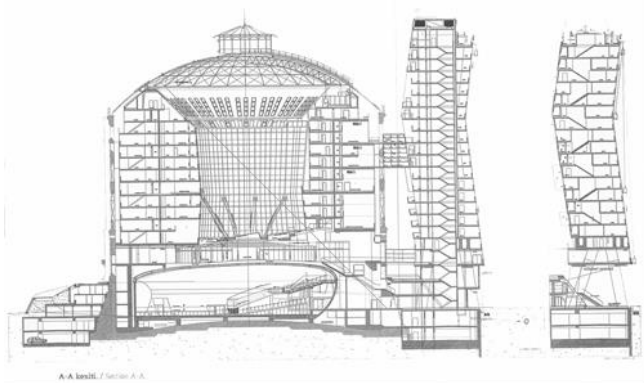


Figure 9. Cross-section view of Gazometre B structure with its shield-like new additional construction (Himmelb(I)au C., 2003).

The "Event Hall", which has an independent structural system, possesses a structure that deviates from the general geometry in both its form and structure. While its sides take on an arched shape, the upper part is amorphous (unstable), slightly inclined, and gains visual complexity in the third

dimension in a radial manner. The stage side is flat (static), while the other three sides focus on the arched form of this structure. Its upper cover, which stands independently and forms an egg-shaped figure, draws a formal resemblance to the original upper covers of the gas storage tanks. In its original state in the old structure, the upper cover relied on the main structural walls and transmitted its load to these load-bearing walls.

In the front part of Gazometre B structure, a modern extension has been designed to obstruct the perception of this structure. Several reasons contribute to this design choice. Firstly, the architects aimed to develop a new accent (design language) for this valuable historic building (See Figure 10). On the other hand, there was a desire to create a structure that would accommodate a specific number of special residential units. However, the circular-plan gasometer structures did not allow for the placement of the required number and quality of residential units. These structures dominate the cityscape from every angle due to their circular shape and scale, offering panoramic views of Vienna and its surrounding shores. In other words, this reflective new structure is strategically positioned to provide the most open view of Vienna's skyline. When viewed from each individual residence, it can be said that 270 different panoramic views of Vienna are perceptible. Besides its openness to the Vienna panorama, this new extension gains a unique quality by being the only structure that allows the observation of all four gasometer structures together (four structures) (See Figure 11).

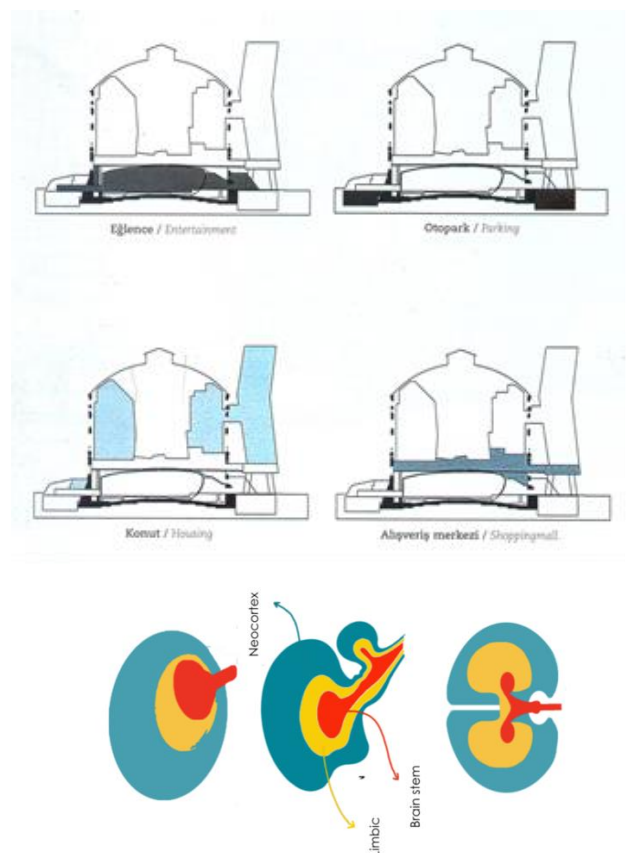


Figure 10. Section diagrams depicting the usage status of Gazometre B structure (Himmelb(I)au C., 2003) and brain model.



Figure 11. The relationship between Gazometre B structure and the shield-like new extension (Himmelb(I)au C., 2003).

The structure, connected to the Gazometre buildings via bridges, serves as a symbol and representative of the new development, arousing curiosity in terms of its design. For visitors, it has become a building that prompts them to question the reason behind this fusion of old and new while also allowing them to learn about the city's history. The structure stands freely on four main supports located on the edges of Guglgasse.

Gasometer C

Gazometre C and D are multifunctional structures designed with an internal height of approximately 70 meters from the base level to the top of the dome. The reconstructions for the entire Gazometre C were based on the simple principle of redesign by architect Manfred. The design principles are grouped under three main headings:

- 1) Clear organization of new functions,
- 2) Maximizing the quality of life,
- 3) Utilizing simple architectural styles (forms).

In terms of functions, the main goal was to create a five-story parking garage, a two-story hall, three-story offices, and six-story residential layers. Gasometer C was constructed with respect to the traditional Viennese urban development method, focusing on creating more green spaces, neighborhood relations, and ease of use. An inner courtyard, planned with top lighting and intermittent gaps, is located in the center of the building (Figure 12). Gasometer C holds a special place among the gasometers in terms of preserving the historical main entrance. Inside, a new entrance integrated into the residential spaces has been created (Figure 13).



Figure 12. The inner courtyard, residential layers, and terraces created within Gazometre C structure (www.gasometer.org, June 2005).



Figure 13. The overall views of the transparent superstructure created in the inner courtyard of Gazometre C structure from the inside and outside (www.gasometer.org, June 2005).

Gasometer D

Gasometer D is designed in the form of a three-armed star. The new structure achieves natural lighting through the organization of units on the upper floors, the central focus of three intersecting axes, and the creation of inner courtyards that face the outer shell, maximizing surface area. Additionally, the courtyard is considered as green space, serving recreational purposes and aiming to visually convey the outer shell (Figure 14). The creation of green areas signifies an attempt to implement "Green House" living criteria throughout the project to maximize gains in water and energy use.

In the approach of this project, which aimed to largely preserve historical and cultural values, a discussion emerged between the historical outer shell and the new interior life. The emphasis on the interior is created with a simple architectural expression, characterized by white-colored and classic Viennese house typology, a design concept with terraced living spaces, and at the same time, a building style where cultural influences are observed (Figure 15).

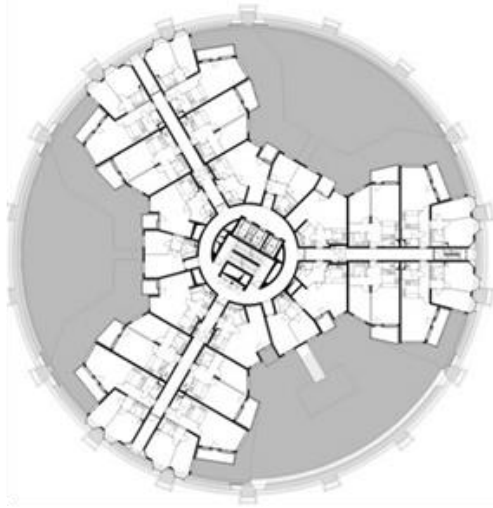


Figure 14. Plan drawing showing the inner courtyards created by the new structure designed in the form of a three-armed star for Gazometre D (www.gasometer.org, June 2005).

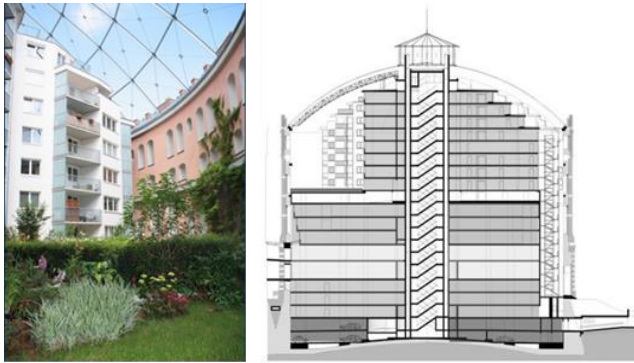


Figure 15. A sectional drawing of the new structure designed in the three-armed star form of Gazometre D, and a view from one of the interior courtyards looking towards the outer shell in the upper floors of the living spaces, showing the intersection of the three axes (www.gasometer.org, June 2005).

The placement of residential spaces to maximize the available area was an important design criterion for the design of the housing units. However, this has resulted in weak circulation spaces. While the central core area is linearly distributed in the form of a three-armed star horizontally, it is not considered an optimal solution in terms of its connection to the vertical circulation area.

4.1.2. The conservation approach in Europe (Vienna) through the Gasometer structures.

Vienna preserve its existing cultural heritage while also embracing contemporary developments and adding new dimensions to its cultural richness. It seeks to reinterpret old buildings, and when a new structure is planned within the context of the urban plan, Vienna strives to ensure that this new building reflects contemporary trends. The Gasometer building complex can be seen as an interesting example of this effort. Vienna demonstrates the continuity and tangible evolution of its culture. In the modern era, Vienna is

evolving while preserving its identity and utilizing technology to safeguard its cultural heritage.

Vienna exemplifies the idea that neither of these values is less important than the other, and both are indispensable elements for a city to be contemporary. Vienna, with its essentially geometric urban layout, is also an important example among Central European cities due to its various squares.

In Vienna, the old historical fabric has been meticulously preserved, and the grand, often neo-baroque style buildings have endured, akin to precious gems, untouched by any form of intervention. While the functions of these structures have evolved to meet contemporary needs, some streets and avenues have been transformed into pedestrian zones for recreational purposes. Throughout this process, the existing facade texture and urban elements have been faithfully preserved, with no alterations to the window proportions in the architecture of these buildings. Changes have been made in terms of elevation to accommodate new units and functions as per contemporary needs. However, the architectural elements themselves have remained unchanged, and elements like granite curb stones bear the traces of centuries. This approach allows old Vienna to continue as a significant cultural heritage, carrying its historical importance forward.

In Vienna's architectural approach, the aim for monumental buildings is to make them accessible to the public, functional, and serve as gathering spaces.

Vienna's activities in its oldest buildings and the new arrangements around these structures provide significant clues to the positive development of the "conservation" approach. Vienna preserves its streets and buildings by keeping them alive. While the functions of the buildings change, their historical qualities remain unchanged, and Vienna's streets and avenues continue to maintain their physical textures and traces of history in terms of appearances. In conservation, there is an approach that comprehensively considers reality and all its social dimensions.

Vienna, like other global metropolises, has undergone certain changes in recent times. These changes necessitate an examination of whether they are alterations that truly disrupt the city's historical image or contributions made to the city in accordance with the requirements of the time. For instance, the introduction of a modern rail system (metro) integrated with the existing rapid rail system (Stadtbahn) and railways has led to a significant portion of urban transportation being placed underground. The influence of a series of service structures considered symbols of the era, such as skyscrapers, on historic buildings is materialized through the addition of multi-story structures. In the design of the Gasometer buildings, the rhythmic patterns on the facades have been aimed to be reflected in the interior design. Spatial organization has been attempted to be organized based on the proportions of solids and voids on the facades. This way, enhancing the perception from both the inside and outside, internal-external connections, and the

play of light and shadow have been integrated into this design.

While the window rhythm created to break the effects of massiveness may evoke architectural column capital arrangements from ancient times (doric, corinthian, ionic), the presence of functional efficiency cannot be denied. In the lower sections, the existence of openings that decrease in size from bottom to top and an increase in their quantity, as well as the occasional creation of a slender and elongated form, aim to enhance vertical effectiveness (Figure 16).



Figure 16. A view of Gazometre D from the south, showing the arrangement of openings and their relationships within the Gazometer structures (www.gasometer.org, June 2005).

The transformation of these industrial structures has been achieved by converting them into spaces where a large number of people live or engage in activities. Therefore, dynamic elements have been created within these spaces, unlike their previous industrial use. These structures are now open for human use. The attempt to crown the structure with elements like a dome or tower signifies a concern for creating space in a modern approach that is connected to the future rather than the past. In this context, it is essential to preserve the historical facade and architectural characters for the ability to trace the past.

While the structures have a defined form, great effort has been made to create a highly dynamic mass through the effects of light and shadow, both from the interior and exterior. The building presents different appearances depending on the time of day and weather conditions. The spatial uses in the residential typology are designed as places that fulfill various new needs emerging from a completely modern understanding. During the construction process, the requirement for constructing a shell structure in the construction program has led to cutting and demolishing processes in some areas of the historical shell.

4.2. CONCLUSIONS

The massive four gasometer structures located in the Simmering district in the eastern part of Vienna have transformed this area into a residential and commercial center. The decision for the transformation of this area was made after analyzing the data related to the area and assessing its potential suitability. Within the scope and boundaries of this study, the examination of architectural features is significant as it initiates both theoretical

arguments related to preservation and assists in reflecting the preservation approach in architecture. The investigation of the practical implications of the preservation approach plays a substantial role in the creation and shaping of preservation plans.

When looking at the gasometer structures, it is evident that certain specific solutions have been attempted to facilitate the flow of daylight into the spaces. The outer shell opens outward like a new cortex of the brain, guiding perceptual and visionary experiences, while the core inside manages the functions and structural experience like the brainstem. The internal-external connection of the structure is achieved by advancing the white structure in between like the axons of the brain and establishing the internal-external balance.

In a, a block layout arrangement with gaps between the massing units has been created to allow the interior spaces to receive natural light. In B, the masses are gradually placed, and gaps are left between the main wall and the new units. In C, terraces have been designed to resolve the issue. In D, three-part cross layouts have been used to create inner courtyards and maximize light intake. In A, the gaps left aim to enhance the perception of historical structures in addition to allowing daylight into the spaces. In B, the goal is to direct attention to the new structure, while in C, it focuses on creating an inward atmosphere, and in D, it enhances the perception of the surroundings. In other words: In A, daylight flows into the spaces through the gaps, and transparent materials cover the surfaces facing the center. In B, light intake is achieved by leaving buffer gaps between historical wall windows. In C, gaps between walls and massing units are created at the lower levels, and terraces are left at the upper levels, shifting the floors on top of each other to allow light to flow into the spaces. In D, staggered gaps between walls and masses are designed at the lower levels, while circulation gaps are created on the other side. Cross-layout plans and inner courtyards are formed on the floors with residential units. The placement of the main circulation space is provided from the center.

In the central space, A and C structures have shopping centers placed within them, and to make use of natural light, the upper covering of these units has been resolved with transparent material in the form of a dome. This situation has led to an inward-oriented spatial arrangement. In B, with the presence of an independent congress center and the new additional unit, the solution is both interrelated and outward-oriented. In D, the circulation spaces are oriented towards the created inner courtyards, allowing the spaces to have views towards the city.

The study, which evaluates the architectural aspects of historical monuments subject to conservation in Vienna, Austria, aims to propose an alternative method for the preservation of historical buildings. By systematically examining the project prepared for the preservation of historical buildings through an architectural analysis approach, this study can serve as an example in the evaluation of similar historical structures. The identification and preservation of architectural features of historical buildings are possible through appropriate and accurate analyses. Creating analyses for the entire complex and each

individual building will provide significant advantages in the process of determining conservation approaches and decisions. Furthermore, emphasizing architectural features will assist in the proper examination of specific intervention strategies and forms. This examination, when strategically aligned with the analogy of the brain and the city, will shed light on the strategic dimension of the fundamental decisions to be made.

In urban development as well as in structural development, the analogical significance of the connections between the existing, i.e., the genotype, and the developmental, i.e., the phenotypic structure can only be achieved with awareness developed at the decision-making stage. This, in turn, provides a technical roadmap for guiding strategies at the level of detail, with a broader vision in mind.

In conclusion, the expected benefit of this study is to systematically generate process data in an exemplary conservation approach and serve as a reference for similar applications. The Vienna example represents a departure from a formalist approach in shaping the object, emphasizing not the object but its symbolic value for the purpose of conservation. In this example, there is no formal reflection of the building's character; instead, it expresses its existence with a completely new, material, and technically modern attitude. This approach goes beyond venerating the old; while respecting this value, it extends beyond the building itself to prevent the totemization of these structures by emerging as a new presence.

The city is a brain, and considering heritage structures as a new phenotype to adapt to the changing era with a fresh vision is important for urban development. It allows for developmental significance, adjusting to the requirements of a different era, and opening up new possibilities with a vision that is in tune with the times.

Acknowledgements

Ethics Committee Approval

N/A

Peer-review

Externally peer-reviewed.

Author Contributions

Conceptualization: Ö.H., K.R.; Investigation: Ö.H., K.R.; Material and Methodology: K.R., Ö.H.; Supervision: Ö.H., K.R.; Visualization: K.R., Ö.H.; Writing-Original Draft: Ö.H., K.R.; Writing-review & Editing: K.R., Ö.H.; Other: All authors have read and agreed to the published version of manuscript.

Conflict of Interest

The authors have no conflicts of interest to declare.

Funding

The authors declared that this study has received no financial support.

REFERENCES

- Blüscher, M., Mogensen, P., Shapiro, D., Wagner, I. (2000). *The Manufaktur- Supporting Work Practice in (Landscape) Architecture*. DESARTE- The Design of Artefacts and Spaces.
- Douet, J. (ed.) (2013). *Industrial heritage re-tooled: The TICCIH guide to industrial heritage conservation*. Routledge. DOI: <https://doi.org/10.4324/9781315426532>
- Enichlmair, C., Kranabether, M., Stein, D. (2005). *Economic Transformation and Urban Planning in Vienna: Emergence of the Service Sector and its' Implications for Urban Regeneration*. 10th International Conference on Information & Communication Technologies (ICT) in Urban Planning and Spatial Development and Impacts of ICT on Physical Space, Proceedings, reviewed paper, Ed. by Manfred SCHRENK, Tagungsband, 261-266.
- Himmelbauer, C. (2003). *Apartment Building Gasometer B*, Yapı Magazine (Yapı Dergisi), No. 259, Istanbul, 70-78.
- Madran, E., & Kılınç, A. (2007). *New Definitions, New Concepts in Conservation: 'Industrial Heritage'*. Publication of the Chamber of Architects Ankara Branch, 44, Ankara, 146-149.
- Mérai D. and Kulikov V. (2021). *From Burden to Resource: Uses of Industrial Heritage in East-Central Europe*. Introduction (eds. Dóra Mérai, Zsuzsanna Sidó, Hanna Szemző, Volodymyr Kulikov). Budapest: *Archaeolingua*, 2021, 5-12. ISBN 978-615-5766-52-7
- Schwarz, M., Wehdorn, M. (2000). *101 Restaurierungen in Wien*. Arbeiten des Wiener Altstadterhaltungsfonds 1990-1999, Vienna- Austria.
- Tekeli, D. (2001). *Industrial Structures*. *Arrademento Architecture*, 2, 62-73.
- TICCIH (2023). *Charter: The Nizhny Tagil Charter for the Industrial Heritage (2003)*. <https://ticcih.org/wp-content/uploads/2013/04/NTagilCharter.pdf>. (Accessed: August 27, 2023).
- Wehdorn, M. (2000). *Social and Economic Integration of Cultural Heritage in Austria*. Technical University of Vienna, Vienna- Austria.
- Gazometers (2005). www.gasometer.org, June 2005.
- Gazometers (2023). <https://www.gasometer.at/de/architektur>, August 2023.

A Bibliometric Analysis of Wearable Health Technology Research

Pelin Yılık^{1*} 

Abstract: The aim of this provision is to include researchers in scientific publications revealing their research activities in the field of wearable health technologies and conducting research on this subject. In this context, bibliometric analysis of English articles in the Web of Science database between 1996 and 2023 was conducted using the R programming language. The search criteria included keywords such as "health," "technology," "physical activity," "devices," "sensors," "design," "adoption," "information technology," "user acceptance," and "acceptance." This search yielded a comprehensive collection of 5,327 studies related to wearable health technologies published between 1996 and 2023.. The data set obtained from these people was analyzed where the "biblioshiny" in the RStudio program was located. As a result of the research, the most frequently used words, the most relevant institutions in the field, and the stored regional growth amounts and citation records were obtained. This study is an important resource for researchers who want to conduct research and studies in the field of wearable health technologies. Since the calendar year 2023 has not been finalised, some graphs do not show the relevant year.

Keywords: technologies, bibliometric analysis, wearable health technologies.

¹**Address:** Kudret International Hospital, 06100, Ankara, Türkiye

***Corresponding author:** pelinyilik@hotmail.com

Citation: Yılık, P. (2023). A Bibliometric Analysis of Wearable Health Technology Research. *Bilge International Journal of Science and Technology Research*, 7(2): 187-197.

1. INTRODUCTION

In our rapidly globalizing and technologically advancing world, the realm of technology progresses at an unprecedented pace. The concept of health, which is the most important factor of human life, also has its share of this development. The healthcare sector, like many other fields, harnesses the power of these technological strides, shifting certain services onto virtual platforms. This transition not only enhances the accessibility of healthcare services but also facilitates easier diagnoses and treatments for patients. Furthermore, the integration of information technology into the healthcare sector enhances service efficiency and quality, while concurrently contributing to the reduction of medication errors, data inaccuracies, and medical mistakes (Ülke and Atilla, 2020).

It is necessary to create an effective health system to ensure the general health of the society and make it sustainable. This health system becomes even more effective with the advancement of technology and the correct integration of health information systems into our lives. In today's world, computers, internet and communication technologies have become an integral part of our daily lives. The widespread use of these technologies in many areas facilitates the work and daily lives of both individuals and institutions.

Institutions in the health sector also use information technologies and health information systems in the planning and management stages of health services (Peker et al., 2018).

Technological advancements have revolutionized healthcare, making it more accessible to people from anywhere and at any time. Key innovations driving this transformation include health informatics, hearing aids, sensor technologies, and mobile devices, with a particular emphasis on smartphones and wearable technological accessories like smartwatches (Şimşir and Mete, 2021).

Thanks to the use of technological advances in healthcare systems, many benefits can be enjoyed, especially during crisis periods such as pandemics. Wearable health technology products can be used to facilitate the isolation of individuals who have the disease or are at risk of infection, especially as in the recent pandemic crisis we have experienced worldwide. In this way, the physical distance between patients and healthcare professionals can be increased and the density in hospitals can be reduced. However, the problem of controlling individuals and thus spreading the epidemic can be solved more easily. For this reason, many countries have developed different solutions for remote patient monitoring. These countries are diligently

crafting strategies aimed not only at minimizing the impact of past epidemics, which continue to affect us, but also at proactively addressing future infectious outbreaks through the utilization of wearable health technology products (Deringöz et al., 2021).

Wearable technology products are designed as special electronic devices that can track data over long periods, usually wirelessly, and they are synchronized with computers or smartphones. These products are among the cutting-edge wearable computers that can be integrated in different ways into different parts of various objects, such as rings, smart glasses, smart watches, shoes, or bracelets. Although wearable technologies that can synchronize with smartphones have begun to appear more frequently in recent times, this process has a longstanding history. . Hearing aids, glasses, overalls and clothing-like products that balance body temperature, and shoes are the products of this technology that were used in the past and are still being developed and used (Büyükgöze, 2019).

It is a necessity to take advantage of the opportunities of technology in the health sector in order to continuously and regularly monitor diseases, perform immediate interventions and contribute to the improvement of preventive and therapeutic health services by providing rapid digital data transmission to relevant health departments. Technological developments can provide positive benefits not only during medical operations, but also before and during the healing process (Dahil, 2023:1). Therefore, just as in every other field, the healthcare sector experiences inevitable changes and developments due to advancing technology. This ongoing transformation process, expected to accelerate in the coming years, is further facilitated by the opportunities offered by wearable technology.

Wearable Health Technologies

The healthcare industry tends to benefit from the assistances of this advancement along with developing technology in order to increase the quality of patient care, reduce costs, improve patients' living standards and increase the efficiency of healthcare services. The ongoing need for technology in healthcare continues to grow, driven by the emergence of new imaging capabilities and the effective utilization of big data for data transmission. This synergy has led to an increased adoption of wearable medical devices, which hold significant promise in disease treatment. Innovative products, born out of the rapid evolution of wearable technology, are swiftly integrating into everyday life (Aydm, 2019).

Wearable technologies refer to electronic devices that can be attached to the skin, can be easily carried, and can be integrated into clothes or accessories and carried along with us. These wearable technologies can perform many functions, especially by having a combined working system with products such as computers and smartphones. However, in some cases, wearable technologies can be more functional than traditional technological devices. Wearable technologies offer the ability to track and monitor features that cannot be detected by mobile phones and computers, such as biofeedback and psychological state monitoring, as

well as the ability to collect data on this feedback. Wearable devices used today include smart watches, smart bracelets, glasses, lenses, smart implants used in dental treatment, e-textile products, smart fabrics, headbands, rings and jewelry such as hearing aids. The most commonly used wearable devices include smart bracelets, hearing aids and smart watches. The history of wearable technologies actually goes back a long way. The first wearable device was produced in 1955 for cheating in games. Since then, wearable technologies have seen remarkable advancements, particularly in the gaming and entertainment sectors, but more notably in the fields of health and fitness (Demirci, 2018; Sağbaş et al., 2016).

Wearable products that can be used in health, sports, jewelry, clothing and many other areas are very common today. These devices make it easier to keep track of daily tasks, such as frequently used mobile phones and computers, and help carry out tasks more efficiently. Swift task completion not only saves time for users but also benefits service providers (Çakır et al., 2018).

Wearable technology products, which provide great benefits in remote treatment processes of individuals and monitoring the data generated during treatment processes, especially in the healthcare sector, will undoubtedly begin to take more part in our lives in the near future. Aging population and increasing population growth rate will further increase the need to benefit from health systems, which will shape new types of current services in health systems. With developing technology, wearable technology products that can provide remote patient control will play an active role in this change, among the methods that will change in parallel with this progress in healthcare systems.

2. MATERIAL AND METHOD

2.1. Material

The research dataset comprises articles sourced from the Web of Science Core Collection database. AND and OR conjunctions were used when searching; Keywords specific to wearable health technologies were selected, focusing on article titles to ensure alignment with the research topic.. Words representing health technologies were searched in the article title and the subject was clarified by searching for the concept of wearable health technologies in the results obtained. At the article level, we employed search terms such as "health," "technology," "physical activity," "devices," "sensors," "design," "adoption," "information technology," "user acceptance," and "acceptance" using the "OR" conjunction . In this way, we tried to access all the studies in the field of wearable health technologies in the database. Another limitation of the search is the time period and indexes. In this context, articles published between 1996 and 2023 were included in the data set.

2.2. Method

The significance of open-source programming languages, known for their cost-free access and abundant resources, continues to grow in the global landscape of data science.. Among these languages, the R programming language holds a

prominent position. For bibliometric analyses in this study, we employed the Biblioshiny algorithm (Cuccurullo et al., 2016), a tool written in the R language, known for its open-source nature. At the same time, the software used is a free web-based interface (R Team, 2014). The R programming language is an open source programming language designed specifically for statistical calculations and provides an environment used in this field. This language was developed in 1996 by Ross Ihaka and Robert Gentleman at the University of Auckland in New Zealand. However, the foundations of this programming language are based on the S programming language developed by John Chambers and his team at Bell Laboratories in the 1960s. The R programming language is well developed and includes features that make it easy to visually present data with graphs, a simple to use and effective programming language (Arslan, 2015). This study includes bibliometric analysis methods analyzed with the R programming language.

As a result of the limitations, 5827 articles were identified and these articles were downloaded in plain text format. For the subsequent bibliometric analysis, a total of 5,327 articles (excluding early access articles) were utilized, and this analysis was conducted using the R package program. Elements of the downloaded articles such as data set, sources, authors and documents were examined in bibliometric analysis. The specific findings and details of these investigations are expounded upon in greater depth

within the results section of the study. The bibliometric study was performed using R using the following commands: `install.packages ("devtools")` and `devtools::install_github (massimoaria/bibliometrix)`. Next, the package's library was activated with the command `library (bibliometrix)`. Finally, the database was accessed using `biblioshiny (maxUploadSize=500)`. Here, the parameter "maxUploadSize=500" means that 5327 documents from the WOSCC database were downloaded as WOSCC text files in eleven groups.

3. RESULTS AND DISCUSSION

3.1. Research Results

The 5327 articles analyzed in our study cover research between 2002 and 2023. Numerical information of the articles is shown in Table 1. When Table 1 is examined, there are 2645 sources in which the mentioned articles are published. The annual citation rate per article is 2,426. Additionally, the annual growth rate of the studies is 23,74. In our study, the number of single-author articles appears to be 333, corresponding to 062% of the average studies done. Another important value of the study is the international co-authorship percentage of 2,282, which indicates that our study is a suitable area for different research to work together.

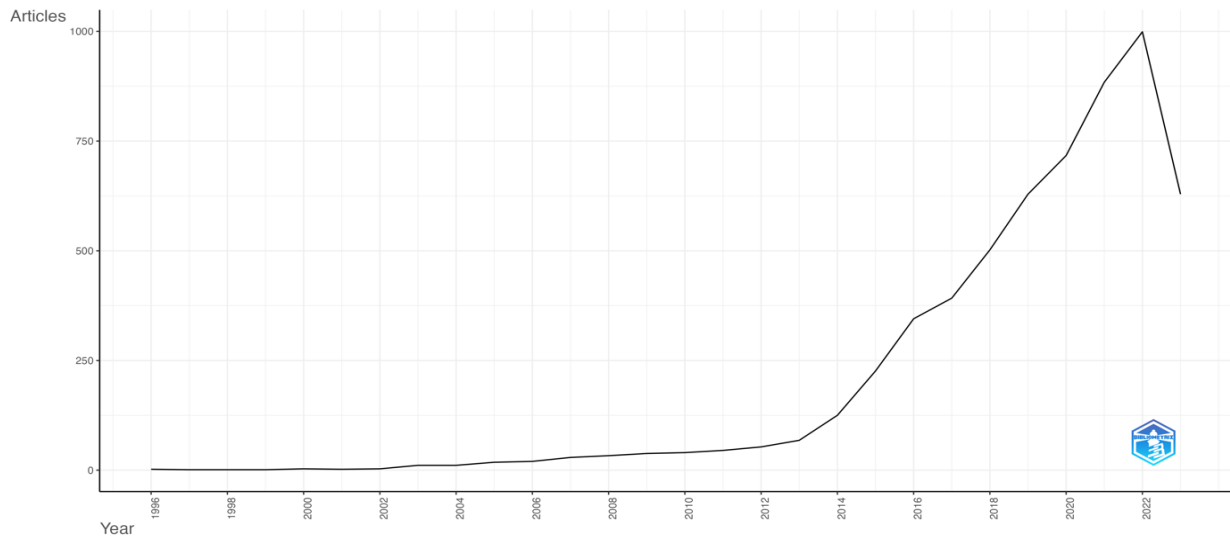
Table 1: Basic Information About the Data Set

DEFINITION	RESULTS
Basic Information About the Data Set	
Time Range	1996:2023
Sources (Journals, Books, etc)	2645
Documents	5327
Document Average Age	3.92
Annual Growth Rate %	23.74
Average Citations Per Doc	2.426
Document Contents	
Keywords Plus (ID)	946
Author's Keywords (DE)	1300
Authors	
Authors	22072
Authors of Single-Authored Docs	296
Authors Collaboration	
Single-Authored Docs	333
Co-Authors Per Doc	5.14
International Co-Authorships %	2.282

Upon examining Figure 1, it becomes evident that there were no studies recorded between 1996 and 2002. However, a gradual increase in research output is discernible over the subsequent decade, spanning from 2002 to 2012. Following this period, a substantial surge in the number of articles is notable until the year 2022. While the number of studies post-2022 does not exhibit a significant decrease, there is a

discernible deceleration compared to the preceding years. Additionally, as we mentioned before, the annual growth rate of the study area is calculated as 23,74. Considering the increasing rate of studies, especially in the last 10 years, it is obvious that the subject matter is a current issue and that it will be the subject of much more research in the coming years.

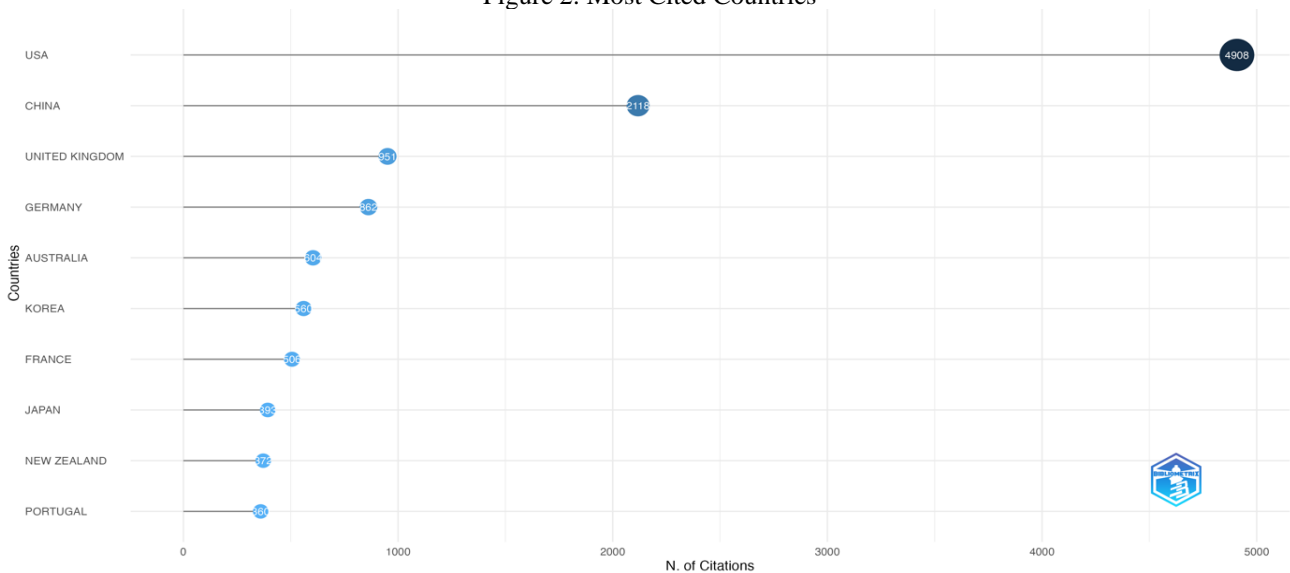
Figure 1: Change in the Number of Articles by Years



The countries where the most cited studies on the subject were conducted are shown in Figure 2. The USA, China and

the United Kingdom are in the top 3 ranks of the most cited studies.

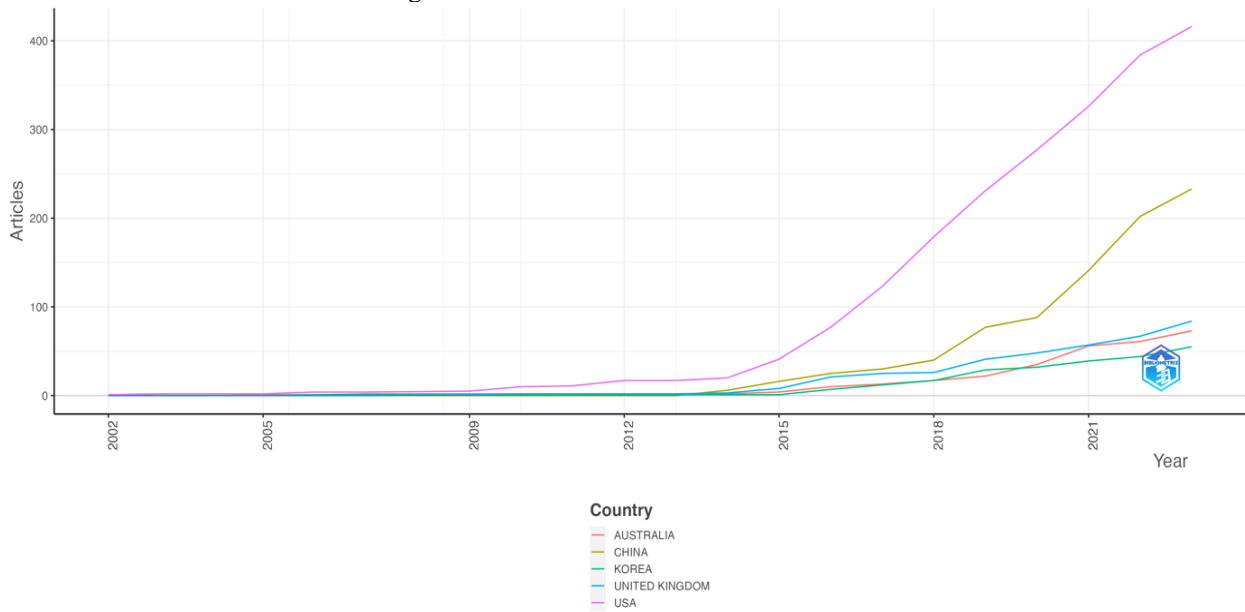
Figure 2: Most Cited Countries



Countries' production over time is shown in the graph in Figure 3. As can be seen in the graph, the increase rate of studies in the last 10 years is remarkable. Especially

considering the production numbers of the USA and China, they differ from other countries in terms of production numbers.

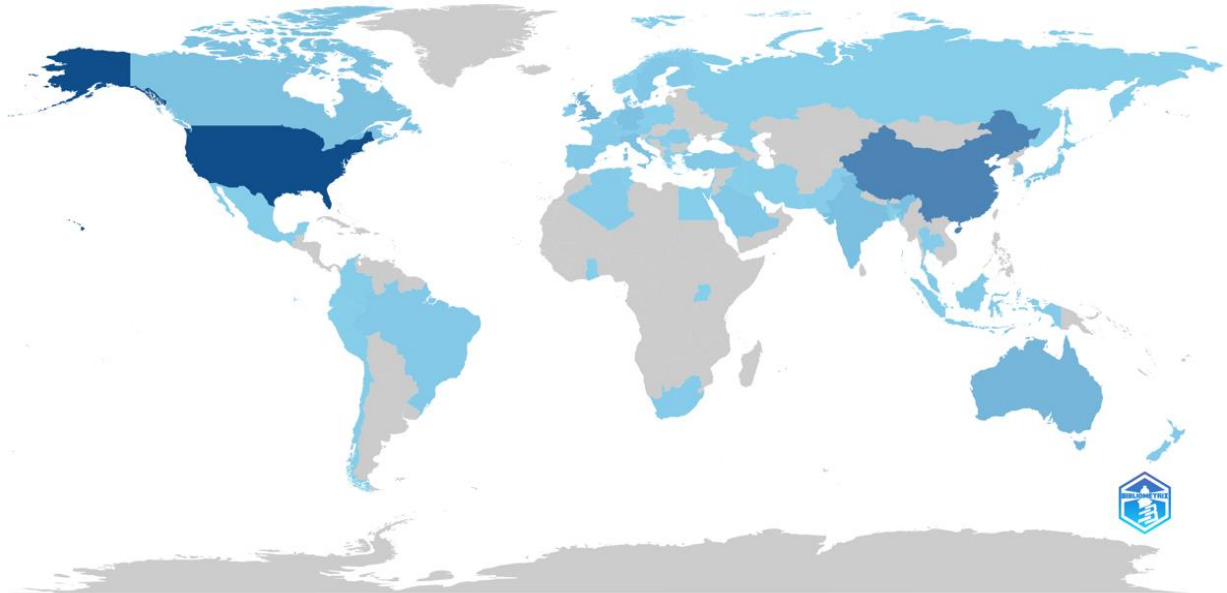
Figure 3: Production of Countries Over Time



The scientific productions of the countries are shown on the colored World Map as in Figure 4. As can be seen in the figure, it is stated that studies are more intense in the USA

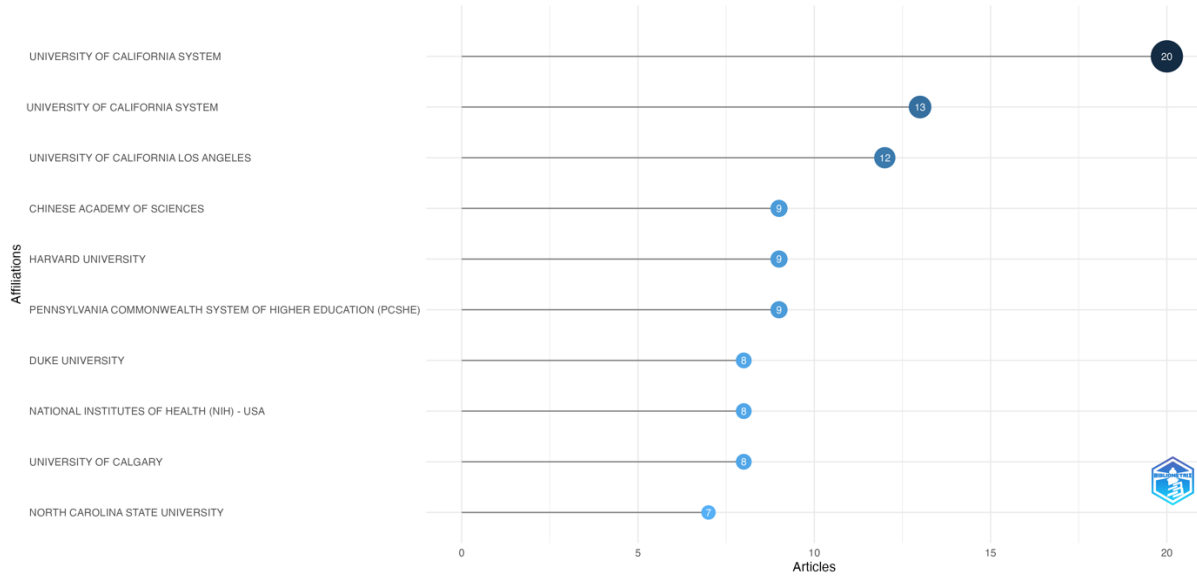
and China, Australia, India, Russia, and Central and Western European countries.

Figure 4: Scientific Production of Countries



When the institutions working on the subject are examined, it can be seen in Figure 5 that universities in the USA and China are predominant.

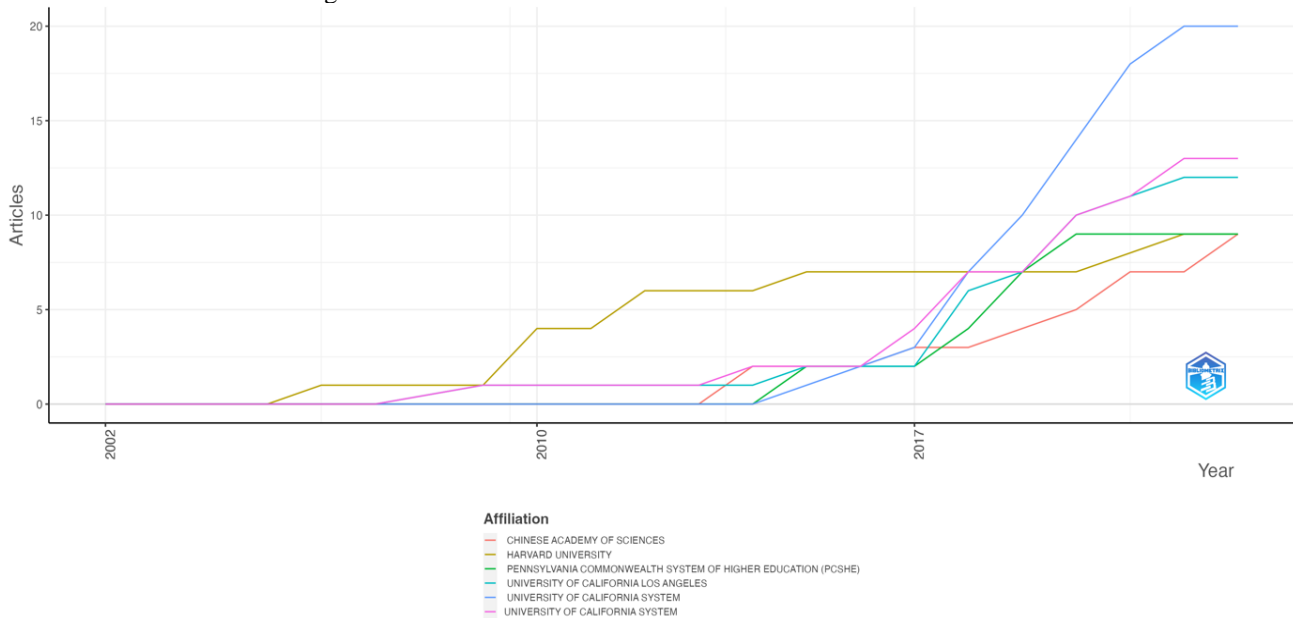
Figure 5: Most Relevant Institutions



When the production of universities on the subject is examined by years, it is seen that the most relevant institution on the subject is Harvard University. However, in the following years, it was observed that other US Universities carried out more studies on the subject, surpassing Harvard

University in terms of the number of studies. We can examine the production numbers of the most relevant institutions related to the subject of the study by year in Figure 6 graphically.

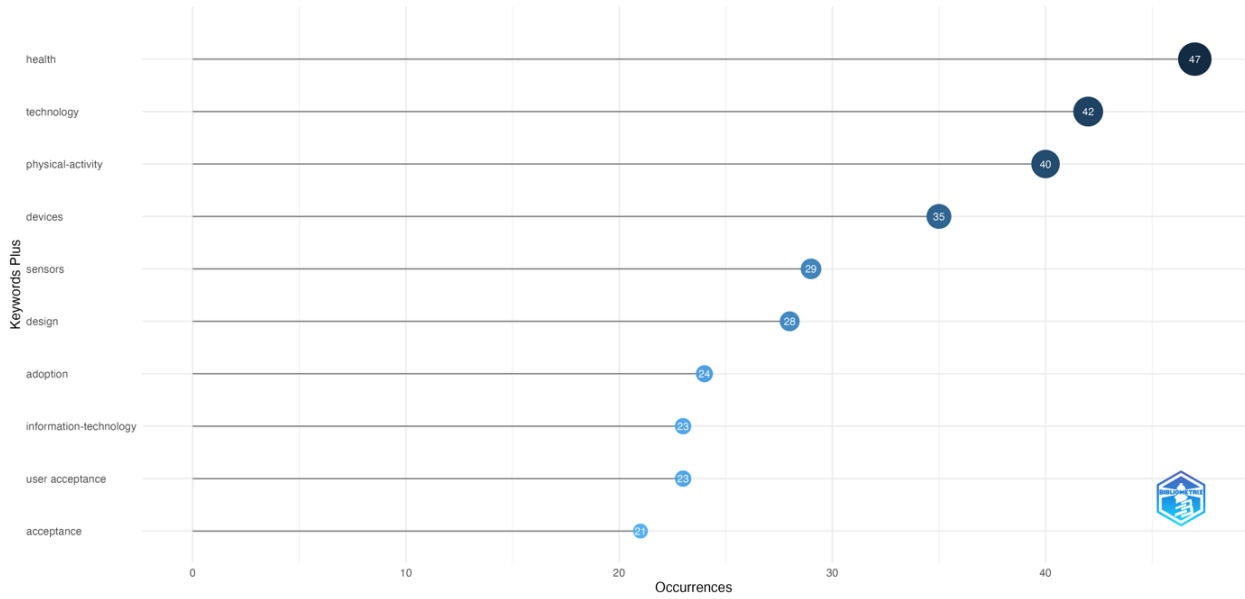
Figure 6: Production of the Most Relevant Institutions Over Time



Upon analyzing the most pertinent words within the scope of our study, we observe that the most frequently used terms include "health," "technology," "physical-activity," "devices," "sensors," "design," "adoption," "information-technology," "user acceptance," and "acceptance," as

illustrated in Figure 6.. As a result of the analysis, it can be concluded that the words mostly used are from the field of health and technology. The analysis of the most relevant words within the research field is seen in Figure 7.

Figure 7: Most Relevant Words



The most frequently used words in the studies are shown in Figure 8 through word cloud graphics. The size of each word within the image corresponds to its frequency of use, with larger fonts indicating higher usage. (Köse and Kurutkan,

2021: 421). As seen in the word cloud analysis, the field of study is closely related to the fields of health and technology.

Figure 8: Word Analysis of Studies



In Figure 9, the proportions of words used in the studies are analyzed. Our analysis, which is parallel to the analyzes in Figure 6 and Figure 7, supports the concepts we have stated before. As seen in our analysis, the word with the highest usage rate is the word "health", followed by the second most

frequently used word, "technology". The main reason for this is that the studies are mainly associated with the fields of health and technology and are carried out within this framework.

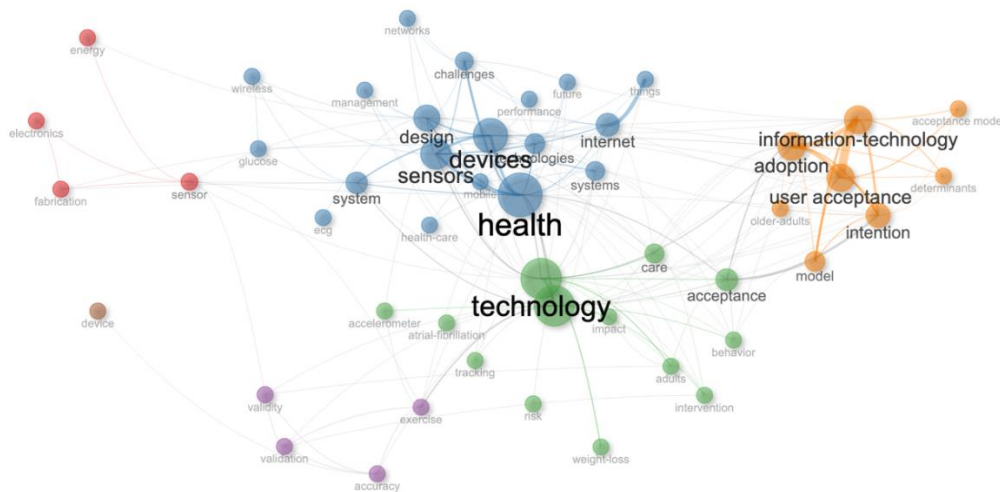
Figure 9: Ratio of Words Used in Studies



Examining keywords for co-occurrence is an extremely critical analysis for a clear understanding of the study's content. The keywords carefully chosen by the authors reflect the basic message of the study and the center of the research. The network also shows us the connection and flow between words. The thickness of the connection lines between the results also illustrates the relationship between words and the strength of interusability (Oraee et al., 2017). Upon examining the co-occurrence of words used in the studies, Figure 10 reveals the formation of six distinct

clusters. Clusters are formed according to the words in the content of the studies and their combined use. In contrast to previously provided graphs such as "Most Relevant Words," "Word Analysis of Studies," and "Ratio of Words Used in Studies," Figure 10 offers insights into the interconnected use of the most frequently employed words in the studies. Moreover, our analysis vividly depicts the interrelationships between disciplinary and interdisciplinary fields.

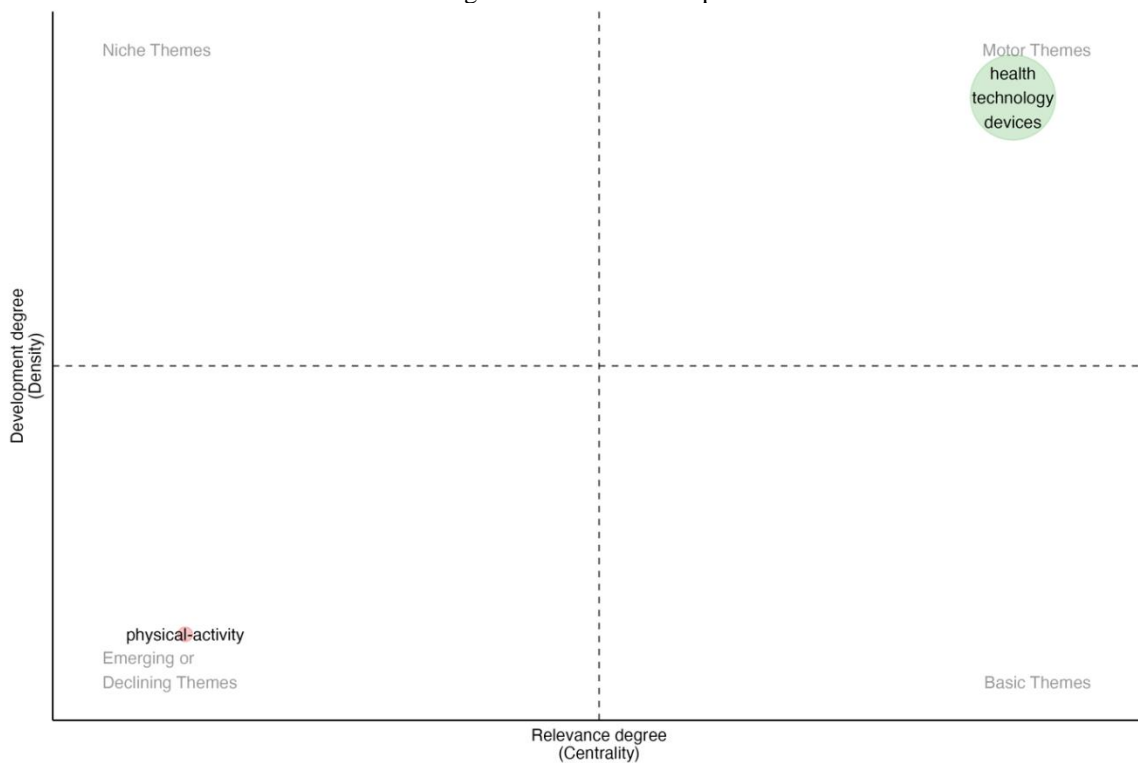
Figure 10: Co-occurrence of Words Used in Studies



The thematic map resembles a 4-section plane, where x and y graphs on the analytical plane show the centrality and density of the results by assigning an impact value to the results. It is expressed with a two-dimensional and four-category diagram based on the centrality and density of the themes. In this diagram, the X-axis denotes a theme's degree of interaction with other networks, referred to as its centrality. The degree of centrality can be considered a measure of importance for a theme in the research field. On the other hand, density represents the strength within a network and can be interpreted as an indicator of theme development (Cobo et al., 2015; Aria et al., 2021:). In the thematic map diagram, the upper right corner is defined by engine themes that are dense and central, indicating that there is intense research in this area. The upper left corner represents highly developed but isolated themes. The lower left corner contains rising or falling themes. The concepts formed in this section are new themes or exist outside the field. The lower right corner contains foundational and

transformational themes. Themes that emerge in this section are generally well-studied concepts with strong internal ties (Cahlik, 2000; Turner and Rojouan, 1991; Flórez-Martínez et al., 2021). As can be seen in Figure 11, two different themes emerged in our analysis. The first theme, centered on the overarching title of "Health," combines the terms "technology" and "devices," suggesting a concentration of research activities in these areas. Studies in this domain are well-documented in the literature, indicative of their extensive exploration. Conversely, the second theme is situated within the context of "physical-activity.". Themes in this section suggest a gradual decline in the topic's prominence. Notably, our thematic analysis reveals that while wearable health technologies initially gained traction in the realm of physical activities, they are progressively expanding and evolving within the broader field of healthcare.

Figure 11: Thematic Map



4. CONCLUSION

The field of wearable health technologies predominantly consists of recent and current studies, characterized by a wide-reaching and interdisciplinary literature.. This broad and interdisciplinary feature of the literature has allowed it to be included in many studies. Our analysis underscores a noteworthy surge in research activities, particularly post-2012, a trend largely driven by the rapid pace of technological advancement.. The abundance of studies conducted in the last 10 years in the literature and the relationship of the subject with different literatures pose difficulties for researchers. At this point, it will be beneficial for researchers to review this study in order to benefit from it in terms of time saving and energy consumption. Our analysis clearly states which literatures researchers will

study, through which institutions they can access productive resources, and which concepts and words they will focus on. Our study identifies the United States and China as the most influential countries in this domain, with the most relevant institutions situated in these nations.. As a result of the study, the most frequently used words in research were listed through figures and it was concluded that especially the fields of health and technology were the two main themes of the subject. It is clearly seen in our study that technological developments, especially in the last decade, have had a positive impact on health technologies. R Programming Language was used as the visualization program of our study, and the visuals created by the program and provided by the system were used within the scope of the study.

In a similar study, Köse and Kurutkan (2021), in their study titled "Bibliometric Analysis of Internet of Things Applications in Health Services", stated that China and the USA stand out as the countries that produce the most in terms of literature contribution. In this study, it is similarly stated that the USA and China are the countries that contribute the most to the field of wearable technology in healthcare services. Furthermore, Köse and Kurutkan (2021) noted that the most frequently used words in their study included "data," "health," "healthcare," "thing," "internet," and "system." Consistently, our study reveals that the most commonly used words align with these findings and include "health," "technology," "physical-activity," "devices," "sensors," "design," "adoption," and "information-technology," mirroring previous research outcomes.

In another similar study, Sikandar et al. (2022) "Digital Technologies in Healthcare: A Systematic Review and Bibliometric Analysis", Sikandar et al. (2022) examined the studies on the use of digital technologies in healthcare organisations. The researchers who analysed the studies in the literature stated that the studies continue to increase. In this study, similarly, it is stated that the researches and studies in the literature are increasing and the importance of the subject is being realised more and more day by day. Sikandar et al. (2022) analysed the studies conducted between 2017 and 2022 and stated that researchers working in the UK, USA and Australia contributed the most to the literature. In this study, the countries that contributed the most to the field were the USA, China, the United Kingdom, Germany and Australia. Although it seems to be in parallel with the other study, there are some minor differences in this section. Sikandar et al. (2022) analysed the studies conducted since 2017 in their study, which resulted in minor differences in the analysis of contributing countries. Again, Sikandar et al. stated the most commonly used words as "digital health", "mhealth", "telemedicine", "covid-19", "ehealth", "digital technologies", "technology" and "mobile apps" in their study. When this study is compared with this section, parallels and minor differences are observed, as in the case of contributing countries. These discrepancies can be attributed to the variation in the starting point of the examination, which Sikandar et al. (2022) based on the year 2017.

Ethics Committee Approval

N/A

Peer-review

Externally peer-reviewed.

Conflict of Interest

The author have no conflicts of interest to declare.

Funding

The author declared that this study has received no financial support.

REFERENCES

- Aria, M., Alterisio, A., Scandurra, A., Pinelli, C., & D'Aniello, B. (2021). The scholar's best friend: Research trends in dog cognitive and behavioral studies. *Animal Cognition*, 24(3), 541-553.
- Arslan, İ. (2015). Statistical programming with R. Pusula.
- Aydın, N. (2019, March). Giyilebilir sağlık teknolojisinin geleceği. In XI. International Balkan and Near Eastern Social Sciences Congress Series, Tekirdağ/Türkiye (pp. 614-619).
- Büyükgöze, S. (2019). A review on sensor patches from wearable technologies in Health 4.0. *European Journal of Science and Technology*, (17), 1239-1247.
- Cahlik, T. (2000). Comparison of the maps of science. *Scientometrics*, 49(3), 373-387.
- Çakır, F. S., Aytekin, A., & Tüminçin, F. (2018). Internet of things and wearable technologies. *Journal of Social Research and Behavioural Sciences*, 4(5), 84-95.
- Cobo, M. J., Martínez, M. Á., Gutiérrez-Salcedo, M., Fujita, H., & Herrera-Viedma, E. (2015). 25 years at knowledge-based systems: a bibliometric analysis. *Knowledge-based systems*, 80, 3-13.
- Cuccurullo C, Aria M, Sarto F. Foundations and trends in performance management. A twenty-five years bibliometric analysis in business and public administration domains. *Scientometrics* 2016;108:595-611.
- Dahil, A. (2023). Investigation of Wearable Health Technologies.
- Demirci, Ş. (2018). The effects of wearable technologies on health services and health service users. *Anemon Muş Alparslan University Journal of Social Sciences*, 6(6), 985-992.
- Deringöz, A., Danişan, T., & Eren, T. (2021). Evaluation of wearable health technologies in the follow-up of Covid-19 with CRCV methods. *Polytechnic Journal*, 25(2), 533-543.
- Flórez-Martínez, D. H., Contreras-Pedraza, C. A., & Rodríguez, J. (2021). A systematic analysis of non-centrifugal sugar cane processing: Research and new trends. *Trends in Food Science & Technology*, 107, 415-428.
- Köse, G. & Kurutkan, M. N. (2021). Bibliometric analysis of internet of things applications in healthcare. *European Journal of Science and Technology*, (27), 412-432.
- Oraee, M., Hosseini, M. R., Papadonikolaki, E., Palliyaguru, R., & Arashpour, M. (2017). Collaboration in BIM-based construction networks: A bibliometric-qualitative literature review. *International Journal of Project Management*, 35(7), 1288-1301.
- Peker, S. V., Van Giersbergen, M. Y., & Biçersoy, G. (2018). Sağlık Bilişimi ve Türkiye'de Hastanelerin Dijitalleşmesi. *Sağlık Akademisi Kastamonu*, 3(3), 228-267.
- R Team, R. D. C. T. (2014). R: A language and environment for statistical computing. Vienna, Austria: R Foundation for Statistical Computing.

- Sağbaşı, E. A., Ballı, S., & Yıldız, T. (2016). Wearable smart devices: past, present and future. *Academic Informatics Symposium*, 30, 749-756.
- Sikandar, H., Abbas, A. F., Khan, N., & Qureshi, M. I. (2022). Digital technologies in healthcare: A systematic review and bibliometric analysis. *International journal of online and biomedical engineering*, 18(8), 34-48.
- Şimşir, İ., & Mete, B. (2021). The Future of Healthcare: Digital Health Technologies. *Journal of Innovative Healthcare Practices (JOINIHP)*, 2(1), 33-39.
- Turner, W., & Rojouan, F. (1991). Evaluating input/output relationships in a regional research network using co-word analysis. *Scientometrics*, 22(1), 139-154.
- Ülke, R., & Atilla, E. A. (2020). Information systems and e-health in health services: The case of Ankara province. *Gazi Journal of Economics and Business*, 6(1), 86-100.

Reading The World With Statistical Literacy: Results of An Empirical Study

Deniz Ünal¹, Begüm Çığsar*¹, Dibanur Alam¹, Şerife Ezgi Atalar¹,
Sait İsmail Gümüş¹, Ali Çakıtlı¹

Abstract: As in all kinds of literacy, this study has been motivated by considering the contribution of statistical literacy to the development reaching from the individual to the society and its ability to bring critical thinking. Statistical literacy scale indexed by Turkish Surveying Index was applied to 398 university students and the correlations between the literacy levels of these participants and some socio-demographic characteristics were examined. As a result of the analyses, it was seen that there was no difference among the statistical literacy scores of the students in terms of years spent at school, parental education status or universities. It was observed that there was a weak positive relationship with grade points averages. The most striking finding is that numerical sciences students got higher scores than social sciences.

Keywords: Critical Interpretation, Critical Thinking, Linear Regression, Logistic Regression, Statistical Literacy

¹**Address:** Çukurova University, Faculty of Arts and Sciences, Dept. of Statistics, Adana, Türkiye.

***Corresponding author:** begumcigsar@gmail.com

Citation: Ünal, D., Cıgsar, B., Alam, D., Atalar, Ş.E., Gümüş, S.İ., Cakitli, A. (2023). Reading The World with Statistical Literacy: Results of An Empirical Study. Bilge International Journal of Science and Technology Research, 7(2): 198-203.

Citation:

1. INTRODUCTION

According to Turkish Language Association (TDK), literacy is defined as the state of being literate, while literate means educated (TDK, 2022).

Literacy according to United Nations Educational, Scientific and Cultural Organization's (UNESCO) definition; It is the ability to identify, understand, interpret, create, communicate and calculate different types and varying types of printed and written materials (UNESCO, 2022). UNESCO also emphasizes that literacy is a continuum of learning that includes the integration and adaptation of individuals into their communities and wider societies by enabling them to develop their potential and knowledge.

Thus, it is emphasized that these people who fully participate in the society will contribute to the acquisition of the right to education and the improvement of their livelihoods. For these reasons, UNESCO (2022) includes global literacy among its targets. In order to emphasize and remind the

public of the importance of literacy, 8 September has been celebrated as the literacy day every year since 1966.

The contribution of literacy to social development and the adaptation of the individual to society over time has caused this concept to go beyond literacy skills. Because the advances and deepening in scientific fields, technology and art in the century we live in have brought with the need to understand, make sense of, and adapt these fields to life.

Thus, concepts such as digital literacy, mathematical literacy, financial literacy, cinema literacy, media literacy, and statistical literacy have emerged.

In this sense, literacy can be defined as having and understanding basic information about an information or problem encountered in daily life, being able to think, comment and criticize this information.

From this perspective, it is clear that literacy will be a driving force for development and will guide societies in issues such as deep poverty, access to health and food, and sustainability,

security, discrimination, media (digital media) which are among the biggest problems of today. Because, literate individuals will be able to comment on the problems they face in the light of their basic knowledge, create solution methods for these problems, and criticize the existing system. The increase of these individuals will reveal social awareness and the power to put the necessary pressure on the decision-makers in this regard.

This variety in the field of literacy and the social driving force it can create has revealed the necessity of including these types of literacy in formal education over time. As a matter of fact, in the report published by the Board of Education and Discipline in 2017 with the title of 21st century skills, has health, environment, financial, media etc. literacy types.

In the same report, the item “acquiring literacy skills” is also included under the heading of competences and skills aimed at gaining students. It has been noticed all over the world as well as in Turkey that literacy skills are criteria that show the development levels of societies.

With this motivation, financial literacy is addressed as a government policy in Australia and New Zealand (Taylor and Wagland, 2011). Similarly, media education is provided for the development of media literacy in Russia and academic studies are carried out to develop this education (Yoon, 2009). In this regard, literacy studies related to the subjects in school curricula have started to increase in the literature. Mathematics also stands out among these subjects. Academic research has also been done on the connections between mathematical literacy and scientific literacy, in addition to studies on the relevance of the mathematics we learn in school to our daily life (Ojose, 2011; Wilkins et.al.,2002). Schields (2005), on the other hand, focused on the relationship between information and data literacy and statistical literacy. While emphasizing the importance of information and data literacy by the relevant researchers in the same study, Schields stated that statistical literacy is necessary for students to make sense of these literacy types by bringing them to the level of critical thinking.

Gal (2004) emphasized that the way to be an informed, questioning citizen and employee is through statistical literacy. Thus, he added that people's ability to make effective decisions in solving their daily problems will develop. In his other work (Gal, 2002), he described statistical literacy as the ability to interpret, critically evaluate and communicate statistical outputs. Engel (2017), on the other hand, emphasized that it is indispensable in the construction of an active citizenship process. In the same study, Engel underlines that it is one of the most important duties of statistics educators to prevent even the false presentation of evidence of empirical data in public, political and social fields. It is stated in the same study that directing public debates from emotional or subjective areas to areas based on evidence and science and making political decisions on these facts will be possible with statistical literacy.

It is clear that learning all types of literacy is necessary for social progress, for moving discussions to a scientific level,

and for speaking objective facts in societies. Statistical literacy, on the other hand, is essential for dealing with, understanding, and considering and criticizing multivariate phenomena together.

In this study, statistical literacy has been specifically addressed with the perspective that all kinds of literacy are an important element of personal and social development. The aim is to introduce the concept of statistical literacy and to draw attention to this area. In the study, which examines the relationship between university students' statistical literacy levels and socio-demographic characteristics, their field of education and universities, it is also examined whether there is a correlation between the students' literacy level and their general grade points averages (GPA), parental education levels, and their knowledge and confidence levels in official statistics.

2. MATERIAL AND METHOD

With the above-mentioned purpose, a questionnaire, including the statistical literacy scale (Şahin, 2012) indexed by TOAD, was prepared. Necessary ethics committee approvals were obtained for the application of the questionnaire and the Google Forms application was used during the implementation of the survey.

Assuming 95% significance level and $p=0.05$, the sample size 398 was obtained by using the sample calculation equation developed by Yamane (1967) according to the population.

All of the individuals participating in the survey are university students. 398 students from different schools such as Çukurova, Mersin, METU, Çağ, Başkent and Boğaziçi universities participated in the survey.

The analysis in Table 2 was carried out by calculating the total score of the Statistical Literacy Scale. In all analyzes, it was concluded that the skewness and kurtosis values of the variables were between -1.5 and +1.5 and the normality assumption was provided by examining the histogram graphs (Tabachnick & Fidell, 2013). Due to the assumption of normality, ANOVA and independent groups t-test were used in the analysis, and the mean and standard deviations of the variables were given with “Mean±S.S.” notation. As a result of the reliability analysis performed for the Statistical Literacy Scale, the Cronbach Alpha value was found to be 0.71. The scale is reliable. (Carmines and Zeller, 1979).

3. EMPIRICAL ANALYSIS

When the participants are examined, it is seen that there are differences both in the universities and in the departments they study. This allows us to see the statistical literacy trends of different departments. For example, in addition to life sciences such as Computer Engineering, Environmental Engineering, Industrial Engineering, Statistics, Mathematics, Chemistry; students studying in social sciences such as Law, Journalism, Public Relations and Advertising, English Language Teaching participated in the survey. When examined percentages, students studying in life sciences are 65.3% of the sample, and students studying

in social sciences constitute 34.7% of the sample. 51% of the study consisted of females and 49% of males. When asked how many years the students have been studying, 16.1% said it was for one year, 17.8% for two years, 27.1% for three years, 24.9% for four years, 14.1% for five years or a longer period of time.

When the education of the parents of the students participating in the study was examined, it was determined that 23.6% of the parents had primary school or lower, 18.1% had secondary school, 33.7% had high school and 24.6% had undergraduate or higher education.

3.1 Literacy Scale

The answers given by the participants to the Statistical Literacy Scale are given in Table 1.

Table 1. Statistical Literacy Scale Questions' Frequency

Questions of Literacy Scale	Incorrect Answers Frequency (Percentage)	Correct Answers Frequency (Percentage)
Question 1	208 (52,3)	190 (47,7)
Question 2	162 (40,7)	236 (59,3)
Question 3	153 (38,4)	245 (61,6)
Question 4	101 (25,4)	297 (74,6)
Question 5	92 (23,1)	306 (76,9)
Question 6	200 (50,3)	198 (49,7)
Question 7	298 (74,9)	100 (25,1)
Question 8	294 (73,9)	104 (26,1)
Question 9	298 (74,9)	100 (25,1)
Question 10	240 (60,3)	158 (39,7)
Question 11	272 (68,3)	126 (31,7)

It was determined that more than half of the students gave incorrect answers to the 1st, 6th, 7th, 8th, 9th, 10th and 11th questions. The questions that most people answered incorrectly were the 7th and 9th questions. More than half of the students had correct answers to the 2nd, 3rd, 4th and 5th questions. The question that most people answered correctly is the 5th question.

In the literacy scale, it is not aimed to measure the level of knowledge, but to measure the cognitive interpretation capacities of individuals and whether they can make these cognitive interpretations critically (Şahin, 2012). In the study (Şahin, 2012), in which the scale was defined, the categories of interpretation or critical interpretation of each question were also defined. What is meant by critical interpretation here is to express the ability to question the data that provide the statistical results, the interpretations made regarding these results, and the arguments based on them.

In Question 7, one of the questions in which the most misinterpretation were recorded, the measurement results of the weight of an object were given by 9 students, and they were asked to comment on the actual weight of this object. The background of this question is related to population, sample means, and outlier. The question aims to measure

both the cognitive interpretation and the critical level of this interpretation that is, the connection between interpretations and statistical information (Şahin, 2012).

Similarly, the 9th question, in which the most misinterpretation were made by the participants, includes the concepts of measures of central tendency in general and concepts such as median, outlier, extreme value or maximum value in particular. In this question, "The median price of a meal in a student cafeteria is \$30. Therefore, she states that most of the students in this sample spend approximately \$30 on food each week." proposition is discussed. It is a noticeable point that this question is one of the most incorrectly answered question whose category is critical interpretation. Because the accompaniment of critical thinking with knowledge and thought is the most important parameter that makes literacy meaningful.

Again, question 8, which 73,9% of the students answered incorrectly, is a question that includes the concept of conditional probability in its background and requires critical interpretation (Şahin, 2012). In this question, the students were asked to comment on probability based on information about the musicians at a flute concert.

The question with the highest number of correct answers is as follows: A decision will be made to give up one of the equipment in a sports center. While making this decision, it is desired to be made by paying attention to the interests and experiences of the athletes. The learning outcome of this question was determined as interpretation in Şahin's (2012) study.

3.2 Relations

Independent groups t-test and ANOVA were used to determine whether there was a difference between the variable groups according to the scale mean. The results can be seen in Table 2.

Table 2. Relations to Statistical Literacy

Variables	Literacy (Mean±S.S.)	Statistics
Gender		t = -1,23 p = 0,22
Female	5,02 ± 2,49	
Male	5,34 ± 2,65	
Departments		t = 4,72 p<0,001
Life Sciences	5,61 ± 2,50	
Social Sciences	4,36 ± 2,51	
Educational Status of Parents		F = 0,55 p = 0,65
Primary school or lower education level	5,14 ± 2,43	
Middle School	5,49 ± 2,50	
High school	5,01 ± 2,67	
Bachelor or Higher	5,21 ± 2,63	
Trust in Official Statistics		F = 3,36 p = 0,04
Yes*	4,63 ± 2,75	
No	5,10 ± 2,53	
Occasionally*	5,48 ± 2,48	
GPA	Pearson Correlation = 0,10	p = 0,04

There was no significant difference between gender groups according to the Statistical Literacy scale (p=0,22).

There is a significant difference between individuals studying in life and social sciences in terms of statistical literacy (p<0,001). Statistical literacy averages of individuals studying in life sciences are higher than individuals studying in social sciences.

There is no significant difference between the educational status of individuals' parents in terms of statistical literacy averages (p=0,65). There is a weak positive correlation between the GPA of students and their statistical literacy scores (p=0,04).

There is a significant difference between people's confidence in official statistics (p=0,04). Accordingly, as a result of the Post-Hoc test, a significant difference was found between individuals who had confidence and those who sometimes (p=0,04). Statistical literacy averages of confident individuals are lower than individuals who say they have confidence occasionally. Those with the lowest average are the group that says having confidence on official statistics.

From this section onwards, models were created using regression analysis. First, a regression model was created by accepting the statistical literacy level as the dependent variable. Since it was noticed that the results obtained in the analysis on trust in official statistics were also worth examining, the second regression model, which accepted the official statistics as the dependent variable, was added to the study.

3.3 Regression Analysis for Statistical Literacy

A multiple linear regression model was created in which statistical literacy score was chosen as the dependent variable, and gender, department status in life/social sciences and GPA were defined as independent variables. All assumptions necessary to build the model are provided. Analysis results are given in Table 3.

Table 3. Statistical Literacy's Regression Analysis

Regression					
	Unstd Coeff		Std Coeff	t	Sig.
	B	Std. Error	Beta		
Const.	3,22	0,65		4,99	p<0,001
Female	-0,25	0,25	-0,05	-0,98	0,33
Life Sciences	1,19	0,26	0,22	4,50	p<0,001
GPA	0,47	0,22	0,11	2,15	0,03
R=0,25 R ² =0,06	F =8,76 p<0,001				

Then,

$$\text{Statistical Literacy} = 3,22 - 0,25 * \text{Female} + 1,19 * \text{Life Sciences} + 0,47 * \text{GPA} \quad (1)$$

The model in which statistical literacy score is chosen as the dependent variable, and gender, reading status in life/social sciences and grade points average is taken as the independent variable is significant (p<0,001). Independent variables have a 6% contribution to statistical literacy.

In our model, reading in life/social sciences makes a significant contribution to the model (p<0,001). Statistical literacy scores of individuals studying in life sciences are 1,19 points higher than individuals studying in social sciences.

GPA predicts statistical literacy positively (p=0,03). A one-unit change in the GPA causes an increase of 0,47 points in the statistical literacy score.

3.4 Logistic Regression Analysis for Official Statistics

The analysis on trust in official statistics which accepted as the dependent variable, and gender, department status in life/social sciences and literacy were defined as independent variables. All assumptions necessary to build the model are provided (Table 4).

Table 4. Official Statistics’ Logistic Regression Analysis

Parameter Estimates							
Confidence in Official Statistics		B	Std. Error	Wald	df	Sig.	ExpB
Sometimes	Intercept	0,65	0,38	2,96	1	0,09	
	Literacy	0,15	0,05	8,03	1	0,005	1,17
	Life Sciences	-0,58	0,29	3,90	1	0,05	0,56
	Social Sciences	0			0		
	Male	-0,44	0,28	2,46	1	0,12	0,65
	Female	0			0		
No	Intercept	1,13	0,39	8,31	1	0,004	
	Literacy	,076	0,058	1,720	1	0,19	1,08
	Life Sciences	-0,49	0,32	2,33	1	0,13	0,61
	Social Sciences	0			0		
	Male	-1,57	0,30	26,85	1	p<0,001	0,21
	Female	0			0		
a. The reference category is: Yes.							
Nagelkerke = 0,12							
Pearson chi-square = 87,573 p = 0,22							

$$\text{Logit}(y_1) = 0.65 + 0.15 * \text{Statistical Literacy} - 0.58 * \text{Life Sciences} - 0.437 * \text{Male} \quad (2)$$

$$\text{Logit}(y_2) = 1.13 + 0.08 * \text{Statistical Literacy} - 0.49 * \text{Life Sciences} - 1.57 * \text{Male} \quad (3)$$

where y_1 denotes “sometimes” and y_2 denotes “no”.

Based on the Pearson chi-square statistic model fits the data well ($p=0.22>0.05$).

One unit increase in total score of scale would be expected to increase relative risk for preferring “Sometimes” to “Yes” by a factor of 1.17. It means that if all variables in the model are held constant, the subject with higher scale score is more likely to select “Sometimes” over “Yes” with the lower scale score.

In other words, as participants' scores on the statistical literacy scale increase, they are more likely to answer "sometimes" to trusting official statistics than "yes". Participants with a high literacy score do not unconditionally trust official statistics and answer the question about trusting the official statistics as "in some cases they trust".

Students in life sciences are more likely than students in social sciences to select “Yes” over “Sometimes”. In other words, individuals studying in life sciences have more confidence in official statistics than those studying in social sciences.

When examined in terms of gender, males are more likely than females to prefer “Yes” over “No”.

4. RESULTS AND DISCUSSION

The Statistical Literacy Scale developed by Şahin (2012) was used in this study to measure the level at which individuals understand and interpret statistical information. The ability of students to interpret and apply statistical information was evaluated by applying a questionnaire to 398 students studying at different universities and departments. In addition to the literacy scale questions, the participants were also asked to answer questions such as gender, family education level, reading status in the life/social sciences, GPA, how long have they been at university, knowledge and confidence in official statistics. It was determined that 51% of the individuals participating in the survey were female and 49% were male, and the majority of the participants' parents were high school graduates.

If we look at the answers given for the scale questions one by one, we see that most incorrectly answered questions are 7th and 9th ones. According to the scale averages, variables of gender, family education, GPA, being in life/social science, knowledge and confidence in official statistics were analyzed by independent groups t-test and ANOVA analysis. Accordingly, no difference was found between the groups in terms of genders and parental education levels, according to statistical literacy averages. However, it has been determined that the statistical literacy averages of the students studying in the life sciences are higher than the students studying in the social sciences. This reveals the necessity of taking measures to increase the statistical literacy levels of the students of the social sciences.

A positive correlation was observed in the correlation between the scale and the GPA. The higher the GPA, the higher the literacy level. When the knowledge and confidence groups on official statistics are compared according to the statistical literacy averages, it is seen that the literacy averages of the individuals who "sometimes" trust are higher than those of the individuals who "trust". This shows that the increase in literacy scores actually increases the ability of individuals to interpret, think and question critically.

In addition, regression model was constructed by gender, being in life/social science and GPA variables and their contribution to statistical literacy was examined. According to this analysis, it has been determined that the statistical literacy level of students studying in life sciences is 1,19 points higher than students studying in social sciences. Again, with the same analysis, it was determined that a one-point increase in GPA caused a 0,47-point increase in statistical literacy.

In addition to all these analyses, further analyzes regarding the trust of the participants in official statistics show that as their statistical interpretation skills increase, they give the answer "sometimes" rather than "yes" for trusting the official statistics. In other words, it has been observed that as the statistical literacy of individuals' increases, their confidence

in official statistics decreases. On the other hand, it is also reflected in the results that males have more confidence in official statistics than females.

As a result of the analysis, it was determined that the statistical literacy levels of the individuals were affected by the students' grade point average and the department they studied. This situation has an impact on the issue of trust in official statistics. With the study, it was aimed to reveal an awareness by associating the statistical literacy levels of the students from different universities and departments with various variables. Thus, regardless of the department or university, it is aimed to contribute to personal and social development by determining the statistical thinking and interpretation abilities of the students.

In order to increase statistical literacy, compulsory courses on reading data, making sense of histograms/graphs, questioning and interpreting statistical results should be added to the curriculum starting from kindergarten age. Currently, due to the belief in the driving force that social enlightenment will bring, the Ministry of National Education has published a report by showing the necessary sensitivity to the issue since 2017.

In addition, the development of the society in this area can be achieved through public service announcements or entertaining cartoons for children. In addition, it is essential that all non-governmental organizations that desire social development, that dream of a more enlightened society, where individuals can question what is presented to them, and which can create the necessary pressure on decision-makers, should take a role in out-of-school education on statistical literacy. In short, anyone who aims to divert public debate from emotional or subjective areas to evidence and science-based areas should take a role in the steps to be taken on statistical literacy. Because political decisions will be based on objective facts instead of subjective areas, and social progress will be possible with statistical literacy.

REFERENCES

- Board of Education (2017). Retrieved from: https://ttkb.meb.gov.tr/meb_iys_dosyalar/2017_07/18160003_basin_aciklamasi-program.pdf.
- Carmines, E. G., & Zeller, R. A. (1979). *Reliability and validity assessment*. Sage publications.
- Engel, J. (2017). Statistical literacy for active citizenship: A call for data science education. *Statistics Education Research Journal*, 16(1), 44-49. <https://doi.org/10.52041/serj.v16i1.213>.
- Gal, I. (2002). Adults' statistical literacy: Meanings, components, responsibilities. *International statistical review*, 70(1), 1-25. <https://doi.org/10.1111/j.1751-5823.2002.tb00336.x>.
- Gal, I. (2004). Statistical literacy. In *The challenge of developing statistical literacy, reasoning and thinking* (pp. 47-78). Springer, Dordrecht. https://doi.org/10.1007/1-4020-2278-6_3.
- Ministry of National Education (2017). Retrieved from: https://ttkb.meb.gov.tr/meb_iys_dosyalar/2017_07/18160003_basin_aciklamasi-program.pdf.
- Ojose, B. (2011). Mathematics literacy: Are we able to put the mathematics we learn into everyday use. *Journal of mathematics education*, 4(1), 89-100. <https://doi.org/10.12691/education-7-10-1>.
- Shields, M. (2005). Information literacy, statistical literacy, data literacy. *IASSIST quarterly*, 28(2-3), 6-6. Retrieved from: https://iassistquarterly.com/public/pdfs/iqvol28_2_3shields.pdf.
- Şahin, F. (2012). A study for development of statistical literacy scale for undergraduate students (Doctoral dissertation, Boğaziçi University). Retrieved from: <https://toad.halileksi.net/sites/default/files/pdf/lisansogrencileri-icin-istatistiksel-okuryazarlik-olcegi-toad.pdf>.
- Tabachnick, B.G., Fidell, L.S. (2013). *Using Multivariate Statistics* (sixth ed.) Pearson, Boston.
- Taylor, S., and Wagland, S. (2011). Financial literacy: A review of government policy and initiatives. *Australasian Accounting, Business and Finance Journal*, 5(2), 101-125. Retrieved from: <https://ro.uow.edu.au/aabfj/vol5/iss2/7/>.
- TDK, Turkish Language Association (2022). Retrieved from: <https://sozluk.gov.tr/>.
- Turkish Surveying Index (TOAD) (2022). Retrieved from: <https://toad.halileksi.net/>.
- UNESCO, United Nations Educational, Scientific and Cultural Organization (2022). Retrieved from: <http://uis.unesco.org/en/glossary-term/literacy>.
- Wilkins, J. L., Zembylas, M., and Travers, K. J. (2002). Investigating correlates of mathematics and science literacy in the final year of secondary school. In *Secondary analysis of the TIMSS data* (pp. 291-316). Springer, Dordrecht. https://doi.org/10.1007/0-306-47642-8_18.
- Yoon, J. (2009). The Development of Media Literacy in Russia: Efforts from Inside and Outside the Country. *Issues in Information and Media Literacy*, 1, 189-213.

Yazar rehberi

Makale A4 sayfa boyutunda, Times New Roman yazı tipinde, 10 punto olarak ve düz metin şeklinde yazılmalıdır. Makaleye sayfa ve satır numarası eklenmelidir.

Kapak sayfası: Kapak sayfasında sırasıyla makale başlığı, yazar adı soyadı, yazar iletişim bilgileri bulunmalıdır.

Başlık ve özet (İngilizce): Özet 500 kelimeyi geçmeyecek şekilde yazılmalıdır. Araştırmanın gerekçesini, amaçlarını, uygulanan yöntemi, sonuç ve önerileri içermelidir. Özet sonuna 3-6 kelimeden oluşan anahtar kelimeler eklenmelidir.

Ana metin: Makale ana metni tek satır aralıklı olarak yazılmalı, çizelge ve şekillerle birlikte toplam 15 sayfayı geçmemelidir. Konu başlıkları 1., 1.1., 1.1.1., şeklinde numaralandırılmalıdır.

Dipnotlar: Metin içerisinde dipnotlardan olabildiğince kaçınılmalıdır. Çizelge ve şekillerde ise gerekli olması halinde ilgili objenin altında yer almalıdır.

Semboller ve kısaltmalar: Birim sembolleri Uluslararası Birimler Sistemine (The International System of Units; SI) göre olmalıdır.

Kaynaklar: Metin içinde geçen kaynaklar yazarların soyadları ve yayın yılı ile birlikte verilmelidir (Örnek: Özkan vd., 2008; Özdemir, 2015). Metin sonundaki kaynaklar önce alfabetik sonra kronolojik sıraya göre sıralanmalıdır. Bir yazarın aynı yılda birden fazla yayınına atıf yapılmışsa, bu kaynaklar yayın yılından sonra gelecek a, b, c... harfleriyle ayrılmalıdır (Örnek: Kandemir, 1999a; 2000b; 2001).

Çizelgeler ve şekiller: Bütün çizelge ve şekiller metin içerisinde atıf sıralarına göre ardışık olarak numaralandırılmalı ve ilgili yere eklenmelidir. Çizelgelerin üzerinde ve şekillerin altında başlıkları yer almalıdır. Çizelge ve şekiller hem elektronik ortamda hem de kağıt baskıda net olarak görünür ve anlaşılabilir olmalıdır. Şekiller en az 300 dpi çözünürlüğünde hazırlanmalıdır. Şekillerde kullanılan karakterler Times New Roman yazı tipinde olmalıdır.

Makalenin gönderilmesi: Dergimizin bütün hakemlik ve yayıncılık işlemleri elektronik sistem üzerinden gerçekleştirilmektedir. Dergimize yayın göndermek isteyen yazarların ilk olarak dergimizin “web sitesine” girerek “kayıt” ekranından üye olmaları gerekmektedir. Kayıtlı yazarlarımız sisteme “giriş” yaptıktan sonra, makaleleri ile birlikte ve hakem önerilerini de içeren “Telif Hakkı Devri Formunu” sisteme ek belge olarak yüklemelidirler.

Kaynaklar

Kaynak kullanımları aşağıda örneklerde belirtilen şekillerde olmalıdır.

Instructions for authors

Manuscript should be written in A4 page size, with Times New Roman font and 10 pt font size, as plain text. Page and line numbers should be included into the manuscript.

Cover page: Cover page should include title of the manuscript, names and contact information of the authors.

Title and abstract (English): Abstract should not written exceed 500 words. Explains rationale, goals, methods, results and recommendations of the study. Keywords with 3-6 words should be included at the end of the abstract.

Main text: Main body of the manuscript should be written in single line spacing, and it should not exceed a total of 15 pages including tables and figures. Headings should be numbered as follows: 1., 1.1., 1.1.1.

Footnotes: Use of footnotes within the text should be avoided as much as possible. If necessary, it can be located below tables and figures.

Symbols and abbreviations: Unit symbols should comply with The International System of Units.

References: In the text, literature should be given with the last name of the author and year of the publication (For example: Özkan et al., 2008; Özdemir, 2015). At the end of the paper, references should be ordered first alphabetically and then chronologically. If there is more than one paper from the same author for a given year, these references should be identified by the letters a, b, c..., after the year of publication (For example: Kandemir, 1999a; 2000b; 2001).

Tables and figures: All tables and figures should be numbered in the order of their citation in the text, and they should be located in suitable places. Titles of the tables should be located above, and titles of the figures should be located below the related table or figure. Tables and figures should be easily visible and understandable both in print and electronic versions. Figures should be prepared in at least 300 dpi resolution. Characters within the figures should be in Times New Roman font type.

Submission of a manuscript: In our journal, all review and publishing processes are conducted within an electronic system. Authors who want to submit their manuscript to our journal should first visit our “web page” and “register” as an author. Our registered members can “log in” to the system and then upload their manuscript and “COPYRIGHT RELEASE FORM” as an appendix, containing their suggested referees.

References

Using of references should be in the form as follows.

Article in periodical journals / Periyodik dergilerde makale

- Akyıldırım, O., Gökce, H., Bahçeli, S., Yüksek, H. (2017). Theoretical and Spectroscopic (FT-IR, NMR and UV-Vis.) Characterizations of 3-p-chlorobenzyl-4-(4-carboxybenzylideneamino)-4,5-dihydro-1H-1,2,4-triazol-5-one Molecule. *Journal of Molecular Structure*, 1127: 114-123.
- Tan, S., Williams, C.T. (2013). An In Situ Spectroscopic Study of Prochiral Reactant–Chiral Modifier Interactions on Palladium Catalyst: Case of Alkenoic Acid and Cinchonidine in Various Solvents. *J. Phys. Chem. C*, 117(35): 18043–18052.

Book / Kitap

- Özkan, K. (2016). *Biyolojik Çeşitlilik Bileşenleri (α , β , γ) Nasıl Ölçülür?* Süleyman Demirel Üniversitesi, Orman Fakültesi Yayın No: 98, ISBN: 976-9944-452-89-2, Isparta, 142 s.
- Whittaker, E. T. (1988). *A treatise on the analytical dynamics of particles and rigid bodies*. Cambridge University Press.

Reference to a chapter in an edited book / Kitapta bölüm

- Westhoff, V., Van Der Maarel, E. (1978). The braun-blanquet approach in classification of plant communities, Reinhold Tüxen (Ed.), *Handbook of Vegetation Science*, Springer Netherlands, pp. 619-704.
- Şencan, A., Sevindir, H.C., Kiliç, M., Karaboyacı, M. (2011). Biosorption of CR+ 6 from Aqueous Solution with Activated Sludge Biosolids (Ref. NO: MT11-OP-475), Gökçekus, H., Türker, U., LaMoreaux, J.W., (Ed, *Survival and Sustainability*, 973-984.

Thesis and dissertation / Tez

- Gülsoy, S. (2011). *Pistacia terebinthus* L. subsp. *palaestina* (Boiss.) Enler (Anacardiaceae)'in Göller Yöresi'ndeki Yetiştirme Ortamı Özellikleri ve Yetiştirme Ortamı-Meyve Uçucu Yağ İçeriği Etkileşimleri. SDÜ, Fen Bilimleri Enstitüsü, Orman Mühendisliği Anabilim Dalı, 194 s.
- Özdemir, S. (2015). Ovacık Dağı Yöresi'nde Türk Kekliği (*Origanum onites* L.) ve Büyük Çiçekli Adaçayı (*Salvia tomentosa* Miller) Türlerinin Ekolojik Özellikleri. SDÜ, Fen Bilimleri Enstitüsü, Orman Mühendisliği Anabilim Dalı. 74s.

Conference proceedings / Konferans bildirisi

- Özkan, K., Kavgacı, A. (2009). Küresel ısınmanın orta dağlık alanlarda tür çeşitliliği üzerine olası etkileri (Acıpayam yöresi örneği). I. Ulusal Kuraklık ve Çölleşme Sempozyumu (Eds: Palta, Ç.), 16-18 Haziran 2009, Konya, Türkiye, 277-284.
- Özkan, K., Negiz, M.G., Şentürk, Ö., Kandemir, H. (2012). Göller Bölgesi'ndeki Bazı Önemli Rekreasyon Alanları ve Onların Ekolojik Özellikleri, I. Rekreasyon Araştırmaları Kongresi 2012, Bildiri Kitabı, 12-15 Nisan, 587-596, Detay Yayıncılık, Kemer-Antalya.

Electronic reference / Elektronik kaynak

- FAO, (2016). *Sustainable Food and Agriculture*. Food and Agriculture Organization of the United Nations, Rome, <http://www.fao.org/sustainability/en/>, Accessed: 14.06.2016.
- Milliparklar, (2017). Doğa Koruma ve Milli Parklar Genel Müdürlüğü. <http://www.milliparklar.gov.tr/korunanalanlar/kavramlar.htm>, Erişim Tarihi: 18.06.2017

Bilge International Journal of Science and Technology Research online ve açık erişimli yayınlanan uluslararası hakemli bir dergidir. Dergi dili İngilizce'dir. Yılda iki sayı yayınlanan dergide Temel bilimler, Doğa bilimleri, Mühendislik ve Teknoloji bilimleri konularında bilimsel makaleler yayınlanmaktadır.

Dergimize gönderilen makalelerin daha önce yayınlanmamış orijinal çalışmalar olması gerekmektedir. Dergide yayımlanacak makalenin atıflarından, bilimsel verilerinden, sonuçlarından ve etik kurallara uygun olup olmadığından yazarlar sorumludur (yazar/yazarlar bu durumu telif hakkı sözleşmesinde kabul eder). Orijinal araştırmaya dayalı çalışmalara öncelik verilmekte, sınırlı sayıda derleme makale yayınlanmaktadır.

Dergiye gönderilen makale, yayın kurulu tarafından yayına uygunluk açısından incelendikten sonra en az iki hakeme gönderilir. Hakemlerin değerlendirmeleri sonucunda en az iki yayınlanabilir raporu alan makale, dergi yönetimince uygun görülen bir sayıda yayınlanır. Hakem raporlarının birisinin olumlu, diğerinin olumsuz olması durumunda makale üçüncü bir hakeme gönderilir. Bu durumda makalenin yayınlanıp yayınlanmamasına üçüncü hakemin raporuna göre karar verilir. Hakemler tarafından düzeltme istenen makaleler gerekli düzeltmeler için yazara geri gönderilir. Düzeltilen metnin belirtilen sürede dergi sistemine yüklenmesi yazarın sorumluluğundadır. Makalenin yayınlanması konusunda son karar, dergi editörlüğüne aittir..

Bilge International Journal of Science and Technology Research is an online, open access, peer-reviewed, international research journal. Language of the journal is English. The journal published two issues a year publishes scientific articles on the subjects of Basic Sciences, Natural Sciences, Engineering and Technology.

Authors should only submit original work, which has not been previously published and is not currently considered for publication elsewhere. The authors are responsible for the citations of the article to be published, its scientific data, its results, and whether it is in line with ethical rules (Author / authors accept that in the copyright agreement). Research papers will be given priority for publication while only a limited number of review papers are published in a given issue.

The articles are sent to least two reviewer after examined by the editor board in terms of compliance with the publication. As a result of the evaluations of the reviewers, the article which received at least two publishable reports will be published at a suitable number for the management of the journal. If one of the reviewer reports is positive and the other is negative, the article will be sent a third reviewer. In this case, the publication of the article is decided according to the third report. The articles corrected by the referees are returned to the author for necessary corrections. It is the responsibility of the author to upload the revised text to the journal system for the specified period. The final decision on the publication of the article belongs to chef editor.

